IMMUNOTHERAPY IN RENAL CELL CARCINOMA

EDITED BY: Walter J. Storkus and Viktor Grünwald
PUBLISHED IN: Frontiers in Oncology

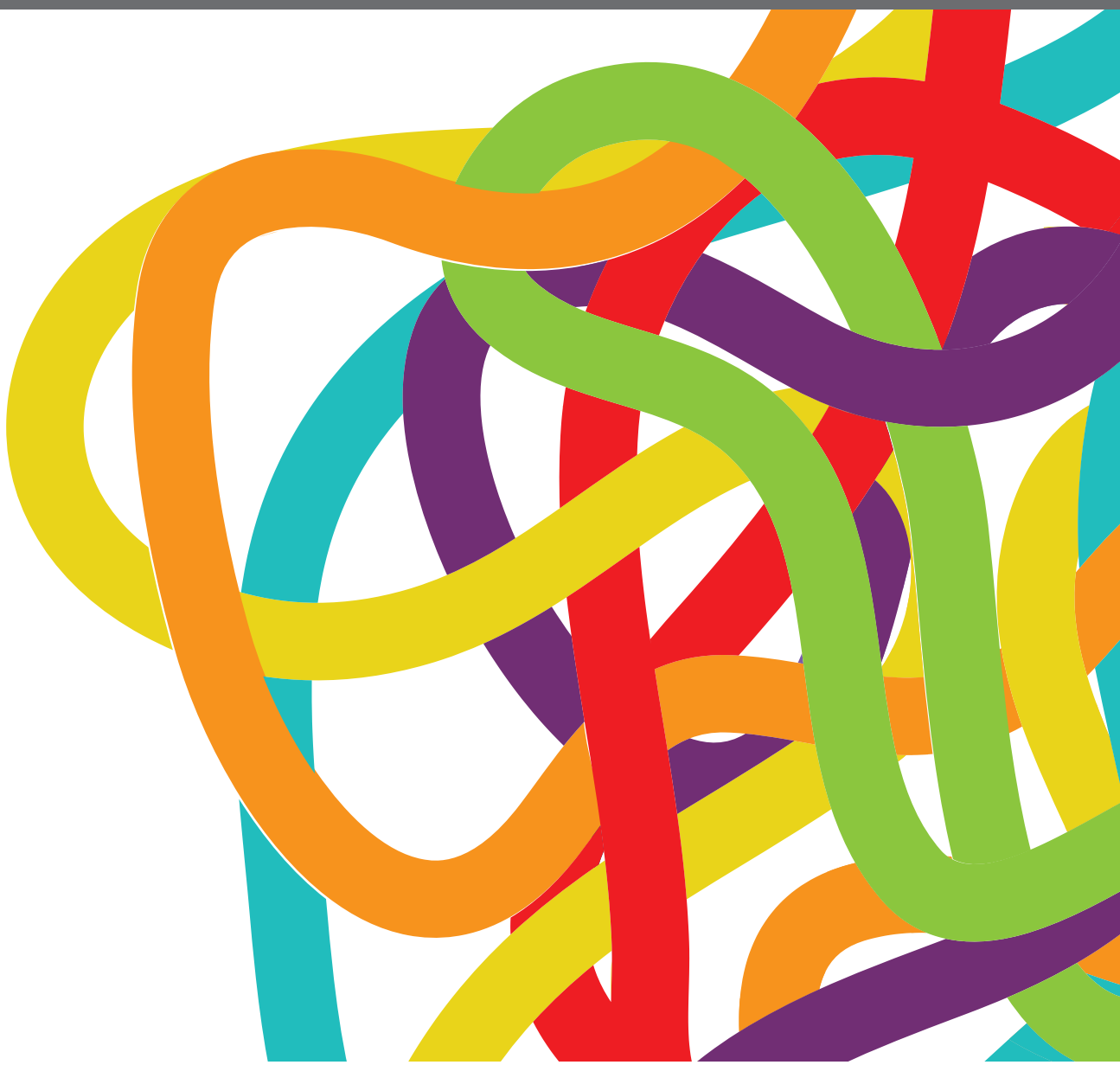

frontiers Research Topics

ISSN 1664-8714
ISBN 978-2-8897-6921-6
DOI 10.3389/978-2-8897-6921-6

About Frontiers

Frontiers is more than just an open-access publisher of scholarly articles: it is a pioneering approach to the world of academia, radically improving the way scholarly research is managed. The grand vision of Frontiers is a world where all people have an equal opportunity to seek, share and generate knowledge. Frontiers provides immediate and permanent online open access to all its publications, but this alone is not enough to realize our grand goals.

Frontiers Journal Series

The Frontiers Journal Series is a multi-tier and interdisciplinary set of open-access, online journals, promising a paradigm shift from the current review, selection and dissemination processes in academic publishing. All Frontiers journals are driven by researchers for researchers; therefore, they constitute a service to the scholarly community. At the same time, the Frontiers Journal Series operates on a revolutionary invention, the tiered publishing system, initially addressing specific communities of scholars, and gradually climbing up to broader public understanding, thus serving the interests of the lay society, too.

Dedication to Quality

Each Frontiers article is a landmark of the highest quality, thanks to genuinely collaborative interactions between authors and review editors, who include some of the world's best academicians. Research must be certified by peers before entering a stream of knowledge that may eventually reach the public - and shape society; therefore, Frontiers only applies the most rigorous and unbiased reviews.
Frontiers revolutionizes research publishing by freely delivering the most outstanding research, evaluated with no bias from both the academic and social point of view. By applying the most advanced information technologies, Frontiers is catapulting scholarly publishing into a new generation.

What are Frontiers Research Topics?

Frontiers Research Topics are very popular trademarks of the Frontiers Journals Series: they are collections of at least ten articles, all centered on a particular subject. With their unique mix of varied contributions from Original Research to Review Articles, Frontiers Research Topics unify the most influential researchers, the latest key findings and historical advances in a hot research area! Find out more on how to host your own Frontiers Research Topic or contribute to one as an author by contacting the Frontiers Editorial Office: frontiersin.org/about/contact

IMMUNOTHERAPY IN RENAL CELL CARCINOMA

Topic Editors:
Walter J. Storkus, University of Pittsburgh, United States
Viktor Grünwald, Westdeutsches Tumorzentrum Essen, Universitätsklinikum Essen, Germany

Citation: Storkus, W. J., Grünwald, V., eds. (2023). Immunotherapy in Renal Cell Carcinoma. Lausanne: Frontiers Media SA. doi: 10.3389/978-2-8897-6921-6

Table of Contents

frontiers | Frontiers in Oncology

TYPE Editorial
PUBLISHED 27 July 2022
DOI 10.3389/fonc.2022.945510

OPEN ACCESS

EDITED AND REVIEWED BY
Ronald M. Bukowski,
Cleveland Clinic, United States

*CORRESPONDENCE
Walter J. Storkus
storkuswj@upmc.edu

SPECIALTY SECTION
This article was submitted to Genitourinary Oncology, a section of the journal Frontiers in Oncology

RECEIVED 16 May 2022
ACCEPTED 31 May 2022
PUBLISHED 27 July 2022

CITATION
Gruenwald V and Storkus WJ (2022) Editorial: Immunotherapy in renal cell carcinoma.
Front. Oncol. 12:945510.
doi: 10.3389/fonc.2022.945510

Editorial: Immunotherapy in renal cell carcinoma

Viktor Gruenwald[1] and Walter J. Storkus[2]*

[1]Interdisciplinary Genitourinary Oncology, Clinic for Medical Oncology and Clinic for Urology, University Hospital Essen, Essen, Germany, [2]Dermatology, Immunology, Pathology and Bioengineering, University of Pittsburgh School of Medicine and the University of Pittsburgh Medical Center (UPMC) Hillman Cancer Center, Pittsburgh, PA, United States

This collection contains 10 reports published In Frontiers in Oncology between August 2020 and March 2022 broadly focused on the immunobiology of renal cell carcinoma (RCC), the impact of immunotherapy in the setting of RCC, and the identification of biomarkers that are prognostic of RCC patient outcomes and response to immunotherapy.

KEYWORDS

immunotherapy, cancer, renal cell carcinoma (RCC), biomarker, urologic oncology

Editorial on the Research Topic:
Editorial: Immunotherapy in renal cell carcinoma

Introduction

Renal cell carcinoma (RCC) accounts for 90-95% of all kidney malignancies. If detected early and managed surgically, the 5-year overall survival rate for RCC patients is ~90% (1). However, one-third of treated patients develop disease recurrence or metastases. Patients diagnosed with advanced-stage metastatic disease have a very poor prognosis, with a 5-year survival rate of 14% in a real-world population (2). There remains a clear and unmet clinical need for the development of effective interventional therapies for RCC patients, particularly for those individuals with advanced-stage disease.

Cytokine-based immunotherapies were developed as standard-of-care treatments for metastatic RCC patients in the 1990s. However, only a minority of patients derived durable clinical benefits. With the advent of refined molecular profiling of RCC, the field witnessed the rapid evolution of targeted therapeutic approaches yielding improved response rates in the early 2000s, with more recent advances (since 2013) including the application of immune checkpoint inhibitors (ICI) to enhance and sustain anti-tumor immune cell function in association with extended progression-free and overall survival in treated RCC patients (1, 3). More recently, ICI-combinations have gained momentum and represent a 1st line standard of care (4), although much work remains to improve current rates of response to ICI-based treatments while coordinately limiting immune-related adverse events (irAEs). In this regard,

biomarkers (at baseline and on-treatment) associated with patient response to immunotherapy are also expected to improve patient diagnoses and therapeutic management, while coordinately serving as monitoring tools to assess patient response to treatment in real-time (5–7).

The current collection advances our understanding of clinically informative biomarkers relevant to patient care and the safety/impact of interventional immunotherapies in the setting of urologic oncology.

RCC immune-associated prognostic biomarkers

Du et al. analyzed immune cell-associated transcripts in the clear cell renal cell carcinoma (ccRCC; KIRK) TCGA database, identifying 7 immune cell type gene signatures associated with patient overall survival (OS). Abundant B (memory, plasma) cells, Treg and M1 macrophage transcripts were linked to poor prognosis, while elevated levels of dendritic cell (DC; resting, activated) and resting mast cells were correlated to extended OS. These data are consistent with higher abundance ratios of DC and activated DC in tumors of patients with better OS and presumed enhanced antigen-presenting cell performance. Low or high expression of 7 HUB genes in the TME also appeared prognostic of prolonged patient OS: BDKRB1 (low), CASR (high), GNG4 (low), MFI2 (low), MMP9 (low), NUM (low) and SAA1 (low). Additional immune-related genes were enriched in neuroactive ligand-receptor binding, cytokine/cytokine receptor interactions, GPCR ligand binding, and APC function that may represent useful prognostic indices and serve to define novel targets for developing prospective interventional approaches.

Long non-coding RNAs (lncRNA) are long RNAs (> 200 nucleotides) that play roles in chromatin remodeling, as well as transcriptional and post-transcriptional gene regulation (Sun et al.). In this collection, (Sun et al.) developed a novel immune-related lncRNA signature based on an analysis of the TCGA KIRC database for prognosis of ccRCC patients. They identified 5 prognostic lncRNAs (3 harmful, 2 protective), which appeared to serve as independent predictors of tumor stage and high-risk (short OS) vs. low-risk (long OS) patient status. Four of these lncRNAs were upregulated in the TME with predicted impact on local expression of immune checkpoint molecules (PD-1, PD-L1, CTLA4), immunomodulatory cytokines, as well as TCR, Wnt/β-catenin and MAPK signaling.

A meta-analysis performed by (Jin et al.) evaluated the systemic immune index (SII) based on neutrophil, platelet, and lymphocyte counts in peripheral blood PBL as a prognostic index in ccRCC patients. High SII was independently associated with aggressive disease and poor OS, but not PFS or cancer-specific survival.

Ferroptosis is a form of immunogenic cell death believed to support improved immune cell recognition of tumor cells (Gao et al.). In this regard, (Gao et al.) described a novel ferroptosis-related 4-gene signature (BID, MT1G, SLC7A11, TAZ) that appears diagnostic/prognostic in ccRCC patients. Notably, TAZ also appears to modulate regulatory factors in the TME favoring recruitment/development of suppressor cells (TAMs, Treg) and upregulated expression of immune checkpoint molecules. High- (poor OS) and low-risk groups based on this 4 gene signature (FeSig) could be distinguished based on differences in immune pathways (Ras-, PPAR- and IL-17A-signaling) and immune cell (macrophages, mast cells, PMNs, $CD4^+$ T cells [Th1, Th2, Tfh], and $CD8^+$ T cells) content within the TME. Expression of PD-1, CTLA4, LAG3, and TIGIT was upregulated in high-risk vs. low-risk patients, with high-risk patients exhibiting superior response to anti-PD-1-based monotherapy. Based on these findings, future immunotherapies coordinately targeting ICI and the TAZ/WNT10B signaling axis are proposed for improved outcomes in ccRCC patients.

Nie et al. report that transcripts for Fcγ receptors (FCGR; FCGR1A/B/C, FCGR2A) were upregulated in ccRCC tumors based on differential gene methylation, where they were linked to tumor grade/stage and associated with poor patient OS. $CD4^+$ T and NK were negatively-, while Treg and M2 macrophage cells were positively-, correlated with FCGR transcript expression levels. Additionally, ccRCC tumors with high FCGR expression exhibited increased expression of immune suppressor/regulatory molecules IL-10, TGFB1 and CTLA4. These results suggest that high tumor expression of FCGRs defines a risk factor for ccRCC patient survival associated with poor prognosis and regulatory immune status in the TME.

RCC immunobiology and immunotherapy

Kuo et al. retrospectively evaluated the safety and efficacy of ICIs (anti-PD-1, anti-PD-L1, anti-CTLA4) in patients with metastatic urothelial carcinoma with/without end-stage renal disease (ESRD). Although small in sample size, the study reports a higher overall response rate (ORR) for ESRD vs. non-ESRD patients (55% vs. 29%), with 6 PR/1 SD documented amongst the 11 ESRD patients treated. Potential prognostic factors in multivariate analyses included leukocytosis and neutrophil-to-lymphocyte ratio.

Stellato et al. retrospectively evaluated the impact of prior nephrectomy on response to ICI-based intervention in 287 metastatic RCC patients. Multivariate analyses revealed that prior nephrectomy was associated with superior patient OS and PFS. These data are consistent with superior outcomes for

advanced-stage mRCC patients treated with biologic modifiers IL-2/IFNA (or anti-PD1/CTLA4 vs. sunitinib in the Checkmate214 trial).

Gopalakrishanan et al. provide a case report in which anti-PD1 triggered (over)exuberant tumor inflammation in association with radiologic hyper-progression and clinical deterioration in 3 patients with advanced ccRCC with diverse visceral sites of disease (Gopalakrishnan et al.). Histologic examination of tumors revealed tissue necrosis with lymphohistiocytic infiltration and evidence of robust immune-mediated tumor-associated killing and macrophage scavenging of debris. The authors suggest these conditions promote the rapid expansion of the anti-tumor T cell repertoire, pro-inflammatory immune cell infiltration and cytokine-release syndrome. To mitigate such immune cell over-reactivity to ICI-based treatment, the authors suggest use of combination regimens including IL-6i (tocilizumab).

Wang et al. evaluated the rare autosomal dominant disorder hereditary leiomyomatosis and RCC (HLRCC) in which patients are at risk of developing multiple skin and uterine leiomyomas and RCC with poor clinical outcomes based on deletion of the tumor suppressor gene fumarate hydratase (FH), an enzyme in the TCA cycle (Wang et al.). While this rare disease has no currently effective standard of care, the authors provide a case study for HLRCC patients who developed a complete response in their PD-L1$^+$PD-1$^+$ tumors after 24 months of treatment with anti-PD1 monotherapy.

Zhou et al. provide a case report and literature review for treatment with tyrosine kinase inhibitors (TKI; pazopanib, axitinib) and ICI in the setting of a collecting duct renal carcinoma (CDC), a rare (0.4-2.0% of RCC cases) and highly aggressive subtype of kidney cancer with poor prognosis with limited effective therapies. In this setting, combination immunotherapy with TKI + ICI after cytoreductive nephrectomy resulted in a clinical PR and extended OS in a patient with CDC, supporting more general testing of such interventional approaches in the future.

Author contributions

All authors listed have made a substantial, direct, and intellectual contribution to the work and approved it for publication.

Funding

This work was supported in part by NIH grant R01 CA249811 (to WJS).

Conflict of interest

The authors declare that the research was conducted in the absence of any commercial or financial relationships that could be construed as a potential conflict of interest.

Publisher's Note

References

1. Goebell PJ, Ivanyi P, Bedke J, Bergmann L, Berthold D, Boegemann M, et al. Consensus paper: current state of first- and second-line therapy in advanced clear-cell renal cell carcinoma. *Future Oncol* (2020) 16:2307–28. doi: 10.2217/fon-2020-0403

2. Siegel RL, Miller KD, Fuchs HE, Jemal A. Cancer statistics, 2022. *CA Cancer J Clin* (2022) 72:7–33. doi: 10.3322/caac.21708

3. Chowdhury N, Drake CG. Kidney cancer: An overview of current therapeutic approaches. *Urol Clin North Am* (2020) 47:419–31. doi: 10.1016/j.ucl.2020.07.009

4. Bedke J, Albiges L, Capitanio U, Giles RH, Hora M, Lam TB, et al. The 2021 updated European association of urology guidelines on renal cell carcinoma: Immune checkpoint inhibitor–based combination therapies for treatment-naive metastatic clear-cell renal cell carcinoma are standard of care. *Eur Urol* (2021) 80:393–7. doi: 10.1016/j.eururo.2021.04.042

5. Walk EE, Yohe SL, Beckman A, Schade A, Zutter MM, Pfeifer J, et al. The cancer immunotherapy biomarker testing landscape. *Arch Pathol Lab Med* (2020) 144:706–24. doi: 10.5858/arpa.2018-0584-CP

6. Music M, Prassas I, Diamandis EP. Optimizing cancer immunotherapy: Is it time for personalized predictive biomarkers? *Crit Rev Clin Lab Sci* (2018) 55:466–79. doi: 10.1080/10408363.2018.1499706

7. Linehan WM, Ricketts CJ. The cancer genome atlas of renal cell carcinoma: findings and clinical implications. *Nat Rev Urol* (2019) 16:539–52. doi: 10.1038/s41585-019-0211-5

frontiers in Oncology

ORIGINAL RESEARCH
published: 20 August 2020
doi: 10.3389/fonc.2020.01430

Long Non-Coding RNA Profile Study Identifies an Immune-Related lncRNA Prognostic Signature for Kidney Renal Clear Cell Carcinoma

Zhuolun Sun[1], *Changying Jing*[2], *Chutian Xiao*[1] *and Tengcheng Li*[1]*

[1] Department of Urology, Third Affiliated Hospital of Sun Yat-sen University, Guangzhou, China, [2] Eye Institute of Shandong University of Traditional Chinese Medicine, Jinan, China

Kidney renal clear cell carcinoma (KIRC) is the predominant pathological subtype of renal cell carcinoma (RCC) in adults. Long non-coding RNAs (lncRNAs) are an important class of gene expression regulators and serve fundamental roles in immune regulation. The intent of this study is to develop a novel immune-related lncRNA signature to accurately predict the prognosis for KIRC patients. Here, we performed genome-wide comparative analysis of lncRNA expression profiles in 537 KIRC patients from The Cancer Genome Atlas (TCGA) database. Cox regression model–identified immune-related lncRNAs were extracted for constructing a novel five immune-related lncRNA signature (AC008105.3, LINC02084, AC243960.1, AC093278.2, and AC108449.2) with the ability to predict the prognosis of KIRC patients. Univariate and multivariate Cox regression analyses demonstrated that the signature could act as an independent prognostic predictor for overall survival (OS). With the further investigation on different clinicopathological parameters, we found that the signature could divide KIRC samples into high-risk groups with shorter OS and low-risk groups with longer OS in different subgroups. Principal component analysis suggested that the five immune-related lncRNA signature drew a clear distinction between high- and low-risk groups based on the immune-related lncRNAs. The different immune status between the two groups was observed in gene set enrichment analysis and the ESTIMATE algorithm. Except for AC093278.2, the expressions of the other four lncRNAs expression were significantly upregulated in tumor tissues. In summary, the identified immune-lncRNA signature had important clinical implications in prognosis prediction and could be exploited as underlying immune therapeutic targets for KIRC patients.

Keywords: immune, kidney renal clear cell carcinoma, long non-coding RNA, overall survival, prognostic signature

OPEN ACCESS

Edited by:
Janice P. Dutcher, Cancer Research Foundation, United States

Reviewed by:
Gabriel Malouf, INSERM U964 Institut de Génétique et de Biologie Moléculaire et Cellulaire (IGBMC), France
Nizar M. Tannir, University of Texas MD Anderson Cancer Center, United States

***Correspondence:**
Tengcheng Li
tengchengli@126.com

Specialty section:
This article was submitted to Genitourinary Oncology, a section of the journal Frontiers in Oncology

Received: *01 May 2020*
Accepted: *06 July 2020*
Published: *20 August 2020*

Citation:
Sun Z, Jing C, Xiao C and Li T (2020) Long Non-Coding RNA Profile Study Identifies an Immune-Related lncRNA Prognostic Signature for Kidney Renal Clear Cell Carcinoma. Front. Oncol. 10:1430. doi: 10.3389/fonc.2020.01430

INTRODUCTION

Renal cell carcinoma (RCC), accounting for ∼2% of adult malignancies, is the third most common malignant tumor of the urinary system worldwide following prostate and bladder cancer (1). Kidney renal clear cell carcinoma (KIRC) is the predominant pathological subtype and represents ∼90% of the total cases of RCC in adults (2). Since the clinical symptoms and signs of early stage RCC are often insidious and non-specific, a great proportion of patients are not diagnosed until

advanced tumor stages (3). Furthermore, KIRC is known for being insensitive to chemotherapy and radiotherapy and characterized by higher rates of recurrence and metastasis compared to other subtypes of RCC (1, 4). The 5-year overall survival (OS) rate for patients with early stage RCC is up to 90% although OS of those with locally advanced RCC and metastatic RCC could drop to 60 and 10%, respectively (5). Immunotherapy has emerged as one of the most promising modalities against cancer, and recent clinical advances have confirmed its value in urological cancer (6). Thus, investigation on immune-related factors is urgently required.

Long non-coding RNAs (lncRNAs) are a class of transcribed non-coding RNAs (ncRNAs) that are longer than 200 nucleotides in length and do not encode any proteins, which are widely distributed in the cytoplasm and nucleus (7, 8). It is well-documented that lncRNAs are implicated in multiple biological functions, such as cell differentiation (9), apoptosis (10), tumor microenvironment (TME) (11), and epigenetic regulation (12). Recent research indicates that lncRNAs exert a complex and comprehensive regulatory role in cancer development and progression (13, 14). Moreover, lncRNAs have emerged as important regulators of gene expression in the immune system, including but not limited to immune activation and immune cell infiltration (15, 16). For example, lncRNA SNHG1 plays a critical role in the immune escape by inhibiting the differentiation of Treg cells in breast cancer (17). Analogously, NKILA, an NF-κB-interacting lncRNA, promotes tumor immune evasion by regulating activation-induced cell death of various T cell subset infiltrating tumors (18). Other research reveals that oncogenic lncRNA LINK-A inactivates tumor suppressor pathways and downregulates antigen presentation through inactivation of PKA pathways (19). The immune system affects oncogenesis greatly, and immunotherapy has emerged as a promising strategy in cancer treatment (20). Therefore, it is crucial to explore immune-related lncRNAs to predict prognosis of KIRC patients and further guide the proper individual treatment strategies.

In this study, we performed a comprehensive comparative genomics analysis of lncRNA expression profiles in 537 KIRC patients from The Cancer Genome Atlas (TCGA) database. The Cox regression model identified five lncRNAs that are related to immune response. We then constructed a novel immune-related lncRNA signature with the ability to predict the prognosis of KIRC patients, which might serve as potential prognostic indicators and could be exploited as underlying immune therapeutic targets for KIRC patients.

MATERIALS AND METHODS

Acquisition of KIRC Expression Data

Both the entire RNA-sequencing profile data and corresponding clinical information of patients with KIRC were downloaded from the TCGA (https://cancergenome.nih.gov/) database. We downloaded the raw reads and fragments per kilobase of transcript per million (FPKM) data for our study. According to the gene annotations in the GENCODE project (https://www.gencodegenes.org/) (21), the lncRNAs and protein-coding genes were further classified. Subsequently, the detailed clinical information of tumor patients, including age, gender, tumor grade, TNM stage, AJCC stage, and survival status were obtained for further analysis. Similarly, the mutation data of patients with KIRC were downloaded as a mutation annotation format (MAF) file from TCGA database. Analysis, visualization, and summarization of MAF files using R package "maftools" (https://github.com/PoisonAlien/maftools) (22). Considering that some patients may die from non-neoplastic factors, samples with overall survival (OS) data less than 30 days were excluded. In addition, a proportion of KIRC subjects with incomplete data were also rejected. No specific ethical approval and informed consent were considered necessary for all of these data were publicly available.

Identification of Immune-Related lncRNAs

List of the immunomodulatory genes was downloaded from the Molecular Signatures Database v7.1 (MSigDB, https://www.gsea-msigdb.org/gsea/index.jsp, IMMUNE_RESPONSE, M19817 and IMMUNE_SYSTEM_PROCESS, M13664) (23). To identify the potential lncRNA related with immune-modulating genes, we performed Pearson correlation analysis in the statistical software R (version 3.6.2). The correlation coefficient (|R|) greater than 0.8 was considered as a strong correlation, and $P < 0.05$ was statistically significant. Based on the above thresholds, candidate immune-related lncRNAs were identified and used for further analysis.

Construction of the Prognostic Signature and Calculation of the Risk Score

To confirm the potential prognostic-related lncRNAs, univariate Cox regression analysis was performed to analyze the association between immune-related lncRNA expression and survival data. Those immune-related lncRNAs significantly related to survival ($P < 0.001$) were selected as prognosis-related lncRNAs of KIRC patients. An HR value greater than one suggested an increased risk; otherwise, it suggested a protective risk. Multivariate Cox regression analysis was employed to confirm target immune-related lncRNAs and its estimated regression coefficients (β) with the lowest Akaike information criterion (AIC) values. We then constructed the optimal lncRNA prognostic signature and calculated the risk score of each PIRC patient on the basis of the risk coefficients as well as the expression levels of target lncRNAs. The risk score was calculated as risk score = $\beta_{\text{lncRNA1}} \times \text{Expression}_{\text{lncRNA1}} + \beta_{\text{lncRNA2}} \times \text{Expression}_{\text{lncRNA2}} + \ldots + \beta_{\text{lncRNA1n}} \times \text{Expression}_{\text{lncRNAn}}$.

Prediction Analysis of Risk Score Model

All KIRC patients were sorted into high- and low-risk groups with the median risk score as the threshold. We depicted the survival curve between two groups using the Kaplan-Meier method with a two-sided *log-rank test*. In addition, the receiver operating characteristic (ROC) curve and area under the ROC curve (AUC value) were utilized to evaluate diagnostic efficacies. Univariate Cox regression analysis was used to evaluate clinicopathological variables that affect the survival of KIRC patients, including age, gender, grade, AJCC stage, T stage, and M stage. N stage was not analyzed due to lacking a large

amount of data. Furthermore, the risk score was analyzed by multivariate Cox regression analysis to confirm whether it is a risk score or not. But beyond all that, we also investigated stratified survival analysis to detect the prognostic value of our risk score model in different subgroups. To further delve into the impact of individual target lncRNA in our prognostic risk model on KIRC patients, the relationship between expression level of each target lncRNA and clinical parameters was compared via Student's *t*-test.

Co-expression Analysis and Immune Status Analysis

Pearson correlation coefficients were calculated to determine co-expressed lncRNA-mRNA pairs. The correlation coefficient threshold was set to >0.6, and the corresponding $P < 0.05$ was considered statistically significant. Principal component analysis (PCA) was carried out to visualize the similarities and differences among grouped samples based on the immune-related lncRNA set and whole gene expression profiles. Gene set enrichment analysis (GSEA) was implemented to determine whether an a priori defined set of genes shows statistically significant, concordant differences between the high- and low-risk groups using GSEA software version 4.0.3. C7 collection set (IMMUNOLOGIC_SIGNATURE) was downloaded from MSigDB for subsequent analysis. The stromal score, immune score, ESTIMATE score, and tumor purity were also calculated by the ESTIMATE algorithm to further explore immune cell infiltration between the low- and high-risk groups.

Statistical Analysis

All statistical analyses were performed using R software (version 3.6.2). Differences between variables were assessed with independent *t*-tests. The association of clinicopathological variables in KIRC patients between predicted high- and low-risk cohorts was subjected to a chi-square test. The correlation was determined by Pearson or Spearman correlation analysis. Kaplan-Meier curves and log-rank tests were used to evaluate the survival data. Independent prognostic factors were assessed by univariate and multivariate Cox regression analyses. $P < 0.05$ was regarded as statistically significant.

RESULTS

Filter Out Immune-Related lncRNAs Associated With Prognosis

A total of 15,142 lncRNAs as well as their expression profiles were screened from the TCGA data sets, and the list of 332 immunoregulatory genes was downloaded from the Molecular Signatures Database. Then, 23 immune-related lncRNAs were screened according to the Pearson correlation analysis with the criteria of $|R| > 0.8$ and $P < 0.05$. Subsequently, we carried out univariate Cox regression analysis to further single out the potential prognostic lncRNAs from the cohort of immune-related lncRNAs and found that 12 lncRNAs were significantly related with the KIRC patients' OS ($P < 0.01$, **Figure 1A**). Remarkably, all but two of these lncRNAs (AC093278.2 and AC108449.2) were considered to be risky factors. Multivariate Cox regression analysis was then applied to confirm the optimal prognostic lncRNAs. Finally, a total of five lncRNAs were filtered out, and its regression coefficients (β) were also determined for further analysis (**Table 1**).

TABLE 1 | The HRs, *P*-values, and Coef of 5 immune-related lncRNAs in the multivariate Cox regression analysis.

lncRNAs	HR (95% CI)	*P*-value	Coef
AC008105.3	1.8743 (1.3319–2.6376)	0.0003	0.6282
AC093278.2	0.6516 (0.5222–0.8129)	0.0001	−0.4284
LINC02084	0.5019 (0.3108–0.8105)	0.0048	−0.6893
AC108449.2	0.6959 (0.5453–0.8881)	0.0036	−0.3625
AC243960.1	2.0658 (1.1331–3.7660)	0.0179	0.7255

HR, hazard ratio; Coef, regression coefficient.

Construction of Five-lncRNA Prognostic Risk Signature

To further investigate whether the above five target lncRNAs could be used as prognosis biomarkers, we developed a five-lncRNA risk signature to predict the outcome of KIRC patients. Then, the risk score for each sample was calculated according to the following formula: risk score $= (0.6282 \times \mathrm{Exp}_{\mathrm{AC008105.3}}) + (-0.4284 \times \mathrm{Exp}_{\mathrm{AC093278.2}}) + (-0.6893 \times \mathrm{Exp}_{\mathrm{LINC02084}}) + (-0.3625 \times \mathrm{Exp}_{\mathrm{AC108449.2}}) + (0.7255 \times \mathrm{Exp}_{\mathrm{AC243960.1}})$. KIRC patients in the TCGA data sets were divided into high- ($n = 253$) and low-risk groups ($n = 254$) based on the median risk score. Significant difference was found in overall survival (OS) between the predicted two subgroups, and patients in the high-risk group suffered shorter survival time than those in the low-risk group (**Figure 1B**). Specifically, the 3-, 5-, and 7-year survival rates of the high-risk group were 69.2, 44.7, and 28.5%, respectively, whereas the corresponding rates in the low-risk group were 84.3, 75.1, and 62.7%. We ranked the risk scores across all KIRC patients and then analyzed their distributions according to the five lncRNAs signature-based risk scores (**Figure 1C**). The distributions of survival status revealed that survival rate and time of patients in the low-risk group were significantly increased compared to the high-risk group (**Figure 1D**). We next assessed the predictive performance of the five-lncRNA model by time-dependent receiver operating characteristic (ROC) curves. The area under the ROC (AUC) value equal to 0.732 indicated the prognostic risk model had a good predictive effect (**Figure 1E**). These findings imply that the prognostic risk model was competent for predicting the prognosis of KIRC patients.

Immune-Related lncRNA Signature Was an Independent Prognostic Factor

To explore whether the five-lncRNA prognostic risk signature was independent of clinical variables, univariate and multivariate Cox regression analyses were performed with the following factors: risk score and relevant clinical factors, including age, gender, grade, AJCC stage, T stage, and M stage

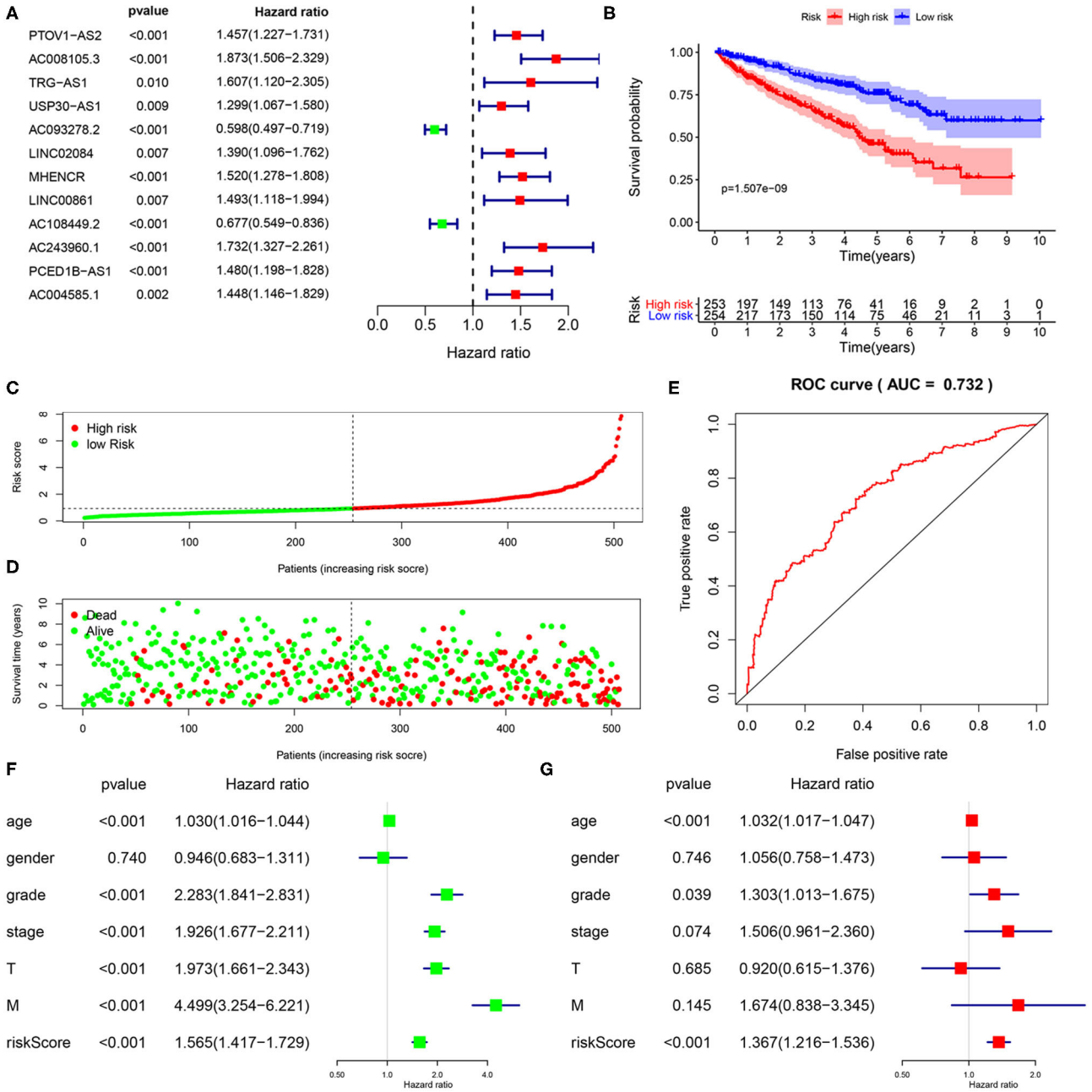

FIGURE 1 | Construction and validation of immune-related lncRNA prognostic signature for KIRC. **(A)** A forest plot illustrating the HR and *P*-value from the univariate Cox regression analysis between immune-related lncRNA expression and survival data. **(B)** Kaplan-Meier overall survival curves for KIRP patients exhibited that the high-risk group suffered significantly shorter OS than those in the low-risk group. **(C)** Predictor scores of KIRP patients were sorted based on the signature. **(D)** The scatterplot of the relationship between the risk scores and the survival status/survival time. **(E)** ROC curve analysis suggests the veracity and reliability for the prognostic signature. Univariate **(F,G)** multivariate Cox regression analysis of the association between clinicopathological factors (including risk score) and overall survival of KIPC patients.

in the TCGA database. N stage was not analyzed for a large amount of missing data. Except the gender, all the others were significantly associated with OS in univariate analysis (**Figure 1F**). Results from multivariate analysis suggested risk score were still significantly linked with OS, and the five immune-related lncRNA signature could serve as an independent prognostic factor for KIRC patients (**Figure 1G**).

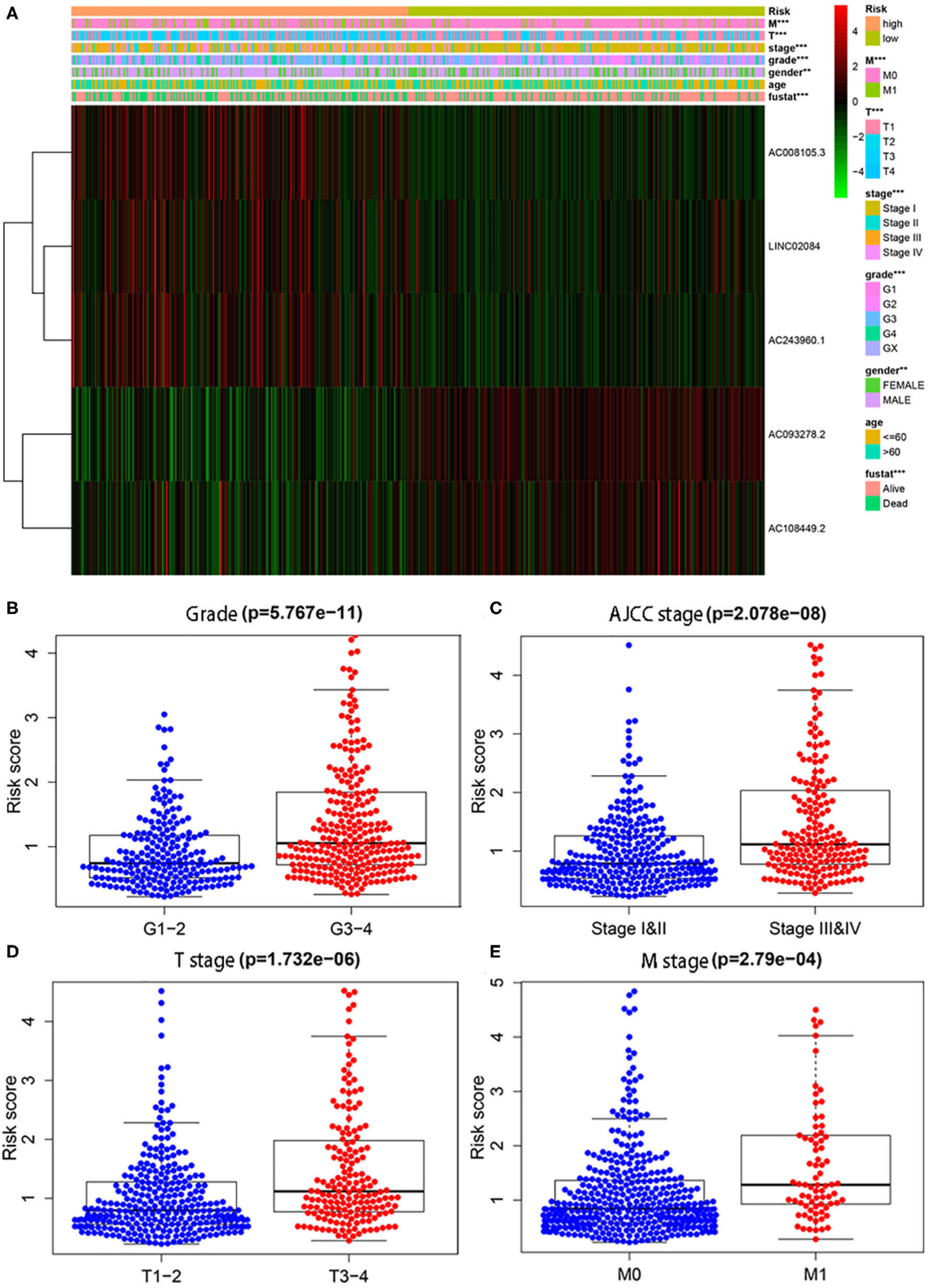

FIGURE 2 | The relationship between the risk score and different clinicopathological features. **(A)** The heat map shows the distribution of clinicopathological factors and the expression of the five immune-related lncRNAs between the low- and high-risk groups. Chi-square test was used for correlation between clinical and risk. $^{**}P < 0.01$ and $^{***}P < 0.001$. **(B–E)** represent grade, AJCC stage, T stage, and M stage, respectively.

Immune-Related lncRNA Signature Was Strongly Related With Clinical Features

In addition, we also conducted chi-square tests to investigate whether the immune-related lncRNA signature could better predict KIPC clinicopathological features. The heat map (**Figure 2A**) showed that there were significant differences between high- and low-risk groups in gender ($P < 0.01$), grade ($P < 0.01$), AJCC stage ($P < 0.01$), M stage ($P < 0.01$), T stage ($P < 0.01$), and survival state ($P < 0.01$). The present study further explored the relationship between the risk score and each clinicopathological characteristic, including grade (**Figure 2B**), AJCC stage (**Figure 2C**), T stage (**Figure 2D**), and M stage (**Figure 2E**). As expected, we discovered that high-grade and advanced-stage tumors were significantly associated with the high-risk group, and low-grade and early stages were related with the low-risk group (**Figure 2**). The results show the immune-related lncRNA signature may serve a pivotal role in oncogenesis and tumor progression of KIRC.

To demonstrate the widespread utility of the signature, we further carried out the stratification analysis using the following clinical variables: age (<60 and ≥60), gender (female and male), tumor grade (G1-2 and G3-4), AJCC stage (I & II and III & IV), T stage (T1-2 and T3-4), and M stage (M0 and M1). Importantly, as we show in **Figure 3**, survival analysis indicates that the signature has predictive significance for all hierarchical cohorts. The low-risk group patients had significantly better survival compared to high-risk group patients for each subgroup. In sum, these results testify that the five-lncRNA prognostic risk signature might exert critical roles in determining the prognosis of KIRC patients.

Finally, we compared the correlation between the expression level of a single lncRNA in the signature and clinical variables to deeply explore the impact of target lncRNAs on KIRC. In terms of age alone, there was no significant difference in the distribution of expression levels of all five lncRNAs (**Figure 4A**). The same results were found for gender (**Figure 4B**). As for different KIRC grades, AC243960.1 and LINC02084 were increased with tumor grade, and AC093278.2 and AC108449.2 were decreased. No significantly different in the expression values of AC008105.3 was detected between different tumor grades (**Figure 4C**). All five immune-related lncRNAs are considered to exert their effects in AJCC stag (**Figure 4D**), T stage (**Figure 4E**), and M stage (**Figure 4F**) to a certain degree. In general, the expression levels

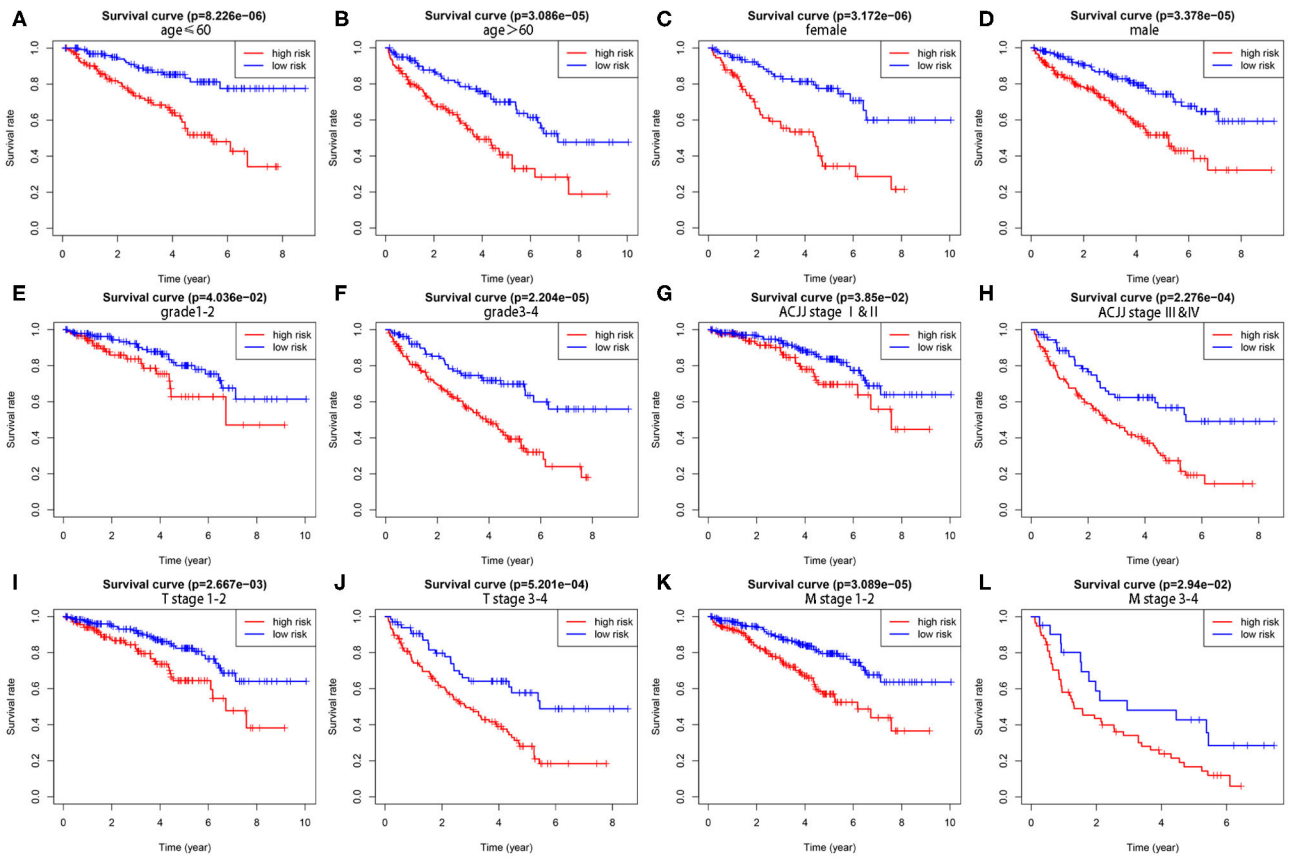

FIGURE 3 | The survival differences between high- and low-risk KIRP patients stratified by clinical factors. **(A,B)** The difference in OS stratified by age (age ≤ 60, age > 60) between two groups. **(C,D)** The difference in OS stratified by gender (male, female) between two groups. **(E,F)** The difference in OS stratified by grade (G1-2, G3-4) between two groups. **(G,H)** The difference in OS stratified by AJCC stage (Stage I/II, Stage III/IV) between two groups. **(I,J)** The difference in OS stratified by T stage (T1-2, T3-4) between two groups. **(K,L)** The difference in OS stratified by M stage (M0, M1) between two groups.

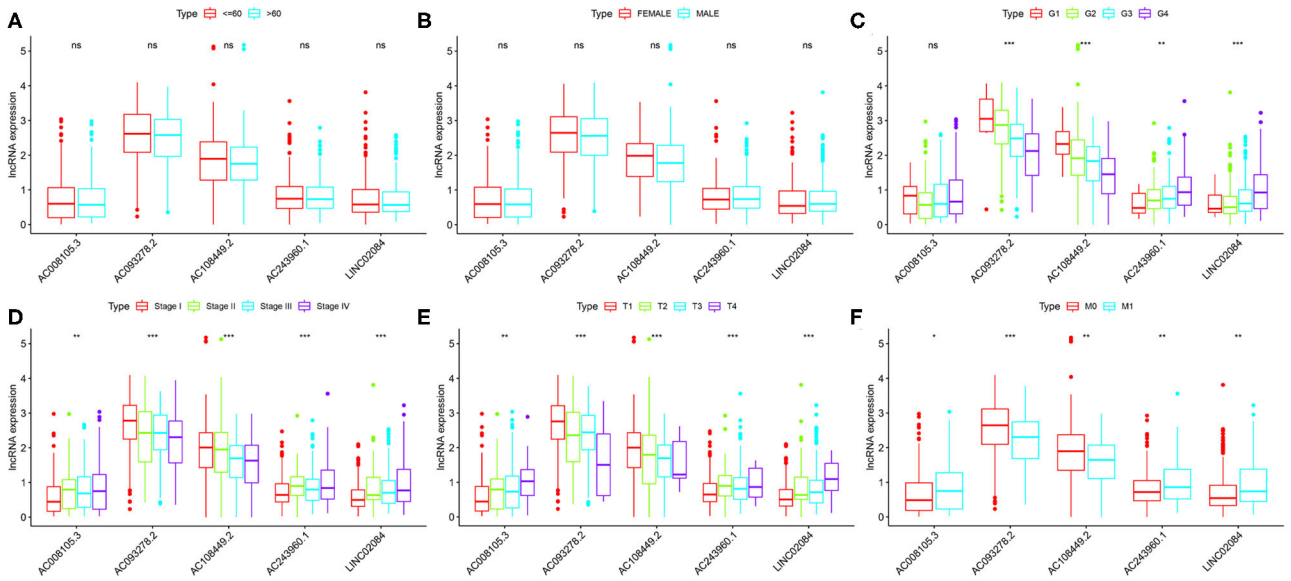

FIGURE 4 | Correlation between the expression level of a single lncRNA in the signature and clinical variables. **(A–F)** represent age, grade, grade, AJCC stage, T stage, and M stage, respectively. NS, not significant. *$P < 0.05$, **$P < 0.01$, and ***$P < 0.001$.

of AC008105.3, AC243960.1, and LINC02084 were positively correlated with tumor staging, and AC093278.2 and AC108449.2 were negatively correlated with tumor staging, which was consistent with the above study.

Somatic Mutations in Different Subgroups Based on Immune-Related lncRNA Signature

Further, the somatic mutation profiles of 336 KIRC patients were utilized to explore common somatic mutations in high- and low-risk group patients. Among these patients, 134 (39.88%) belonged to the high-risk group, 178 (52.98%) belonged to the low-risk group, and the remaining 24 (7.14%) were excluded based on the above exclusion criteria. Mutation data were analyzed and visualized using the "maftools" package. Mutation information for each gene in each sample of the high- and low-risk groups were demonstrated by waterfall plots (**Figures 5A,B**), and we found that the top 10 mutated genes in the high-risk group were VHL, PBRM1, TTN, BAP1, SETD2, MTOR, KDM5C, DNAH9, FLG, and PRKDC, and in the low-risk group were VHL, PBRM1, TTN, SETD2, ATM, BAP1, ARID1A, MTOR, MUC16, and ANK3. Interestingly, TP53 was one of the most common mutated genes in cancer, occurring more frequently in the high- than in the low-risk group. In addition, mutations were further sorted based on the different classifications in detail, and missense mutations are the biggest fraction among these mutations in both groups (**Figures 5C,D**). The most frequently mutation type in both groups was single nucleotide polymorphism (SNP) (**Figures 5E,F**), and C > T transversion accounted for the most common of single nucleotide variants (**Figures 5G,H**). Gene cloud plots showed the mutated frequencies of other genes (**Figures 5I,J**).

lncRNA-mRNA Co-expression Network Analysis

Considering that lncRNA and miRNA can affect the development of tumors through mutual regulation, the lncRNA-mRNA co-expression relationship network was constructed using Cytoscape software. As shown in **Figure 6A**, we found that these five target lncRNAs had obvious correlation with 44 mRNAs ($|R| > 0.6$ and $P < 0.05$). A Sankey diagram was depicted to visualize the co-occurrences of lncRNAs, mRNAs, and factors (**Figure 6B**). Results suggest that AC243960.1 and LINC02084 may be the major components among lncRNAs, as are CTLA4, ZAP70, NLRC3, and MAP4K1 in mRNAs. In addition, 72 significantly co-expressed lncRNA-mRNA pairs were identified as relevant. And among them all, MAP4K1, involved in regulation of the mitogen-activated protein kinase (MAPK) signaling pathway, was the closest correlation with AC243960.1. According to the KEGG analysis for mRNAs co-expressed with five lncRNAs, as expected, we observed that the majority of the enriched pathways manifested the immunomodulatory functions, and the top five significantly enriched pathways involved in cytokine–cytokine receptor interaction, PD–L1 expression, and PD−1 checkpoint pathway in cancer, Th1 and Th2 cell differentiation, viral protein interaction, with cytokine and cytokine receptor as well as T cell receptor signaling pathway (**Figure 6C**).

Analysis of Immune Status Between Low- and High-Risk Groups

We performed principal component analysis (PCA) to further assay the distinct distribution between high- and low-risk groups using the immune-related lncRNA set and whole gene expression profiles. As a result, the samples tended to be

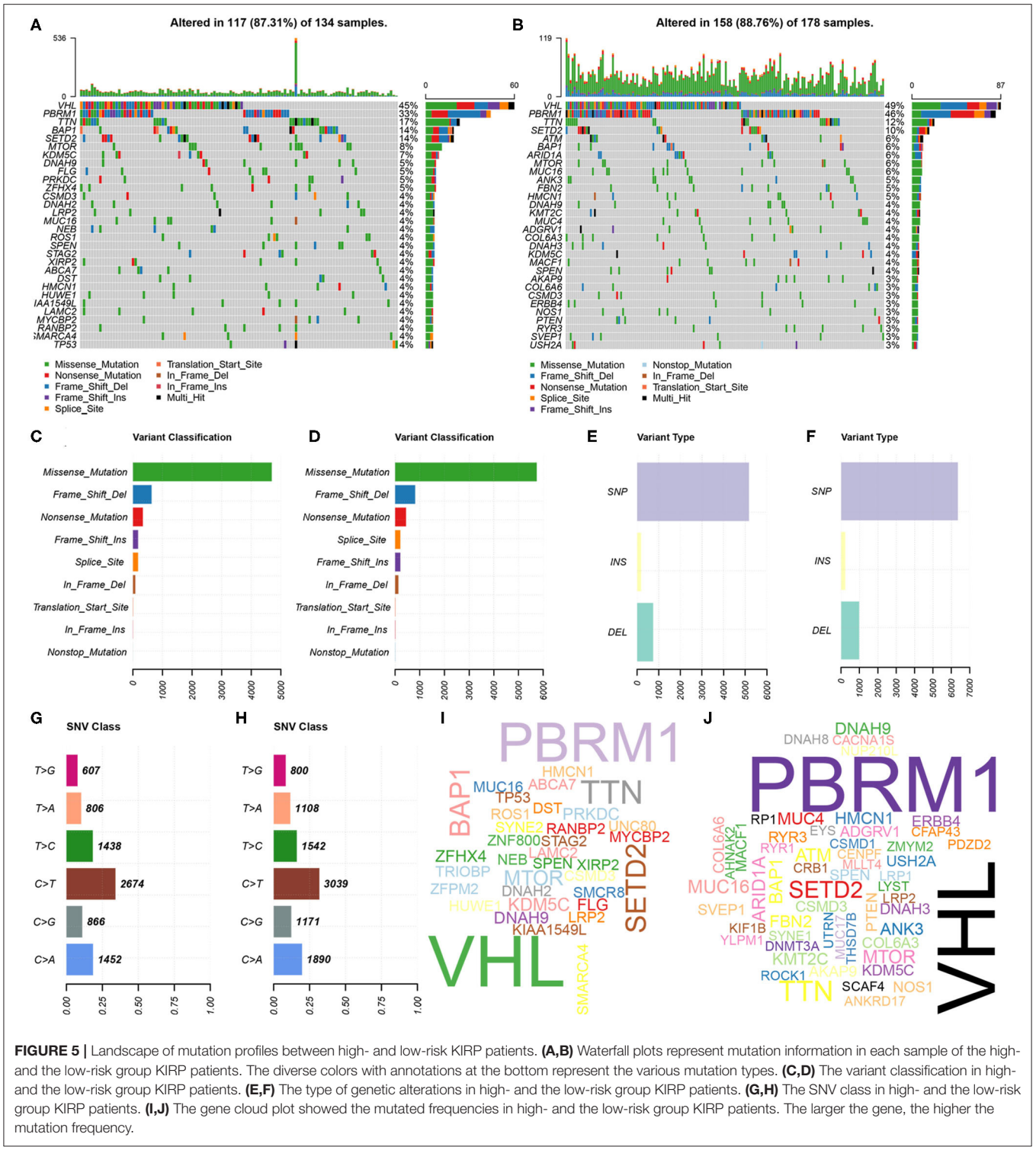

FIGURE 5 | Landscape of mutation profiles between high- and low-risk KIRP patients. **(A,B)** Waterfall plots represent mutation information in each sample of the high- and the low-risk group KIRP patients. The diverse colors with annotations at the bottom represent the various mutation types. **(C,D)** The variant classification in high- and the low-risk group KIRP patients. **(E,F)** The type of genetic alterations in high- and the low-risk group KIRP patients. **(G,H)** The SNV class in high- and the low-risk group KIRP patients. **(I,J)** The gene cloud plot showed the mutated frequencies in high- and the low-risk group KIRP patients. The larger the gene, the higher the mutation frequency.

sorted into two sections, and the immune status of KIRC patients in the high-risk group was significantly different from those in the low-risk group according to immune-related lncRNAs sets (**Figures 7A,B**). However, there was no significant separation in the immune status of each group when PCA was done based on the genome-wide expression profiles (**Figure 7C**).

Furthermore, GSEA analysis was performed, and the results exhibited that both IMMUNE_RESPONSE (**Figure 7D**) and IMMUNE_SYSTEM_PROCESS (**Figure 7E**) were enriched in

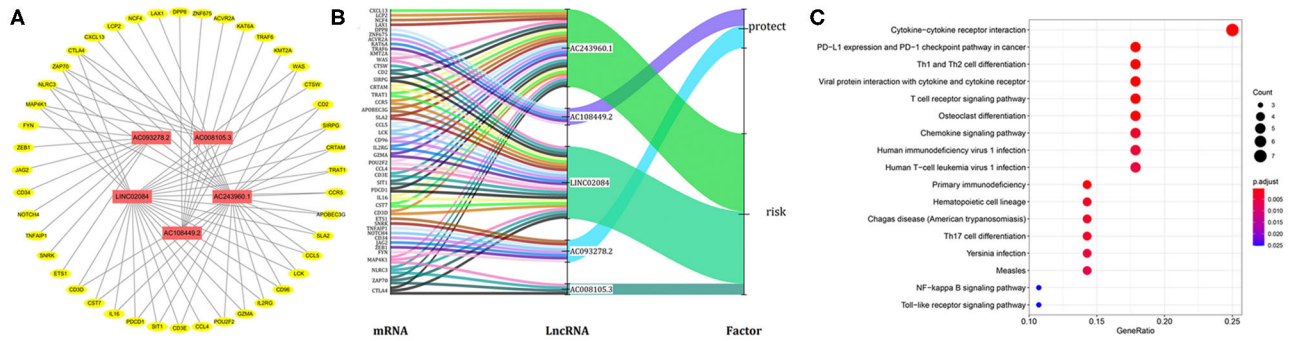

FIGURE 6 | Functional annotation analysis of the five-immune-related lncRNAs prognostic signature according to co-expressed lncRNA-mRNA. **(A)** The lncRNA-mRNA co-expression regulatory network based on five immune-related lncRNAs and their highly related genes ($|R| > 0.6$, $P < 0.05$). **(B)** A Sankey diagram was depicted to visualize the co-occurrences of lncRNAs, mRNAs, and factors. **(C)** Results for KEGG enrichment analysis of the mRNAs co-expressed with five lncRNAs.

the high-risk group compared with the low-risk group. For the present study, we also used C7 collection sets (IMMUNOLOGIC_SIGNATURE) for GSEA analysis to further analyze differentially expressed genes. We observed that a total of 4,281 gene sets were significantly enriched (cutoff FDR < 0.25 and NOM $P < 0.05$). Among them, 709 and 3,572 gene sets were significantly enriched in the high- and low-risk groups, respectively. The five most significant gene sets in the high- and low-risk groups are shown in **Figure 7F**.

Besides this, to further explore immune cell infiltration between the low- and high-risk groups, we calculated stromal score, immune score, ESTIMATE score, and tumor purity according to the ESTIMATE algorithm. The high-risk group had lower stromal score and tumor purity but higher immune score and ESTIMATE score compared with the low-risk group (**Figure 7G**). In a word, a five-lncRNA prognostic risk signature was closely related to the immune status of KIRC patients, and the different immune status was showed between the low- and high-risk groups.

Validation of the Expression Levels of Those Five lncRNAs Between Tumor and Normal Samples

Additionally, to further verify our analysis, the expression levels of five lncRNAs were assessed in 539 KIRC tumor tissues and 72 non-tumor tissues in the TCGA data set. The mean expression levels of AC008105.3, LINC02084, and AC243960.1 in KIRC samples were significantly lower, nd AC108449.2 was significantly higher than that in non-tumor tissues (**Figures 8A,B**), which were consistent with our analysis findings. The results proved the reliability of our analysis. However, it was interesting that AC093278.2 was considered to be a protective factor on the above analysis but was represented significantly higher in KIRC samples than in non-tumor liver samples. This may be because AC093278.2 could exert various functions at different stages of KIRC tumorigenesis and development.

DISCUSSION

Although the efficacy of surgical resection had been proven to be central to the cure for localized RCC and achieved high cure rates, the treatment outcome for advanced and metastatic RCC remains unsatisfactory (24). For some KIRC patients with similar clinical risk factors, their responses to treatment and prognosis are different due to molecular heterogeneity (25). Thus, in addition to traditional clinical risk factors, identifying additional molecular prognostic indicators is imperative. Previous research has reached a consensus that the immune system plays complex and extensive roles in both the positive and negative regulation of tumor development and progression (26). Correspondingly, lncRNAs are emerging as critical regulators of gene expression in the immune system (17). It is worth noting that immune-related lncRNAs may be more highly expressed in immune cells and are significantly correlated with immune cell infiltration (14).

In the current study, 332 immunoregulatory genes were obtained from two immune-related pathways for further subsequent analysis. One of the major findings in our study was that we constructed a five immune-related lncRNA signature and verified its reliability and stability through a time-dependent ROC curve. In addition, we observed that KIRC samples with a good or poor prognosis could be distinguished based on the signature generated by these lncRNAs. Univariate and multivariate Cox regression analyses demonstrated that the signature was an independent prognostic predictor for OS in KIRC patients. We further investigated stratified survival analysis for different clinicopathological parameters to verify wide applicability of the signature and discovered that the signature could also divide KIRC samples into high-risk groups with shorter OS and low-risk groups with longer OS in different subgroups. Additionally, we compared correlation between the expression level of a single lncRNA in the signature and clinical variables and confirmed that, among these lncRNAs, AC008105.3, LINC02084, and AC243960.1 were risk-associated genes, and AC093278.2 and AC108449.2 were regarded as

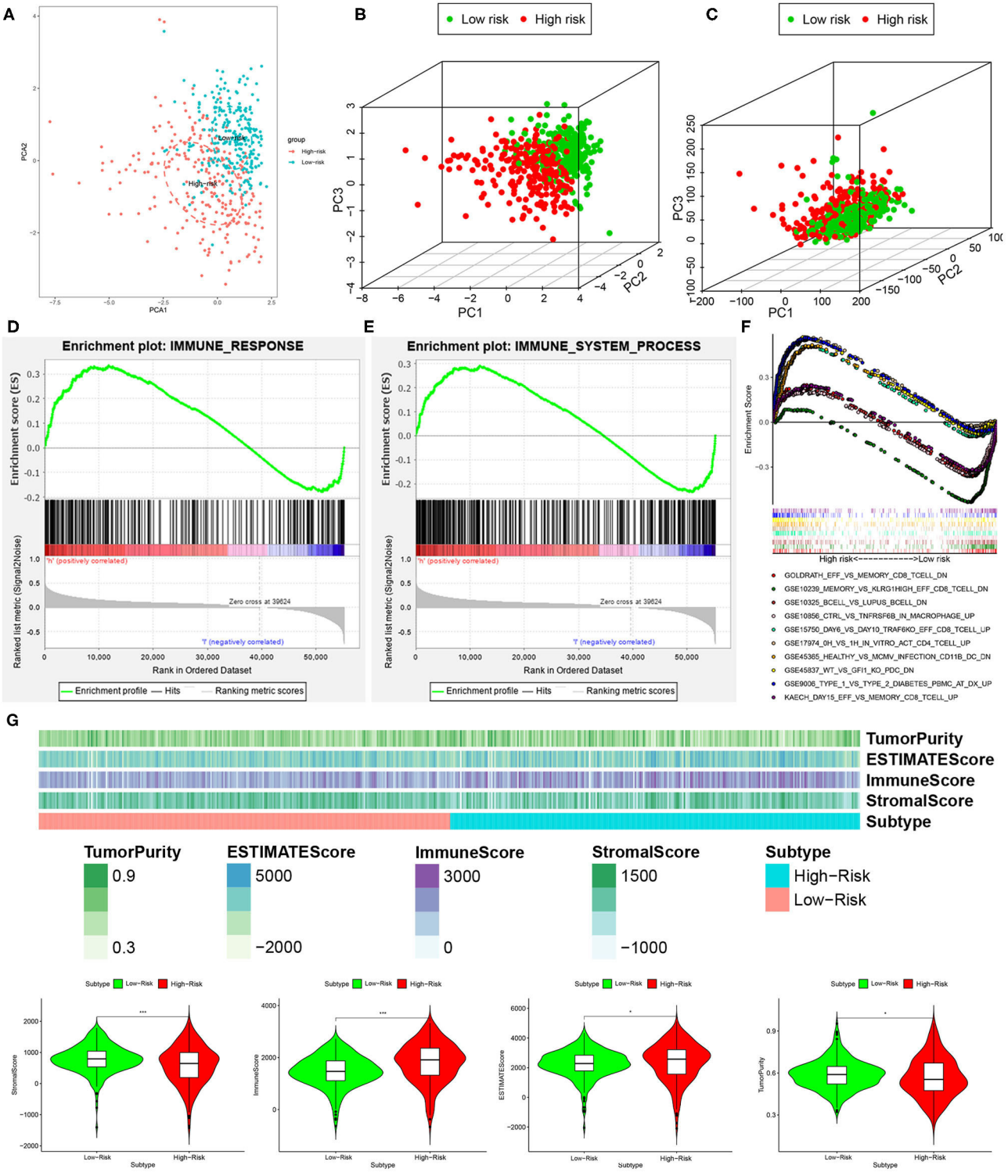

FIGURE 7 | High- and low-risk groups showed different immune status. **(A,B)** Principal component analysis for immune-related lncRNAs sets between the high- and low-risk groups, showing a remarkable difference between two patterns. **(C)** Principal component analysis for genome-wide expression profiles between high- and low-risk groups, no significant separation in the immune status between two patterns. GSEA analysis exhibited that both IMMUNE_RESPONSE **(D)** and IMMUNE_SYSTEM_PROCESS **(E)** were enriched in the high- compared with low-risk group. **(F)** The five most significant gene sets in C7 collection sets (IMMUNOLOGIC_SIGNATURE) between two groups. **(G)** The high-risk group had a lower stromal score and tumor purity but higher immune score and Estimate score compared with the low-risk group. $^{*}P < 0.05$ and $^{***}P < 0.001$.

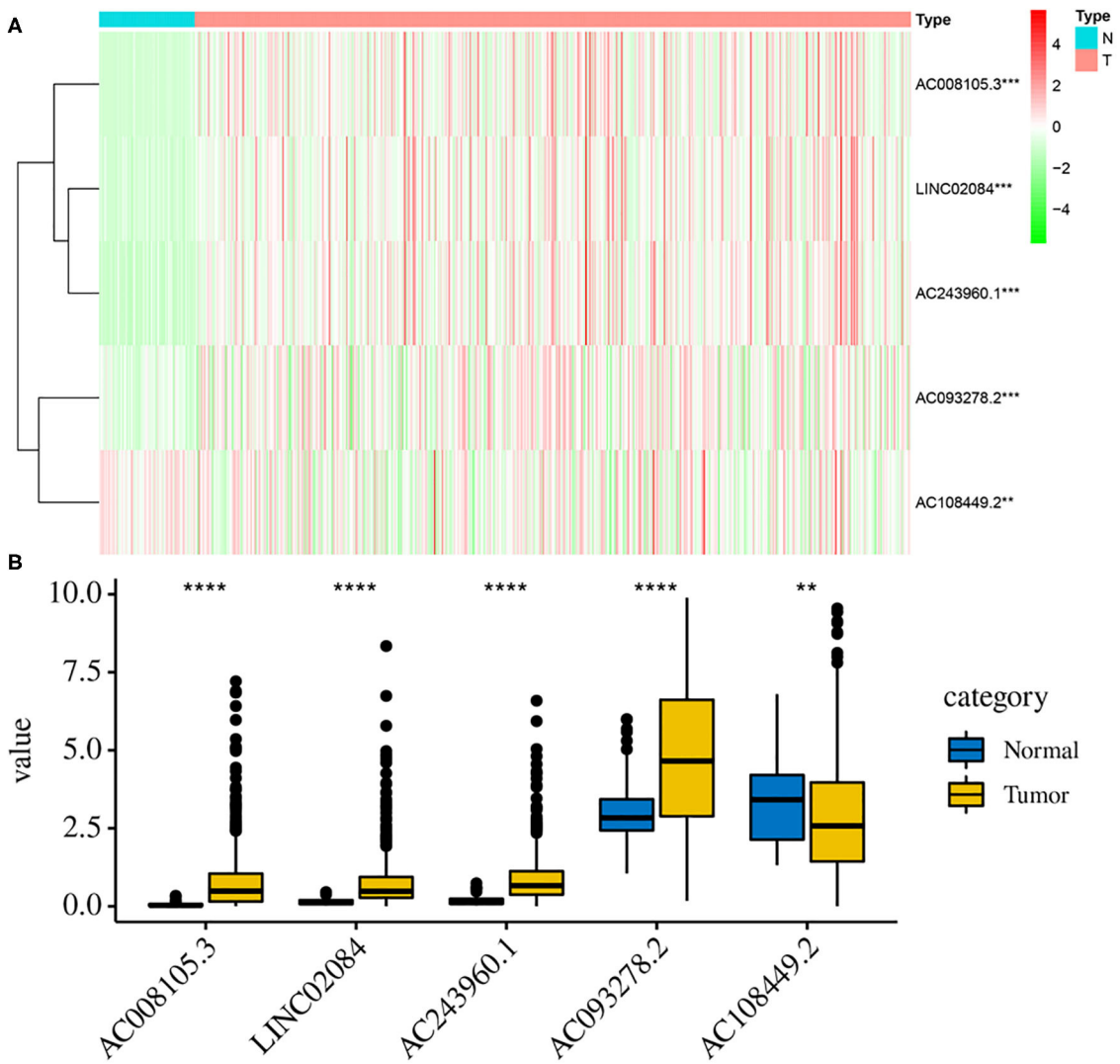

FIGURE 8 | Validation the expression levels of those 5 lncRNAs between tumor and normal samples. The heat map **(A)** and bar graph **(B)** showed the expression levels of 5 lncRNAs between 539 KIRC tumor tissues and 72 non-tumor tissues in the TCGA data set. The mean expression levels of AC008105.3, LINC02084, AC243960.1, and AC093278.2 in KIRC samples were significantly lower while AC108449.2 was significantly higher than that in non-tumor tissues. $^{**}P < 0.01$, $^{***}P < 0.001$, and $^{****}P < 0.0001$.

protective genes. PCA suggested that the five immune-related lncRNA set drew a clear distinction between high- and low-risk groups based on the immune-related lncRNAs compared with whole gene expression profiles. Furthermore, GSEA analysis was performed, and the results exhibited differentially expressed genes between the high- and low-risk groups. These findings indicate the value of the five immune-related lncRNAs signature for KIRC patients' prognosis and may be beneficial for clinicians to more precisely identify patients with high-risk scores, develop novel therapeutic strategies, and further potentially improve patient prognosis.

Undoubtedly, lncRNAs may contribute to the development of different tumors (including KIRC) via diverse mechanisms. Previous studies have reported that elevated expression of MRCCAT1, ATB, and SNHG14 in KIRC were correlated with poor prognosis, and this is also the case for low expression of OTUD6B-AS1 and ADAMTS9-AS2. More specifically, lncRNA MRCCAT1 promotes metastasis of KIRC via inhibiting NPR3 and activating p38-MAPK signaling (27). Song et al. implied high expression of lncRNA ATB could accelerate the proliferative and migratory rates of RCC cells and inhibit cell apoptosis through downregulating p53 via binding to DNMT1 (28). Another study revealed that SNHG14 is a critical lncRNA that promotes KIRC migration and invasion via sponging miR-203 and elevating N-WASP (29). On the other hand, Wang et al. demonstrated that the antioncogenic effect of OTUD6B-AS1 is partly mediated through the inhibition of the activity of the Wnt/β-catenin pathway and the EMT-related pathway (30). As reported previously, lncRNA ADAMTS9-AS2 inhibits the progression and impairs the chemoresistance of KIRC via

miR-27a-3p-mediated regulation of FOXO1 (31). Despite some progress achieved in the field of lncRNA research, the functions of most lncRNAs still remain elusive, and the detailed molecular mechanism requires further investigation.

Recently, immunotherapy has gained more attention as a new paradigm in cancer treatment (32). In this article, the lncRNA-mRNA co-expression relationship network was further analyzed to dig deeper into the function of related lncRNAs, which is of great significance for innovation of immunotherapy strategies. The GSEA analysis was performed, and the results exhibited that both IMMUNE_RESPONSE and IMMUNE_SYSTEM_PROCESS were enriched in high-risk groups. Additionally, C7 collection sets (IMMUNOLOGIC_SIGNATURE) were used to further analyze differentially expressed genes and verify the effectiveness of the signature. It has been shown that immune infiltration was closely associated with the therapeutic responsiveness and prognosis of KIRC patients (33). Therefore, the five immune-related lncRNAs may serve as potential immunotherapy targets of KIRC.

Given that immunotherapy is emerging as a promising approach for cancer treatment, our studies have the advantage of comprehensive analysis of high-throughput sequencing data and construction of the immune-related lncRNA signature with predicting prognosis. These results and conclusions could provide significant clues for thorough dissection of lncRNAs in future experimental work. Nevertheless, several limitations of this pilot study should be acknowledged. The differences between normal and tumor samples that are visible to the immune system is essential for cancer immunotherapy and should be further analyzed. In addition, the construction and evaluation of the model depended on the public database, which requires additional experimental (for example, immunohistochemistry, PCR, and flow cytometry) and clinical data to verify our results. More research should also focus on the detailed relationship between the expression level of immune-related lncRNA and the immunophenotype.

In conclusion, we here systematically identified a five immune-related lncRNA signature, which may be beneficial for clinicians to more precisely identify patients with high-risk and further potentially improve prognosis of KIRC patients. In addition, the signature may serve as potential immunotherapy targets for the research of the molecular mechanisms.

DATA AVAILABILITY STATEMENT

Publicly available datasets were analyzed in this study. This data can be found here: the TCGA database (https://cancergenome.nih.gov/) and the Molecular Signatures Database v7.1 (MSigDB, https://www.gsea-msigdb.org/gsea/index.jsp).

ETHICS STATEMENT

Ethical review and approval was not required for the study on human participants in accordance with the local legislation and institutional requirements. Written informed consent for participation was not required for this study in accordance with the national legislation and the institutional requirements.

AUTHOR CONTRIBUTIONS

ZS was responsible for study design, data acquisition, and analysis and was a major contributor to writing the manuscript. CJ was responsible for the bioinformatics analysis and the statistical analysis. CX was responsible for the figures and tables. TL was responsible for the integrity of the entire study and manuscript review. All authors read and approved the final manuscript.

REFERENCES

1. Ljungberg B, Bensalah K, Canfield S, Dabestani S, Hofmann F, Hora M, et al. EAU guidelines on renal cell carcinoma: 2014 update. *Eur Urol*. (2015) 67:913–24. doi: 10.1016/j.eururo.2015.01.005
2. Siegel RL, Miller KD, Jemal A. Cancer statistics, 2017. *CA Cancer J Clin*. (2017) 67:7–30. doi: 10.3322/caac.21387
3. Gupta K, Miller JD, Li JZ, Russell MW, Charbonneau C. Epidemiologic and socioeconomic burden of metastatic renal cell carcinoma (mRCC): a literature review. *Cancer Treat Rev*. (2008) 34:193–205. doi: 10.1016/j.ctrv.2007.12.001
4. Lu J, Zhu L, Zheng LP, Cui Q, Zhu HH, Zhao H, et al. Overexpression of ULK1 represents a potential diagnostic marker for clear cell renal carcinoma and the antitumor effects of SBI-0206965. *EBioMedicine*. (2018) 34:85–93. doi: 10.1016/j.ebiom.2018.07.034
5. De Mulder PH, van Herpen CM, Mulders PA. Current treatment of renal cell carcinoma. *Ann Oncol*. (2004) 15(Suppl. 4):iv319–28. doi: 10.1093/annonc/mdh946
6. Obara W, Kanehira M, Katagiri T, Kato R, Kato Y, Takata R. Present status and future perspective of peptide-based vaccine therapy for urological cancer. *Cancer Sci*. (2018) 109:550–9. doi: 10.1111/cas.13506
7. Guttman M, Rinn JL. Modular regulatory principles of large non-coding RNAs. *Nature*. (2012) 482:339–46. doi: 10.1038/nature10887
8. Gutschner T, Diederichs S. The hallmarks of cancer: a long non-coding RNA point of view. *RNA Biol*. (2012) 9:703–19. doi: 10.4161/rna.20481
9. Fatica A, Bozzoni I. Long non-coding RNAs: new players in cell differentiation and development. *Nat Rev Genet*. (2014) 15:7–21. doi: 10.1038/nrg3606
10. Han CL, Ge M, Liu YP, Zhao XM, Wang KL, Chen N, et al. Long non-coding RNA H19 contributes to apoptosis of hippocampal neurons by inhibiting let-7b in a rat model of temporal lobe epilepsy. *Cell Death Dis*. (2018) 9:617. doi: 10.1038/s41419-018-0496-y
11. Lin YH, Wu MH, Yeh CT, Lin KH. Long non-coding RNAs as mediators of tumor microenvironment and liver cancer cell communication. *Int J Mol Sci*. (2018) 19:3742. doi: 10.3390/ijms19123742
12. Dykes IM, Emanueli C. Transcriptional and post-transcriptional gene regulation by long non-coding RNA. *Genomics Proteomics Bioinformatics*. (2017) 15:177–86. doi: 10.1016/j.gpb.2016.12.005
13. Bhan A, Soleimani M, Mandal SS. Long noncoding RNA and cancer: a new paradigm. *Cancer Res*. (2017) 77:3965–81. doi: 10.1158/0008-5472.can-16-2634
14. Li Y, Jiang T, Zhou W, Li J, Li X, Wang Q, et al. Pan-cancer characterization of immune-related lncRNAs identifies potential oncogenic biomarkers. *Nat Commun*. (2020) 11:1000. doi: 10.1038/s41467-020-14802-2
15. Atianand MK, Fitzgerald KA. Long non-coding RNAs and control of gene expression in the immune system. *Trends Mol Med*. (2014) 20:623–31. doi: 10.1016/j.molmed.2014.09.002
16. Chen YG, Satpathy AT, Chang HY. Gene regulation in the immune system by long noncoding RNAs. *Nat Immunol*. (2017) 18:962–72. doi: 10.1038/ni.3771

17. Pei X, Wang X, Li H. LncRNA SNHG1 regulates the differentiation of Treg cells and affects the immune escape of breast cancer via regulating miR-448/IDO. *Int J Biol Macromol*. (2018) 118:24–30. doi: 10.1016/j.ijbiomac.2018.06.033
18. Huang D, Chen J, Yang L, Ouyang Q, Li J, Lao L, et al. NKILA lncRNA promotes tumor immune evasion by sensitizing T cells to activation-induced cell death. *Nat Immunol*. (2018) 19:1112–25. doi: 10.1038/s41590-018-0207-y
19. Hu Q, Ye Y, Chan LC, Li Y, Liang K, Lin A, et al. Oncogenic lncRNA downregulates cancer cell antigen presentation and intrinsic tumor suppression. *Nat Immunol*. (2019) 20:835–51. doi: 10.1038/s41590-019-0400-7
20. Miller JF, Sadelain M. The journey from discoveries in fundamental immunology to cancer immunotherapy. *Cancer Cell*. (2015) 27:439–49. doi: 10.1016/j.ccell.2015.03.007
21. Derrien T, Johnson R, Bussotti G, Tanzer A, Djebali S, Tilgner H, et al. The GENCODE v7 catalog of human long noncoding RNAs: analysis of their gene structure, evolution, and expression. *Genome Res*. (2012) 22:1775–89. doi: 10.1101/gr.132159.111
22. Mayakonda A, Lin DC, Assenov Y, Plass C, Koeffler HP. Maftools: efficient and comprehensive analysis of somatic variants in cancer. *Genome Res*. (2018) 28:1747–56. doi: 10.1101/gr.239244.118
23. Wang W, Zhao Z, Yang F, Wang H, Wu F, Liang T, et al. An immune-related lncRNA signature for patients with anaplastic gliomas. *J Neuro Oncol*. (2018) 136:263–71. doi: 10.1007/s11060-017-2667-6
24. MacLennan S, Imamura M, Lapitan MC, Omar MI, Lam TB, Hilvano-Cabungcal AM, et al. Systematic review of perioperative and quality-of-life outcomes following surgical management of localised renal cancer. *Eur Urol*. (2012) 62:1097–117. doi: 10.1016/j.eururo.2012.07.028
25. Signoretti S, Flaifel A, Chen YB, Reuter VE. Renal cell carcinoma in the era of precision medicine: from molecular pathology to tissue-based biomarkers. *J Clin Oncol*. (2018) 36:Jco2018792259. doi: 10.1200/jco.2018.79.2259
26. Kaufmann SHE. Immunology's coming of age. *Front Immunol*. (2019) 10:684. doi: 10.3389/fimmu.2019.00684
27. Li JK, Chen C, Liu JY, Shi JZ, Liu SP, Liu B, et al. Long noncoding RNA MRCCAT1 promotes metastasis of clear cell renal cell carcinoma via inhibiting NPR3 and activating p38-MAPK signaling. *Mol Cancer*. (2017) 16:111. doi: 10.1186/s12943-017-0681-0
28. Song C, Xiong Y, Liao W, Meng L, Yang S. Long noncoding RNA ATB participates in the development of renal cell carcinoma by downregulating p53 via binding to DNMT1. *J Cell Physiol*. (2019) 234:12910–7. doi: 10.1002/jcp.27957
29. Liu G, Ye Z, Zhao X, Ji Z. SP1-induced up-regulation of lncRNA SNHG14 as a ceRNA promotes migration and invasion of clear cell renal cell carcinoma by regulating N-WASP. *Am J Cancer Res*. (2017) 7:2515–25.
30. Wang G, Zhang ZJ, Jian WG, Liu PH, Xue W, Wang TD, et al. Novel long noncoding RNA OTUD6B-AS1 indicates poor prognosis and inhibits clear cell renal cell carcinoma proliferation via the Wnt/β-catenin signaling pathway. *Mol Cancer*. (2019) 18:15. doi: 10.1186/s12943-019-0942-1
31. Song EL, Xing L, Wang L, Song WT, Li DB, Wang Y, et al. LncRNA ADAMTS9-AS2 inhibits cell proliferation and decreases chemoresistance in clear cell renal cell carcinoma via the miR-27a-3p/FOXO1 axis. *Aging*. (2019) 11:5705-25. doi: 10.18632/aging.102154
32. Kelly PN. The cancer immunotherapy revolution. *Science*. (2018) 359:1344–5. doi: 10.1126/science.359.6382.1344
33. Senbabaoglu Y, Gejman RS, Winer AG, Liu M, Van Allen EM, de Velasco G, et al. Tumor immune microenvironment characterization in clear cell renal cell carcinoma identifies prognostic and immunotherapeutically relevant messenger RNA signatures. *Genome Biol*. (2016) 17:231. doi: 10.1186/s13059-016-1092-z

Conflict of Interest: The authors declare that the research was conducted in the absence of any commercial or financial relationships that could be construed as a potential conflict of interest.

frontiers in Oncology

ORIGINAL RESEARCH
published: 02 September 2020
doi: 10.3389/fonc.2020.01770

Identification of Immune-Related Cells and Genes in Tumor Microenvironment of Clear Cell Renal Cell Carcinoma

Bowen Du†, Yulin Zhou†, Xiaoming Yi, Tangliang Zhao, Chaopeng Tang, Tianyi Shen, Kai Zhou, Huixian Wei, Song Xu, Jie Dong*, Le Qu*, Haowei He* and Wenquan Zhou**

Department of Urology, Jinling Hospital, Medical School, Nanjing University, Nanjing, China

Clear cell renal cell carcinoma (ccRCC) is one of the most common tumors in the urinary system. Progression in immunotherapy has provided novel options for the ccRCC treatment. However, the understanding of the ccRCC microenvironment and the potential therapeutic targets in the microenvironment is still unclear. Here, we analyzed the gene expression profile of ccRCC tumors from the Cancer Genome Atlas (TCGA) and calculated the abundance ratios of immune cells for each sample. Then, seven types of immune cells were found to be correlated to overall survival, and 3863 immune-related genes were identified by analyzing differentially expressed genes. We also found that the function of immune-related genes was mainly focused on ligand-receptor binding and signaling pathway transductions. Additionally, we identified 13 hub genes by analyzing the protein-protein interaction network, and seven of them are related to overall survival. Our study not only expands the understanding of fundamental biological features of microenvironment but also provides potential therapeutic targets.

Keywords: ccRCC, tumor microenvironment, immunotherapy, TCGA, hub gene

OPEN ACCESS

Edited by:
Viktor Grünwald,
Essen University Hospital, Germany

Reviewed by:
Jan Hinrich Bräsen,
Hannover Medical School, Germany
Henning Reis,
Essen University Hospital, Germany

****Correspondence:***
Song Xu
songxu1963@gmail.com
Jie Dong
smiledongjie@163.com
Le Qu
septsoul@hotmail.com
Haowei He
hohowell@163.com
Wenquan Zhou
shzwqzsl@163.com

† These authors have contributed equally to this work

Specialty section:
This article was submitted to Genitourinary Oncology, a section of the journal Frontiers in Oncology

Received: *01 May 2020*
Accepted: *07 August 2020*
Published: *02 September 2020*

Citation:
Du B, Zhou Y, Yi X, Zhao T, Tang C, Shen T, Zhou K, Wei H, Xu S, Dong J, Qu L, He H and Zhou W (2020) Identification of Immune-Related Cells and Genes in Tumor Microenvironment of Clear Cell Renal Cell Carcinoma. Front. Oncol. 10:1770. doi: 10.3389/fonc.2020.01770

INTRODUCTION

Kidney cancer is one of the most common cancer in the world (1). Renal cell carcinoma (RCC) accounts for 85–90% of kidney cancer, while clear cell renal cell carcinoma (ccRCC) accounts for about 70–75% of RCC (2–6). ccRCC is frequently characterized by the von Hippel Lindau (VHL) tumor suppressor gene lose or inactivation, which leads to the overexpression of the hypoxia-inducible factor-2α (HIF2α), vascular endothelial growth factor (VEGF), and their downstream kinases (7–9). Multiple tyrosine kinase inhibitors (TKIs) have been developed as novel therapies (10), but the 5-year overall survival rate for advanced ccRCC remains under 30% (11, 12). Thus, it is necessary to develop novel therapies for ccRCC treatment.

The tumor microenvironment has been increasingly studied in the field of cancer immunotherapy in recent years. The tumor microenvironment is the non-cancerous cells and molecules surrounding the tumor cells, which consist of immune cells, blood vessels, adipocytes, mesenchymal stem cells, cancer-associated fibroblasts, and extracellular matrix (13, 14). The tumor microenvironment significantly influences therapeutic response and clinical outcomes through

multiple signaling pathways (15). Thus, a better understanding of tumor microenvironment may help us develop novel therapies for ccRCC treatments.

To explore the immune microenvironment component in the ccRCC tumor and its interaction with the tumor cells, we first screened the survival-related immune cells in the ccRCC microenvironment. Then, we identified the immune-cell-specific genes by analyzing differentially expressed genes. To study the biological function of the immune-specific genes, we also enriched those genes in the Kyoto Encyclopedia of Genes and Genomes (KEGG), and Reactome pathways. Finally, we identified 13 hub genes by studying protein-protein interaction (PPI) networks and found seven genes correlated to overall survival. Our study not only revealed the biological features of the ccRCC microenvironment but also provided a novel view of ccRCC therapies.

MATERIALS AND METHODS

Samples and Data Process

We selected 530 ccRCC patients from the Cancer Genome Atlas (TCGA) dataset and excluded 11 patients owing to the incomplete clinical data. The raw count data were downloaded from the TCGA website[1]. The transcripts per million (TPM) values were calculated with R software as the mRNA level of each gene. The clinical data were downloaded from the cbioportal website[2] and summarized in **Table 1**.

[1]https://portal.gdc.cancer.gov

[2]http://www.cbioportal.org

TABLE 1 | Patient clinical characteristics of The Cancer Genome Atlas cohort.

	Case (No.)	Percent (%)
Gender		
Male	337	64.9
Female	182	35.1
Age		
Median	60	
Range	26–90	
Fuhrman grade		
G1	14	2.7
G2	225	43.4
G3	206	39.7
G4	74	14.3
Stage		
I	261	50.3
II	54	10.4
III	122	23.5
IV	82	15.8
T Stage		
pT1	267	51.4
pT2	66	12.7
pT3	175	33.7
pT4	11	2.1

Identification of Survival-Related Immune Cells

The abundance ratios of 22 types of immune cells were calculated with CIBERSORTx (16). The matrix of TPM values for all samples was uploaded to the CIBERSORTx website[3] as the Mixture file. The LM22 matrix within the software was selected as the Signature gene file. The software was run in relative mode. Batch correction and quantile normalization were not performed in this run. The permutations for significance analysis were set to 100. Then, the Kaplan–Meier analysis was performed to identify the survival-related immune cells with the Survival R package based on the abundance ratio of each cell type. The Log-Rank test was used to analyze the survival data, and the medians of the abundance ratios for cell types were as the cut-off values. The relationship between the abundance ratios of immune cells and the pathological grades and the clinical stages were analyzed with the one-way ANOVA test.

Identification of Immune-Related Genes

We identified the specific genes for each type of the survival-related immune cells by calculating the differentially expressed genes between the high- and low-immuno-infiltrated samples with the median of abundance ratios as the cut-off value. The differentially expressed genes were analyzed with the DEseq2 R package. The genes with $|\log_2(\text{foldchange})| > 1$ and p-value < 0.05 were considered as specific genes for that cell type. The results were visualized with the UpSetR R package.

Enrichment Analysis of Immune-Related Genes

The KEGG enrichment analysis was performed with the enrichKEGG function in the Clusterprofiler R package. The list of gene IDs was used as the input file. The Benjamini-Hochberg method was used to adjust the p-values. The cut-off of p-values was set to 0.05. The Reactome enrichment analysis was performed with the enrichPathway function in the ReactomePA R packages. The list of gene IDs was used as the input file. The parameters were set as follow: pAdjustMethod = "BH," pvalueCutoff = 0.05, minGSSize = 10, and maxGSSize = 500. The enrichment results were visualized with the ggplot2 R package.

Constriction of PPI Network and Identification of Hub Genes

The 933 immune-related protein-coding genes were imported into the STRING database[4]. The results with combined scores over 0.7 were kept and visualized with the Cytoscape software. To identify the hub genes, we clustered the genes within the PPI network with the MCODE plugin of the Cytoscape software using the following parameter: Degree Cutoff = 4, Node Score Cutoff = 0.3, K-core = 2, and Max. Depth = 100. The clusters containing over 40 proteins were used to extract hub genes. The hub genes were obtained with the CytoHubba plugin of the Cytoscape software.

[3]https://cibersortx.stanford.edu

[4]https://string-db.org

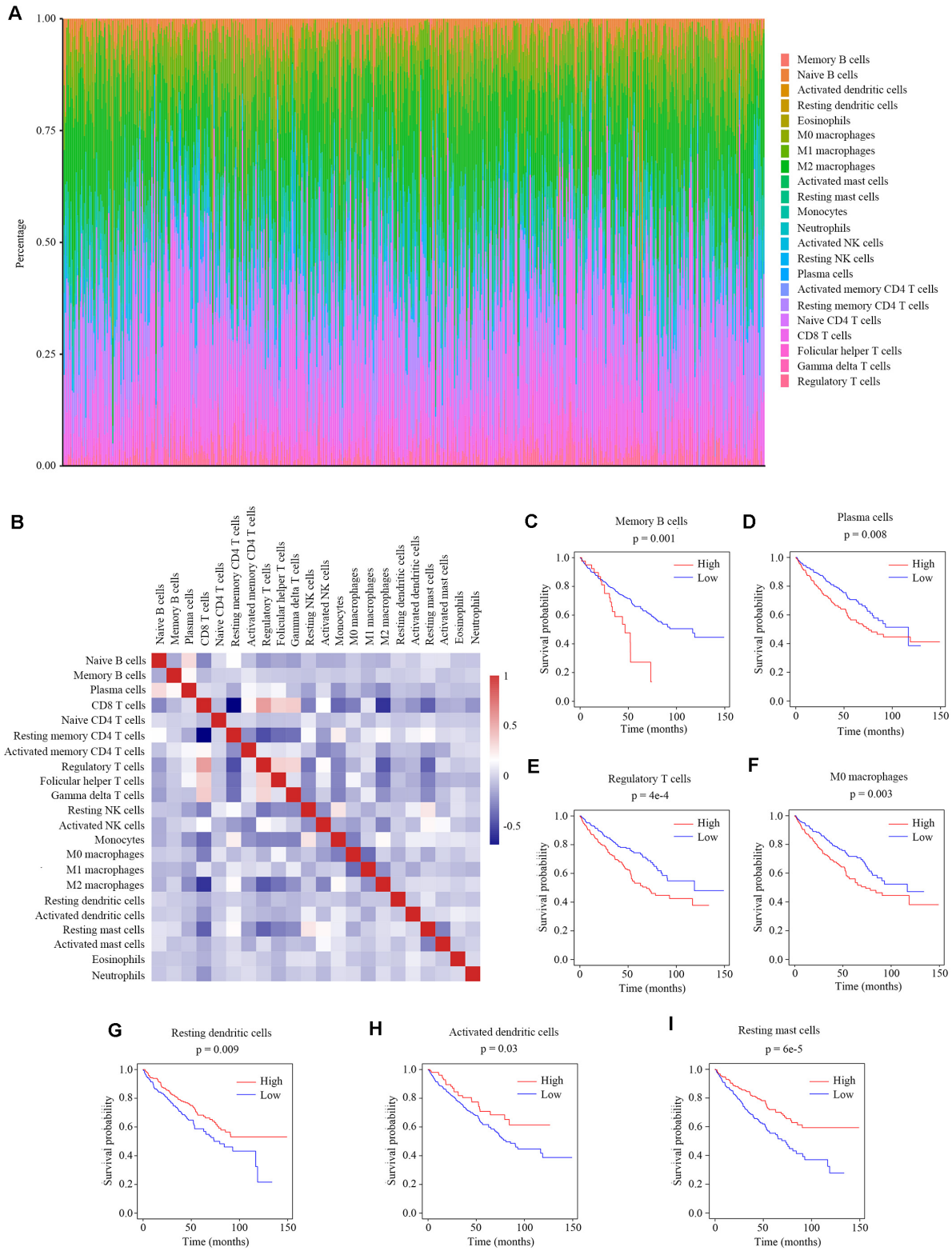

FIGURE 1 | The relationship between the abundance ratios of immune cells and overall survival. **(A)** The abundance ratios of immune cells in the ccRCC samples. Each column represents a sample, and the column height indicates the abundance ratios of the certain immune cells in that sample. **(B)** The correlation coefficient between the abundance ratios of distinct immune cells. **(C–I)** The survival analysis for the abundance ratios of memory B cells, plasma cells, regulatory T cells, M0 macrophages, resting dendritic cells, activated dendritic cells, and resting mast cells.

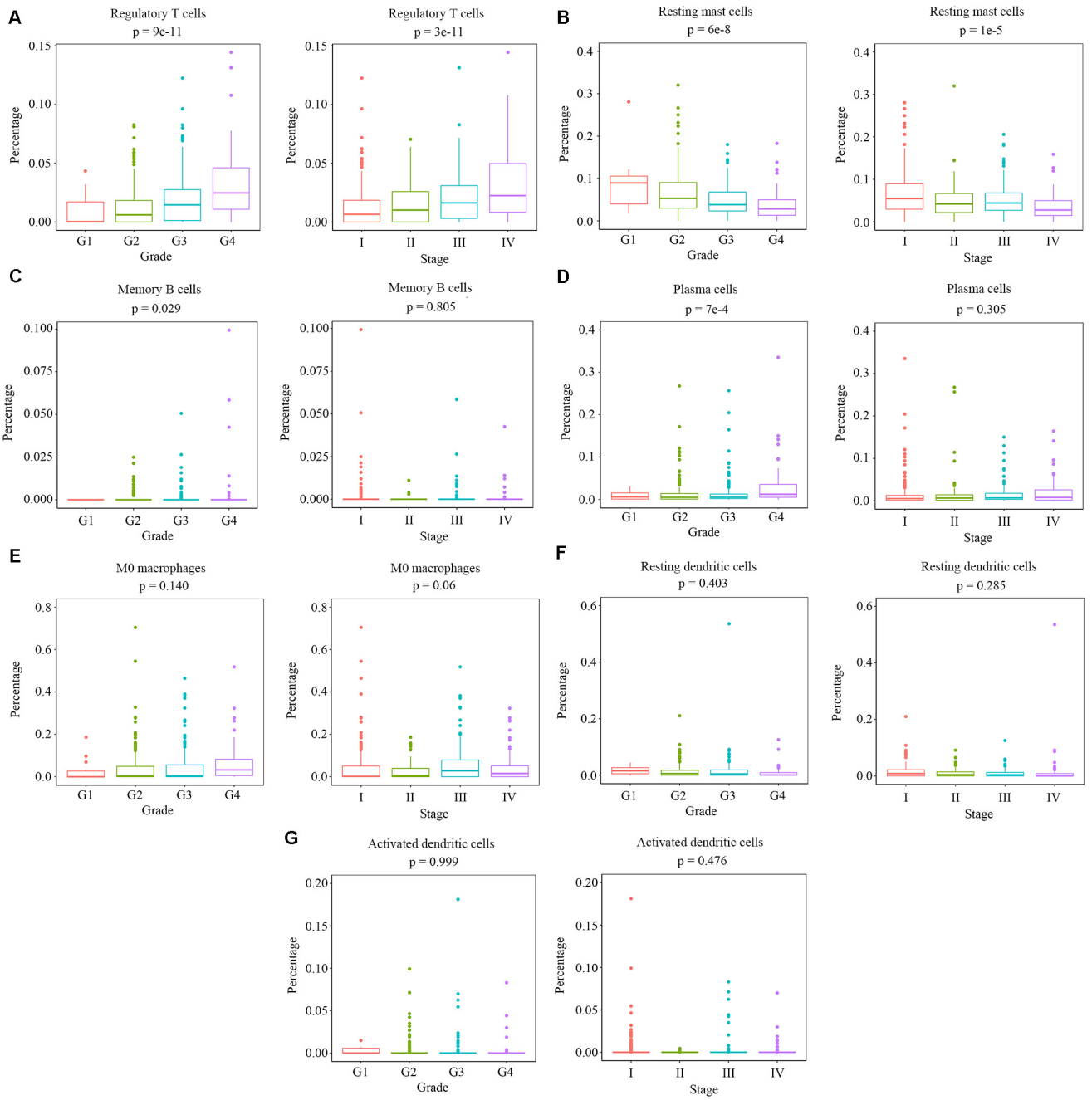

FIGURE 2 | The relationship between the abundance ratios of the immune cells and clinical characteristics. **(A–G)** The abundance ratios of memory B cells, plasma cells, regulatory T cells, M0 macrophages, resting dendritic cells, activated dendritic cells, and resting mast cells in different pathological grades and clinical stages. Data are shown in boxplot format, and the dots represent the outliers.

Relationship Between Immune Infiltration and Hub Genes

The Pearson correlation between the hub genes and all the 22 types of immune cells was calculated, and the result was visualized with the ggplot2 R package. Also, the correlation between the hub genes and the overall survival was calculated with the Log-Rank test.

RESULTS

Identifying Survival-Related Immune Cells

Previous studies have reported the immune infiltration in the ccRCC tumors (17–20). Thus we explored the microenvironment components of ccRCC tumors by calculating the abundance

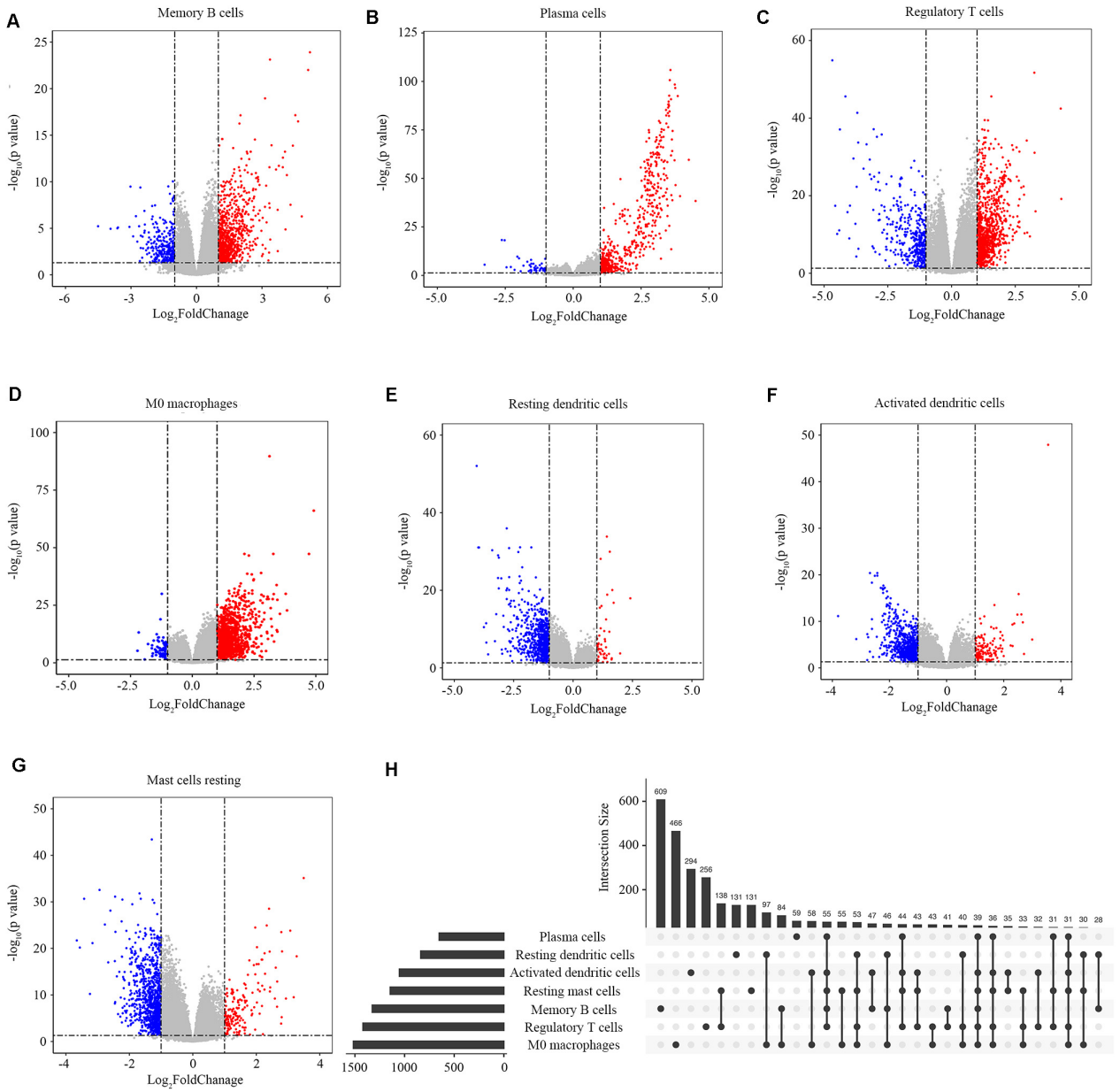

FIGURE 3 | Identification of immune-related genes. **(A–G)** Gene expression profiles related to memory B cells, plasma cells, regulatory T cells, M0 macrophages, resting dendritic cells, activated dendritic cells, and resting mast cells. Data are presented with Volcano plots. The red/blue dots represent the upregulated/downregulated genes according to the criteria: $|\log_2 \text{Foldchange}| > 1$ and adjusted p-value < 0.05. **(H)** The distribution of immune-related genes in the seven types of immune cells. Each black dot represents a set of genes that distributed in one type of immune cell. The numbers on the bar represent the counts of genes in this gene set. The dots connected with a black line represent a common set of genes distributed in more than one type of immune cell.

ratios of 22 types of immune cells with the online software CIBERSORTx (**Figure 1A**). We found the T cells accounted for the most proportion (42.2 ± 14.2%), followed by the macrophages (33.7 ± 11.7%). We also found that the abundance ratios of some types of immune cells were correlated with each other (**Figure 1B**).

The abundance ratios of memory B cells, plasma cells, regulatory T cells, M0 macrophages, resting dendritic cells, activated dendritic cells, and resting mast cells were significantly correlated with the overall survival of ccRCC patients (**Figures 1C–I**). The higher abundance ratios of memory B cells, plasma cells, regulatory T cells, and M0 macrophages identified patients with worse prognosis, while the higher abundance ratios of resting dendritic cells, activated dendritic cells, and resting mast cells identified patients with better prognosis. These seven types of immune cells were considered as survival-related cells and analyzed in further study.

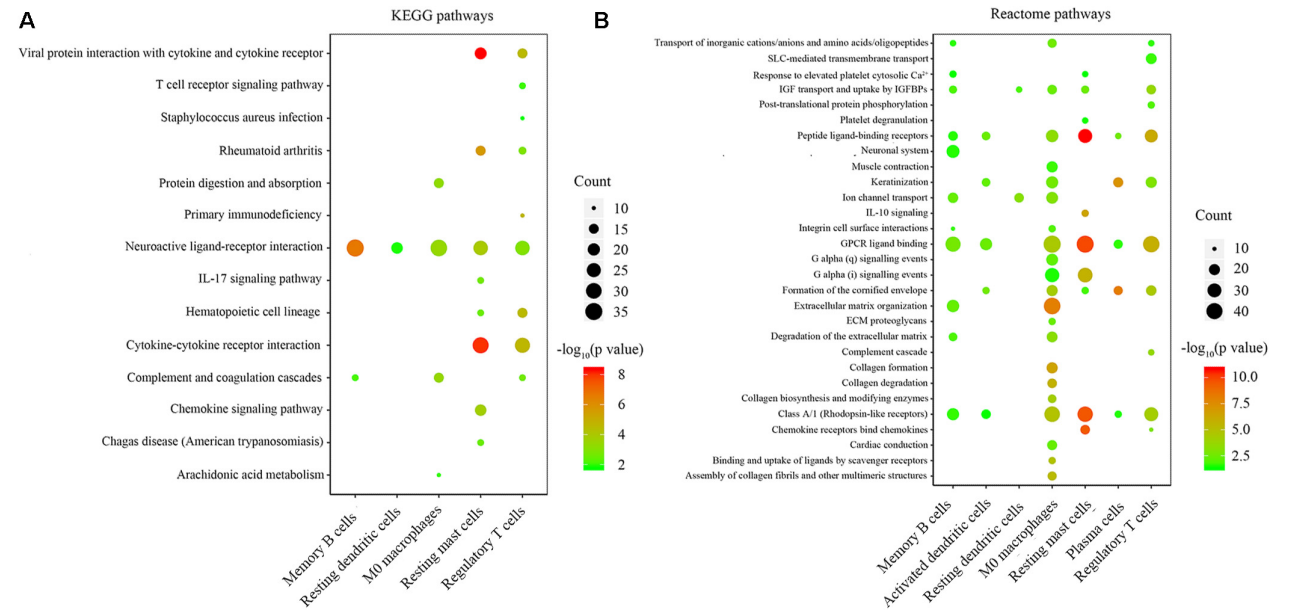

FIGURE 4 | Enrichment analysis of genes related to immune cell infiltration. **(A,B)** the KEGG and Reactome pathway enrichment results of genes involved in each type of immune cells. The color indicates the significance of enrichment results, and the dot size indicates the count of genes enriched for each result.

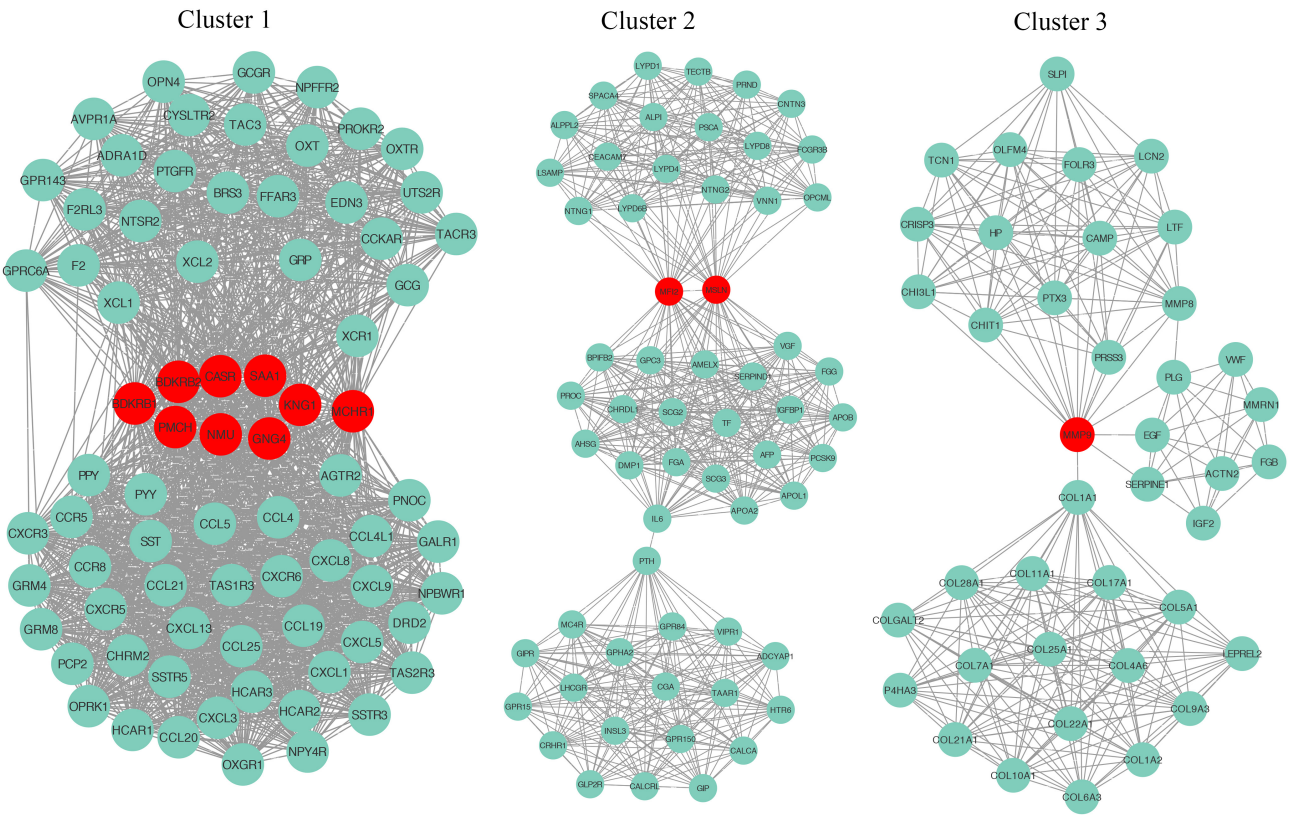

FIGURE 5 | The identification of hub genes. Three gene clusters were identified from the PPI network by the MCODE plugin. The hub genes are highlighted in red dots.

TABLE 2 | List of the 13 hub genes.

Gene	Full name
CASR	Calcium sensing receptor
BDKRB1	Bradykinin receptor B1
MMP9	Matrix metallopeptidase 9
MSLN	Mesothelin
COL1A1	Collagen type I alpha 1 chain
NMU	Neuromedin U
KNG1	Kininogen 1
MCHR1	melanin concentrating hormone receptor 1
MFI2	Melanotransferrin 2
GNG4	G protein subunit gamma 4
BDKRB2	Bradykinin receptor B2
SAA1	Serum amyloid A1
PMCH	Pro-melanin concentrating hormone

Relationship Between Clinical Traits and Survival-Related Immune Cells

We measured the relationship between clinical traits and the abundance ratios of survival-related immune cells. The abundance ratio of regulatory T cells increased with the increase of pathological grades and clinical stages (**Figure 2A**), while the abundance ratio of resting mast cells decreased with the increase of pathological grades and clinical stages (**Figure 2B**). The abundance ratio of memory B cells was statistically different in distinct pathological grades ($p < 0.05$). However, we still suggest that there was no change with the increase of pathological grades since the abundance ratio of memory B cells in most cases was relatively small and the difference probably attributed to the outliers (**Figure 2C**). The abundance ratio of plasma cells slightly increased in pathological grade 4 (**Figure 2D**). The abundance ratios of M0 macrophages, resting dendritic cells, and activated dendritic cells showed no significant difference in distinct grades or stages (**Figures 2E–G**). These results indicate that the abundance ratios of survival-related immune cells are not necessarily related to the pathological grade or clinical stage.

Identification of Immune-Related Genes

We screened the genes related to the abundance ratios of the survival-related immune cells with the method described in the Materials and Methods and found 3863 genes related to the abundance of the seven types of survival-related immune cells. In all these genes, 1325 genes were related to memory B cells, 651 to plasma cells, 1419 to regulatory T cells, 1515 to M0 macrophages, 837 to resting dendritic cells, 1052 to activated dendritic cells, and 1144 to resting mast cells (**Figures 3A–G**). The distribution of immune-related genes is shown in **Figure 3H**.

Pathway Analysis of Immune-Related Genes

We performed KEGG and Reactome pathway enrichment for each group of immune-related genes to explore the biological function of immune-related genes. The results are listed in **Supplementary Tables S1, S2**. The results with gene counts over ten are shown in **Figure 4**. The KEGG pathway enrichment results showed that the immune-related genes were mainly enriched in neuroactive ligand-receptor binding, cytokine-cytokine receptor interaction (**Figure 4A**). The Reactome

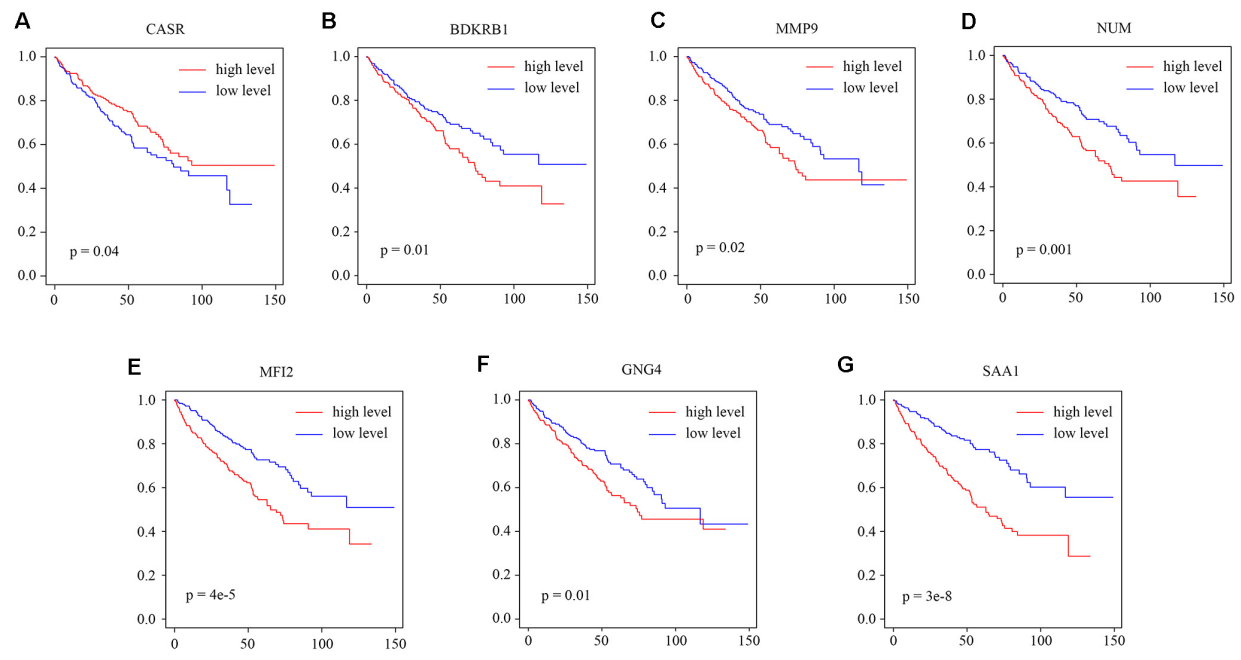

FIGURE 6 | The relationship between the hub genes and overall survival. **(A–G)** The survival analysis for the hub gene CASR, BDKRB1, MMP9, NMU, MFI2, GNG4, and SAA1.

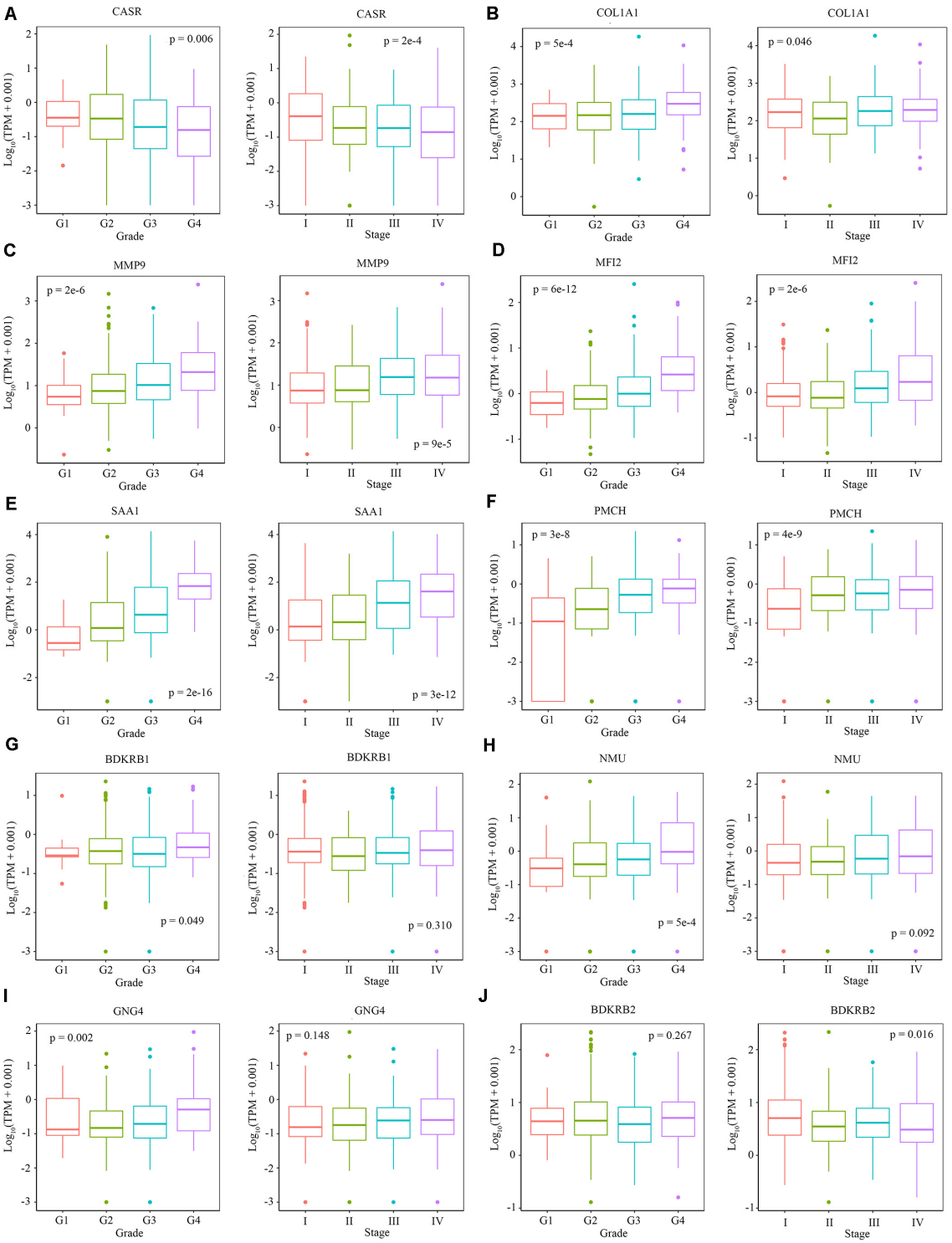

FIGURE 7 | The relationship between the level of hub genes and clinical characteristics. **(A–J)** The level of CARS, COL1A1, MMP9, MFI2, SAA1, PMCH, BDKRB1, NMU, GNG4, and BDKRB2 in different pathological grades and clinical stages. Data are shown in boxplot format, and the dots represent the outliers.

pathways enrichment results showed that the immune-related genes were mainly enriched in G protein-coupled receptor (GPCR) ligand binding, peptide ligand-binding receptors (**Figure 4B**). These results indicate that the immune-related genes might be involved in ligand-receptor binding and signaling pathway transduction.

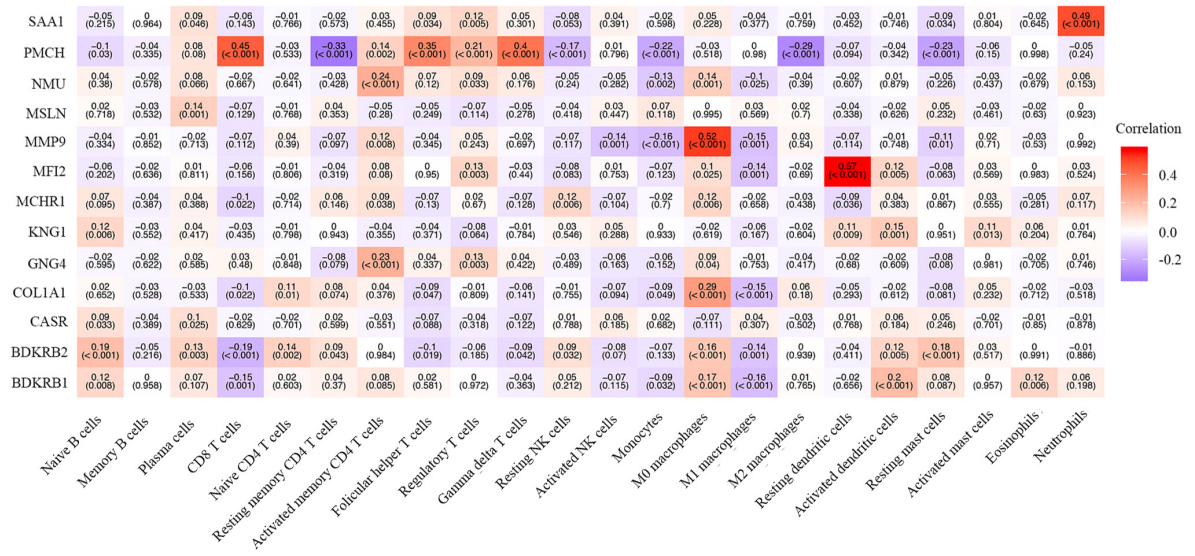

FIGURE 8 | The correlation between the hub genes and immune cells. The Pearson correlation coefficients are presented with a heatmap. The number without brackets is the Pearson correlation coefficients, and the number with brackets is the *p*-value.

Identification of Hub Genes

To explore the detail of immune-related gene relationships, we constructed the PPI with all the protein-coding genes in the immune-related gene set. To identify the critical immune-related gene, we explored the gene clusters within the PPI network with the MCODE plugin of the Cytoscape software. Three clusters with no less than 40 genes were found and applied to identify the hub genes. Here, the Hub genes were those genes with the most interacted genes in the cluster. Finally, 13 genes were identified as the hub genes (**Figure 5** and **Table 2**).

Relationship Between Clinical Traits and Hub Genes

We explored the relationship between the overall survival and the hub genes. We found that 7 out of 13 hub genes (CASR, BDKRB1, MMP9, NMU, MFI2, GNG4, and SAA1) are correlated to overall survival (**Figure 6**). We also explored the relationship between the clinical traits and the hub genes. The level of CASR decreased with the increase of pathological grades and clinical stages (**Figure 7A**). The level of COL1A1 increased in pathological grade 4 but decreased in clinical stage II (**Figure 7B**). Meanwhile, the levels of MMP9, MFI2, SAA1, and PMCH increased with the increase of pathological grades and clinical stages (**Figures 7C–F**). The levels of BDKRB1, NMU, and GNG4 increased only with the increase of pathological grades (**Figures 7G–I**). The level of BDKRB2 decreased with the increase of clinical stages (**Figure 7J**). The levels of MSLN, KNG1, and MCHR1 showed no difference in distinct pathological grades or clinical stages (**Supplementary Figure S1**).

We also explored the correlation between hub genes and the abundance ratios of 22 types of immune cells. We found that multiple hub genes were correlated to the abundance ratio of certain types of immune cells (**Figure 8**). For instance, the level of MMP9 was positively correlated to the abundance ratio of M0 macrophages, while the level of PMCH was negatively correlated to the abundance ratio of resting mast cells. These results indicate that the hub genes might play a vital role in the function of the immune cells.

DISCUSSION

As the comprehensive molecular characterization of ccRCC has been performed (3, 20–23), genetic and epigenetic prognostic markers have been widely studied (24, 25). Since immune cell infiltration has been widely reported in ccRCC (3, 17–20), the prognostic value of the immune-based markers has emerged. Prognostic models based on tumor-associated immune cells and genes have been developed (26–28). In this study, we pursued to expand the range of immune prognostic tools by exploring microenvironment component of ccRCC. We analyzed the ccRCC microenvironment by calculating the abundance ratios of 22 types of immune cells. The results showed a variation of the abundance ratios among distinct patients, which not only supported those previous research but also indicated that the ccRCC microenvironment might be complex.

We found that seven types of survival-related immune cells, including memory B cells, plasma cells, regulatory T cells, M0 macrophages, resting dendritic cells, activated dendritic cells, and resting mast cells, were correlated with overall survival. A previous study has identified ICOS + Treg cells as a prognostic marker in localized ccRCC, which is consistent with our results (29). Also, Eckl et al. analyzed immune cell infiltration of 41 ccRCC samples with flow cytometry and found that patients with a high level of NK cell infiltration had better cancer-specific survival (30). This result is consistent with our results that the higher abundance ratios of resting dendritic cells and activated

dendritic cells identify patients with better prognosis. These research, to a certain extent, indicate that these seven types of immune cells might be predictors for ccRCC prognosis.

The survival-related immune cells in the microenvironment may be the potential therapeutic targets. Several studies demonstrated that macrophages constitute up to 50% of a tumor mass, forming a major component of the tumor microenvironment (31, 32). A widely accepted theory on macrophage subtypes is the plastic modal that macrophages can be activated into classically polarized tumor-suppressive M1 and alternatively polarized tumor-promoting M2 subtypes. M2 macrophages promote ccRCC progression due to their immune-suppressive property (33, 34). Several therapeutic agents targeting macrophages have been developed in recent years (35, 36). According to our data, the abundance ratio of macrophages is over 30% in ccRCC tumors. Therefore, macrophages might be a potential target for ccRCC treatment.

We also screened the immune-related genes and analyzed their biological functions. Most of the immune-related genes were enriched in neuroactive ligand-receptor binding, cytokine-cytokine receptor interaction, GPCR ligand binding, peptide ligand-binding receptors. These results imply that the immune-related genes may be associated with ligand-receptor binding and its downstream signaling pathways that may be potential therapeutic targets. For instance, G protein-coupled receptor 68 (GPR68), a proton-sensing GPCR, plays a vital role in multiple types of tumors (37, 38). Additionally, several immune-related genes were enriched in the interleukin (IL)-17 signaling pathway. IL-17 is mainly produced by Th17 cells, a subtype of T helper cells (39). The activation of IL-17 signaling pathways leads to the overexpression of Chemokines, Cytokines and matrix metallopeptidases (MMPs) through multiple signaling pathways (40).

We also identified 13 hub genes from the immune-related genes and found seven of them (CASR, BDKRB1, MMP9, NMU, MFI2, GNG4, and SAA1) are correlated with overall survival. CASR, a Calcium-sensing receptor, is expressed in the immune cells including macrophages, eosinophils, and monocytes (41–43). Several studies have reported that CASR expression can be induced by multiple cytokines (44, 45). In murine macrophages, the CASR activates the NACHT, LRR, and NLRP3 inflammasome in a cAMP-dependent manner (46). Additionally, MMP9 is a downstream matrix metallopeptidase of the IL-17 signaling pathway. MMP9 promotes metastasis by degrading the extracellular matrix. Ma et al. reported that the level of MMP9 is higher in metastatic ccRCC than in primary ccRCC (47). The level of MMP9 is associated with poor prognosis in ccRCC patients (48). These results indicate that the hub genes may play a key role in the network of immune-related genes.

There are still limitations in our study. First, the analysis of immune-cell infiltration is based on the TCGA dataset and needs to be validated with samples from other sources. Second, the hub genes are identified from PPI networks based on the String database, which needs to be proved by experiment on cell line models. Third, the abundance ratio of memory B cells is zero in most cases, which means the conclusion on memory B cells relays on outliers. Although these results are statistically reliable, we should be cautious with the conclusion on memory B cells. Fourth, intra-tumor heterogeneity of pathological grades in ccRCC has been reported (49). Thus, we need to be cautious about the conclusion on the relation between pathological grades and immune-related cells and genes.

In the past decade, immune checkpoint inhibition therapy has been developed. Nivolumab, a monoclonal antibody targeting programmed death-1 (PD-1), was approved as the second-line treatment for advanced RCC in 2015. Mikami et al. explored the level of PD-1 and programmed death ligand 1 (PD-1L) in tumor-infiltrating immune cells in the tumor microenvironment of untreated and VEGF-TKI-treated primary ccRCC tissues. They found that the high level of PD-1 and PD-L1 in tumor-infiltrating immune cells was associated with the poor prognosis and the clinical response to VEGF-TKI treatment for metastatic ccRCC (50). These results indicate the potential effect of microenvironment on the immune checkpoint inhibition therapy. In conclusion, we identified seven types of survival-related immune cells and 13 hub genes, and seven of these genes were correlated to overall survival in ccRCC patients. These cells and genes can be considered predictors for prognosis, or as therapeutic targets for ccRCC. Our research not only provides a critical understanding of ccRCC microenvironments but also identifies the potential therapeutic targets.

DATA AVAILABILITY STATEMENT

Publicly available datasets were analyzed in this study. This data can be found here: The Cancer Genome Atlas (https://portal.gdc.cancer.gov/).

AUTHOR CONTRIBUTIONS

BD, SX, JD, LQ, HH, and WZ: study concept and design. BD, XY, and TZ: analysis and interpretation of data. BD and YZ: drafting of the manuscript. SX, CT, TS, KZ, and HH: critical revision of the manuscript. All authors contributed to the article and approved the submitted version.

FUNDING

This study was supported by the National Natural Science Foundation of China (No. 81972402) and China Postdoctoral Science Foundation (No. 2019t120970).

SUPPLEMENTARY MATERIAL

The Supplementary Material for this article can be found online at: https://www.frontiersin.org/articles/10.3389/fonc.2020.01770/full#supplementary-material

FIGURE S1 | The relationship between the level of hub genes and clinical characteristics. **(A–C)** The level of MSLN, KNG1 and MCHR1 in different pathological grades and clinical stages. Data are shown in boxplot format, and the dots represent the outliers.

REFERENCES

1. Siegel RL, Miller KD, Jemal A. Cancer statistics, 2020. *CA Cancer J Clin.* (2020) 70:7–30. doi: 10.3322/caac.21590
2. Hsieh JJ, Purdue MP, Signoretti S, Swanton C, Albiges L, Schmidinger M, et al. Renal cell carcinoma. *Nat Rev Dis Prim.* (2017) 3:17009. doi: 10.1038/nrdp.2017.9
3. Ricketts CJ, De Cubas AA, Fan H, Smith CC, Lang M, Reznik E, et al. The cancer genome atlas comprehensive molecular characterization of renal cell carcinoma. *Cell Rep.* (2018) 23:3698. doi: 10.1016/j.celrep.2018.06.032
4. Lopez-Beltran A, Scarpelli M, Montironi R, Kirkali Z. 2004 WHO classification of the renal tumors of the adults. *Eur Urol.* (2006) 49:798–805. doi: 10.1016/j.eururo.2005.11.035
5. Frew IJ, Moch H. A clearer view of the molecular complexity of clear cell renal cell carcinoma. *Ann Rev Pathol.* (2015) 10:263–89. doi: 10.1146/annurev-pathol-012414-040306
6. Barata PC, Rini BI. Treatment of renal cell carcinoma: current status and future directions. *CA Cancer J Clin.* (2017) 67:507–24. doi: 10.3322/caac.21411
7. Qian CN, Huang D, Wondergem B, Teh BT. Complexity of tumor vasculature in clear cell renal cell carcinoma. *Cancer.* (2009) 115(Suppl. 10):2282–9. doi: 10.1002/cncr.24238
8. Shen C, Kaelin WG Jr. The VHL/HIF axis in clear cell renal carcinoma. *Sem Cancer Biol.* (2013) 23:18–25. doi: 10.1016/j.semcancer.2012.06.001
9. Gossage L, Eisen T, Maher ER. VHL, the story of a tumour suppressor gene. *Nat Rev Cancer.* (2015) 15:55–64. doi: 10.1038/nrc3844
10. Atkins MB, Tannir NM. Current and emerging therapies for first-line treatment of metastatic clear cell renal cell carcinoma. *Cancer Treat Rev.* (2018) 70:127–37. doi: 10.1016/j.ctrv.2018.07.009
11. Motzer RJ, Escudier B, McDermott DF, George S, Hammers HJ, Srinivas S, et al. Nivolumab versus everolimus in advanced renal-cell carcinoma. *New Engl J Med.* (2015) 373:1803–13. doi: 10.1056/NEJMoa1510665
12. Soultati A, Stares M, Swanton C, Larkin J, Turajlic S. How should clinicians address intratumour heterogeneity in clear cell renal cell carcinoma? *Curr Opin Urol.* (2015) 25:358–66. doi: 10.1097/MOU.0000000000000204
13. Yuan Y. Spatial heterogeneity in the tumor microenvironment. *Cold Spring Harb Perspect Med.* (2016) 6:26583. doi: 10.1101/cshperspect.a026583
14. Denton AE, Roberts EW, Fearon DT. Stromal cells in the tumor microenvironment. *Adv Exp Med Biol.* (2018) 1060:99–114. doi: 10.1007/978-3-319-78127-3_6
15. Wu T, Dai Y. Tumor microenvironment and therapeutic response. *Cancer Lett.* (2017) 387:61–8. doi: 10.1016/j.canlet.2016.01.043
16. Newman AM, Steen CB, Liu CL, Gentles AJ, Chaudhuri AA, Scherer F, et al. Determining cell type abundance and expression from bulk tissues with digital cytometry. *Nat Biotechnol.* (2019) 37:773–82. doi: 10.1038/s41587-019-0114-2
17. Senbabaoglu Y, Gejman RS, Winer AG, Liu M, Van Allen EM, de Velasco G, et al. Tumor immune microenvironment characterization in clear cell renal cell carcinoma identifies prognostic and immunotherapeutically relevant messenger RNA signatures. *Genome Biol.* (2016) 17:231. doi: 10.1186/s13059-016-1092-z
18. Chevrier S, Levine JH, Zanotelli VRT, Silina K, Schulz D, Bacac M, et al. An Immune atlas of clear cell renal cell carcinoma. *Cell.* (2017) 169:736–49e18. doi: 10.1016/j.cell.2017.04.016
19. Hakimi AA, Voss MH, Kuo F, Sanchez A, Liu M, Nixon BG, et al. Transcriptomic profiling of the tumor microenvironment reveals distinct subgroups of clear cell renal cell cancer: data from a randomized phase iii trial. *Cancer Discover.* (2019) 9:510–25. doi: 10.1158/2159-8290.CD-18-0957
20. Clark DJ, Dhanasekaran SM, Petralia F, Pan J, Song X, Hu Y, et al. Integrated proteogenomic characterization of clear cell renal cell carcinoma. *Cell.* (2019) 179:964–83.e31. doi: 10.1016/j.cell.2019.10.007
21. Cancer Genome Atlas Research Network. Comprehensive molecular characterization of clear cell renal cell carcinoma. *Nature.* (2013) 499:43–9. doi: 10.1038/nature12222
22. Sato Y, Yoshizato T, Shiraishi Y, Maekawa S, Okuno Y, Kamura T, et al. Integrated molecular analysis of clear-cell renal cell carcinoma. *Nat Genet.* (2013) 45:860–7. doi: 10.1038/ng.2699
23. Chen F, Zhang Y, Senbabaoglu Y, Ciriello G, Yang L, Reznik E, et al. Multilevel genomics-based taxonomy of renal cell carcinoma. *Cell Rep.* (2016) 14:2476–89. doi: 10.1016/j.celrep.2016.02.024
24. Liu H, Ye T, Yang X, Lv P, Wu X, Zhou H, et al. A panel of four-lncRNA signature as a potential biomarker for predicting survival in clear cell renal cell carcinoma. *J Cancer.* (2020) 11:4274–83. doi: 10.7150/jca.40421
25. Zhou J, Wang J, Hong B, Ma K, Xie H, Li L, et al. Gene signatures and prognostic values of m6A regulators in clear cell renal cell carcinoma–a retrospective study using TCGA database. *Aging.* (2019) 11:1633–47. doi: 10.18632/aging.101856
26. Geissler K, Fornara P, Lautenschlager C, Holzhausen HJ, Seliger B, Riemann D. Immune signature of tumor infiltrating immune cells in renal cancer. *Oncoimmunology.* (2015) 4:e985082. doi: 10.4161/2162402X.2014.985082
27. Xu WH, Xu Y, Wang J, Wan FN, Wang HK, Cao DL, et al. Prognostic value and immune infiltration of novel signatures in clear cell renal cell carcinoma microenvironment. *Aging.* (2019) 11:6999–7020. doi: 10.18632/aging.102233
28. Ghatalia P, Gordetsky J, Kuo F, Dulaimi E, Cai KQ, Devarajan K, et al. Prognostic impact of immune gene expression signature and tumor infiltrating immune cells in localized clear cell renal cell carcinoma. *J Immunother Cancer.* (2019) 7:139. doi: 10.1186/s40425-019-0621-1
29. Giraldo NA, Becht E, Vano Y, Petitprez F, Lacroix L, Validire P, et al. Tumor-infiltrating and peripheral blood T-cell immunophenotypes predict early relapse in localized clear cell renal cell carcinoma. *Clin Cancer Res.* (2017) 23:4416–28. doi: 10.1158/1078-0432.CCR-16-2848
30. Eckl J, Buchner A, Prinz PU, Riesenberg R, Siegert SI, Kammerer R, et al. Transcript signature predicts tissue NK cell content and defines renal cell carcinoma subgroups independent of TNM staging. *J Mol Med (Berlin Germany).* (2012) 90:55–66. doi: 10.1007/s00109-011-0806-7
31. Van Overmeire E, Laoui D, Keirsse J, Van Ginderachter JA, Sarukhan A. Mechanisms driving macrophage diversity and specialization in distinct tumor microenvironments and parallelisms with other tissues. *Front Immunol.* (2014) 5:127. doi: 10.3389/fimmu.2014.00127
32. Qian BZ, Pollard JW. Macrophage diversity enhances tumor progression and metastasis. *Cell.* (2010) 141:39–51. doi: 10.1016/j.cell.2010.03.014
33. Ginhoux F, Schultze JL, Murray PJ, Ochando J, Biswas SK. New insights into the multidimensional concept of macrophage ontogeny, activation and function. *Nat Immunol.* (2016) 17:34–40. doi: 10.1038/ni.3324
34. Poltavets AS, Vishnyakova PA, Elchaninov AV, Sukhikh GT, Fatkhudinov TK. Macrophage modification strategies for efficient cell therapy. *Cells.* (2020) 9:1535. doi: 10.3390/cells9061535
35. Allavena P, Germano G, Belgiovine C, D'Incalci M, Mantovani A. Trabectedin: a drug from the sea that strikes tumor-associated macrophages. *Oncoimmunology.* (2013) 2:e24614. doi: 10.4161/onci.24614
36. Zhou J, Tang Z, Gao S, Li C, Feng Y, Zhou X. Tumor-associated macrophages: recent insights and therapies. *Front Oncol.* (2020) 10:188. doi: 10.3389/fonc.2020.00188
37. Wiley SZ, Sriram K, Liang W, Chang SE, French R, McCann T, et al. GPR68, a proton-sensing GPCR, mediates interaction of cancer-associated fibroblasts and cancer cells. *FASEB J.* (2018) 32:1170–83. doi: 10.1096/fj.201700834R
38. Wiley SZ, Sriram K, Salmeron C, Insel PA. GPR68: an emerging drug target in cancer. *Int J Mol Sci.* (2019) 20:559. doi: 10.3390/ijms20030559
39. Hemdan NY. Anti-cancer versus cancer-promoting effects of the interleukin-17-producing T helper cells. *Immunol Lett.* (2013) 149:123–33. doi: 10.1016/j.imlet.2012.11.002
40. Li X, Bechara R, Zhao J, McGeachy MJ, Gaffen SL. IL-17 receptor-based signaling and implications for disease. *Nat Immunol.* (2019) 20:1594–602. doi: 10.1038/s41590-019-0514-y
41. Yamaguchi T, Kifor O, Chattopadhyay N, Bai M, Brown EM. Extracellular calcium (Ca2+o)-sensing receptor in a mouse monocyte-macrophage cell line (J774): potential mediator of the actions of Ca2+o on the function of J774 cells. *J Bone Mineral Res.* (1998) 13:1390–7. doi: 10.1359/jbmr.1998.13.9.1390
42. Yarova PL, Stewart AL, Sathish V, Britt RD Jr., Thompson MA, Lowe APP, et al. Calcium-sensing receptor antagonists abrogate airway hyperresponsiveness

and inflammation in allergic asthma. *Sci Trans Med.* (2015) 7:284ra60. doi: 10.1126/scitranslmed.aaa0282
43. Yamaguchi T, Olozak I, Chattopadhyay N, Butters RR, Kifor O, Scadden DT, et al. Expression of extracellular calcium (Ca2+o)-sensing receptor in human peripheral blood monocytes. *Biochem Biophys Res Commun.* (1998) 246:501–6. doi: 10.1006/bbrc.1998.8648
44. Canaff L, Hendy GN. Calcium-sensing receptor gene transcription is up-regulated by the proinflammatory cytokine, interleukin-1beta. Role of the NF-kappaB PATHWAY and kappaB elements. *J Biol Chem.* (2005) 280:14177–88. doi: 10.1074/jbc.M408587200
45. Fetahu IS, Hummel DM, Manhardt T, Aggarwal A, Baumgartner-Parzer S, Kallay E. Regulation of the calcium-sensing receptor expression by 1,25-dihydroxyvitamin D3, interleukin-6, and tumor necrosis factor alpha in colon cancer cells. *J Steroid Biochem Mol Biol.* (2014) 144(Pt A):228–31. doi: 10.1016/j.jsbmb.2013.10.015
46. Lee GS, Subramanian N, Kim AI, Aksentijevich I, Goldbach-Mansky R, Sacks DB, et al. The calcium-sensing receptor regulates the NLRP3 inflammasome through Ca2+ and cAMP. *Nature.* (2012) 492:123–7. doi: 10.1038/nature11588
47. Ma J, Li M, Chai J, Wang K, Li P, Liu Y, et al. Expression of RSK4, CD44 and MMP-9 is upregulated and positively correlated in metastatic ccRCC. *Diagnostic Pathol.* (2020) 15:28. doi: 10.1186/s13000-020-00948-6
48. Niu H, Li F, Wang Q, Ye Z, Chen Q, Lin Y. High expression level of MMP9 is associated with poor prognosis in patients with clear cell renal carcinoma. *PeerJ.* (2018) 6:e5050. doi: 10.7717/peerj.5050
49. Ball MW, Bezerra SM, Gorin MA, Cowan M, Pavlovich CP, Pierorazio PM, et al. Grade heterogeneity in small renal masses: potential implications for renal mass biopsy. *J Urol.* (2015) 193:36–40. doi: 10.1016/j.juro.2014.06.067
50. Mikami S, Mizuno R, Kondo T, Shinohara N, Nonomura N, Ozono S, et al. Clinical significance of programmed death-1 and programmed death-ligand 1 expression in the tumor microenvironment of clear cell renal cell carcinoma. *Cancer Sci.* (2019) 110:1820–8. doi: 10.1111/cas.14019

Conflict of Interest: The authors declare that the research was conducted in the absence of any commercial or financial relationships that could be construed as a potential conflict of interest.

frontiers in Oncology

ORIGINAL RESEARCH
published: 27 November 2020
doi: 10.3389/fonc.2020.584834

Safety and Efficacy of Immune Checkpoint Inhibitors for Patients With Metastatic Urothelial Carcinoma and End-Stage Renal Disease: Experiences From Real-World Practice

*Ming-Chun Kuo[1], Po-Jung Su[2], Chun-Chieh Huang[3], Hao-Lun Luo[4], Tai-Jan Chiu[1], Shau-Hsuan Li[1], Chia-Che Wu[1], Ting-Ting Liu[5], Yuan-Tso Cheng[4], Chih-Hsiung Kang[4] and Yu-Li Su[1,6]**

[1] Division of Hematology Oncology, Department of Internal Medicine, Kaohsiung Chang Gung Memorial Hospital and Chang Gung University, College of Medicine, Kaohsiung, Taiwan, [2] Division of Hematology Oncology, Chang Gung Memorial Hospital at Linkou and College of Medicine, Chang Gung University, Tao-Yuan, Taiwan, [3] Department of Radiation Oncology, Kaohsiung Chang Gung Memorial Hospital and Chang Gung University, College of Medicine, Kaohsiung, Taiwan, [4] Department of Urology, Kaohsiung Chang Gung Memorial Hospital and Chang Gung University, College of Medicine, Kaohsiung, Taiwan, [5] Department of Pathology, Kaohsiung Chang Gung Memorial Hospital and Chang Gung University, College of Medicine, Kaohsiung, Taiwan, [6] Clinical Trial Center, Kaohsiung Chang Gung Memorial Hospital, Kaohsiung, Taiwan

OPEN ACCESS

Edited by:
Sumit Kumar Subudhi,
University of Texas MD Anderson Cancer Center, United States

Reviewed by:
Jamie S. Lin,
University of Texas MD Anderson Cancer Center, United States
Mehmet Asim Bilen,
Emory University, United States

***Correspondence:**
Yu-Li Su
yolisu@mac.com

Specialty section:
This article was submitted to Genitourinary Oncology, a section of the journal Frontiers in Oncology

Received: 18 July 2020
Accepted: 29 October 2020
Published: 27 November 2020

Citation:
Kuo M-C, Su P-J, Huang C-C, Luo H-L, Chiu T-J, Li S-H, Wu C-C, Liu T-T, Cheng Y-T, Kang C-H and Su Y-L (2020) Safety and Efficacy of Immune Checkpoint Inhibitors for Patients With Metastatic Urothelial Carcinoma and End-Stage Renal Disease: Experiences From Real-World Practice. Front. Oncol. 10:584834. doi: 10.3389/fonc.2020.584834

Background: Immune checkpoint inhibitors (ICIs) are used widely for treating metastatic urothelial carcinoma (mUC). In practical settings, evidence is lacking on the efficacy of ICIs in some difficult-to-treat patients, such as those with end-stage renal disease (ESRD). Herein, we evaluate the safety and efficacy of ICIs for patients with mUC and ESRD.

Methods: For this retrospective study, patients with mUC who were given ICIs at Kaohsiung Chang Gang Memorial Hospital and Linkou Chang Gung Memorial Hospital between April 2016 and November 2019 were consecutively enrolled. All clinicopathologic data, treatment responses, and adverse events were recorded. The immune-related adverse events (AEs), objective response rate (ORR), progression-free survival (PFS), and overall survival (OS) were compared between ESRD and non-ESRD groups.

Results: In total, 129 patients with mUC were enrolled, with 11 patients categorized as the ESRD group. Among these patients with ESRD receiving ICIs, 7 of 11 (63.6%) had high-grade (grade ≥3) AEs, chiefly hematologic toxicity. Some rarely encountered AEs were noted, including toxic epidermal necrolysis, tuberculosis reactivation, ascites, and cytokine release syndrome. Patients in the ESRD group had numerically higher ORR (54.5% vs. 28.8%, p = 0.09), PFS (7.1 vs. 3.5 months, p = 0.42), and OS (not reached vs. 15.4 months) than the non-ESRD group. A multivariate Cox regression model demonstrated that leukocytosis (hazard ratio [HR]: 2.63; 95% confidence interval [CI]:

1.23–5.63; p = 0.01) and neutrophil-to-lymphocyte ratio (HR 2.91; 95% CI: 1.30–6.53; p = 0.01) were independent prognostic factors.

Conclusion: Administration of ICIs in patients with mUC and ESRD demonstrated a modest antitumor activity, and should be used with caution for increasing risk of hematologic toxicity.

Keywords: immune checkpoint inhibitor, end-stage renal disease, metastatic urothelial carcinoma, safety, survival

INTRODUCTION

Urothelial carcinoma (UC) is a common cancer worldwide, with approximately 500,000 new cases diagnosed annually and an estimated 150,000 cancer-related deaths (1). Early-stage UC can be cured through radical surgery, including cystectomy for bladder cancer and nephroureterectomy for upper tract urothelial carcinoma (UTUC). Nevertheless, approximately 10–30% of these patients experience local recurrence or distant metastasis, leading to mortality from such diseases (2). Cisplatin-based chemotherapy has been the gold standard therapy since 1990, with an objective response rate (ORR) of 40–50% and an overall survival (OS) of 14–15 months (3). As the recent breakthrough of immune checkpoint inhibitors (ICIs) has been widely studied for various cancer types, the paradigm of treatment has shifted to ICIs for patients failing to respond to platinum-based chemotherapy and those who are ineligible for cisplatin (4–8). In the pivotal phase 3 KEYNOTE-045 study, compared with conventional chemotherapy, pembrolizumab conferred a significant survival benefit on patients with metastatic UC (mUC) whose conditions were refractory to first-line platinum-based chemotherapy, regardless of the patients' PD-L1 expression (4). At this time, five ICIs have been approved by the U.S. Food and Drug Administration (FDA) for mUC treatment.

The efficacy of cisplatin-based chemotherapy in patients with mUC is generally limited by poor Eastern Cooperative Oncology Group (ECOG) performance status or chronic kidney disease. In general, the proportion of patients for whom cisplatin is unsuitable may be 30–50% of the population with stage IV mUC (9). Given their more favorable toxicity profile, ICIs have been investigated as first-line treatments for cisplatin-ineligible patients with mUC. The promising OS results from the IMVigor 210 trial demonstrated that atezolizumab monotherapy provided an excellent OS of 15.8 months, prompting the FDA to grant accelerated approval for ICIs as first-line treatment for cisplatin-ineligible patients with mUC (10). However, many patients have been excluded from prospective trials owing to poor ECOG performance status or having coexisting autoimmune disease or end-stage renal disease (ESRD) requiring hemodialysis. Treatment options for patients with such rare conditions remain uncertain, and related evidence is lacking.

ESRD is a common comorbidity in patients with mUC. UTUC and urothelial carcinoma of the bladder (UCB) independently increase the risk of ESRD, with hazard ratios (HRs) for ESRD up to 7.75 and 3.12 in patients with UTUC and UCB, respectively (11). Patients with ESRD, especially women aged 50 to 60 years, also have a high risk of developing UC (12). As ICIs are eliminated through the reticuloendothelial system and are not excreted through renal filtration, their use in patients receiving dialysis provides an alternative therapeutic choice to avoid cumulative toxicity from conventional chemotherapy (13). Only small case series have provided evidence of the safety and efficacy of ICIs in patients with ESRD, and most of such studies have been on melanoma, lung cancer, and renal cell carcinoma (14, 15). To assist such difficult-to-treat patients, data on the safety and efficacy of ICIs are urgently required. The aim of this retrospective study was to evaluate the safety and efficacy of immune ICIs in patients with mUC and ESRD.

METHODS

Patients

We retrospectively reviewed patients with mUC who received ICIs between April 2016 and November 2019 at Kaohsiung Chang Gung Memorial Hospital and Linkou Chang Gung Memorial Hospital in Taiwan. All clinicopathologic data were collected from electrical medical recording systems by physicians and trained assistants. Database variables included age, sex, ECOG performance status, primary tumor site, visceral or lymph node metastasis, PD-L1 expression by tumor proportion score, ICI type, regimen of combination treatment or previous systemic treatment, laboratory data, treatment response, and adverse events (AEs). The study was approved by the Institutional Review Board of Chang Gung Medical Foundation.

Treatment

All patients received an anti-PD-1 (nivolumab, pembrolizumab) or anti-PD-L1 (atezolizumab, durvalumab, or avelumab) medication. The regimen, treatment sequence, and combined treatment regimen were at the discretion of the physician. The regimen of combined treatment included chemotherapy, a cytotoxic T-lymphocyte antigen 4 (CTLA-4) inhibitor, and a poly ADP-ribose polymerase (PARP) inhibitor.

Response Evaluation and Endpoints

All patients had attended scheduled appointments during treatment until disease progression, treatment intolerance, or death. The follow-up visit procedures included physical examinations, laboratory tests, and imaging studies. Patients were subjected to computed tomography scans of the chest or

abdomen for tumor response assessments using the Response Evaluation Criteria in Solid Tumors (version 1.1).

The primary endpoint was treatment-related AEs in patients with ESRD. The observed AEs during any round of ICIs were graded according to the Common Terminology Criteria for Adverse Events (CTCAE) version 4.0 (**Supplementary Table 1**). All patients who received at least one cycle of immunotherapy were included in the analysis. The secondary endpoints of the study were treatment response, OS, and progression-free survival (PFS). OS was defined as the time interval from the date of ICIs commencement (any cycle) to the date of death or final patient contact.

Statistical Analysis

All statistical analyses were performed using SPSS version 21.0 (SPSS Inc., Chicago, IL, USA), and survival curves were plotted using GraphPad Prism version 6.04 (GraphPad Software, La Jolla California, USA). The differences between the ESRD subgroup and patients without ESRD were examined using chi-squared (χ^2) and t tests for categorical and continuous variables, respectively. We constructed OS and PFS curves using the Kaplan–Meier method. Univariate and multivariate analyses were performed using the Cox proportional hazards regression analysis. A p value <0.05 was considered statistically significant.

RESULTS

Patient Characteristics

In total, 129 patients were included in this study, including 11 patients (8.5%) with ESRD who were on maintenance hemodialysis; they were categorized into the ESRD group. Basic patient characteristics are shown in **Table 1**. According to group comparison, the ESRD group had a significantly higher proportion of patients with an ECOG scale score of ≥2 (45.5 vs. 16.1%, p = 0.05), UTUC (72.7% vs. 59.3%, p = 0.05), and anemia (90.0 vs. 35.1%, p = 0.001). No significant difference was noted in age, gender, site of visceral metastasis, tumor proportion score, regimen and sequence of ICIs, white blood cell count, and neutrophil to lymphocyte ratio (NLR) between the two groups. Two-thirds of patients (65.1%) were given anti-PD-1 therapy, and the majority of ICIs were used as monotherapy (64.3%) and as a first-line treatment (75.2%). The individual details of the ESRD group are listed in **Table 2**.

TABLE 1 | Patients demographics and baseline characteristics.

	N (%)	ESRD (%)	Non-ESRD (%)	*p* value
N	129	11	118	
Age (median, years)	66	64	66	0.55
Male	76 (58.9)	4 (36.4)	72 (61.0)	0.2
Tumor location				0.05
UCB	49 (38.0)	2 (18.2)	47 (39.8)	
UTUC	78 (60.5)	8 (72.7)	70 (59.3)	
Multifocal	2 (1.5)	1 (9.1)	1 (0.8)	
ECOG				0.05
0-1	102 (79.1)	6 (54.5)	96 (81.4)	
≧2	24 (18.6)	5 (45.5)	19 (16.1)	
Missing	3 (2.3)	0	3 (2.5)	
ICI sequence				0.25
1st line	97 (75.2)	6 (54.5)	91 (77.1)	
2nd line	19 (14.7)	3 (27.3)	16 (13.6)	
3rd line or later	13 (10.1)	2 (18.2)	11 (9.3)	
ICI type				0.75
Anti-PD-1	84 (65.1)	8 (72.7)	76 (64.4)	
Anti-PD-L1	45 (34.9)	3 (27.3)	42 (35.6)	
Treatment partner				0.63
Monotherapy	83 (64.3)	7 (63.6)	76 (64.4)	
Chemotherapy	38 (29.5)	4 (36.4)	34 (28.8)	
Anti-CTLA-4	8 (6.2)	0	8 (6.8)	
PD-L1 testing*	71 (55.0)	7 (63.6)	64 (54.2)	0.75
PD-L1 result¶				
≧1	37 (52.1)	4 (57.1)	33 (51.6)	0.78
≧10	27 (38.0)	2 (28.6)	25 (39.1)	0.59
Visceral metastasis	70 (54.3)	4 (36.4)	66 (55.9)	0.34
Liver	25 (19.4)	2 (18.2)	23 (19.5)	0.99
Lung	46 (35.7)	1 (9.1)	45 (38.1)	0.10
Bone	25 (19.4)	2 (18.2)	23 (19.5)	0.99
Laboratory tests				
WBC ≧10,000/μl	102 (79.1)	6 (54.5)	96 (81.4)	0.70
Hgb <10 g/dl	49 (39.5)	9 (90.0)	40 (35.1)	0.001
NLR ≧5	49 (41.2)	5 (50.0)	44 (40.4)	0.74

CTLA-4, cytotoxic T-lymphocyte-associated protein 4; ECOG, Eastern Cooperative Oncology Group; ESRD, end-stage renal disease; Hgb, hemoglobin; ICI, immune checkpoint inhibitor; PD-1, programmed cell death protein 1; UCB, urothelial cancer of the bladder; UTUC, upper tract urothelial carcinoma; NLR, neutrophil to lymphocyte ratio; WBC, while blood cell count.

**PD-L1 immunohistochemistry testing used Dako 22C3 antibody.*

¶Scoring by tumor proportion score (TPS) criteria.

Treatment-Related AEs

All patients in the ESRD group experienced at least one treatment-related AE during the treatment period, and seven of them (63.6%) had high-grade (grade ≥3) AEs (**Table 3**). AEs of all grades included hematologic toxicity (neutropenia 54.5%; anemia 100%; and thrombocytopenia 72%), hepatitis (27.3%), fatigue (18.2%), anorexia (27.3%), and dermatologic toxicity (18.2%). Regarding hematologic toxicity, four patients (36.4%) had grade 3 neutropenia or higher, six (54.5%) had grade 3 anemia or higher, and one (9.1%) had grade 3 thrombocytopenia or higher. However, given the nature of defective function on hematopoiesis for patients with ESRD, the median baseline hemoglobin (Hb) of ESRD group was 8.75 g/dl. The low level of baseline Hb in ESRD group can actually be categorized in CTCAE grade 2 anemia, indicating that any decline of Hb will classified into grade 3 anemia. Although a considerable number of grade 3–4 anemia were observed in the ESRD group, the decrease in mean Hb between baseline and post-ICI administration was 1.6 g/dl, which was not substantially significant (**Figure 1**). For one who developed toxic epidermal necrolysis (TEN), a grade 4 dermatologic AE was recorded. Two patients presented with refractory ascites after receiving a PD-1 inhibitor. The ascites subsided after ICI usage was discontinued and recurred again after the re-administration of ICIs for disease relapse. One patient had disseminated tuberculosis reactivation. A cytokine release syndrome (CRS)-like syndrome was observed in one patient who presented with intermittent spiking fever and respiratory failure after receiving a PD-1 inhibitor.

We also compared the incidence of all grade AE and hematologic AE between ESRD and non-ESRD groups. As shown in **Table 3**, patients with ESRD on ICIs treatment had a higher incidence of all grade of neutropenia (54.5 vs. 22.9%, $p = 0.02$), anemia (100 vs.

TABLE 2 | Patient profiles, treatment, response, and adverse events of ESRD group.

Patient	Age	Primary site	Therapy	Combination	Line	Response	OS (months)	Status	Hematologic AE	Other AE
1	58	Right renal pelvis	Atezolizumab	Paclitaxel	3	PD	8.05	AWD	Gr.4 neutropenia Gr.3 anemia Gr.1 thrombocytopenia	Gr.1 hepatitis Gr.1 anorexia Gr.1 fatigue
2	79	Left ureter	Pembrolizumab	–	1	PR	4.80	AWD	Gr.2 anemia	Gr.2 ascites
3	82	Left renal pelvis and ureter	Pembrolizumab	Gemcitabine	1	PD	0.72	DOD	Gr.3 neutropenia Gr.3 anemia Gr.3 thrombocytopenia	–
4	69	Left renal pelvis	Pembrolizumab	–	1	PD	5.85	DOD	Gr.2 anemia	Gr.1 hepatitis Gr.3 anorexia
5	68	Right renal pelvis	Nivolumab	Gemcitabine	1	PR	12.16	AWD	Gr.3 neutropenia Gr.4 anemia Gr.2 thrombocytopenia	Gr.1 hepatitis Gr.3 ascites
6	63	Left renal pelvis	Nivolumab	–	3	PD	0.23	DOD	Gr.2 anemia Gr.1 thrombocytopenia	Gr.4 CRS
7	45	Right renal pelvis and bladder	Atezolizumab	Paclitaxel	2	SD	19.68	AWD	Gr.4 anemia	–
8	65	Right renal pelvis	Pembrolizumab	–	2	PR	27.17	AWD	Gr.2 neutropenia Gr.2 anemia Gr.1 thrombocytopenia	Gr.2 eczema
9	66	Right renal pelvis	Atezolizumab	–	1	PR	15.54	AWD	Gr.4 neutropenia Gr.4 anemia Gr.1 thrombocytopenia	Gr.3 TB peritonitis Gr.4 TEN
10	74	Bladder	Pembrolizumab	–	2	PR	14.26	AWD	Gr.3 anemia Gr.1 thrombocytopenia Gr.2 anorexia	Gr.2 fatigue
11	35	Bladder	Pembrolizumab	–	1	PR	4.63	AWD	Gr.2 neutropenia Gr.2 anemia Gr.1 thrombocytopenia	–

OS, overall survival; AE, adverse event; PD, progressive disease; PR, partial response; SD, stable disease; AWD, alive with disease; DOD, dead of disease; Gr, grade; CRS, cytokine release syndrome; TB, tuberculosis; TEN, toxic epidermal necrolysis.

TABLE 3 | Adverse events in ESRD and non-ESRD group.

Adverse events	ESRD (%)	Non-ESRD (%)	*p* value
Any grade	11 (100)	84 (71.2)	0.04
Grade 3/4	7 (63.6)	42 (35.6)	0.07
Neutropenia	6 (54.5)	27 (22.9)	0.02
Grade 3/4	4 (36.4)	10 (8.5)	0.004
Anemia	11 (100)	54 (45.8)	0.001
Grade 3/4	6 (54.5)	32 (27.1)	0.07
Thrombocytopenia	8 (72.0)	43 (36.4)	0.02
Grade 3/4	1 (9.1)	16 (13.6)	0.68
Hepatitis	3 (27.3)	34 (28.8)	0.91
Fatigue	2 (18.2)		
Anorexia	3 (27.3)		
Skin*	2 (18.2)		
AE of specific interest			
Ascites	2 (18.2)		
TB reactivation	1 (9.1)		
TENS	1 (9.1)		
CRS-like syndrome	1 (9.1)		

AE, adverse event; TB, tuberculosis; TENS, toxic epidermal necrolysis; CRS, cytokine release syndrome; ESRD, end-stage renal disease.
**One TENS classified as grade 4 dermatologic toxicity.*

45.8%, $p = 0.001$) and thrombocytopenia (72.0 vs. 36.4%, $p = 0.02$) than non-ESRD patients. Except for hematologic toxicity, there was no new additional safety concerns emerged from this comparative study between ESRD and non-ESRD group.

Treatment Responses

The objective response rate (ORR) was significantly higher in the ESRD group than in the non-ESRD group (54.5 vs. 28.8%, p = 0.09). In terms of the disease control rate (DCR), the ESRD group benefited more (63.6%) than the non-ESRD group did (50.0%); in the ESRD group, six patients achieved partial response (54.5%), and one patient achieved stable disease status (9.1%). All details are provided in **Table 4**.

Survival Outcomes

The median PFS of patients in the ESRD and non-ESRD groups was 7.1 and 3.5 months, respectively (p = 0.42; the PFS curve is plotted in **Figure 2**). The median OS of patients in the ESRD group was not reached and was 15.4 months in the non-ESRD group (the OS curve is plotted in **Figure 3**). In the univariate analysis of OS, the

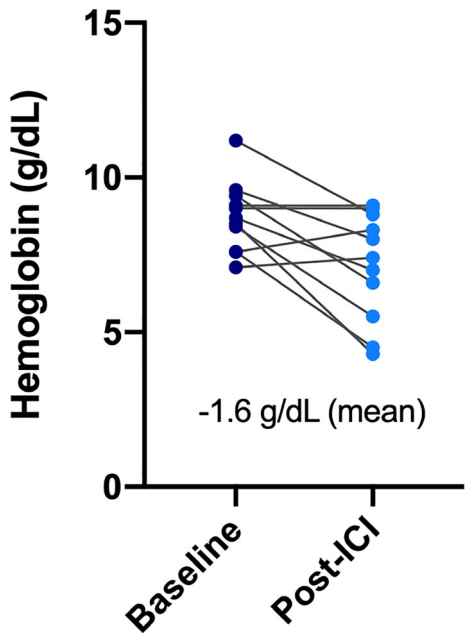

FIGURE 1 | Change of hemoglobin before and after ICIs administration in the ESRD group.

TABLE 4 | Treatment response.

	ESRD (%)	Non-ESRD (%)	*p* value
Complete response (CR)	0	15 (12.7)	
Partial response (PR)	6 (54.5)	19 (16.1)	
Stable disease (SD)	1 (9.1)	25 (21.2)	
Progressive disease (PD)	4 (36.4)	59 (50.0)	
Overall response rate (ORR)	6 (54.5)	34 (28.8)	0.09
Disease control rate (DCR)	7 (63.6)	59 (50.0)	0.53

ESRD, end-stage renal disease.

prognostic factors included ECOG (≥2 vs. <1; HR: 1.96; 95% CI: 1.06–3.65; p <0.03), leukocytosis (≥10,000/μl vs. <10,000/μL; HR: 3.80; 95% CI: 2.22–6.51; p <0.001), anemia (<10 g/dl vs. ≥10 g/dl; HR: 2.41; 95% CI: 1.43–4.04; p = 0.001) and NLR (≥5 vs. <5; HR: 3.93; 95% CI: 2.29–6.77; p <0.001). In the univariate analysis, a trend of survival benefits was observed for patients without liver metastasis (HR: 1.65; 95% CI: 0.92–2.98; p = 0.09) and without lung metastasis (HR: 1.59; 95% CI: 0.95–2.66; p = 0.08). After adjustments were made for all potential prognostic factors in the multivariate analysis, the only independent factor was leukocytosis (HR: 2.63; 95% CI: 1.23–5.63; p = 0.01) and NLR (HR: 2.91; 95% CI: 1.30–6.53; p = 0.01). All details are presented in **Table 5**.

DISCUSSION

The present study reports the treatment experience of 11 consecutive patients with ESRD who received ICIs for mUC. Although some unexpected AEs occurred, generally, in patients with ESRD, the ICIs were well tolerated without additional

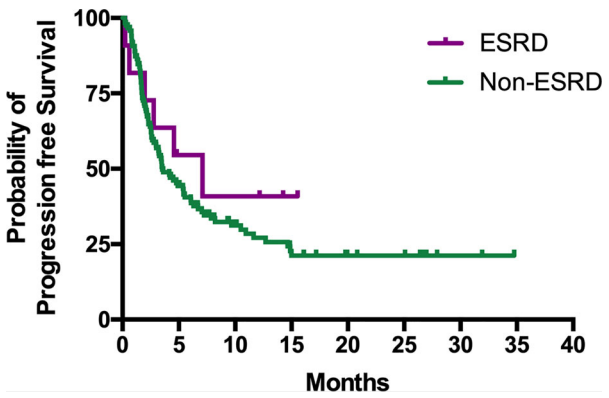

FIGURE 2 | Kaplan–Meier curves of PFS for mUC patients with or without ESRD receiving ICIs.

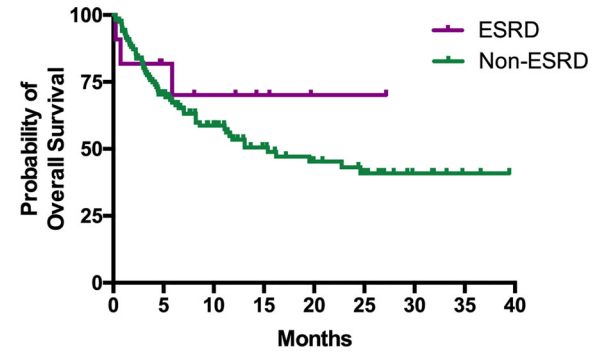

FIGURE 3 | Kaplan–Meier curves of OS for mUC patients with or without ESRD receiving ICIs.

toxicity. Furthermore, the major efficacy endpoints of ORR, PFS, and OS suggested benefits of ICI use in patients with ESRD. To our knowledge, this is the largest case series on the safety and efficacy of ICIs for patients with cancer who require maintenance hemodialysis. Our real-world data indicate that the administration of ICIs may be beneficial in such difficult treatment scenarios.

A few case reports and case series had examined the efficacy and safety of administrating ICIs in patients with ESRD on dialysis. In reviewing literature, only 41 patients had been reported; most of them were metastatic melanoma, NSCLC and renal cell carcinoma (RCC), only five cases were mUC (13–31) (**Table 6**) Vitale et al. reported eight ESRD patients with metastatic RCC who received dialysis (seven on hemodialysis, one on peritoneal dialysis) and nivolumab as cancer treatment. Only two patients (25%) experienced grade 3 AEs (diarrhea, asthenia, and anorexia), and five patients (62.5%) had grade 1–2 AEs, including cutaneous toxicities, anorexia, diarrhea, nausea, vomiting, arthralgia, and hematologic toxicities. These irAEs were appropriately managed with systemic corticosteroid and symptomatic treatment (15).

TABLE 5 | Univariate and multivariate analysis of overall survival.

Characteristics	Median OS	Univariate		Multivariate	
	(month)	HR (95% CI)	*p* value	HR (95% CI)	*p* value
Age (year)			0.50		0.19
<65	13.1	1		1	
≧65	22.7	0.84 (0.50–1.40)		0.65 (0.35–1.23)	
Gender			0.59		0.52
Female	15.4	1		1	
Male	19.5	0.87 (0.52–1.45)		1.26 (0.62–2.55)	
Primary tumor			0.21		0.28
UCB	22.7	1		1	
UTUC	11.9	1.42 (0.82–2.47)		1.45 (0.74–2.85)	
ECOG			0.03		0.35
0–1	16.2	1		1	
≧2	4.4	1.96 (1.06–3.65)		1.47 (0.66–3.29)	
ICI sequence					
1st line	19.5	1	0.37	1	0.14
2nd line	16.2	0.95 (0.46–1.95)	0.89	2.22 (0.93–5.28)	0.07
3rd line or later	5.2	1.69 (0.79–3.61)	0.18	0.83 (0.28–2.43)	0.73
ICI type			0.68		0.78
Anti-PD-1	15.4	1		1	
Anti-PD-L1	19.5	0.89 (0.52–1.54)		0.91 (0.45–1.83)	
Treatment partner					
Monotherapy	13.1	1	0.83	1	0.64
Chemotherapy	NR	0.84 (0.47–1.52)	0.57	0.85 (0.43–1.69)	0.64
Anti-CTLA-4	13.1	1.05 (0.41–2.68)	0.92	0.57 (0.15–2.12)	0.40
Visceral metastasis			0.29		0.91
No	16.2	1		1	
Yes	13.4	1.33 (0.81–2.29)		0.94 (0.29–3.05)	
Liver metastasis			0.09		0.30
No	22.7	1		1	
Yes	8.2	1.65 (0.92–2.98)		1.53 (0.68–3.42)	
Lung metastasis			0.08		0.17
No	NR	1		1	
Yes	8.6	1.59 (0.95–2.66)		1.95 (0.75–5.07)	
Bone metastasis			0.49		0.42
No	15.4	1		1	
Yes	8.6	1.24 (0.67–2.31)		0.72 (0.33–1.60)	
Leukocytosis			<0.001		0.01
WBC <10,000/μl	24.6	1		1	
WBC ≧10,000/μl	3.9	3.80 (2.22–6.51)		2.63 (1.23–5.63)	
Anemia			0.001		0.38
Hgb ≧10 g/dl	22.7	1		1	
Hgb <10 g/dl	4.4	2.41 (1.43–4.04)		1.45 (0.64–3.28)	
Neutrophil to lymphocyte ratio			<0.001		0.01
NLR <5	NR	1		1	
NLR ≧5	4.1	3.93 (2.29–6.77)		2.91(1.30–6.53)	

CTLA-4, cytotoxic T-lymphocyte-associated protein 4; ECOG, Eastern Cooperative Oncology Group; ESRD, end-stage renal disease; Hgb, hemoglobin; ICI, immune checkpoint inhibitor; OS, overall survival; PD-1, programmed cell death protein 1; NLR, neutrophil to lymphocyte ratio; NR, non-reach; UCB, urothelial cancer of the bladder; UTUC, upper tract urothelial carcinoma; WBC, while blood cell count.

Strohbehn et al. presented a brief report of treatment response and side effects in 19 ESRD patients received ICI therapy. However, the study population were quite heterogeneous in cancer types (six genitourinary cancer, three melanoma, three merkel cell carcinoma, three head and neck cancer), ICI regimen (90% anti-PD-1/PD-L1, 5% anti-CTLA-4 and 5% combined anti-PD-1/CTLA-4), and dialysis modality (79% hemodialysis, 21% peritoneal dialysis), which limited to achieve a definite conclusion (32). Compared with previous reports, our study revealed more hematologic AEs, 36.4% of which were grade 3–4 neutropenia. However, a standard chemotherapy regimen, either of gemcitabine plus cisplatin or MVAC (methotrexate, vinblastine, doxorubicin, and cisplatin), caused more than 70% of patients to experience grade 3–4 neutropenia (3). Given concerns related to neutropenia and risk of infection, ICI is a safe treatment for patients with mUC and ESRD.

We also reported some notable irAEs in this study. A 65-year-old woman had disseminated tuberculosis reactivation and TEN after anti-PD-L1 administration. The patient fully recovered from TEN after systemic steroid administration and intensive skin care, and her tuberculosis was appropriately controlled by anti-tuberculosis agents. It is worthwhile to highlight the relationship between ICI use and TB reactivation. Barber et al. hypothesized that ICIs may boost T_H1 function and increase the

TABLE 6 | Summary of 41 published cases of the use of immune checkpoint inhibitors in dialysis patients.

Reference	n	Age	Dialysis	Cancer	ICI	Response	Toxicity
Cavalcante et al. (14)	2	56,69	HD	Melanoma	Ipilimumab	CR (1),PR (1)	G2 fatigue, G1-2 pruritus, G3 pemphigoid rash
Boils et al. (16)	1	74	HD*	NSCLC-SCC	Nivolumab	NA	Renal allograft rejection (3 doses)
Ong et al. (17)	1	76	HD*	Melanoma	Nivolumab	PR	Renal allograft rejection (8 days)
Carlo et al. (18)	1	77	HD	mRCC	Nivolumab	PR	Pseudo-progression with respiratory failure
Chang et al. (19)	1	63	HD	Melanoma	Pembrolizumab	CR	G1 fatigue
Lipson et al. (20)	1	57	HD*	Cutaneous SCC	Pembrolizumab	PR (85% reduction)	Renal allograft rejection (2 months)
Spain et al. (21)	1	48	HD*	Melanoma	Ipilimumab (1) Nivolumab (2)	PR	Renal allograft rejection (8 days of nivolumab)
Alhamad et al. (22)	1	68	HD*	Melanoma	Ipilimumab (1) Pembrolizumab (2)	Progression (1) NA (Pembrolizumab)	Renal allograft rejection (3 weeks of pembrolizumab)
Jose et al. (23)	1	40	HD/PD*	Melanoma†	Ipilimumab	Progression	Renal allograft rejection (after two cycles)
Tabei et al. (24)	1	49	HD	RCC	Nivolumab	PR	No AEs
Boyle et al. (25)	1	57	HD	Melanoma‡	Nivolumab	PR	No AEs
Park and Daniels (26)	4	66–71	HD (3) PD (1)	RCC (2) Cutaneous SCC (2)	Nivolumab (2) Pembrolizumab (2)	SD (1), PR (3)	G2 rash, G2 fatigue G3 pneumonitis, G4 encephalitis¶
Ishizuka et al. (27)	1	66	HD	NSCLC-SCC	Pembrolizumab	PR	G1 rash
Ansari et al. (28)	1	72	HD	RCC	Nivolumab	PR	No G2-4 AEs
Cheun et al. (13)	3	64–68	HD	RCC (2) Renal pelvic UC (1)	Nivolumab (2) Atezolizumab (1)	PR (1), SD (1), Progression (1)	G2 pneumonitis
Vitale et al. (15)	8	51–77	HD (7) PD (1)	RCC (8)	Nivolumab	PR (1), SD (5), Progression (2)	G2 Nausea, G1 Vomiting, G2-3 Diarrhea G2-3 Anorexia, G1-3 Asthenia, G1 Arthralgia G1-2 Cutaneous, G1-2 Hematologic
Parisi et al. (29)	1	NA	HD	UC§	Atezolizumab	PR	G1 itching, G1 asthenia G1 nausea, G1 dysgeusia, G1 constipation
Osmán-García et al. (30)	3	60–77	HD (2) PD (1)	RCC	Nivolumab	PR (2), PD (1)	No G2-4 AEs
Hirsch et al. (31)	8	35–83	HD (7) PD (1)	UC (3), HCC (1), CCA (1), HL (1), NET (1), RCC (1)	Pembrolizumab (4) Nivolumab (3)‖ lipilimumab (1)‖ Atezolizumab (1)	SD (3) Progression (5)	Dermatitis (1) Renal allograft rejection (1)
Current study	11	35–82	HD	UC (11)	Pembrolizumab (6) Nivolumab (2) Atezolizumab (3)	PR (6), SD (1) Progression (4)	G1-4 cytopenia, G1 hepatitis, G2-3 ascites G4 CRS, G3 TB peritonitis, G4 TEN G1-3 anorexia, G1-2 fatigue, G2 eczema

n, case number; NA, not available; HD, hemodialysis; PD, peritoneal dialysis; NSCLC, non-small cell lung cancer; SCC, squamous cell carcinoma; RCC, renal cell carcinoma; UC, urothelial carcinoma; HCC, hepatocellular carcinoma; CCA, cholangiocarcinoma; HL, Hodgkin lymphoma; NET, neuroendocrine tumor; ICI, immune checkpoint inhibitor; CR, complete response; PR, partial response; SD; stable disease; G, grade; AE, adverse event; CRS, cytokine release syndrome; TB, tuberculosis; TEN, toxic epidermal necrolysis.

**Dialysis dependence after renal graft rejection.*

†Choroid melanoma.

‡Donor derived melanoma.

§Bladder sarcomatoid carcinoma.

‖One patient received both nivolumab and ipilimumab.

¶In this case report, one patient died from possible treatment-related causes.

level of interferon γ-producing *Mycobacterium tuberculosis*-specific CD4 T-cells in the blood (33). The pathogenesis of TEN is also related to cell-mediated cytotoxic reactions and the clonal expansion of drug-specific T-cells with cytotoxicity against keratinocytes directly and indirectly through the recruitment of other cells (34). Cavalcante et al. reported that a patient with ESRD developed a grade 3 pemphigoid rash and bullous lesion after ipilimumab administration, achieving a complete response (14). Further studies are required to clarify the incidence of severe dermatologic irAEs in patients with ESRD and to elucidate the relationship between the intensity of cell-mediated cytotoxic reactions and the durable response rate.

One patient in our study presented with daily spiking fever, hypotension, altered mental status, hypoxia, and respiratory failure after administration of the first cycle of anti-PD-1 treatment. The clinical manifestation was thought to be severe sepsis but also resembled an unusual form of CRS, an inflammatory systemic disorder resulting from an overwhelming elevation of cytokine levels and T-cell engagement and proliferation. CRS severity can range from mild symptoms to a fulminant disease with multiple organ failure and death. CRS has been observed to be triggered by several monoclonal antibodies, systemic interleukin-2, and more recently, the CD19-CD3 chimeric antigen receptor T-cell therapy (35). A few case reports have detailed life-threatening CRS in patients after the administration of ICIs, with occurrences ranging from cycles 1 to 17 (36–39). The culprit medications were anti-PD-1 and anti-LAG-3. Alexander et al. reported the case of a patient with stage IV melanoma who received nivolumab on cycle 17 and had a CRS episode; it was controlled by tocilizumab initially, but the patient died 6 weeks later because of another CRS episode (39). Seth et al. also reported a patient with alveolar soft part sarcoma who received nivolumab and had a CRS event that was resolved by tocilizumab and corticosteroids (38). Although CRS is an uncommon complication associated with ICIs, early

recognition and prompt management of CRS is crucial owing to its high mortality risk.

Among patients with ESRD in this report, ICIs conferred a significantly higher ORR and better DCR on patients with ERSD than those without. The response rate benefits reflect the trends of better PFS and median OS. Our results showed that the efficacy of ICIs for patients with ESRD was not inferior to that for patients without ESRD. A possible explanation of the superior antitumor efficacy of ICIs may be related to pharmacokinetics. Renal failure or hemodialysis seems to have no effect on the pharmacokinetics of ICIs, possibly because the clearance of ICIs is governed by numerous physiological mechanisms; this clearance predominantly occurs through nonspecific degradation within plasma and tissues. This nonspecific route of degradation reduces the influence of age, hepatic impairment, and renal failure on clearance (40). Considering the large molecular weights of ICIs (nivolumab: 146 kDa; ipilimumab: 148 kDa; pembrolizumab: 149 kDa; atezolizumab: 145 kDa), which cannot penetrate dialysis pores, drug removal and elimination through hemodialysis are unlikely (13). The pharmacokinetic characteristics of ICIs, which are unaffected by renal failure and hemodialysis, were also demonstrated by a similar incidence of AEs among patients in the ESRD and non-ESRD groups.

This study had some inevitable limitations owing to its retrospective nature; furthermore, it was limited by the relatively small sample size of the ESRD group. However, it is difficult to conduct a prospective clinical trial through recruiting patients with advanced UC or mUC to receive ICIs. The difficulty is not simply due to sample size; additionally, ESRD may develop during the treatment period among such patients with UC. Finally, the study had unpreventable bias in terms of the choice of ICIs being governed by physicians' decisions, patients' financial considerations, and the instructions of the National Health Insurance system in Taiwan. However, our results demonstrated that the administration of ICIs in patients with ESRD resulted in them having a better survival trend than did patients without ESRD, and no notable safety concerns arose.

In conclusion, our study revealed that administration of ICIs in patients with mUC and ESRD demonstrated a modest antitumor activity, and should be used with caution for increasing risk of hematologic toxicity. Further confirmatory studies are required to validate our findings.

DATA AVAILABILITY STATEMENT

The raw data supporting the conclusions of this article will be made available by the authors, without undue reservation.

ETHICS STATEMENT

The studies involving human participants were reviewed and approved by Institutional Review Board of Chang Gung Medical Foundation. Written informed consent for participation was not required for this study in accordance with the national legislation and the institutional requirements.

AUTHOR CONTRIBUTIONS

M-CK analyzed and interpreted data, prepared the tables, and wrote the original manuscript. Y-LS designed the conceptualization and methodology, prepared the figures, and reviewed and edited the manuscript. P-JS, C-CH, H-LL, T-JC, S-HL, C-CW, T-TL, Y-TC, and C-HK contributed the resources. All authors contributed to the article and approved the submitted version.

ACKNOWLEDGMENTS

We thank the multidisciplinary team of the genitourinary cancer at our hospital for their generous assistance and cooperation. The study was supported in part by a grant from Chang Gung Memorial Hospital, Kaohsiung, Taiwan (CMRPG8H1381, CMRPG8G1432). This manuscript was edited by Wallace Academic Editing.

SUPPLEMENTARY MATERIAL

The Supplementary Material for this article can be found online at: https://www.frontiersin.org/articles/10.3389/fonc.2020.584834/full#supplementary-material

REFERENCES

1. Ferlay J, Soerjomataram I, Dikshit R, Eser S, Mathers C, Rebelo M, et al. Cancer incidence and mortality worldwide: Sources, methods and major patterns in GLOBOCAN 2012. *Int J Cancer* (2014) 136:E359–86. doi: 10.1002/ijc.29210
2. Mari A, Campi R, Tellini R, Gandaglia G, Albisinni S, Abufaraj M, et al. Patterns and predictors of recurrence after open radical cystectomy for bladder cancer: a comprehensive review of the literature. *World J Urol* (2018) 36:157–70. doi: 10.1007/s00345-017-2115-4
3. Maase H, Hansen SW, Roberts JT, Dogliotti L, Oliver T, Moore MJ, et al. Gemcitabine and Cisplatin Versus Methotrexate, Vinblastine, Doxorubicin, and Cisplatin in Advanced or Metastatic Bladder Cancer: Results of a Large, Randomized, Multinational, Multicenter, Phase III Study. *J Clin Oncol* (2000) 17(17):3068–77. doi: 10.1200/JCO.2000.18.17.3068
4. Bellmunt J, de Wit R, Vaughn DJ, Fradet Y, Lee JL, Fong L, et al. Pembrolizumab as Second-Line Therapy for Advanced Urothelial Carcinoma. *N Engl J Med* (2017) 376:1015–26. doi: 10.1056/NEJMoa1613683
5. Rosenberg JE, Hoffman-Censits J, Powles T, van der Heijden MS, Balar AV, Necchi A, et al. Atezolizumab in patients with locally advanced and metastatic urothelial carcinoma who have progressed following treatment with platinum-based chemotherapy: a single-arm, multicentre, phase 2 trial. *Lancet* (2016) 387(10031):1909–20. doi: 10.1016/S0140-6736(16)00561-4
6. Sharma P, Retz M, Siefker-Radtke A, Baron A, Necchi A, Bedke J, et al. Nivolumab in metastatic urothelial carcinoma after platinum therapy (CheckMate 275): a multicentre, single-arm, phase 2 trial. *Lancet Oncol* (2017) 18(3):312–22. doi: 10.1016/S1470-2045(17)30065-7
7. Powles T, O'Donnell PH, Massard C, Arkenau HT, Friedlander TW, Hoimes C, et al. Updated efficacy and tolerability of durvalumab in locally advanced or metastatic urothelial carcinoma [abstract]. *J Clin Oncol* (2018) 35. doi: 10.1200/JCO.2017.35.6_suppl.286

8. Apolo AB, Infante JR, Balmanoukian A, Patel MR, Wang D, Kelly K, et al. Avelumab, an Anti-Programmed Death-Ligand 1 Antibody, In Patients With Refractory Metastatic Urothelial Carcinoma: Results From a Multicenter, Phase Ib Study. *J Clin Oncol* (2017) 35(19):2117–24. doi: 10.1200/JCO.2016.71.6795
9. Gómez De Liaño A, Duran I. The continuing role of chemotherapy in the management of advanced urothelial cancer. *Ther Adv Urol* (2018) 10 (12):455–80. doi: 10.1177/1756287218814100
10. Balar AV, Galsky MD, Rosenberg JE, Powles T, Petrylak DP, Bellmunt J, et al. Atezolizumab as first-line treatment in cisplatin-ineligible patients with locally advanced and metastatic urothelial carcinoma: a single-arm, multicentre, phase 2 trial. *Lancet* (2017) 389:67–76. doi: 10.1016/S0140-6736(16)32455-2
11. Hung PH, Tsai HB, Hung KY, Muo CH, Chung MC, Chang CH, et al. Patients with urothelial carcinoma have poor renal outcome regardless of whether they receive nephrouretectomy. *Oncotarget* (2016) 7(38):61679–89. doi: 10.18632/oncotarget.11223
12. Wang SM, Lai MN, Chen PC, Wang JD. Increased risk of urothelial cancer in young and middle aged patients with end-stage renal disease. *J Formos Med Assoc* (2015) 114:52–7. doi: 10.1016/j.jfma.2013.10.022
13. Cheun H, Kim M, Lee H, Oh KH, Keam B. Safety and efficacy of immune checkpoint inhibitors for end-stage renal disease patients undergoing dialysis: a retrospective case series and literature review. *Invest New Drugs* (2019) 37 (3):579–83. doi: 10.1007/s10637-018-0673-y
14. Cavalcante L, Amin A, Lutzky J. Ipilimumab was safe and effective in two patients with metastatic melanoma and end-stage renal disease. *Cancer Manage Res* (2015) 7:47–50. doi: 10.2147/CMAR.S73389
15. Vitale MG, Baldessari C, Milella M, Buti S, Militello AM, Di Girolamo S, et al. Immunotherapy in Dialysis-Dependent Cancer Patients: Our Experience in Patients With Metastatic Renal Cell Carcinoma and a Review of the Literature. *Clin Genitourin Cancer* (2019) 17(5):E903–8. doi: 10.1016/j.clgc.2019.06.009
16. Postow MA, Callahan MK, Wolchok JD. Use of the PD-1 Pathway Inhibitor Nivolumab in a Renal Transplant Patient With Malignancy. *Am J Transplant* (2016) 16:2496–7. doi: 10.1111/ajt.13786
17. Ong M, Ibrahim AM, Bourassa-Blanchette S, Canil C, Fairhead T, Knoll G, et al. Antitumor activity of nivolumab on hemodialysis after renal allograft rejection. *J Immunother Cancer* (2016) 4:64. doi: 10.1186/s40425-016-0171-8
18. Carlo MI, Feldman DR. Response to Nivolumab in a Patient With Metastatic Clear Cell Renal Cell Carcinoma and End-stage Renal Disease on Dialysis. *Eur Urol* (2016) 70(6):1082–3. doi: 10.1016/j.eururo.2016.05.040
19. Chang R, Shirai K. Safety and efficacy of pembrolizumab in a patient with advanced melanoma on haemodialysis. *BMJ Case Rep* (2016) 2016: bcr2016216426. doi: 10.1136/bcr-2016-216426
20. Lipson EJ, Bagnasco SM, Moore JJr, Jang S, Patel MJ, Zachary AA, et al. Tumor Regression and Allograft Rejection after Administration of Anti-PD-1. *N Engl J Med* (2016) 374(9):896–8. doi: 10.1056/NEJMc1509268
21. Spain L, Higgins R, Gopalakrishnan K, Turajlic S, Gore M, Larkin J. Acute renal allograft rejection after immune checkpoint inhibitor therapy for metastatic melanoma. *Ann Oncol* (2016) 27(6):1135–7. doi: 10.1093/annonc/mdw130
22. Alhamad T, Venkatachalam K, Linette GP, Brennan DC. Checkpoint Inhibitors in Kidney Transplant Recipients and the Potential Risk of Rejection. *Am J Transplant* (2016) 16:1332–3. doi: 10.1111/ajt.13711
23. Jose A, Yiannoullou P, Bhutani S, Denley H, Morton M, Picton M, et al. Renal Allograft Failure After Ipilimumab Therapy for Metastatic Melanoma: A Case Report and Review of the Literature. *Transplant Proc* (2016) 48(9):3137–41. doi: 10.1016/j.transproceed.2016.07.019
24. Tabei T, Natsume I, Kobayashi K. Successful treatment of metastatic clear cell carcinoma with nivolumab in a patient receiving dialysis treatment. *Int J Urol* (2017) 24(9):708–10. doi: 10.1111/iju.13420
25. Boyle SM, Ali N, Olszanski AJ, Park DJ, Xiao G, Guy S, et al. Donor-Derived Metastatic Melanoma and Checkpoint Inhibition. *Transplant Proc* (2017) 49 (7):1551–4. doi: 10.1016/j.transproceed.2017.06.007
26. Park S, Daniels GA. Anti-PD-1 therapy in patients with end-stage renal disease on dialysis: A single-center case series. *J Clin Oncol* (2017) 35 (15_suppl):e14553–3. doi: 10.1200/JCO.2017.35.15_suppl.e14553
27. Ishizuka S, Sakata S, Yoshida C, Takaki A, Saeki S, Nakamura K, et al. Successful treatment by pembrolizumab in a patient with end-stage renal disease with advanced non-small cell lung cancer and high PD-L1 expression. *Respir Investig* (2018) 56(4):361–4. doi: 10.1016/j.resinv.2018.03.005
28. Ansari J, Ali M, Farrag A, Ali AM, Alhamad A. Efficacy of Nivolumab in a Patient with Metastatic Renal Cell Carcinoma and End-Stage Renal Disease on Dialysis: Case Report and Literature Review. *Case Rep Immunol* (2018) 2018:1623957. doi: 10.1155/2018/1623957
29. Parisi A, Cortellini A, Cannita K, Bersanelli M, Ficorella C. Safe Administration of anti-PD-L1 Atezolizumab in a Patient with Metastatic Urothelial Cell Carcinoma and End-Stage Renal Disease on Dialysis. *Case Rep Oncol Med* (2019) 2019:3452762. doi: 10.1155/2019/3452762
30. Osmán-García I, Congregado-Ruiz CB, Lendínez-Cano G, Baena-Villamarin C, Conde-Sanchez JM, Medina-López RA. Outcomes and Safety of Biweekly and Monthly Nivolumab in Patients with Metastatic Renal Cell Carcinoma and Dialysis: Three Case Reports and Literature Review. *Urol Int* (2020) 104 (3-4):323–6. doi: 10.1159/000504515
31. Hirsch JS, Wanchoo R, Ng JH, Khanin Y, Jhaveri KD. Use of Immune Checkpoint Inhibitors in End Stage Kidney Disease Patients, Single Center Experience and Review of the Literature. *Kidney360* (2020) 1(5):399–402. doi: 10.34067/KID.0000422020
32. Strohbehn IA, Lee M, Seethapathy H, Chute D, Rahma O, Guidon A, et al. Safety and Efficacy of Immune Checkpoint Inhibitors in Patients on Dialysis: A Retrospective Case Series. *Am J Kidney Dis* (2020) 76(2):299–302. doi: 10.1053/j.ajkd.2020.02.451
33. Barber DL, Sakai S, Kudchadkar RR, Fling SP, Day TA, Vergara JA, et al. Tuberculosis following PD-1 blockade for cancer immunotherapy. *Sci Transl Med* (2019) 11(475):eaat2702. doi: 10.1126/scitranslmed.aat2702
34. Ko TM, Chung WH, Wei CY, Shih HY, Chen JK, Lin CH, et al. Shared and restricted T-cell receptor use is crucial for carbamazepine-induced Stevens-Johnson syndrome. *J Allergy Clin Immunol* (2011) 128(6):1266–76.e11. doi: 10.1016/j.jaci.2011.08.013
35. Shimabukuro-Vornhagen A, Gödel P, Subklewe M, Stemmler HJ, Schlößer HA, Schlaak M, et al. Cytokine release syndrome. *J ImmunoTher Cancer* (2018) 6:56. doi: 10.1186/s40425-018-0343-9
36. Dimitriou F, Matter AV, Mangana J, Urosevic-Maiwald M, Micaletto S, Braun RP, et al. Cytokine Release Syndrome During Sequential Treatment With Immune Checkpoint Inhibitors and Kinase Inhibitors for Metastatic Melanoma. *J Immunother* (2019) 42:29–32. doi: 10.1097/CJI.0000000000000236
37. Oda H, Ishihara M, Miyahara Y, Nakamura J, Kozuka Y, Iwasa M, et al. First Case of Cytokine Release Syndrome after Nivolumab for Gastric Cancer. *Case Rep Oncol* (2019) 12:147–56. doi: 10.1159/000496933
38. Rotz SJ, Leino D, Szabo S, Mangino JL, Turpin BK, Pressey JG. Severe cytokine release syndrome in a patient receiving PD-1-directed therapy. *Pediatr Blood Cancer* (2017) e26642. doi: 10.1002/pbc.26642
39. Slota A, Khan R, Rahman A, Warner EA. Cytokine Release Syndrome As a Rare Complication of Nivolumab: A Case Report. *Blood* (2019) 134 (Supplement_1):5630. doi: 10.1182/blood-2019-127586
40. Centanni M, Moes DJAR, Trocóniz I, Ciccolini J, van Hasselt JGC. Clinical Pharmacokinetics and Pharmacodynamics of Immune Checkpoint Inhibitors. *Clin Pharmacokinet* (2019) 58:835–57. doi: 10.1007/s40262-019-00748-2

Conflict of Interest: The authors declare that the research was conducted in the absence of any commercial or financial relationships that could be construed as a potential conflict of interest.

frontiers in Oncology

CASE REPORT
published: 29 April 2021
doi: 10.3389/fonc.2021.679177

Case Report: Immune Checkpoint Inhibitor-Induced Exuberant Tumor Inflammation With Accelerated Clinical Deterioration in Metastatic Renal Cell Carcinoma

Dharmesh Gopalakrishnan[1*†], *Rohit K. Jain*[2†], *Laurie Herbst*[1], *Marcus Sikorski*[1], *Silpa Mandava*[1], *Gissou Azabdaftari*[3], *Bo Xu*[3], *Charles LeVea*[3], *Kevin Robillard*[1], *Marc S. Ernstoff*[4] *and Saby George*[1]

[1] Department of Medicine, Roswell Park Comprehensive Cancer Center, Buffalo, NY, United States, [2] Department of Genitourinary Oncology, Moffitt Cancer Center and Research Institute, Tampa, FL, United States, [3] Department of Pathology, Roswell Park Comprehensive Cancer Center, Buffalo, NY, United States, [4] ImmunoOncology Branch, Developmental Therapeutics Program, National Cancer Institute, Bethesda, MD, United States

OPEN ACCESS

Edited by:
Walter J. Storkus,
University of Pittsburgh, United States

Reviewed by:
Benjamin A. Teply,
University of Nebraska Medical Center, United States
Katy Beckermann,
Vanderbilt University, United States

***Correspondence:**
Dharmesh Gopalakrishnan
dharmesh.gopalakrishnan@roswellpark.org

[†]These authors share first authorship

Specialty section:
This article was submitted to Genitourinary Oncology, a section of the journal Frontiers in Oncology

Received: 11 March 2021
Accepted: 12 April 2021
Published: 29 April 2021

Citation:
Gopalakrishnan D, Jain RK, Herbst L, Sikorski M, Mandava S, Azabdaftari G, Xu B, LeVea C, Robillard K, Ernstoff MS and George S (2021) Case Report: Immune Checkpoint Inhibitor-Induced Exuberant Tumor Inflammation With Accelerated Clinical Deterioration in Metastatic Renal Cell Carcinoma. Front. Oncol. 11:679177. doi: 10.3389/fonc.2021.679177

Immune checkpoint inhibitors (ICIs) have revolutionized cancer therapy. Nivolumab, an anti-PD-1 monoclonal antibody, markedly improved overall survival in advanced renal cell carcinoma (RCC). However, ICIs can rarely trigger massive inflammation, a phenomenon characterized by rapid acceleration in radiographic tumor growth, the mechanisms underlying which are largely unknown. We report three patients with metastatic RCC who experienced rapid radiographic progression and clinical deterioration following treatment with nivolumab. However, histological analysis revealed no viable cancer despite the evidence of radiological progression. Instead, extensive necrosis and lymphohistiocytic infiltration were noted, as described previously in patients with ICI-induced pseudoprogression. Based on these observations, we postulate that exuberant antitumor inflammatory responses may contribute to adverse clinical outcomes in some patients with ICI-induced radiographic progression. Prospective studies incorporating tumor biopsies may shed more light on this rare phenomenon.

Keywords: renal-cell carcinoma, immune checkpoint inhibitor, tumor inflammation, nivolumab, pseudoprogression

BACKGROUND

Monoclonal antibodies against programmed cell death protein-1(PD-1) and other co-inhibitory immune checkpoints act by reinvigorating antitumor effector T-cell responses (1). Nivolumab, a fully human Ig4 anti-PD-1 antibody, was demonstrated to significantly improve overall survival compared to everolimus among patients with previously treated clear cell RCC (RCC) in CheckMate-025, a phase 3 randomized open-label trial (2). Immune checkpoint inhibitors (ICIs) can occasionally lead to atypical responses such as pseudoprogression and hyperprogression. Pseudoprogression is defined as a transient radiological worsening followed by shrinkage of tumors with continued therapy (3). This phenomenon partly explains the benefit from treatment beyond

radiological progression in patients who do not experience overt clinical deterioration (4, 5). A small minority of patients experience a more dramatic acceleration in tumor growth along with rapid clinical deterioration when exposed to ICIs, a phenomenon termed hyperprogression (3, 6). The mechanisms underlying ICI-related hyperprogressive disease remain poorly defined. We describe three patients with metastatic RCC who experienced rapid radiographic progression on nivolumab and analyze their tumor histologies. This study was approved by our Institutional Review Board (BDR No. 120019) and Informed consent was obtained from the next of kin.

CASE PRESENTATION

Case 1: A 68-year-old male who underwent left radical nephrectomy for a 10.5 cm pT3aNx, Fuhrman grade 2, clear cell RCC, developed radiographic recurrence in the nephrectomy bed a year later. Over the next 4.5 years, he was treated sequentially with sunitinib, axitinib, everolimus, and pazopanib. He also underwent metastasectomy with excision of retroperitoneal masses, resection of the diaphragm, and splenectomy. He also received palliative radiation after T10-T11 laminectomy for epidural metastasis with spinal cord compression. He was eventually started on nivolumab 3mg/kg every 2 weeks. Staging scans at this time showed lung, liver, omental and skeletal metastases. Also noted was a small anterior right thigh intramuscular lesion which had been stable for several preceding months. Follow-up CT scans after 6 doses of nivolumab showed marked enlargement of the right thigh intramuscular mass to 4.0 x 5.4 cm with contrast enhancement (**Figure 1A**), but stable disease in the lungs, liver, bones, omentum, and the nephrectomy bed. A dedicated CT scan of the right thigh showed that the mass involved the entire length of the anterior muscle compartment. Core biopsies, performed to rule out extremity soft tissue sarcoma, revealed minute fragments of fibrous proliferation with mixed inflammatory infiltrate containing plasma cells, $CD3^+/CD5^+$ lymphocytes and $CD68^+$ histiocytes, with no evidence of viable tumor cells (**Figures 1B–D** and **Table 1**). Patient received 6 more doses of nivolumab before developing immune-related encephalitis, with no evidence of brain parenchymal or leptomeningeal metastases. This was

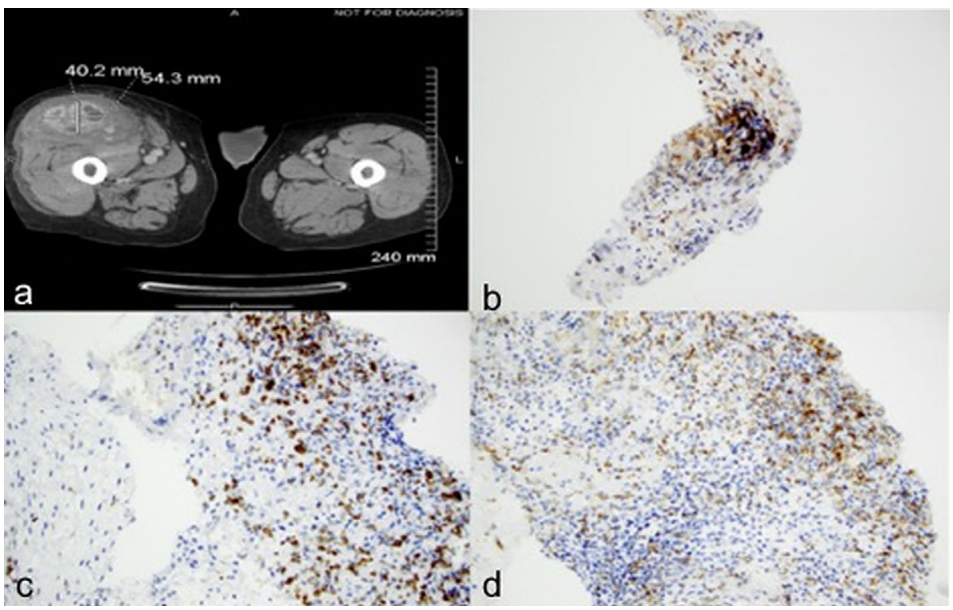

FIGURE 1 | Case 1 demonstrating **(A)** Increase in size of right thigh mass **(B)** CD3 positive **(C)** CD5 positive **(D)** CD 68 positive immunohistochemical staining.

TABLE 1 | Description of clinical and pathological characteristics of the three patients.

	Age/Sex	Prior systemic therapies	Type of ICI	Site(s) of hyperprogression	Biopsy site	Immunohistochemistry
Case 1	68/M	Sunitinib, Axitinib, Everolimus, Pazopanib	Nivolumab	Right thigh muscle	Thigh	$CD3^+$, $CD4^+$, $CD5^+$ lymphocytes $CD68^+$ histiocytes $PAX8^-$, CK AE1/3$^-$, S100$^-$, Desmin$^-$
Case 2	72/M	Sunitinib, Axitinib, Everolimus	Nivolumab	Colon, lung, lymph nodes, liver, adrenal	Colon	$CD3^+$, $CD4^+$, $CD5^-$ lymphocytes $CD68^+$ histiocytes $PAX8^-$, $CD10^-$, Renal Cell$^-$
Case 3	70/M	Sunitinib, Everolimus, Axitinib, Sorafenib	Nivolumab	Lymph nodes, liver, adrenal, stomach	Stomach	Not performed

treated with steroids, intravenous immunoglobulin, and rituximab with improvement. Though restaging studies showed stable disease, he was transitioned to hospice care due to marked deterioration in performance status.

Case 2: A 72-year-old male underwent left radical nephrectomy for a 7.5 cm pT3aNx, Fuhrman grade 3, clear cell RCC. CT scans 9 months later showed enlarging bilateral pulmonary nodules, biopsy of which confirmed metastatic RCC. Over the next two years he was treated with sunitinib, axitinib, and everolimus on various clinical trials. Eventually, due to disease progression, he was initiated on nivolumab 3 mg/kg every 2 weeks. Staging scans at this time revealed multiple bilateral pulmonary nodules, an enlarged left external iliac lymph node, and a small descending colon mass. Follow up CT after 6 doses of nivolumab showed interval worsening of lung metastases, left hilar adenopathy, new liver and right adrenal metastases, and marked enlargement of the descending colon mass from 2.1 x 3.1 cm to 8.8 x 10.6 cm (**Figures 2A, B**). He later developed bloody stools with left lower quadrant abdominal pain. Colonoscopy revealed a large nearly-obstructing mass in the descending colon, biopsies of which showed necrosis, acute and chronic inflammation with fibrin, but no evidence of viable malignancy. Immunohistochemistry revealed $CD4^+$ infiltrating lymphocytes and $CD68^+$ histiocytes (**Figures 2C, D** and **Table 1**). After recovery from the acute event, he received 3 more treatments with nivolumab but experienced marked decline in performance status before subsequent restaging, and eventually opted for hospice care.

Case 3: A 70-year-old male presented with abdominal pain and gastrointestinal bleeding and was found to have a large fatty tumor in the gastric body and a bulky lobulated mass in the superior pole of left kidney. He underwent resection of the gastric mass and a left radical nephrectomy. Pathology on the former showed a lipoma while nephrectomy revealed a 7.2 cm pT3aNx, Fuhrman grade 2, clear cell RCC. CT scans three years later revealed a solitary left lower lobe lung nodule, which was biopsied to confirm RCC, and treated with VATS resection. MRI brain 6 months later revealed a large temporal lobe lesion which was resected followed by gamma knife radiosurgery to the resection cavity. He then developed another brain lesion 4 months later and underwent a second gamma knife treatment. Subsequently, he received multiple systemic therapies including sunitinib, everolimus, axitinib, and sorafenib over the subsequent 4.5 years but had interval progression in hepatic, right adrenal and subcarinal lymph node metastases. Nivolumab was then initiated at 3 mg/Kg every 2 weeks. CT scans after 6 doses demonstrated interval increase in mediastinal/hilar lymphadenopathy, right adrenal gland and development of new hypodense liver lesions. There was also marked interval enlargement of a multilobular mass tethered to the gastric wall, from 1.3 x 1.5 cm to 5.0 x 7.0 cm, concerning for metastasis versus a second primary cancer (**Figures 3A, B**). Upper endoscopy demonstrated a large, bulky mass in the proximal stomach, highly suggestive of malignancy. However, biopsies revealed only extensive necrosis and inflammatory changes with focal granulation tissue response, and no evidence of viable

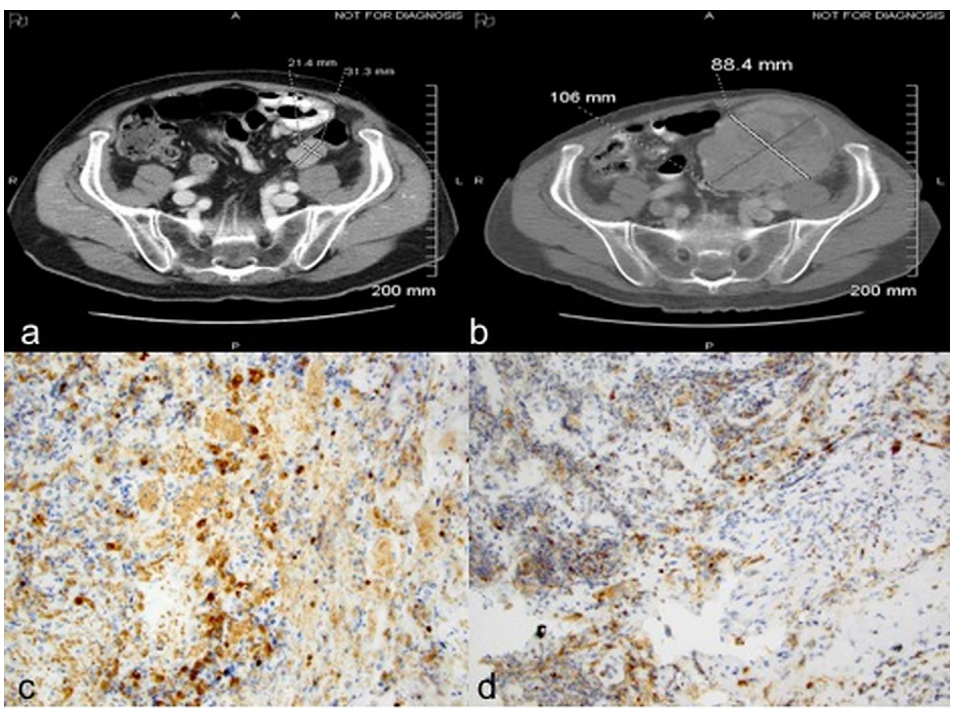

FIGURE 2 | Case 2 demonstrating descending colon mass before **(A)** and after **(B)** nivolumab treatment; **(C)** CD4 positive **(D)** CD 68 positive immunohistochemical staining.

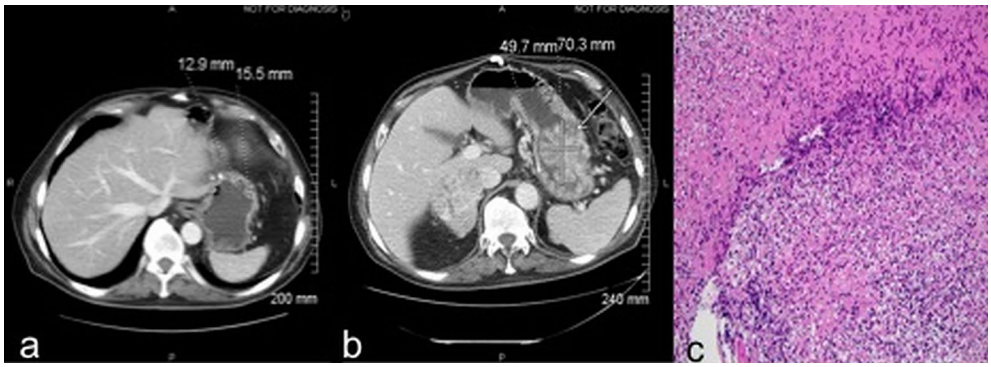

FIGURE 3 | Case 3 demonstrating stomach mass before **(A)** and after **(B)** nivolumab treatment **(C)** extensive necrosis with no viable tumor (H&E, x100).

malignancy (**Figure 3C**). He then received 6 more doses of nivolumab and follow up imaging showed disease progression within the hepatic, splenic and adrenal metastases as well as further enlargement of the gastric mass, thus nivolumab had to be discontinued. The patient was eventually transitioned to hospice care due to rapidly deteriorating performance status.

DISCUSSION

PD-1 and other checkpoints are critical to tumor-induced immune evasion, and antibodies against immune checkpoints have emerged as principal tools in the therapeutic arsenal against many cancers (1). While on ICIs, differentiating normal tumor progression from atypical responses, such as pseudoprogression and hyperprogression, can prove to be challenging. Pseudoprogression is characterized by an initial increase in tumor size or appearance of new lesions followed by tumor regression and clinical benefit with continued treatment (4, 6). The underlying pathophysiology includes effector immune-cell infiltration with resultant tumor inflammation and/or interval tumor growth before immune mechanisms are primed to trigger an antitumor response (7–9). The appearance of new lesions may reflect enlargement of preexisting radiographically undetectable metastases due to similar mechanisms. Hyperprogression, on the other hand, is a rarer and more dramatic acceleration in tumor progression after the initiation of ICIs, usually with prompt clinical deterioration (10). Precise mechanisms underlying hyperprogression remain unclear.

Here, we describe three patients with metastatic clear cell RCC who had striking acceleration in tumor growth on cross-sectional imaging after the initiation of nivolumab, associated with detrimental outcomes. Biopsies from sites of radiographic progression revealed extensive areas of necrosis and lymphohistiocytic infiltration with no viable tumor. These changes indicate exuberant antigen presentation, T-cell cytotoxicity, and macrophage-mediated scavenging, findings previously reported in patients with ICI-induced pseudoprogression (7–9). However, our patients had marked acceleration in tumor growth with profound clinical deterioration suggesting rapid loss of response and resulting in transition to hospice.

Tumor histology after hyperprogression has not been well-characterized. One study examining gastric cancer tissue samples before and after anti-PD1 therapy, demonstrated marked increase in tumor-infiltrating proliferative ($Ki67^+$) regulatory T-cells (T_{regs}) in patients with HPD (n = 2), contrasting with their reduction in those without HPD (n=12) (11). Arasanz et al. (12) described expansion of $CD28^-$ $CD4^+$ highly differentiated T-cells (T_{HD}) in the peripheral blood of NSCLC patients who developed HPD. Another study observed tumor infiltration by M2-like $CD163^+$ $CD33^+$ $PD\text{-}L1^+$ macrophages, albeit in pretreatment tissue samples, in NSCLC patients who went on to develop hyperprogression (n = 39) (13). Recently, it was observed that the expansion of intratumoral clonal T cells is associated with a similar proliferation of non-exhausted T cells in the peripheral blood and adjacent non-tumor tissue, suggesting an extratumoral source of tumor-targeted T cells (14). We had previously postulated that patients with metastatic RCC treated with interleukin 2-based immunotherapy respond because of a pre-existing state of immune preparedness (15). Mechanisms underlying rapid tumor progression in RCC after ICI therapy are largely unknown. Our current observations in these three patients support the hypothesis that rapid proliferation of pre-existing T cell clones with exuberant tumor inflammation can result in a cytokine release syndrome-like picture and subsequent clinical deterioration.

ICI-induced hyperprogression is a rare complication in metastatic RCC. Two previous studies reported incidence rates lower than 1% (16, 17). Remarkably, all patients in our study demonstrated a pattern of rapid progression that was either confined to or disproportionately faster in one of the involved anatomic locations. Kobari et al. described three patients with advanced RCC who had rapid radiographic progression confined to a few sites with clinical deterioration after exposure to an ICI, though post-progression biopsies were not analyzed (18). Very little is known about the incidence and mechanisms underlying organ tendencies in hyperprogression across tumor types.

Our report points to a possible discordance between tumor growth kinetics and histology in some patients with rapid

radiographic progression while on treatment with ICIs, as demonstrated by the absence of viable cancer on biopsies from sites of such progression. Exuberant antitumor immunity and cytokine release secondary to overwhelming inflammation may contribute to rapidly declining performance status and other detrimental outcomes in these patients (19). Tumor biopsies should be carefully considered in such patients, preferably in the context of well-designed prospective studies, to further characterize these immune responses and identify potential therapeutic targets. We also hypothesize that evaluation of serum cytokine profiles in such cases may inform potential salvage strategies, such as the IL-6 inhibitor tocilizumab (20).

Our study was limited by its retrospective nature and small sample size. We cannot rule-out that sampling bias due to intratumor heterogeneity could have accounted for the absence of viable tumor in biopsy specimens, though multiple cores were examined in these three patients. Since biopsies were performed as part of routine care, primarily to rule out second primary neoplasms, immune-cell subpopulations in the inflammatory infiltrates could not be further characterized, and immunohistochemical staining was performed at the discretion of the pathologist. Baseline biopsies prior to the initiation of ICI, from the sites of subsequent rapid radiographic progression, were not available for comparison. Also, serum cytokine levels were not measured in these patients.

CONCLUSIONS

Overwhelming antitumor immune responses may contribute to detrimental outcomes in some patients with ICI-induced radiographic progression. Tumor biopsies and cytokine analyses, preferably in the context of prospective studies, may help elucidate the pathophysiology underlying these aberrant responses.

DATA AVAILABILITY STATEMENT

The original contributions presented in the study are included in the article/supplementary material. Further inquiries can be directed to the corresponding author.

ETHICS STATEMENT

The studies involving human participants were reviewed and approved by Roswell Park Comprehensive Cancer Center Institutional Review Board. Informed consent was obtained from the individuals' next of kin as they were deceased. Written informed consent was obtained from the individual(s) for the publication of any potentially identifiable images or data included in this article.

AUTHOR CONTRIBUTIONS

DG and RJ compiled the data and wrote the manuscript. SG proposed the concept, data acquisition, interpretation and made substantial edits to the manuscript. SM, GA, BX, CL, LH, MS, KR, and ME made major contributions to data acquisition and interpretation. All authors contributed to the article and approved the submitted version.

REFERENCES

1. Wei SC, Duffy CR, Allison JP. Fundamental Mechanisms of Immune Checkpoint Blockade Therapy. *Cancer Discovery* (2018) 8(9):1069–86. doi: 10.1158/2159-8290.CD-18-0367
2. Motzer RJ, Escudier B, George S, Hammers HJ, Srinivas S, Tykodi SS, et al. Nivolumab Versus Everolimus in Patients With Advanced Renal Cell Carcinoma: Updated Results With Long-Term Follow-Up of the Randomized, Open-Label, Phase 3 CheckMate 025 Trial. *Cancer* (2020) 126 (18):4156–67. doi: 10.1002/cncr.33033
3. Wang Q, Gao J, Wu X. Pseudoprogression and Hyperprogression After Checkpoint Blockade. *Int Immunopharmacol* (2018) 58:125–35. doi: 10.1016/j.intimp.2018.03.018
4. Borcoman E, Nandikolla A, Long G, Goel S, Le Tourneau C. Patterns of Response and Progression to Immunotherapy. *Am Soc Clin Oncol Educ Book* (2018) 38:169–78. doi: 10.1200/EDBK_200643
5. George S, Motzer RJ, Hammers HJ, Redman BG, Kuzel TM, Tykodi SS, et al. Safety and Efficacy of Nivolumab in Patients With Metastatic Renal Cell Carcinoma Treated Beyond Progression: A Subgroup Analysis of a Randomized Clinical Trial. *JAMA Oncol* (2016) 2(9):1179–86. doi: 10.1001/jamaoncol.2016.0775
6. Ferrara R, Matos I. Atypical Patterns of Response and Progression in the Era of Immunotherapy Combinations. *Future Oncol* (2020) 16(23):1707–13. doi: 10.2217/fon-2020-0186
7. Rocha P, Hardy-Werbin M, Naranjo D, Taus Á, Rodrigo M, Zuccarino F, et al. Cd103+Cd8+ Lymphocytes Characterize the Immune Infiltration in a Case With Pseudoprogression in Squamous Nsclc. *J Thorac Oncol* (2018) 13 (10):e193–6. doi: 10.1016/j.jtho.2018.05.008
8. Tabei T, Tsuura Y, Kobayashi K. Pseudoprogression: A Case of Metastatic Renal Clear Cell Carcinoma Treated With Nivolumab. *Pathol Int* (2018) 68 (11):627–9. doi: 10.1111/pin.12714
9. Tanizaki J, Hayashi H, Kimura M, Tanaka K, Takeda M, Shimizu S, et al. Report of Two Cases of Pseudoprogression in Patients With non-Small Cell Lung Cancer Treated With Nivolumab-Including Histological Analysis of One Case After Tumor Regression. *Lung Cancer* (2016) 102:44–8. doi: 10.1016/j.lungcan.2016.10.014
10. Frelaut M, Le Tourneau C, Borcoman E. Hyperprogression Under Immunotherapy. *Int J Mol Sci* (2019) 20(11):2674. doi: 10.3390/ijms20112674
11. Kamada T, Togashi Y, Tay C, Ha D, Sasaki A, Nakamura Y, et al. Pd-1(+) Regulatory T Cells Amplified by PD-1 Blockade Promote Hyperprogression of Cancer. *Proc Natl Acad Sci U S A* (2019) 116(20):9999–10008. doi: 10.1073/pnas.1822001116
12. Arasanz H, Zuazo M, Bocanegra A, Gato M, Martínez-Aguillo M, Morilla I, et al. Early Detection of Hyperprogressive Disease in Non-Small Cell Lung Cancer by Monitoring of Systemic T Cell Dynamics. *Cancers (Basel)* (2020) 12 (2):344. doi: 10.3390/cancers12020344
13. Lo Russo G, Moro M, Sommariva M, Cancila V, Boeri M, Centonze G, et al. Antibody-Fc/Fcr Interaction on Macrophages as a Mechanism for Hyperprogressive Disease in Non-small Cell Lung Cancer Subsequent to PD-1/PD-L1 Blockade. *Clin Cancer Res* (2019) 25(3):989–99. doi: 10.1158/1078-0432.CCR-18-1390
14. Wu TD, Madireddi S, de Almeida PE, Banchereau R, Chen YJ, Chitre AS, et al. Peripheral T Cell Expansion Predicts Tumour Infiltration and Clinical Response. *Nature* (2020) 579(7798):274–8. doi: 10.1038/s41586-020-2056-8
15. Schwaab T, Schwarzer A, Wolf B, Crocenzi TS, Seigne JD, Crosby NA, et al. Clinical and Immunologic Effects of Intranodal Autologous Tumor Lysate-Dendritic Cell Vaccine With Aldesleukin (Interleukin 2) and IFN-{alpha}2a

Therapy in Metastatic Renal Cell Carcinoma Patients. *Clin Cancer Res* (2009) 15(15):4986–92. doi: 10.1158/1078-0432.CCR-08-3240
16. Dionese M, Pierantoni F, Maruzzo M, Bimbatti D, Deppieri FM, Maran M, et al. Fatal Hyperprogression Induced by Nivolumab in Metastatic Renal Cell Carcinoma With Sarcomatoid Features: A Case Report. *Anticancer Drugs* (2021) 32(2):222–5. doi: 10.1097/CAD.0000000000000991
17. Hwang I, Park I, Yoon SK, Lee JL. Hyperprogressive Disease in Patients With Urothelial Carcinoma or Renal Cell Carcinoma Treated With Pd-1/Pd-L1 Inhibitors. *Clin Genitourin Cancer* (2020) 18(2):e122–33. doi: 10.1016/j.clgc.2019.09.009
18. Kobari Y, Kondo T, Takagi T, Omae K, Nakazawa H, Tanabe K. Rapid Progressive Disease After Nivolumab Therapy in Three Patients With Metastatic Renal Cell Carcinoma. *In Vivo* (2017) 31(4):769–71. doi: 10.21873/invivo.11129
19. Slota A, Khan R, Rahman A, Warner EA. Cytokine Release Syndrome As a Rare Complication of Nivolumab: A Case Report. *Blood* (2019) 134 (Supplement_1):5630–0. doi: 10.1182/blood-2019-127586
20. Shimabukuro-Vornhagen A, Godel P, Subklewe M, Stemmler HJ, Schlößer HA, Schlaak M, et al. Cytokine Release Syndrome. *J Immunother Cancer* (2018) 6(1):56. doi: 10.1186/s40425-018-0343-9

Conflict of Interest: The authors declare that the research was conducted in the absence of any commercial or financial relationships that could be construed as a potential conflict of interest.

frontiers in Oncology

ORIGINAL RESEARCH
published: 08 June 2021
doi: 10.3389/fonc.2021.682449

Impact of Previous Nephrectomy on Clinical Outcome of Metastatic Renal Carcinoma Treated With Immune-Oncology: A Real-World Study on Behalf of Meet-URO Group (MeetUro-7b)

Marco Stellato[1], Daniele Santini[1], Elena Verzoni[2], Ugo De Giorgi[3], Francesco Pantano[1], Chiara Casadei[3], Giuseppe Fornarini[4], Marco Maruzzo[5], Andrea Sbrana[6], Giuseppe Di Lorenzo[7], Mariella Soraru[8], Emanuele Naglieri[9], Sebastiano Buti[10], Rocco De Vivo[11], Andrea Napolitano[1], Francesca Vignani[12], Claudia Mucciarini[13], Francesco Grillone[14], Giandomenico Roviello[15], Marilena Di Napoli[16], Giuseppe Procopio[2] and on behalf of the MeetUro group*

[1] Department of Medical Oncology, Campus Bio-Medico University of Rome, Rome, Italy, [2] Medical Oncology Department, Fondazione IRCCS Istituto Nazionale dei Tumori, Milan, Italy, [3] Department of Medical Oncology, IRCCS Istituto Romagnolo per lo Studio dei Tumori (IRST) Dino Amadori, Meldola, Italy, [4] Onco-ematological Department, IRCCS Ospedale Policlinico San Martino, Genova, Italy, [5] Medical Oncology Unit 1, Department of Oncology, Istituto Oncologico Veneto IOV IRCCS, Padua, Italy, [6] Department of Surgical, Medical and Molecular Pathology and Critical Area Medicine, University of Pisa, Pisa, Italy, [7] Oncologia, Università del Molise, Campobasso, Italy, [8] Oncology Unit, Camposampiero General Hospital, Padova, Italy, [9] Division of Medical Oncology, Istituto Tumori Bari Giovanni Paolo II—IRCCS, Bari, Italy, [10] Medical Oncology Unit, University Hospital of Parma, Parma, Italy, [11] Department of Oncology, San Bortolo General Hospital, Vicenza, Italy, [12] AO Ordine Mauriziano, SCDU Oncologia, Turin, Italy, [13] U.O. Medicina Oncologica, Ospedale Ramazzini, Carpi-AUSL Modena, Carpi, Italy, [14] Azienda Ospedaliero-Universitario "Mater Domini", Policlinico of Catanzaro, Catanzaro, Italy, [15] Department of Health Sciences, University of Florence, Firenze, Italy, [16] Department of Urology and Gynecology, Istituto Nazionale Tumori IRCCS Fondazione "G. Pascale", Napoli, Italy

OPEN ACCESS

Edited by:
Antonio Augusto Ornellas, National Cancer Institute (INCA), Brazil

Reviewed by:
Amin Nassar, Brigham and Women's Hospital and Harvard Medical School, United States
Ahmet Murat Aydin, Moffitt Cancer Center, United States

***Correspondence:**
Marco Stellato
m.stellato@unicampus.it

Specialty section:
This article was submitted to Genitourinary Oncology, a section of the journal Frontiers in Oncology

Received: *18 March 2021*
Accepted: *11 May 2021*
Published: *08 June 2021*

Citation:
Stellato M, Santini D, Verzoni E, De Giorgi U, Pantano F, Casadei C, Fornarini G, Maruzzo M, Sbrana A, Di Lorenzo G, Soraru M, Naglieri E, Buti S, De Vivo R, Napolitano A, Vignani F, Mucciarini C, Grillone F, Roviello G, Di Napoli M and Procopio G (2021) Impact of Previous Nephrectomy on Clinical Outcome of Metastatic Renal Carcinoma Treated With Immune-Oncology: A Real-World Study on Behalf of Meet-URO Group (MeetUro-7b). Front. Oncol. 11:682449. doi: 10.3389/fonc.2021.682449

Background: Immune-Oncology (IO) improves Overall Survival (OS) in metastatic Renal Cell Carcinoma (mRCC). The prognostic impact of previous Cytoreductive Nephrectomy (CN) and radical nephrectomy (RN), with curative intent, in patients treated with IO is not well defined. The aim of our paper is to evaluate the impact of previous nephrectomy on outcome of mRCC patients treated with IO.

Methods: 287 eligible patients were retrospectively collected from 16 Italian referral centers adhering to the MeetUro association. Patients treated with IO as second and third line were included, whereas patients treated with IO as first line were excluded. Kaplan–Meier method and log-rank test were performed to compare Progression Free Survival (PFS) and OS between groups. In our analysis, both CN and RN were included. The association between nephrectomy and other variables was analyzed in univariate and multivariate setting using the Cox proportional hazard model.

Results: 246/287 (85.7%) patients had nephrectomy before IO treatment. Median PFS in patients who underwent nephrectomy (246/287) was 4.8 months (95%CI 3.9–5.7) vs 3.7 months (95%CI 1.9–5.5) in patients who did not it (HR log rank 0.78; 95%CI 0.53 to 1.15; $p = 0.186$). Median OS in patients who had previous nephrectomy (246/287) was 20.9 months (95%CI 17.6–24.1) *vs* 13 months (95%CI 7.7–18.2) in patients who did not it (HR log rank 0.504; 95%CI 0.337 to 0.755; $p = 0.001$). In the multivariate model, nephrectomy showed a significant association with OS (HR log rank 0.638; 95%CI 0.416 to 0.980), whereas gland metastases were still associated with better outcome in terms of both OS (HR log rank 0.487; 95%CI 0.279 to 0.852) and PFS (HR log rank 0.646; 95%CI 0.435 to 0.958).

Conclusions: IO treatment, in patients who had previously undergone nephrectomy, was associated with a better outcome in terms of OS. Further prospective trials would assess this issue in order to guide clinicians in real word practice.

Keywords: nephrectomy, immune-oncology, metastatic renal cell carcinoma, immunotherapy, nivolumab

INTRODUCTION

Kidney cancer represents 5% of estimated new cases of cancer in men and 3% in women, being the 13th most commonly diagnosed solid malignancy (1, 2).

Approximately 20% of patients will develop metastases after nephrectomy, while 15% patients have already developed synchronous metastatic disease at the time of diagnosis (2, 3).

Radical Nephrectomy (RN) and Partial Nephrectomy (PR) with curative intent can be considered standard of care in patients with localized disease (4–7). In the management of metastatic renal cell carcinoma (mRCC) patients, randomized data from the "interferon era" demonstrated that Cytoreductive Nephrectomy (CN) improves survival, decreasing the risk of death (8). Despite the retrospective data from IMDC by Heng et al. and the prospective results from CARMENA and SURTIME trial (9, 10), CN remains controversial in patients treated with VEGF-targeted therapy. Recently, Immune-Oncology (IO), alone or in combination, has changed the standard of care in mRCC due to the high rate of survival in pretreated and treatment-naïve patients (11–13). In CHECKMATE214, Overall Survival (OS) favored nivolumab plus ipilimumab over sunitinib, also in patients who had previous nephrectomy. Updated analysis confirms that median OS was longer among those randomized to nivolumab-ipilimumab with target kidney lesion (14). Nevertheless, in patients treated with IO, the role of previous CN or RN has not been defined. It is unclear if previous nephrectomy affects outcome in patients treated with IO. Data about response of primary renal tumor to IO are partial and prospective trials evaluating the effect of nephrectomy in patients treated with IO are lacking.

Previous reports demonstrated some changes in the immune system after nephrectomy, but data are not conclusive (15). Therefore, the aim of our study was to retrospectively evaluate the impact of previous nephrectomy on mRCC patients treated with IO.

PATIENTS AND METHODS

We retrospectively collected data of mRCC patients treated with IO in 16 Italian referral centers adhering to the Meet-Uro group, between February 2017 and January 2020.

Inclusion criteria were at least 18 years old at the time of enrollment, histological diagnosis of RCC and radiological diagnosis of metastatic disease.

Patients treated with IO, as single agent or in combination, were considered eligible. Patients enrolled in the expanded access program of nivolumab or nivolumab–ipilimumab were excluded. Patients treated with first line IO were excluded to homogenize our population, whereas patients treated with IO as second and third line were included.

Baseline characteristics were collected at the start of immunotherapy. Outcome data, including PFS and toxicities, were collected too. Data included site of metastatic disease, duration of first line and subsequent IO therapy, previous CN or RN. Glandular metastasis included metastasis in glandular organs such as thyroid, pancreas and adrenal gland.

The International Metastatic RCC Database Consortium (IMDC) prognostic risk group was computed at the index date based on the presence of six individual risk factors including time from diagnosis to systemic treatment <1 year, hemoglobin < lower limit of normal, calcium >10 mg/dl, platelet > upper limit of normal, neutrophil > upper limit of normal, Performance Status (PS) <80% (Karnofsky) (16).

Primary endpoint was to evaluate difference in IO-OS between patients who previously received nephrectomy and patients who did not it. IO-OS was defined as the time from the start of IO to death.

Secondary endpoints were to evaluate difference in PFS between the twogroups of patients. PFS was defined as the time from the start of IO to radiological or clinical progression.

Patients with no evidence of death were censored at the date of last tumor assessment.

Real-world physician-assessed progression and response was based on clinical criteria or radiographic criteria using Response Evaluation Criteria in Solid Tumors (RECIST) guidelines (17), with imaging assessments occurring at clinically variable time points.

Baseline demographic and clinical characteristics have been described using frequencies and percentages for categorical variables.

Descriptive analysis was made using median values and ranges. Kaplan–Meier method and Mantel–Haenszel log-rank test were performed to compare differences in OS and PFS between groups. The association between nephrectomy and other variables was analyzed in univariate and multivariable setting using the Cox proportional hazard model. Variables to be included in multivariate analysis were selected according to the levels of significance in cox regression univariate analysis. P-values <0.05 were considered significant. All statistical analyses were performed using SPSS software (version 19.00, SPSS, Chicago).

Written informed consent for patient information to be published was provided by the patients or a legally authorized representative. All participating centers received local ethics approval for data collections. The study was conducted in accordance with good clinical practice and the Declaration of Helsinki.

RESULTS

287 patients were considered eligible. Characteristics of patients are described in **Table 1**. All patients received nivolumab as IO.

246/287 (85.7%) patients had nephrectomy, whereas 41 (14.3%) patients did not it. 95 (33.1%) patients had CN and 151 (52.6%) patients had RN with curative intent. Nephrectomy was performed before IO treatment.

136/287 patients (47.4%) had synchronous metastatic disease, whereas 151/287 patients (52.6%) had metachronous disease.

G3–G4 immune-related Adverse Events (irAEs) were reported in 24/287 patients (8.3%).

At a median follow up of 24.7 months, 114/287 patients (56.4%) received target therapy (TT), such as mTOR inhibitors and VEGFR inhibitors at progression to IO, whereas 68/287 patients (25.4%) did not receive further treatment for clinical deterioration. 68/287 patients (23.7%) continued IO beyond progression.

52/287 patients (18.2%) were still in treatment at the time of analysis.

Median IO-PFS was 4.6 months (95%CI 3.85–5.42). Median PFS in patients who underwent nephrectomy (246/287) was 4.8 months (95%CI 3.9–5.7) vs 3.7 months (95%CI 1.9–5.5) in patients who did not it (HR log rank 0.78; 95%CI 0.53 to 1.15; $p = 0.186$) (**Figure 1**) (**Table 2**).

Median IO-OS in the entire population was 18.5 months (95%CI 15.5–21.4). In patients with metastasis to glandular organs (37/287), mOS was 39.3 months (95%CI 22.5–43.5) compared to 16.2 months (95%CI 13.9–23.8) in patients without gland metastasis (250/287) (**Figure 2**).

TABLE 1 | Characteristics of patients.

	N (%)
Age	
median	69.4 y
Sex	
M	206 (71.7)
F	81 (28.3)
Nephrectomy	
Y	246 (85.7)
N	41 (14.3)
Cytoreductive Nephrectomy	95 (33.1)
Clear cell	
Y	246 (86.0)
N	41 (14.0)
Sarcomatoid	
Y	36 (12.5)
N	251 (87.5)
IO Line	
2	195 (68)
3	73 (25.4)
further line	19 (6.6)
ECOG PS at IO start	
0	145 (50.5)
1	116 (40.4)
2	26 (9.0)
Previous TKI treatment	
sunitinib	178 (62.0)
pazopanib	97 (33.8)
cabozantinib	22 (7.6)
sorafenib	6 (2.0)
everolimus	19 (6.6)
axitinib	36 (12.5)
lenvatinib everolimus	6 (2.0)
tivozanib	4 (1.4)
lenvatinib	1 (0.3)
Metastatic sites	
lynphonodes	128 (44.6)
lung	122 (42.5)
bone	84 (29.2)
liver	33 (11.5)
brain	12 (4.2)
gland	37 (12.9)
peritoneum	14 (4.8)
IMDC score	
good	82 (28.6)
Intermediate	176 (61.3)
poor	29 (10.1)

M, male; F, female; IO, Immune-Oncology; ECOG PS, Eastern Cooperative Oncology Group Performance status; TKI, tyrosine-Kinase Inhibitor; IMDC, International Metastatic renal cell carcinoma Database Consortium.

Median OS in patients who had previous nephrectomy (246/287) was 20.9 months (95%CI 17.6–24.1) vs 13 months (95%CI 7.7–08.2) in patients who did not it (HR log rank 0.504; 95%CI 0.337 to 0.755; $p = 0.001$) (**Figure 3**).

In patients with synchronous metastatic disease (136/287), mOS was 20.5 months for those who underwent CN, compared to 13 months in patients who did not it (HR log rank 0.51; 95%CI 0.305 to 0.855; $p = 0.0024$). On the other hand, mPFS was 4.6 months in patients who underwent CN vs 3.7 months in patients who did not it (HR log rank 0.83; 95%CI 0.554 to 1.247; $p = 0.34$) (**Table 3**).

In the multivariate model, including gland metastasis and IMDC score, nephrectomy showed significant association with

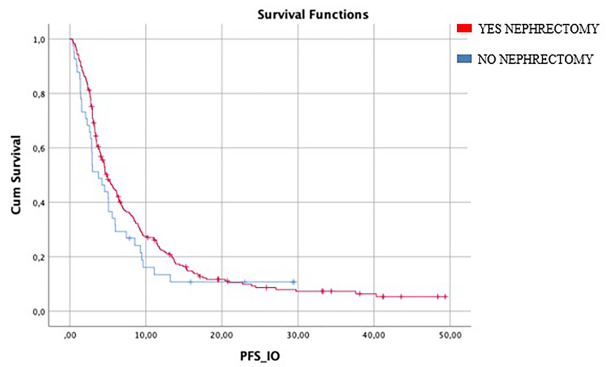

FIGURE 1 | Median mIO-PFS in patients who underwent nephrectomy (246/287) was 4.8 months *vs* 3.7 months in patients who did not (HR log rank 0.78; 95%CI 0.53 to 1.15; $p = 0.186$). mIO-PFS (mPFS in patient treated with IO).

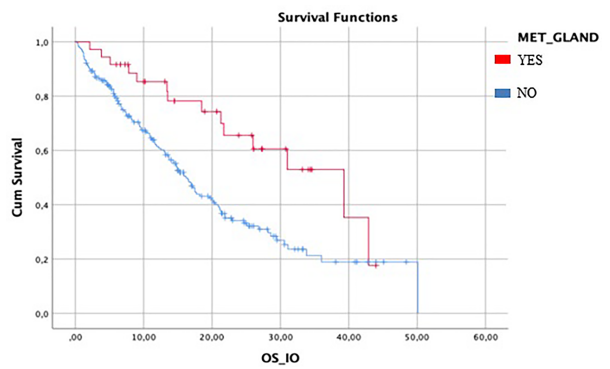

FIGURE 2 | Difference between mIO-OS between patient with gland metastasis and patient without gland metastasis. Median IO-OS was longer in patients with gland metastasis.

TABLE 2 | Median PFS difference between groups of patients treated with IO.

	mPFS	*p* value
Nephrectomy		
Y	4.8 (3.9–5.7)	0.186
N	3.7 (1.9–5.5)	
Histology		
Clear cell	4.8 (3.9–5.7)	0.829
Non clear cell	4.6 (2.8–6.4)	
Sarcomatoid variant		
Y	4.3 (2.0–6.6)	0.97
N	4.8 (3.9–5.7)	
Bone metastasis		
Y	4.1 (3.0–5.2)	0.093
N	5.0 (4.0–5.9)	
Lynphonodes metastasis		
Y	5.0 (3.4–6.6)	0.216
N	4.6 (3.9–5.3)	
Lung metastasis		
Y	5.5 (3.6–6.7)	0.089
N	4.5 (4.2–5.3)	
Liver metastasis		
Y	4.6 (0.7–5.3)	0.813
N	5.0 (4.0–6.1)	
Gland metastasis		
Y	6.5 (2.8–6.9)	**0.022**
N	4.6 (3.8–5.5)	
IMDC SCORE		
0	6.1 (1.0–4.0)	**0.044**
1	4.5 (0.4–3.6)	
2	3.3 (2.1–0.0)	
ECOG PS		
0	5.5 (3.8–7.3)	0.25
1	4.5 (3.9–5.1)	
2	3.0 (2.2–3.8)	
G3–G4 toxicities		
Y	5.0 (3.2–6.7)	0.9
N	4.8 (3.9–5.7)	

Y, Yes; N, No; IMDC, International Metastatic Renal Cell Carcinoma Database Consortium; ECOG PS, Eastern Cooperative Oncology Group Performance status; G, Grade; mPFS, Median Progression Free Survival; IO, Immune-Oncology.
Groups of patients with different IMDC score and with gland metastasis had statistically difference in PFS when treated with IO.
Bold values represent statistically significant value.

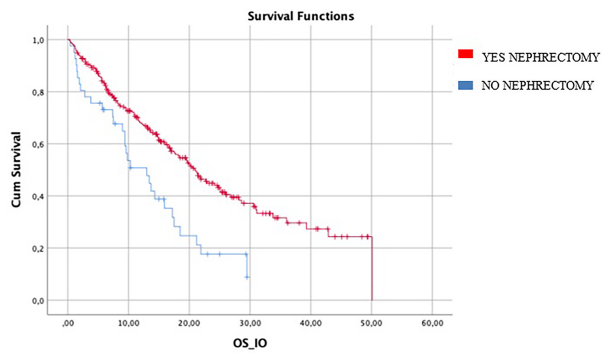

FIGURE 3 | difference in mIO-OS between who underwent nephrectomy was 20.9 (95%CI 17.6–24.1) *vs* 13.0 (95%CI 7.7–18.2) in patients who did not. IO-OS (median OS in patients treated with IO).

OS (HR log rank 0.638; 95%CI 0.416 to 0.980), whereas gland metastases were still associated with better outcome in terms of both OS (HR log rank 0.487; 95%CI 0.279 to 0.852) and PFS (HR log rank 0.646; 95%CI 0.435 to 0.958). However, IMDC score showed significant association with both OS (HR log rank 1.352; 95%CI 1.020 to 1.791) and PFS (HR log rank 1.27; 95%CI 1.016 to 1.587).

DISCUSSION

IMDC and Memorial Sloan-Kettering Cancer Center (MSKCC) score are currently the gold standard for predicting survival in patients with mRCC but metastatic sites influence prognosis too. Indeed, gland metastasis, such as pancreatic metastasis, are related to more favorable prognostic features, long response to TTs and prolonged survival (18). Lung and nodes metastasis, instead, are related to higher complete response rate in patients treated with nivolumab–ipilimumab (19). Bone metastasis has

TABLE 3 | mOS differences between groups of patients treated with IO.

	mIO-OS	*p* value
Nephrectomy		
Y	20.9 (17.6–24.1)	**0.001**
N	13.0 (7.7–18.2)	
Histology		
Clear cell	18.5 (15.4–21.5)	0.654
Non-clear cell	17.0 (0.0–38.9)	
Sarcomatoid component		
Y	19.7 (11.3–28.0)	0.923
N	18.5 (15.3–21.6)	
Bone metastasis		
Y	18.5 (11.5–27.6)	0.814
N	19.5 (16.1–26.1)	
Lynphonodes metastasis		
Y	17.5 (14.0–20.9)	0.908
N	20.2 (16.3–24.0)	
Lung metastasis		
Y	16.6 (11.6–26.0)	0.576
N	18.5 (14.8–27.1)	
Liver metastasis		
Y	16.6 (10.7–24.7)	0.280
N	18.5 (14.9–26.6)	
Gland metastasis		
Y	39.3 (22.5–43.5)	**0.004**
N	16.2 (13.9–23.8)	
IMDC SCORE		
0	22.9 (15.7–33.3)	**0.004**
1	17.2 (12.3–25.1)	
2	15.3 (8.3–20.2)	
ECOG PS		
0	19.7 (15.9–23.4)	0.208
1	20.9 (14.3–27.4)	
2	10.9 (5.6–16.1)	
IO line		
2	19.7 (15.9–23.4)	
3	20.5 (14.5–26.4)	
4	11.9 (3.8–19.9)	
5	1.3 (NR-NR)	
G3–G4 toxicities		
Y	17.0 (4.7–29.2)	0.761
N	19.7 (16.6–22.7)	

Y, Ye; N, No; mOS, median Overall Survival; IO, Immune-Oncology; IMDC, International Metastatic Renal Cell Carcinoma Database Consortium; ECOG PS, Eastern Cooperative Oncology Group Performance Status; G, Grade.

Nephrectomy, gland metastasis and IMDC score demonstrated a significant difference in mOS between groups.

Bold values represent statistically significant value.

been identified as an independent prognostic variable associated with poor survival in patients with mRCC (20) and brain metastasis seem to influence prognosis when they are more than 4 (21, 22). Even though nephrectomy has not been reported as a prognostic factor or in prognostic scores, patients who underwent nephrectomy are usually patients with metachronous disease or more indolent disease, compared to patients with synchronous disease.

The first evidence regarding the role of nephrectomy in mRCC refers to patients treated with cytokines (IL-2, IFN-a). CN demonstrated improved survival rate in them (8, 23). Later, Heng et al. retrospectively reported data from IMDC. CN was related to OS and PFS benefit in patients treated with TT, compared to patients who did not it. Patients with four or more IMDC prognostic criteria did not benefit from CN, as well as patients with reduced life expectancy (24).

Recently, the phase III CARMENA trial has investigated the role of immediate CN followed by sunitinib versus sunitinib alone and the phase III SURTIME trial has compared immediate CN followed by sunitinib therapy, versus treatment with three cycles of sunitinib followed by CN. Results from both trials have showed that patients with intermediate and poor risk, according to MSKCC and IMDC criteria, should be more appropriately treated with systemic therapy, deferring upfront CN, whereas CN might be considered in good risk patients with low burden disease (9, 10).

Retrospective data from 1,541 patients included in an international, multicenter, prospective database, confirm that deferred CN in mRCC patients treated with upfront sunitinib is associated with improved OS, in appropriately selected patients, whereas upfront CN followed by sunitinib is associated to a lower probability of OS. Authors suggest that initial course of systemic treatment might be a way to identify patients with more aggressive biology, already destined to low survival and who consequently would not benefit from CN (25).

Nowadays, it is difficult to put into practice data about CN, because the influence on outcome of previous nephrectomy in mRCC patients treated with IO is not well defined.

Most of the patients included in the CHECKMATE025 (88%) underwent nephrectomy, so that a subgroup analysis was not performed and data about outcome of patients treated with IO stratified by nephrectomy are not available (11, 12).

Nevertheless, CN after receipt of IO currently remains limited to case reports (26–29), whereas results from CHECKMATE214 showed OS benefit for patients, who had previous nephrectomy (CN or RN), receiving Nivolumab–Ipilimumab versus Sunitinib.

Recently, update results from Javelin Renal 101 favor avelumab plus axitinib over sunitinib across prespecified subgroups, including prior nephrectomy (30). Post hoc analysis of the same trial showed that almost 20% of patients who did not undergo prior nephrectomy and 34.5% of patients, treated with avelumab–axitinib, had 30% or greater shrinkage of primary renal tumor from baseline compared to 9.7% in sunitinib arm (31). These results demonstrate that IO-Tyrosine Kinase Inhibitors (TKIs) combination is active on primary disease, even if in a small number of patients.

The above-mentioned reports seem to suggest an interplay between IO, immune system and primary tumor that need to be researched further.

Our study reported difference in IO-OS between patients who had previous nephrectomy and patients who did not it. Previous nephrectomy seems to extend OS in mRCC patients treated with immunotherapy. Analyzing patients with synchronous metastatic disease, who underwent CN, the benefit in OS was confirmed, compared to patients who did not have CN. This result confirms the findings of Bakouny et al. reported at the ASCO GU 2020. The authors, in a propensity score-based analysis, found that CN was associated with a significant OS benefit in patients treated with IO and TT both. 198 patients treated with IO were included in the analysis (32).

In our multivariate analysis, nephrectomy retained a significant association with OS irrespective of the gland metastases and IMDC score.

Reported PFS' results do not demonstrate difference between patients who underwent nephrectomy and patients who did not it (4.8 *vs* 3.7 *p* 0.186). This result confirms that PFS is not a surrogate for OS in patients treated with IO and confirms the delayed benefit in PFS with nivolumab, as previously reported in CHECKMATE025.

Furthermore, our study demonstrates that gland metastases are related to better prognosis and outcome, as demonstrated in univariate and multivariate analysis. Biological and immunological effects of the primary tumor on IO, which are mostly unknown, might explain the different outcome between patients who underwent nephrectomy and patients who did not it.

Previous report from Wald et al. analyzed how RN could influence immune response, collecting the immune signature in subjects with RCC before and after nephrectomy. Authors reported that the removal of the tumor produced few changes in the cellular immune response at 1 month post-nephrectomy, for example the level of circulating BTLA(B and T lymphocyte attenuator)-expressing CD8+ T cells decreased significantly, suggesting a reversal of T-cell exhaustion and dysfunction (15).

Finally, it is noteworthy to mention the retrospective study by Pignot et al. regarding patients who underwent delayed nephrectomy following IO. Patients who received IO and who experienced complete response on metastatic sites, underwent nephrectomy to achieve complete response. At a median follow up of 15 months, 73% of patients were free from progression, but inflammatory infiltration after long exposure to IO resulted in challenging surgery (33).

Our study covered a well-balanced population and represented all risk categories according to IMDC (**Table 4**).

Specifically, it included 30% of patients with bone metastasis, already known poor prognostic factor in mRCC, which is consistent with frequency of bone metastasis in RCC.

We analyzed patients who received IO mostly as second or third therapy, to homogenize our population and minimize the selection bias between patients with metachronous disease, or patients with low burden disease referred to CN, and patients with synchronous disease or with higher burden of disease referred to upfront systemic therapy. Indeed, recently, Donskov et al. demonstrated that, in patients treated with first line TKI, synchronous disease was associated with poorer OS and shorter Time to Treatment Failure (TTF) (34).

The purpose of our trial was to suggest that the persistence of primary renal cell tumor could influence the efficacy of Immunotherapy because it could influence the immune system. This is the reason why patients who had CN or RN were not divided into two groups.

In spite of the novel treatments available for renal cell carcinoma, our paper remains relevant because TKI monotherapy can still be considered as a standard of care for many patients. Indeed, IO-TKI failed to show an OS advantage over sunitinib in favorable risk patients according to IMDC and MSKCC score. Moreover, we included patients treated with IO as second line treatment since in Europe IO and IO-TKI has not been available for long time.

TABLE 4 | Differences between patients who had nephrectomy *vs* patients who had not nephrectomy.

	Nephrectomy246 (85.7%)	No Nephrecomy41 (14.3%)
Histology		
Clear cell	218 (88.6)	37 (90.2)
Non-clear cell	28 (11.4)	4 (9.8)
Sarcomatoid component		
Y	34 (13.8)	2 (4.8)
N	212 (86.2)	39 (95.2)
Bone metastasis		
Y	67 (27.0)	17 (41.4)
N	182 (73.0)	24 (58.6)
Lynphonodes metastasis		
Y	105 (46.7)	23 (56.0)
N	141 (57.3)	18 (44.0)
Lung metastasis		
Y	102 (41.4)	20 (48.7)
N	144 (58.6)	21 (51.3)
Liver metastasis		
Y	25 (10.1)	8 (19.5)
N	221 (89.9)	33 (80.5)
Gland metastasis		
Y	29 (11.7)	3 (7.3)
N	217 (88.3)	38 (82.7)
IMDC SCORE		
0	80 (32.5)	2 (4.8)
1	143 (58.1)	33 (80.5)
2	23 (9.3)	6 (14.7)
ECOG PS		
0	128 (52.0)	17 (41.5)
1	96 (39.0)	20 (48.8)
2	22 (9.0)	4 (9.7)
IO line		
2	164 (66.6)	31 (75.6)
3	65 (26.4)	8 (19.6)
Further line	17 (7.0)	2 (4.8)

Y, Yes; N, No; mOS, median Overall Survival; IO, Immune-Oncology; IMDC, International Metastatic Renal Cell Carcinoma Database Consortium; ECOG PS, Eastern Cooperative Oncology Group Performance Status; G, Grade.

Limits of our study include the retrospective collection of data, the small sample size and the lack of central radiological review. As basis for further considerations, there is significant residual confounding in the analysis of nephrectomy versus no nephrectomy, particularly in the metachronous group. Those patients, who are not offered curative intent surgery, are likely more unwell and less fit and thus, perhaps, destined to do poorly regardless of type of systemic therapy received at the time of metastatic diagnosis.

Furthermore, patients who had nephrectomy were more likely to be favorable risk and this might bias results of multivariate analysis.

Our assumption can be made that resection of primary tumor could have an effect on immune system and IO response, even if

IO treatment is administered long after surgical intervention. Data are still unclear and further prospective trials would assess this issue.

CONCLUSION

In our real-world experience in mRCC patients treated with IO, previous nephrectomy, including CN, seems to be associated with a better outcome, in terms of OS, with all the limitations of a retrospective collection. The benefit of previous nephrectomy persisted also in multivariate analysis.

DATA AVAILABILITY STATEMENT

The raw data supporting the conclusions of this article will be made available by the authors, without undue reservation.

ETHICS STATEMENT

The studies involving human participants were reviewed and approved by the Campus Bio-Medico University of Rome. The patients/participants provided their written informed consent to participate in this study.

AUTHOR CONTRIBUTIONS

MSt and DS provided study conception and design. GP made critical revisions. All authors contributed to the article and approved the submitted version.

SUPPLEMENTARY MATERIAL

The Supplementary Material for this article can be found online at: https://www.frontiersin.org/articles/10.3389/fonc.2021.682449/full#supplementary-material

REFERENCES

1. Bray F, Ferlay J, Soerjomataram I, Siegel RL, Torre LA, Jemal A. Global Cancer Statistics 2018: GLOBOCAN Estimates of Incidence and Mortality Worldwide for 36 Cancers in 185 Countries. *CA Cancer J Clin* (2018) 68 (6):394–424. doi: 10.3322/caac.21492
2. Siegel RL, Miller KD, Jemal A. Cancer Statistics, 2018. *CA Cancer J Clin* (2018) 68(1):7–30. doi: 10.3322/caac.21442
3. Dabestani S, Thorstenson A, Lindblad P, Harmenberg U, Ljungberg B, Lundstam S. Renal Cell Carcinoma Recurrences and Metastases in Primary Non-Metastatic Patients: A Population-Based Study. *World J Urol* (2016) 34 (8):1081–6. doi: 10.1007/s00345-016-1773-y
4. Van Poppel H, Da Pozzo L, Albrecht W, Matveev V, Bono A, Borkowski A, et al. A Prospective, Randomised EORTC Intergroup Phase 3 Study Comparing the Oncologic Outcome of Elective Nephron-Sparing Surgery and Radical Nephrectomy for Low-Stage Renal Cell Carcinoma. *Eur Urol* (2011) 59(4):543–52. doi: 10.1016/j.eururo.2010.12.013
5. Lee JH, You CH, Min GE, Park JS, Lee SB, Ahn H, et al. Comparison of the Surgical Outcome and Renal Function Between Radical and Nephron-Sparing Surgery for Renal Cell Carcinomas. *Korean J Urol* (2007) 48(7):671–6. doi: 10.4111/kju.2007.48.7.671
6. Gratzke C, Seitz M, Bayrle F, Schlenker B, Bastian PJ, Haseke N, et al. Quality of Life and Perioperative Outcomes After Retroperitoneoscopic Radical Nephrectomy (RN), Open RN and Nephron-Sparing Surgery in Patients With Renal Cell Carcinoma. *BJU Int* (2009) 104(4):470–5. doi: 10.1111/j.1464-410X.2009.08439.x
7. Butler BP, Novick AC, Miller DP, Campbell SA, Licht MR. Management of Small Unilateral Renal Cell Carcinomas: Radical Versus Nephron-Sparing Surgery. *Urology* (1995) 45(1):34–40. doi: 10.1016/S0090-4295(95)96306-5
8. Mickisch GHJ, Garin A, van Poppel H, de Prijck L, Sylvester R. Radical Nephrectomy Plus Interferon-Alfa-Based Immunotherapy Compared With Interferon Alfa Alone in Metastatic Renal-Cell Carcinoma: A Randomised Trial. *Lancet* (2001) 358(9286):966–70. doi: 10.1016/S0140-6736(01)06103-7
9. Méjean A, Ravaud A, Thezenas S, Colas S, Beauval J-B, Bensalah K, et al. Sunitinib Alone or After Nephrectomy in Metastatic Renal-Cell Carcinoma. *N Engl J Med* (2018) 379(5):417–27. doi: 10.1056/NEJMoa1803675
10. Bex A, Mulders P, Jewett M, Wagstaff J, van Thienen JV, Blank CU, et al. Comparison of Immediate vs Deferred Cytoreductive Nephrectomy in Patients With Synchronous Metastatic Renal Cell Carcinoma Receiving Sunitinib: The SURTIME Randomized Clinical Trial. *JAMA Oncol* (2019) 5 (2):164–70. doi: 10.1001/jamaoncol.2018.5543
11. Motzer RJ, Escudier B, McDermott DF, George S, Hammers HJ, Srinivas S, et al. Nivolumab Versus Everolimus in Advanced Renal-Cell Carcinoma. *N Engl J Med* (2015) 373(19):1803–13. doi: 10.1056/NEJMoa1510665
12. Motzer RJ, Tannir NM, McDermott DF, Arén Frontera O, Melichar B, Choueiri TK, et al. Nivolumab Plus Ipilimumab Versus Sunitinib in Advanced Renal-Cell Carcinoma. *N Engl J Med* (2018) 378(14):1277–90. doi: 10.1056/NEJMoa1712126
13. Santini D, Stellato M, De Giorgi U, Pantano F, De Lisi D, Casadei C, et al. Clinical Outcomes of Metastatic Renal Carcinoma Following Disease Progression to Programmed Death (PD)-1 or PD-L1 Inhibitors (Io): A Meet-Uro Group Real World Study (Meet-Uro 7). *Am J Clin Oncol* (2021) 44(3):121–5. doi: 10.1097/COC.0000000000000791
14. Albiges L, Tannir N, Burotto M, McDermott DF, Plimack ER , Barthélémy P, et al. 711p - Nivolumab + Ipilimumab (N+I) vs Sunitinib (s) for First-Line Treatment of Advanced Renal Cell Carcinoma (aRCC) in CheckMate 214: 4-Year Follow-Up and Subgroup Analysis of Patients (Pts) Without Nephrectomy. *Ann Oncol* (2020) 31:S550–0. doi: 10.1016/j.annonc.2020.08.783
15. Wald G, Barnes KT, Bing MT, Kresowik TP, Tomanek-Chalkley A, Kucaba TA, et al. Minimal Changes in the Systemic Immune Response After Nephrectomy of Localized Renal Masses. *Urol Oncol Semin Orig Investig* (2014) 32(5):589–600. doi: 10.1016/j.urolonc.2014.01.023
16. Heng DYC, Xie W, Regan MM, Harshman LC, Bjarnason GA, Vaishampayan UN, et al. External Validation and Comparison With Other Models of the International Metastatic Renal-Cell Carcinoma Database Consortium Prognostic Model: A Population-Based Study. *Lancet Oncol* (2013) 14 (2):141–8. doi: 10.1016/S1470-2045(12)70559-4
17. Watanabe H, Okada M, Kaji Y, Satouchi M, Sato Y, Yamabe Y, et al. New Response Evaluation Criteria in Solid Tumours - Revised Recist Guideline (Version 1.1). *Japanese J Cancer Chemotherapy* (2009) 36:2495–501. doi: 10.1016/j.ejca.2008.10.026
18. Grassi P, Doucet L, Giglione P, Grünwald V, Melichar B, Galli L, et al. Clinical Impact of Pancreatic Metastases From Renal Cell Carcinoma: A Multicenter Retrospective Analysis. *PloS One* (2016) 11(4):e0151662. doi: 10.1371/journal.pone.0151662
19. Motzer RJ, Rini BI, McDermott DF, Arén Frontera O, Hammers HJ, Carducci MA, et al. Nivolumab Plus Ipilimumab Versus Sunitinib in First-Line Treatment for Advanced Renal Cell Carcinoma: Extended Follow-Up of Efficacy and Safety Results From a Randomised, Controlled, Phase 3 Trial. *Lancet Oncol* (2019) 20(10):1370–85. doi: 10.1016/S1470-2045(19)30413-9
20. Kankuri M, Pelliniemi T-T, Pyrhönen S, Nikkanen V, Helenius H, Salminen E. Feasibility of Prolonged Use of Interferon-α in Metastatic Kidney Carcinoma.

Cancer (2001) 92(4):761–7. doi: 10.1002/1097-0142(20010815)92:4<761::AID-CNCR1380>3.0.CO;2-#
21. Vickers MM, Al-Harbi H, Choueiri TK, Kollmannsberger C, North S, MacKenzie M, et al. Prognostic Factors of Survival for Patients With Metastatic Renal Cell Carcinoma With Brain Metastases Treated With Targeted Therapy: Results From the International Metastatic Renal Cell Carcinoma Database Consortium. *Clin Genitourin Cancer* (2013) 11(3):311–5. doi: 10.1016/j.clgc.2013.04.012
22. Peverelli G, Raimondi A, Ratta R, Verzoni E, Bregni M, Cortesi E, et al. Cabozantinib in Renal Cell Carcinoma With Brain Metastases: Safety and Efficacy in a Real-World Population. *Clin Genitourin Cancer* (2019) 17(4):291–8. doi: 10.1016/j.clgc.2019.05.002
23. Flanigan RC, Mickisch G, Sylvester R, Tangen C, Van Poppel H, Crawford ED. Cytoreductive Nephrectomy in Patients With Metastatic Renal Cancer: A Combined Analysis. *J Urol* (2004) 171(3):1071–6. doi: 10.1097/01.ju.0000110610.61545.ae
24. Heng DYC, Wells JC, Rini BI, Beuselinck B, Lee J-L, Knox JJ, et al. Cytoreductive Nephrectomy in Patients With Synchronous Metastases From Renal Cell Carcinoma: Results From the International Metastatic Renal Cell Carcinoma Database Consortium. *Eur Urol* (2014) 66(4):704–10. doi: 10.1016/j.eururo.2014.05.034
25. Bhindi B, Graham J, Wells JC, Bakouny Z, Donskov F, Fraccon A, et al. Deferred Cytoreductive Nephrectomy in Patients With Newly Diagnosed Metastatic Renal Cell Carcinoma. *Eur Urol* (2020) 78(4):615–23. doi: 10.1016/j.eururo.2020.04.038
26. Woldu SL, Brugarolas J, Kapur P, Margulis V. What Is the Role of Nephrectomy Following Complete Response to Checkpoint Inhibitors? *Urol Case Rep* (2018) 18:60–3. doi: 10.1016/j.eucr.2018.02.016
27. Singla N, Elias R, Ghandour R, Freifeld YN, Bowman AI, Woldu SL, et al. Safety and Feasibility of Nephrectomy After Receipt of Immune Checkpoint Inhibitors for Renal Cell Carcinoma. *J Clin Oncol* (2019) 37(7_suppl):619. doi: 10.1200/JCO.2019.37.7_suppl.619
28. Ikarashi D, Kato Y, Katagiri H, Takahara T, Uesugi N, Shiomi E, et al. Case of Complete Response to Neoadjuvant Therapy Using Nivolumab in a Patient With Metastatic Renal Cell Carcinoma. *Int J Urol* (2018) 25(6):630–2. doi: 10.1111/iju.13590
29. Labbate C, Hatogai K, Werntz R, Stadler WM, Steinberg GD, Eggener S, et al. Complete Response of Renal Cell Carcinoma Vena Cava Tumor Thrombus to Neoadjuvant Immunotherapy. *J Immunother Cancer* (2019) 7(1):1–6. doi: 10.1186/s40425-019-0546-8
30. Choueiri TK, Motzer RJ, Rini BI, Haanen J, Campbell MT, Venugopal B, et al. Updated Efficacy Results From the JAVELIN Renal 101 Trial: First-Line Avelumab Plus Axitinib Versus Sunitinib in Patients With Advanced Renal Cell Carcinoma. *Ann Oncol [Internet]* (2020) 31(8):1030–9. doi: 10.1016/j.annonc.2020.04.010
31. Albiges L, Rini BI, Haanen JBAG, Motzer RJ, Kollmannsberger CK, Negrier S, et al. Primary Renal Tumour Shrinkage in Patients (Pts) Who did Not Undergo Upfront Cytoreductive Nephrectomy (uCN): Subgroup Analysis From the Phase 3 JAVELIN Renal 101 Trial of First-Line Avelumab + Axitinib (a + Ax) vs Sunitinib (s) for Advanced Renal Cell Ca. *Ann Oncol* (2019) 30:v356–402. doi: 10.1093/annonc/mdz249.007
32. Bakouny Z, Xie W, Dudani S, Wells C, Gan CL, Donskov F, et al. Cytoreductive Nephrectomy (CN) for Metastatic Renal Cell Carcinoma (mRCC) Treated With Immune Checkpoint Inhibitors (ICI) or Targeted Therapy (TT): A Propensity Score-Based Analysis. *J Clin Oncol* (2020) 38(6_suppl):608. doi: 10.1200/JCO.2020.38.6_suppl.608
33. Pignot G, Thiery-Vuillemin A, Walz J, Lang H, Bigot P, Werle P, et al. Nephrectomy After Complete Response to Immune Checkpoint Inhibitors for Metastatic Renal Cell Carcinoma: A New Surgical Challenge? *Eur Urol* (2020) 77(6):761–3. doi: 10.1016/j.eururo.2019.12.018
34. Donskov F, Xie W, Overby A, Wells JC, Fraccon AP, Sacco CS, et al. Synchronous Versus Metachronous Metastatic Disease: Impact of Time to Metastasis on Patient Outcome—Results From the International Metastatic Renal Cell Carcinoma Database Consortium. *Eur Urol Oncol* (2020) 3(4):530–9. doi: 10.1016/j.euo.2020.01.001

Conflict of Interest: The authors declare that the research was conducted in the absence of any commercial or financial relationships that could be construed as a potential conflict of interest.

frontiers in Oncology

ORIGINAL RESEARCH
published: 21 July 2021
doi: 10.3389/fonc.2021.678694

A Novel Ferroptosis-Related Pathway for Regulating Immune Checkpoints in Clear Cell Renal Cell Carcinoma

Su Gao[1,2], Hailong Ruan[3], Jingchong Liu[3], Yuenan Liu[3], Di Liu[3], Junwei Tong[3], Jian Shi[3], Hongmei Yang[4], Tianbo Xu[3] and Xiaoping Zhang[3]**

[1] Department of Geriatrics, Union Hospital, Tongji Medical College, Huazhong University of Science and Technology, Wuhan, China, [2] Institute of Gerontology, Union Hospital, Tongji Medical College, Huazhong University of Science and Technology, Wuhan, China, [3] Department of Urology, Union Hospital, Tongji Medical College, Huazhong University of Science and Technology, Wuhan, China, [4] Department of Pathogenic Biology, School of Basic Medicine, Huazhong University of Science and Technology, Wuhan, China

OPEN ACCESS

Edited by:
Walter J. Storkus,
University of Pittsburgh,
United States

Reviewed by:
Mariusz Lukasz Hartman,
Medical University of Lodz,
Poland
Di Gu,
First Affiliated Hospital of
Guangzhou Medical University,
China

***Correspondence:**
Xiaoping Zhang
xzhang@hust.edu.cn
Tianbo Xu
tianboxu@hust.edu.cn

Specialty section:
This article was submitted to
Genitourinary Oncology,
a section of the journal
Frontiers in Oncology

Received: 10 March 2021
Accepted: 25 June 2021
Published: 21 July 2021

Citation:
Gao S, Ruan H, Liu J, Liu Y, Liu D, Tong J, Shi J, Yang H, Xu T and Zhang X (2021) A Novel Ferroptosis-Related Pathway for Regulating Immune Checkpoints in Clear Cell Renal Cell Carcinoma. Front. Oncol. 11:678694. doi: 10.3389/fonc.2021.678694

Ferroptosis is a novel form of cell death and plays a role in various diseases, especially tumors. It has been reported that ferroptosis is involved in the growth and progression of clear cell renal cell carcinoma (ccRCC); however, the specific molecular mechanisms are still unclear. In this study, we constructed a four-gene signature (FeSig) of ferroptosis-related genes *via* Cox regression analysis. ROC and survival analyses indicated that FeSig had good diagnostic and prognostic value. Further analysis revealed that ferroptosis was associated with tumor immunity in ccRCC. Next, weighted gene co-expression network analysis was performed to identify the potential regulatory mechanisms. Combined with correlation and survival analyses, the TAZ/WNT10B axis was identified as a tumor immune-related regulatory pathway. In conclusion, these findings suggest that ferroptosis is correlated with tumor immunity. The TAZ/WNT10B axis may be a novel biomarker and therapeutic target for immunotherapy in ccRCC.

Keywords: clear cell renal cell carcinoma, ferroptosis, TAZ, WNT10B, immune checkpoints, PD-1

INTRODUCTION

Renal cell carcinoma (RCC) is a common neoplasm that originates from renal tubular epithelial cells and accounts for 2–3% of all malignant tumors in adults (1). In the USA, it is estimated that there will be approximately 70,000 new cases and 14,000 deaths due to this cancer in 2020. The 5-year relative survival is 75.2% (2). Clear cell renal cell carcinoma (ccRCC) is the most common histological subtype and accounts for over 70% of RCCs (1). Due to high resistance to conventional chemoradiotherapy, only limited

Abbreviations: ccRCC, clear cell renal cell carcinoma; RCC, renal cell carcinoma; ICIs, immune checkpoint inhibitors; ROS, reactive oxygen radicals; FeSig, ferroptosis-related gene signature; TCGA, The Cancer Genome Atlas; ICGC, International Cancer Genome Consortium; DEGs, differentially expressed genes; DE-FRGs, differentially ferroptosis-related genes; PPI, protein–protein interaction; LASSO, least absolute shrinkage and selection operator; RS: risk score; PCA: principal component analysis; t-SNE: t-distributed stochastic neighbor embedding; ROC, receiver operator characteristic; GSEA, gene set enrichment analysis; GSVA, gene set variation analysis; KEGG, Kyoto Encyclopedia of Genes and Genomes; WGCNA, weighted gene co-expression network analysis; TOM, topological overlap matrix; MEs, module eigengenes; OS, overall survival; AUC, area under the curve; DFS, disease-free survival; TAM, tumor associated macrophages.

therapies are currently available (3, 4). At present, immunotherapy, as a novel treatment, is gradually being applied in ccRCC therapy (5). Immune checkpoint inhibitors (ICIs), such as PD-1 and CTLA-4 inhibitors (6, 7), have improved clinical responses and quality of life for some patients. However, some patients are insensitive to ICIs (8). Therefore, it is necessary to further study the regulatory mechanisms of immune checkpoints in ccRCC.

Ferroptosis is a novel form of cell death caused by iron-dependent oxidative damage (9). Due to the failure of glutathione peroxidase (GPX4), a large number of reactive oxygen radicals (ROS) accumulate on membrane lipids (10). In recent years, many studies have verified that ferroptosis plays a vital role in degenerative diseases (*i.e.*, Alzheimer's and Parkinson's diseases) (11, 12), ischemia–reperfusion injury (13), and tumors (14). Zhang et al. showed that BAP1 inhibits tumor progression by promoting cellular ferroptosis (15). Furthermore, it has been reported that ferroptosis is closely associated with the therapeutic effect of immunotherapy. Wang et al. verified that CD8+ T cells enhanced the effect of immunotherapy by promoting ferroptosis of tumor cells (16). Interestingly, Lang et al. indicated that immunotherapy sensitizes tumors to radiotherapy by inhibiting SLC7A11 and reducing cystine uptake (17). However, the interaction between ferroptosis and immunotherapy in ccRCC is still unclear. In this study, we constructed a ferroptosis-related gene signature (FeSig) and analyzed the correlation between FeSig and immune checkpoints to identify novel therapeutic targets in ccRCC.

METHODS AND MATERIALS

Data Download and Study Design

The gene expression data and clinical data were obtained from The Cancer Genome Atlas (TCGA-KIRC, https://www.cancer.gov/tcga) and International Cancer Genome Consortium (ICGC-RECA-EU, https://dcc.icgc.org/) databases. An immunotherapy (immune checkpoint inhibitor, ICI) dataset of clear cell renal cell carcinoma (ccRCC) with clinical data and gene expression data was obtained from the study of Miao et al. (18). In addition, the study process is shown in a flow chart (**Figure 1**).

Identification of Differentially Expressed Genes and Ferroptosis-Related Genes

The "DESeq2" (19) and "edgeR" (20) packages were used to screen DEGs with p-value <0.05 and |log2FC| > 1.5. The Wilcoxon test was performed to identify DE-FRGs with a p-value <0.05 and |log2FC| >1.

Protein–Protein Interaction Network Analysis

The DE-FRGs were inputted into the STRING online tool (https://string-db.org) to construct the PPI network. Then, Cytoscape software (21) was used to analyze the PPI network.

Cox Regression Analysis and Construction of a Proportional Hazards Model

The "survival" package (https://CRAN.R-project.org/package=survival) was utilized to perform univariate and multivariate Cox regression analyses. The "glmnet" (22) and "survival" packages were used to perform least absolute shrinkage and selection operator (LASSO) regression analysis. Through integrated Cox analysis, four key FRGs were screened to construct the risk model (FeSig). The risk score (RS) formula was as follows:

$$\mathrm{RS} = \sum_{i=1}^{n} Coef(i)X(i)$$

Where *Coef* (*i*) represents the coefficient, and *X*(*i*) represents the expression of selected genes.

Principal Component Analysis and T-Distributed Stochastic Neighbor Embedding Analysis

The "stats" and "limma" packages (23) were used to perform PCA. The "Rtsne" package (https://CRAN.R-project.org/package=Rtsne) was utilized to perform t-SNE analysis. PCA and t-SNE analysis were both used to explore the distribution of different groups.

Survival Analysis and Receiver Operator Characteristic Curve Analysis

According to the median gene expression/risk score, ccRCC patients were divided into a high group and a low group. Then, survival curves of overall survival (OS) and disease-free survival (DFS) were drawn by the "survival" package in R and GraphPad software (version 7.0). A p-value <0.05 was considered statistically significant. Moreover, the "survivalROC" (https://CRAN.R-project.org/package=survivalROC) package was used to generate a time-dependent ROC curve to evaluate the predictive value of the risk model.

Gene Set Enrichment Analysis and Gene Set Variation Analysis

All patients were divided into two groups (high group and low group) according to the median gene expression/risk score. GSEA (24) was performed to discover potential mechanisms and downstream signaling pathways. Moreover, the "GSVA" package (25) was utilized to find differential signaling pathways between the high group and the low group.

Kyoto Encyclopedia of Genes and Genomes Pathway Enrichment Analysis

The "clusterProfiler" package (26) was used to conduct KEGG enrichment analysis of DEGs. The results were visualized by the "ggplot2" package (https://CRAN.R-project.org/package=ggplot2) in the R programme. A p-value <0.05 was selected as the cut-off point.

Weighted Gene Co-Expression Network Analysis

The "WGCNA" package (27) was applied to construct the weighted gene co-expression network of DEGs. First, the TCGA-KIRC cohort was evaluated *via* sample clustering to detect outliers with a height cut-off point = 60. Then, Pearson's correlation was calculated between each of the gene pairs. Second, a matrix of adjacencies was constructed according to Pearson's

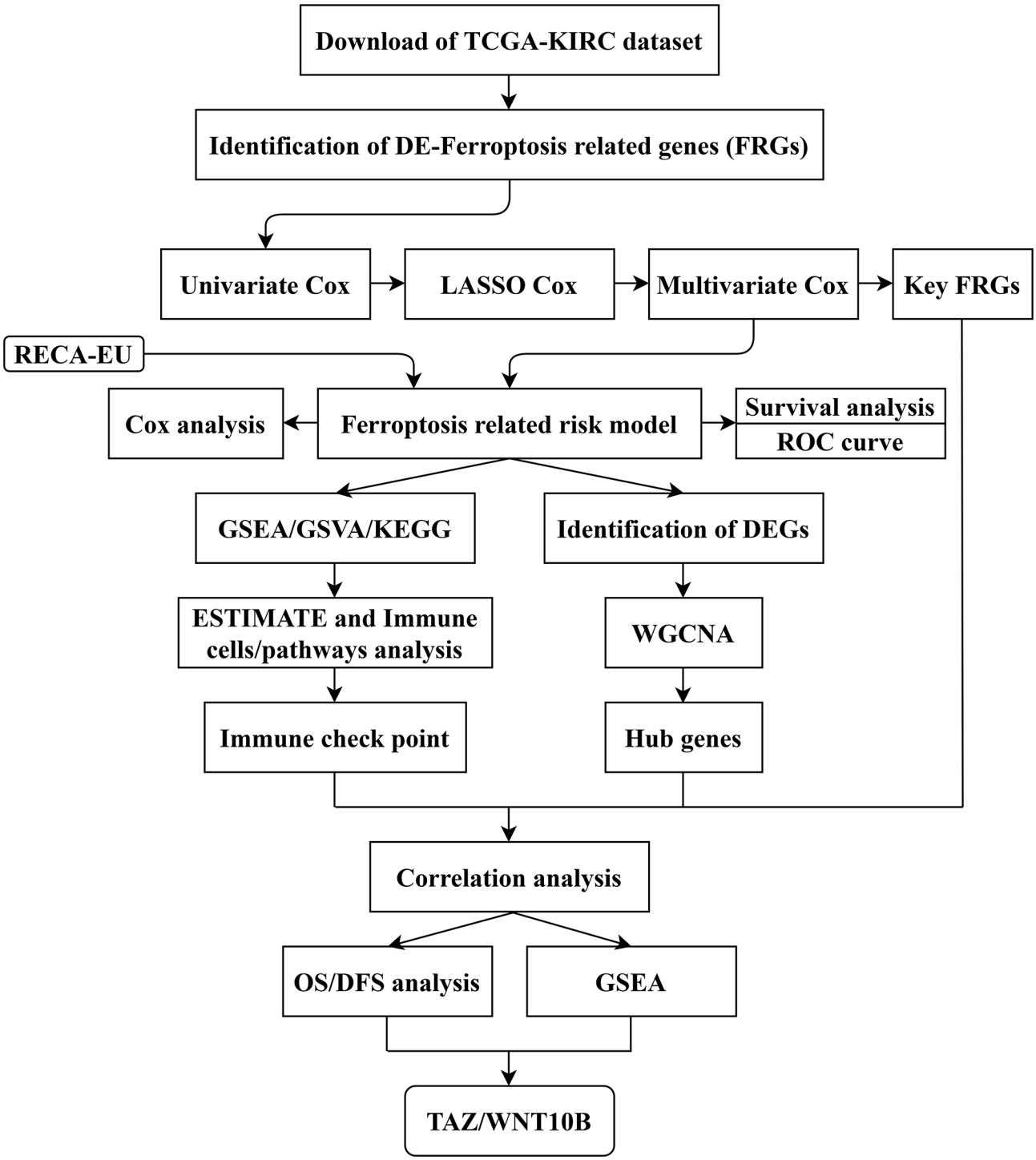

FIGURE 1 | Flow chart of study design. The data collection and study process were shown in a flow chart. TCGA, The Cancer Genome Atlas; KIRC, kidney clear cell carcinoma; FRGs, ferroptosis-related genes; LASSO, least absolute shrinkage and selection operator; ROC, receiver operating characteristic; GSEA, gene set enrichment analysis; GSVA, gene set variation analysis; KEGG: Kyoto Encyclopedia of Genes and Genomes; DEGs, differentially expressed genes; ESTIMATE, Estimation of STromal and Immune cells in Malignant Tumor tissues using Expression data; WGCNA, weighted gene co-expression network analysis; OS, overall survival; DFS, disease-free survival.

correlation. Then, the adjacencies achieved scale-free topology based on the soft threshold power β (**Figure 7A**). Third, the adjacencies were transformed into a topological overlap matrix (TOM). Genes with a high absolute correlation were clustered into the same module. Finally, combined with clinical traits, we calculated the correlation between the module eigengenes (MEs) and clinical traits to screen the clinically significant modules. After that, the correlation between genes and clinical traits (cor.geneTraitSignificance) and the correlation between genes and MEs (cor.geneModuleMembership) were conducted to identify hub genes. In this study, cor.geneTraitSignificance >0.2 and cor.geneModuleMembership >0.6 were selected as the cut-off criteria.

Human Clinical Specimens

A total of 19 pairs of ccRCC samples and adjacent normal samples (4 cm away from the margin of the tumor tissues) were obtained from Wuhan Union Hospital between 2018 and 2020. The study was approved by the Human Research Ethics Committee of Huazhong University of Science and Technology (HUST), and all patients signed the informed consent.

RNA Extraction and qRT-PCR

Total RNA was extracted from ccRCC samples and adjacent normal samples using Trizol Reagent (Sigma, USA). Then, cDNA was synthesized using qPCR RT Kit (Vazyme, China). After that, quantitative real time PCR (qRT-PCR) was performed to amplify cDNA.

Primer sequences were listed as follows:

GAPDH Forward: 5′-GCACCGTCAAGGCTGAGAAC-3′;
GAPDH Reverse: 5′-TGGTGAAGACGCCAGTGGA-3′;
TAZ Forward: 5′-CACCGTGTCCAATCACCAGTC-3′;
TAZ Reverse: 5′-TCCAACGCATCAACTTCAGGT-3′;
WNT10B Forward: 5′-CATCCAGGCACGAATGCGA-3′;
WNT10B Reverse: 5′-CGGTTGTGGGTATCAATGAAGA-3′.

Statistical Analysis

In this study, all data are presented as the mean ± SD. SPSS (version 22.0) and GraphPad Prism (version 7.0) were used to analyze the data. Student's t-test, Mann–Whitney test, and Pearson's χ^2 test were used to conduct statistical analyses. A p-value <0.05 was considered statistically significant.

RESULTS

Identification of DE-FRGs and Construction of a Proportional Hazards Model

The gene expression data were obtained from the TCGA-KIRC cohort. According to the cut-off criteria, 46 DE-FRGs were identified (**Figure 2A**). The protein–protein interactions of DE-FRGs were shown in **Figure 2B**. Further analysis indicated that there were 20 DE-FRGs with good prognostic value (**Figure 2C**). The correlation was close and high between these DE-FRGs (**Figure 2D**). Then, LASSO and multivariate Cox regression analyses were applied to construct a prognostic model. A four-gene signature (FeSig) was identified (**Figures 2E–G**). The risk score = 0.49*expression of BID + 0.70*expression of TAZ + 0.09*expression of MT1G + 0.45*expression of SLC7A11.

The Diagnostic and Prognostic Value of the Four-Gene Signature

PCA and t-SNE analysis proved that FeSig could significantly divide patients into different risk groups (**Figures 3A, B**). In the TCGA-KIRC cohort, patients were divided into two groups (high-risk group and low-risk group) according to the median risk score (**Figure 3C**). As shown in **Figure 3D**, patients with a high-risk score had a higher probability of death earlier than those with a low risk score. Further Cox regression analysis revealed that the risk score was an independent prognostic factor (**Figures 3E, F**). Time-dependent ROC curves indicated that the risk score had good predictive performance in both the TCGA-KIRC (**Figure 3G**) cohort and the ICGC-RECA-EU (**Figure 3H**) cohort. Moreover, survival analysis also uncovered that the high-risk group predicted poor OS (**Figures 3I, J**). These findings suggested that FeSig had good diagnostic and prognostic value.

FeSig Is Closely Correlated With Immune-Related Pathways

GSEA, GSVA, and KEGG analyses were performed to identify potential downstream signaling pathways of FeSig. As shown in **Figure 4A**, FeSig was associated with immune cell-related pathways. Analogously, GSVA also verified that there were many differentially enriched immune cell-related pathways between the high-risk group and the low-risk group (**Figures 4B, C**). Then, 314 DEGs were identified *via* DESeq2 and edgeR package in the R programme (**Figures 4D, E**). Further KEGG pathway enrichment analysis indicated that these DEGs were mainly enriched in immune-related pathways (**Figure 4F**, Ras signaling pathway, PPAR signaling pathway, and IL-17 signaling pathway). To further study the correlation between FeSig and immune status, we quantified the enrichment scores of diverse immune cell subpopulations, related functions, or pathways with ssGSEA. As shown in **Figure 5A**, nine immune cell subpopulations (CD8+ T cells, macrophages, mast cells, neutrophils, T helper cells, Tfhs, Th1 cells, Th2 cells, and TILs) were clearly different between the high-risk group and the low-risk group. For immune-related functions, seven pathways (CCR, checkpoint, cytolytic activity, inflammation promotion, parainflammation, T cell coinhibition, and T cell costimulation) had higher scores in the high-risk group, and only the type II IFN response had higher scores in the low-risk group (**Figure 5B**). These findings revealed that FeSig is significantly associated with the regulation of tumor immunity.

Potential of the FeSig as an Indicator of Response to Anti-PD-1 Therapy

Due to the wide popularization of immune checkpoint inhibitors in ccRCC, we further focused on the correlation between FeSig

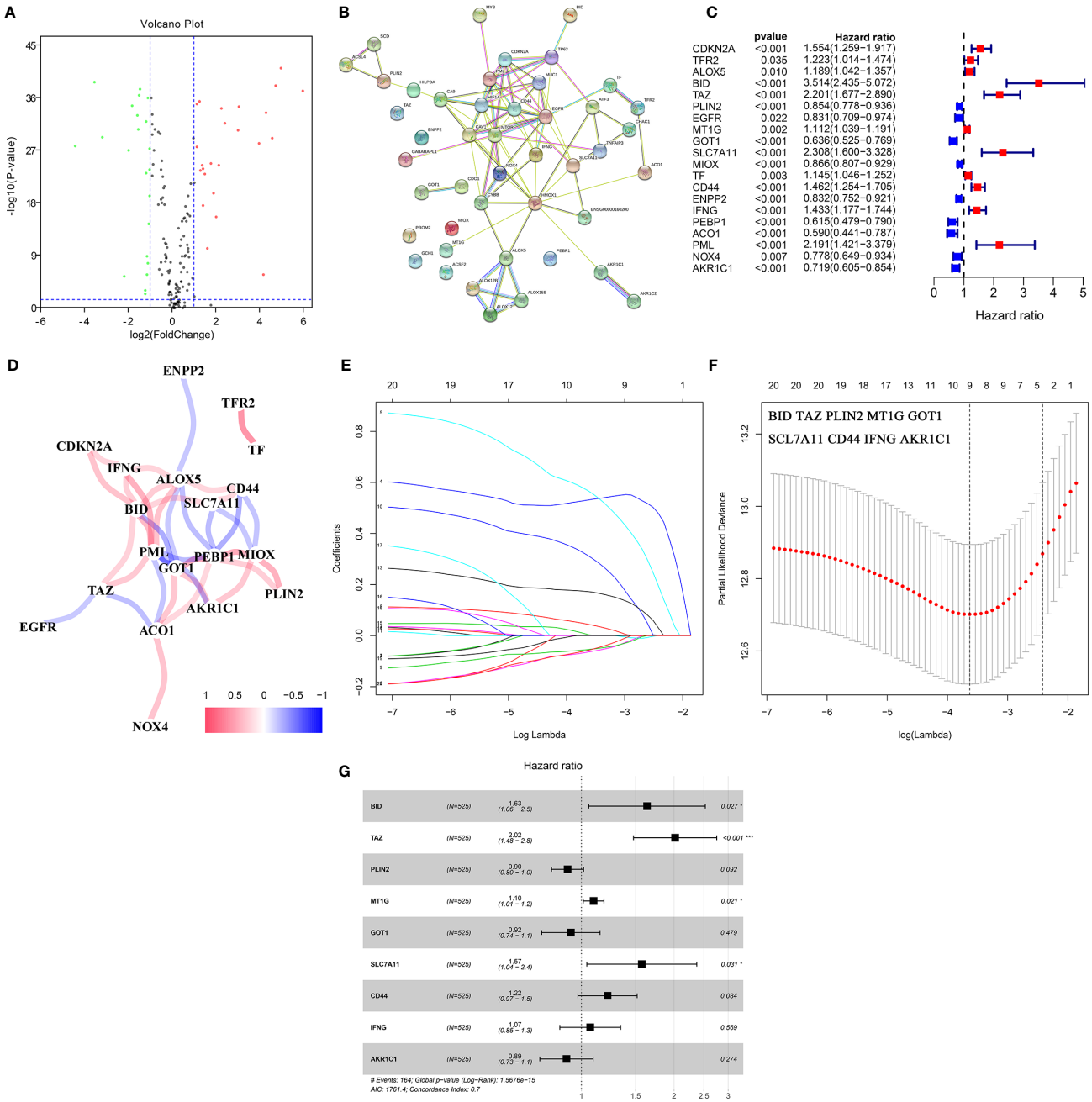

FIGURE 2 | Identification of key DE-FRGs *via* Cox regression analysis. **(A)** The volcano plot of FRGs. **(B)** The protein–protein interaction between FRGs. **(C)** Univariate cox regression analysis revealed that a total of twenty DE-FRGs had prognostic value. **(D)** The correlation network of DE-FRGs. **(E, F)** Through LASSO Cox regression, nine genes were selected as key DE-FRGs for further analysis. **(G)** Four genes (BID, TAZ, MT1G, and SCL7A11) were identified as independent prognostic factors *via* multivariate Cox regression analysis. DE-FRGs, differentially expressed ferroptosis-related genes; LASSO, least absolute shrinkage and selection operator. ***P < 0.001; *P < 0.05.

and immune checkpoint pathways. As shown in **Figure 6A**, we found that PD-1, CTLA4, LAG3, and TIGIT were upregulated in the high-risk group and TIM-3 was downregulated in the high-risk group. Moreover, correlation analysis indicated that the riskScore was significantly positively correlated with PD-1, CTLA4, LAG3, and TIGIT (**Figures 6B–H**). These findings suggested that FeSig may be a biomarker of the response to immunotherapy. Therefore, the predictive value of FeSig was tested in an immunotherapy dataset of ccRCC. Survival analysis verified that there was a significant difference

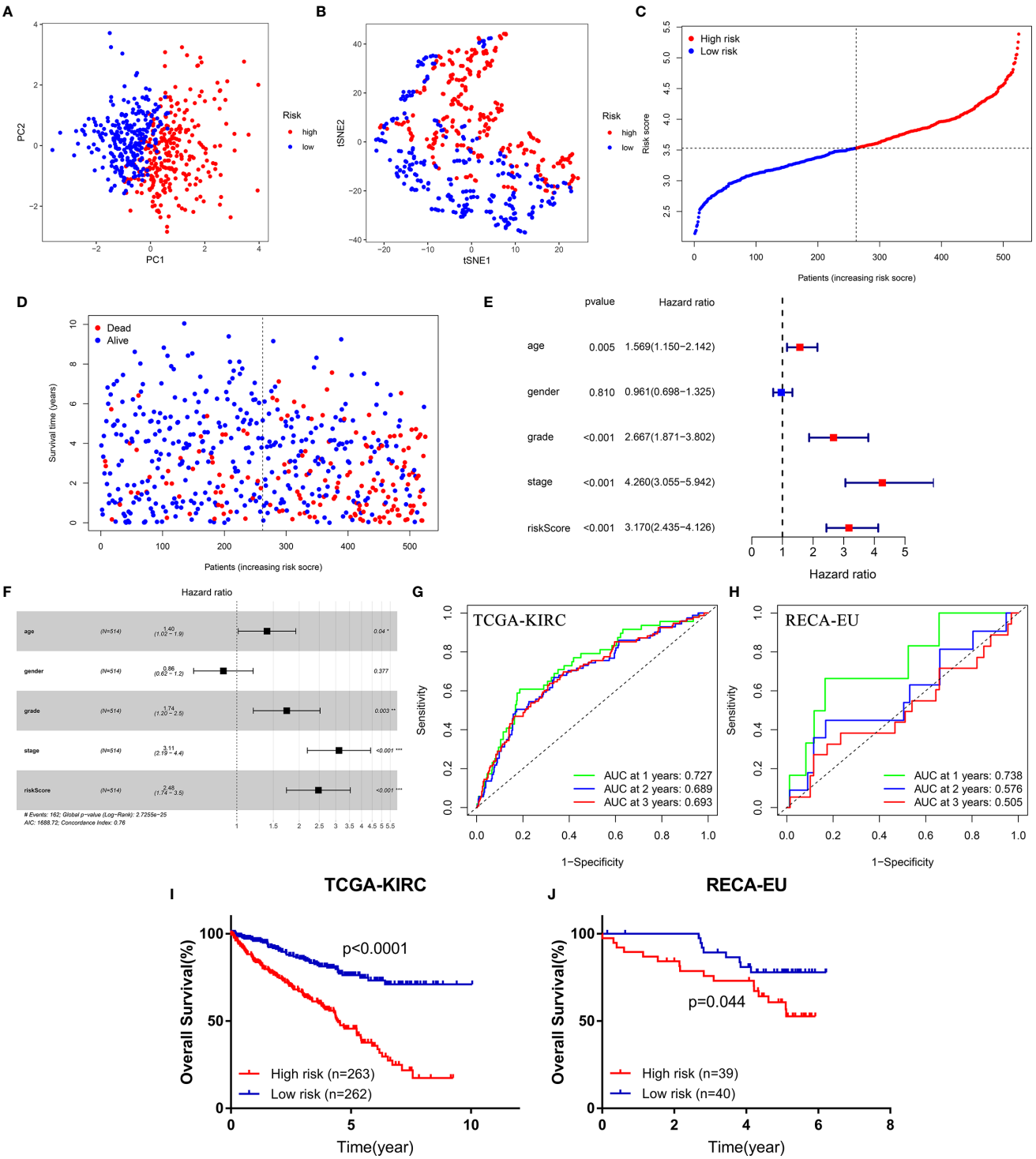

FIGURE 3 | The diagnostic and prognostic value of the four-gene signature (FeSig). **(A, B)** PCA and t-SNE analysis both verified that FeSig could significantly divide patients into different risk groups. **(C)** The distribution and median value of the risk scores in the TCGA cohort. **(D)** Patients with high-risk score had poor OS. **(E, F)** Univariate and multivariate Cox regression analyses indicated that risk score was an independent prognostic factor (HR = 2.48, p < 0.001). **(G, H)** The risk score had good diagnostic value. **(I, J)** High-risk group predicted poor OS both in TCGA and ICGC cohort. FeSig, ferroptosis-related gene signature; PCA, principal component analysis; t-SNE, t-distributed stochastic neighbor embedding; TCGA, The Cancer Genome Atlas; OS, overall survival; ICGC, International Cancer Genome Consortium.

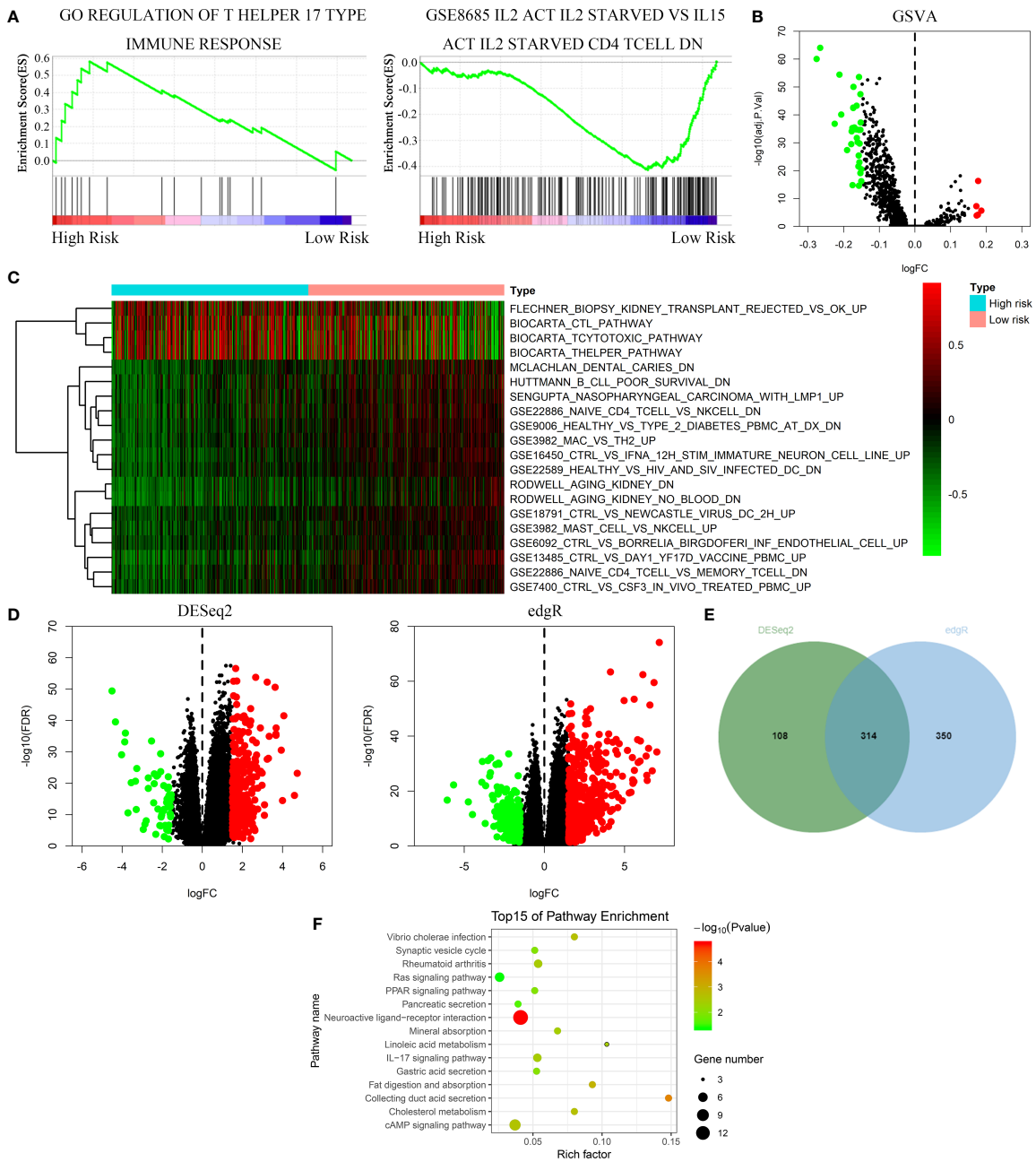

FIGURE 4 | The FeSig was obviously closely associated with immune-related pathways. **(A–C)** GSEA and GSVA showed that FeSig was correlated to immune cell related pathways. **(D, E)** A total of 314 DEGs were identified *via* DESeq2 and edgR package. **(F)** The DEGs were mainly enriched in immune-related signaling pathways. FeSig, ferroptosis-related gene signature; GSEA, gene set enrichment analysis; GSVA, gene set variation analysis; DEGs, differentially expressed genes.

(log-rank p = 0.038) between the high- and low-risk groups of patients with anti-PD-1 monotherapy. Patients in the high-risk group had longer OS than those in the low-risk group (**Figure 6I**). The ROC curve of ICI response (**Figure 6J**) revealed that the diagnostic value of FeSig (AUC = 0.603) was better than that of PD-1 (AUC = 0.544).

Identification of the TAZ/WNT10B Axis as an Immune Checkpoint Regulatory Pathway in ccRCC

The WGCNA algorithm was performed to find further downstream targets of four-gene signature (FeSig). As shown in **Figure 7A**, $\beta = 5$ was selected as the soft threshold power in this study. The DEGs

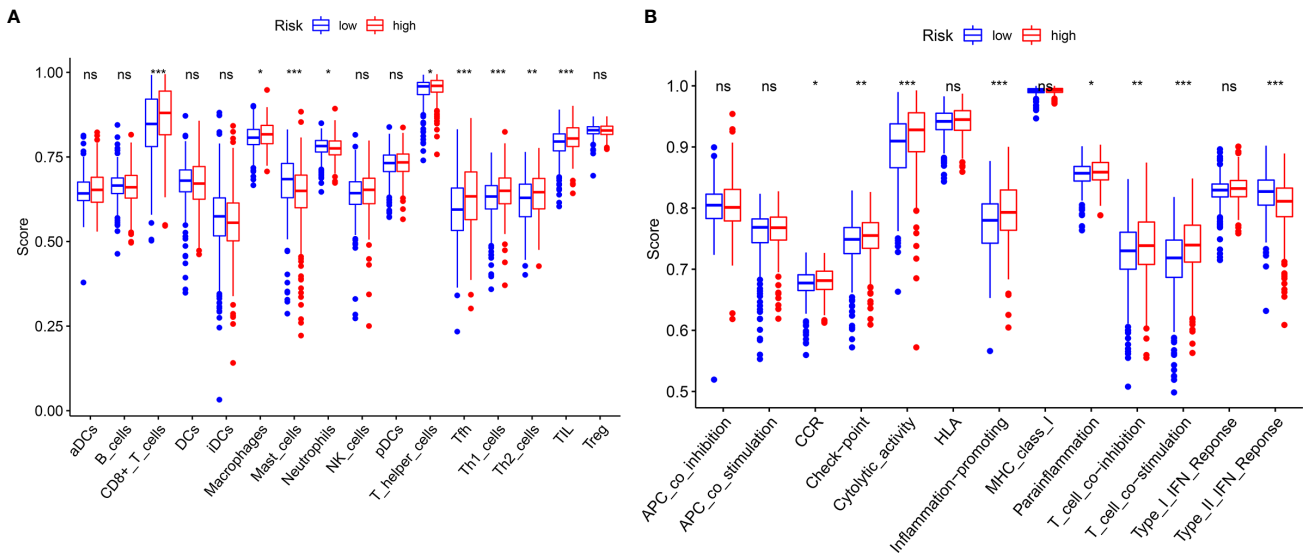

FIGURE 5 | ssGSEA analysis of FeSig. **(A, B)** The ssGSEA score of 16 immune cells and 13 immune-related functions between high-risk group and low-risk group. ssGSEA, single sample gene set enrichment analysis. ***P < 0.001; **P < 0.01; *P < 0.05; ns, no significance.

between high-risk group and low-risk group were divided into four modules according to the expression level of each gene (**Figure 7B**). Combined with the clinical information, we found that the MEturquoise module was significantly positively associated with grade (R = 0.23, p = 2e-07), TNM stage (R = 0.29, p = 3e-11), risk (R = 0.66, p = 2e-66), and ImmuneScore (R = 0.2, p = 6e-06) (**Figure 7C**). According to cor.geneTraitSignificance >0.2 and cor.geneModuleMembership >0.6, CPNE7, WNT10B, ADAMTS14, and RUFY4 were regarded as downstream hub genes of FesSig (**Table 1**, **Figures 7D–H**). Moreover, we analyzed the correlation among four-gene signature (FeSig) (BID, TAZ, MT1G, and SLC7A11), downstream hub genes (CPNE7, WNT10B, ADAMTS14, and RUFY4), and immune checkpoints (PD-1, CTLA4, LAG3, and TIGIT) to further discover potential molecular mechanisms of tumor immunity. According to the correlation value, BID, TAZ, CPNE7, WNT10B, and RUFY4 were selected for subsequent analysis (**Figure 7I**). Survival analyses of OS and DFS proved that WNT10B had better prognostic prediction performance than CPNE7 and RUFY4 (**Figures 8A–F**). Similarly, TAZ had better prognostic value than BID (**Figures 8G, H**). Therefore, TAZ and WNT10B were selected for further study. In addition, the expression of TAZ was clearly positively correlated with WNT10B (**Figure 8I**, R = 0.66, p = 2e-67). Interestingly, GSEA verified that the low TAZ group was enriched in WNT signaling pathway (**Figures 8J, K**). These findings indicated that TAZ might regulate tumor immunity through mediating WNT10B (WNT signaling pathway) in ccRCC.

TAZ/WNT10B Was Closely Correlated With TNM/Grade Stage and UpRegulated in ccRCC Tissue

We further analyzed the correlation between the expression level of TAZ/WNT10B and TNM/Grade stage and verified their mRNA expression level in ccRCC tissues. As shown in **Figures 9A, B**, TAZ and WNT10B were both elevated and positively correlated with TNM/Grade stage in ccRCC. Moreover, qRT-PCR assay also indicated that TAZ and WNT10B were upregulated in ccRCC tissues (**Figure 9C**).

DISCUSSION

Recently, immunotherapy has emerged as a promising approach for cancer treatment, which mainly includes non-specific immunostimulation, immune checkpoint inhibitors (ICIs), tumor vaccines, and adoptive cellular immunotherapy (28). In metastatic RCC (mRCC), immune checkpoint inhibitors have changed the treatment paradigm because most patients with newly diagnosed mRCC are now treated with these medicines. It has been reported that immune checkpoint inhibitors have provided significant clinical benefit for mRCC patients in multiple clinical trials (29). However, there are still some patients without good effects due to adverse reactions and drug resistance to ICIs (30). Therefore, it is necessary to study the molecular mechanisms of drug resistance and reduce the adverse reactions to ICIs. At present, some studies have reported that the induction of ferroptosis enhances the effect of ICIs (16). Interestingly, many ferroptosis-related genes are abnormally expressed in ccRCC and might be potential therapeutic targets. However, the correlation between ferroptosis and immune checkpoints in ccRCC is still unclear.

In this study, a ferroptosis-related risk model (FeSig) was constructed through Cox regression analysis. We found that FeSig had good diagnostic/prognostic value and was closely associated with immune checkpoints. Moreover, patients with high-risk scores had better OS than those with low-risk scores

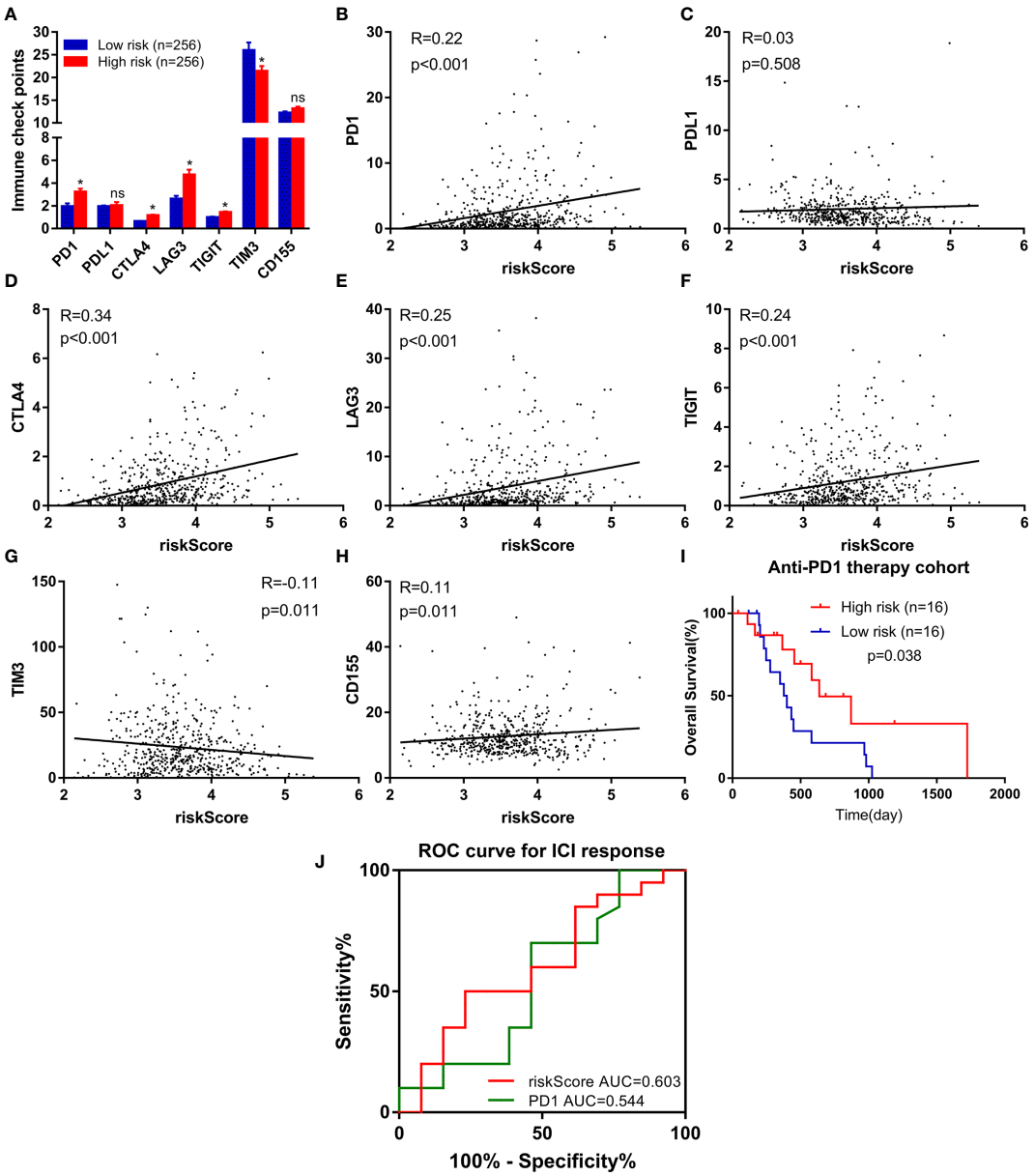

FIGURE 6 | FeSig was a potential indicator of response to anti-PD-1 therapy. **(A)** The expression level of immune checkpoints between high-risk group and low-risk group. **(B–H)** The correlation between immune checkpoints and risk score. **(I)** High risk group of patients with anti-PD-1 monotherapy had better OS. **(J)** ROC curve of ICI response showed that FeSig had good diagnostic value. OS, overall survival; ROC, receiver operating characteristic; ICI, immune checkpoint inhibitor.
*P < 0.05; ns, no significance.

TABLE 1 | Hub genes were identified *via* WGCNA.

Gene	cor.geneModuleMembership	cor.geneTraitSignificance			
	Turquoise	Grade	TNM	Risk	ImmuneScore
CPNE7	0.63	0.29	0.27	0.49	0.41
WNT10B	0.81	0.21	0.21	0.55	0.31
ADAMTS14	0.66	0.29	0.26	0.46	0.22
RUFY4	0.75	0.20	0.24	0.49	0.40

WGCNA, weighted gene co-expression network analysis.

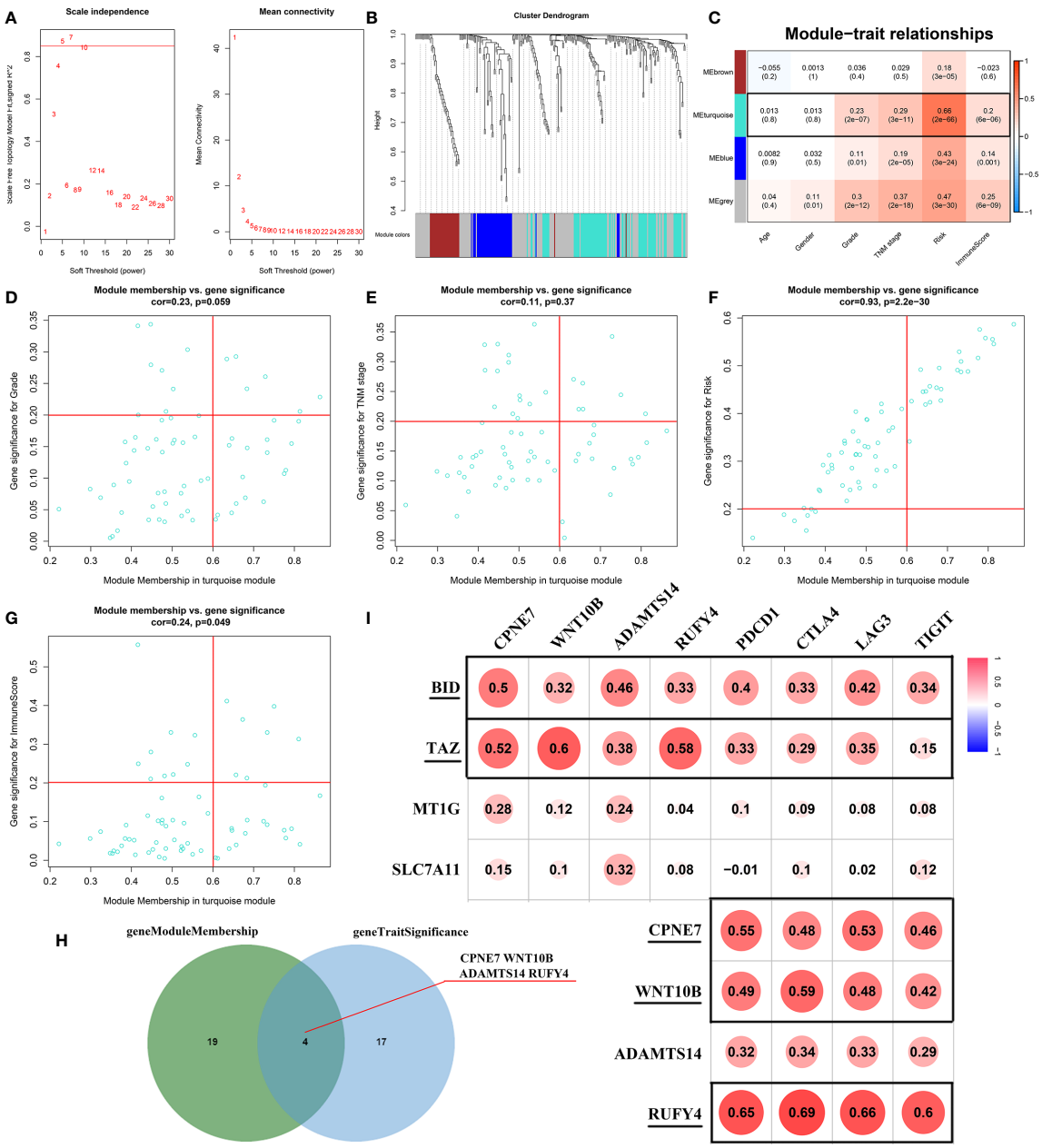

FIGURE 7 | Identification of key genes of regulating immune checkpoints. **(A)** Analysis of scale-free fit parameter and mean connectivity for various soft-thresholding power. **(B)** Dendrogram of DEGs clustered based on a dissimilarity measure (1-TOM). The DEGs were divided into four modules (brown, turquoise, blue, and gray). **(C)** The correlation between clinical traits and modules. MEturquoise was selected as the hub module. **(D–H)** Four genes (CPNE7, WNT10B, ADAMTS14, and RUFY4) were regarded as downstream hub genes. **(I)** The correlation among the FeSig (BID, TAZ, MT1G, and SLC7A11), downstream hub genes (CPNE7, WNT10B, ADAMTS14, and RUFY4), and immune checkpoints (PD-1, CTLA4, LAG3, and TIGIT). BID, TAZ, CPNE7, WNT10B, and RUFY4 were selected for further analysis. DEGs, differentially expressed genes; TOM, topological overlap matrix.

after PD-1 inhibitor treatment, which indicated that FeSig was a potential prognostic biomarker for immunotherapy. Then, the TAZ/WNT10B axis was identified as a potential regulatory pathway of immune checkpoints *via* WGCNA and correlation analysis.

TAZ (Tafazzin) is a transcriptional regulator and plays a vital role in tumorigenesis and tumor progression of most solid tumors (31). TAZ stimulates cell proliferation by regulating DNA duplication and mitosis (32). It has been reported that TAZ maintains plasticity in cell–ECM adhesion and favors

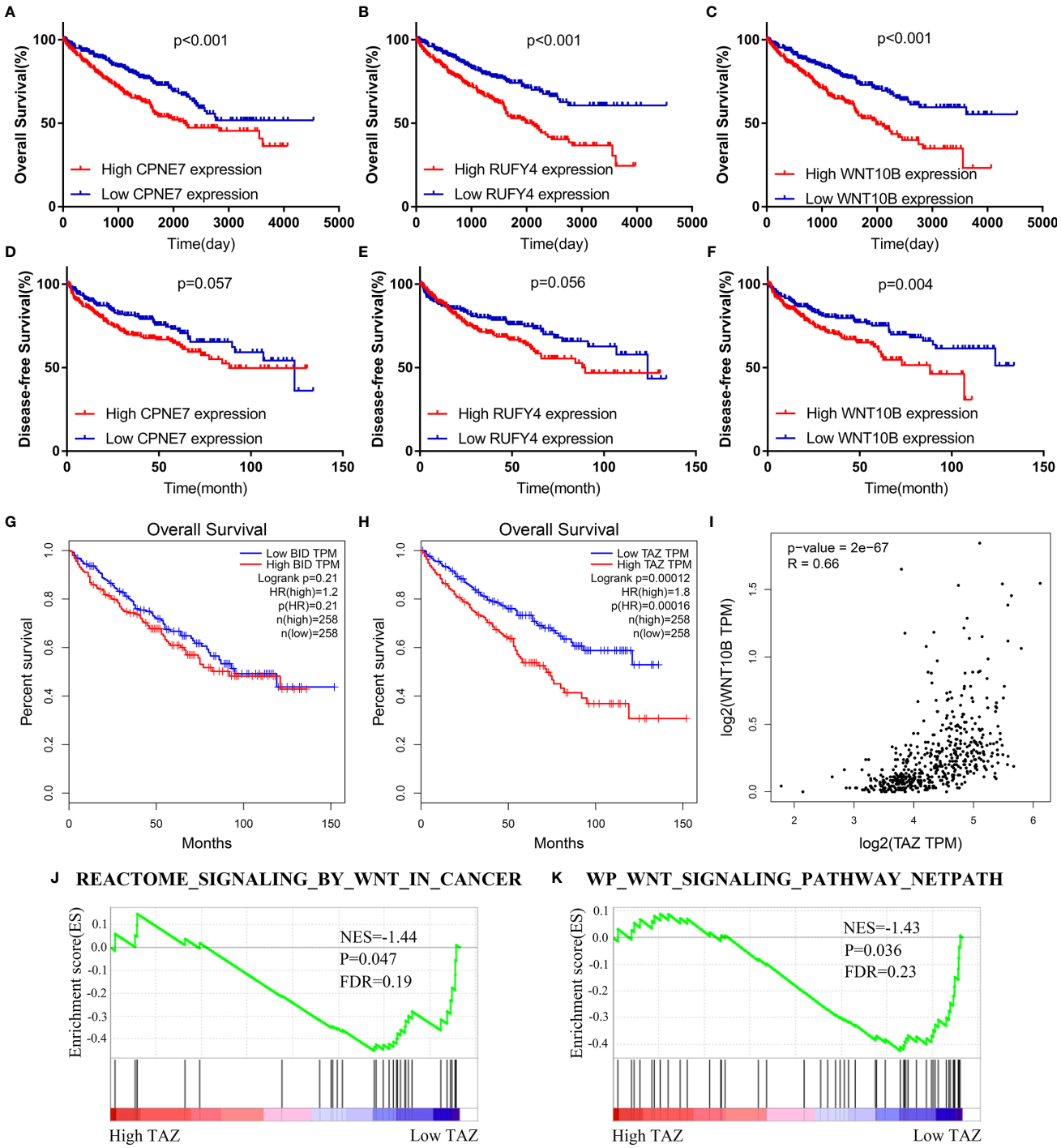

FIGURE 8 | TAZ/WNT10B axis was identified as a potential immune checkpoint regulatory pathway. **(A–F)** WNT10B had better prognostic value than CPNE7 and RUFY4 according to survival analysis of OS and DFS. **(G, H)** Survival analysis revealed that TAZ had better prognostic value than BID. **(I)** TAZ was closely positively correlated to WNT10B (R = 0.66). **(J, K)** Low TAZ group was enriched in WNT signaling pathways. OS, overall survival; DFS, disease-free survival.

cytoskeletal remodeling to promote tumor metastasis (33). TAZ is also regarded as an important regulator of ferroptosis. Two research groups recently reported that TAZ promoted tumor cell ferroptosis by regulating members of the NOX family (34, 35). Furthermore, many studies have verified that TAZ is closely involved in tumor immunity and the microenvironment. TAZ mediates the expression of tumor-secreted factors to drive the differentiation and recruitment of immune suppressive cells,

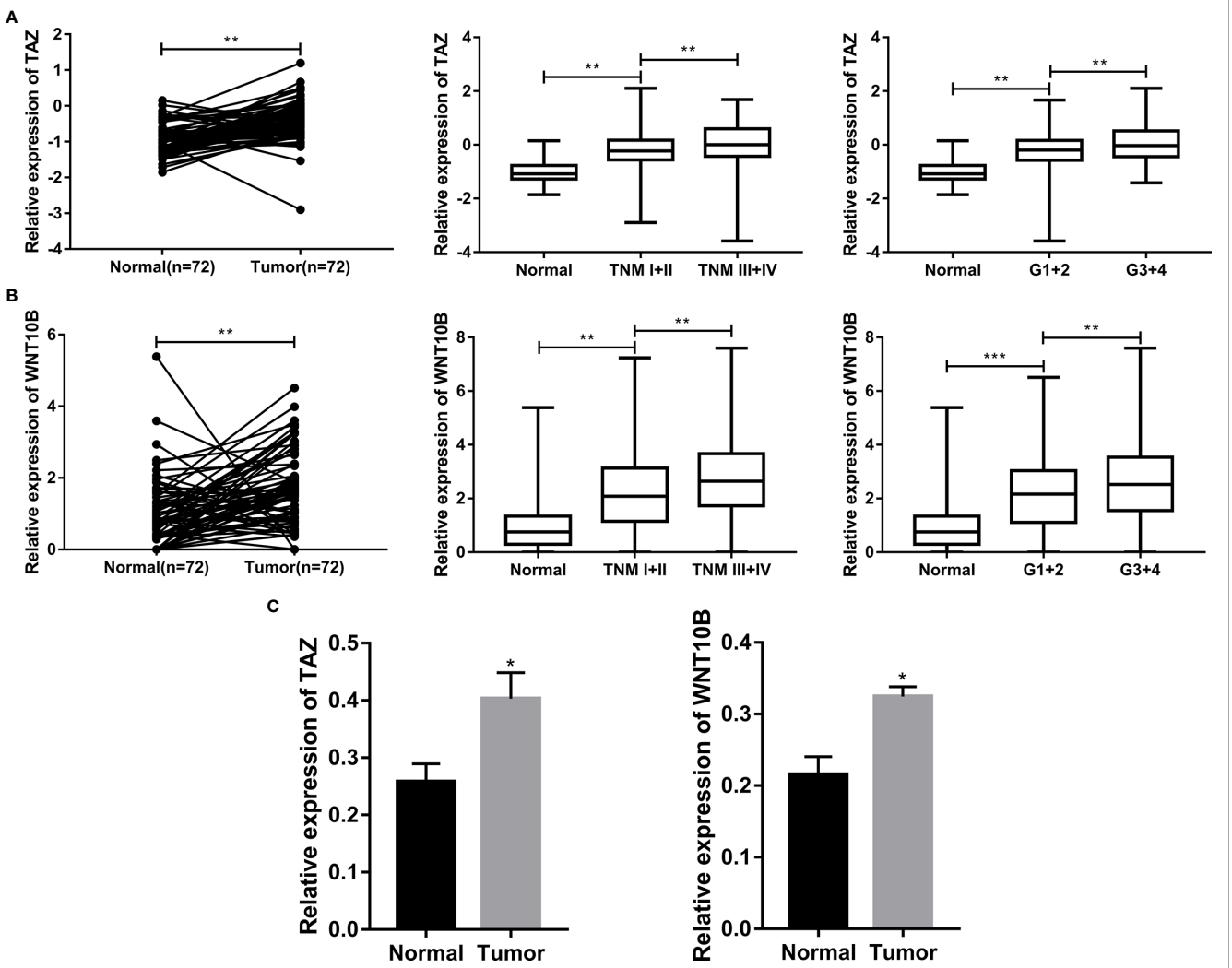

FIGURE 9 | TAZ/WNT10B was closely correlated with TNM/Grade stage and up-regulated in ccRCC tissue. **(A)** In TCGA-KIRC dataset, TAZ was elevated in ccRCC and positively correlated with TNM/Grade stage. **(B)** In TCGA-KIRC dataset, WNT10B was elevated in ccRCC and positively correlated with TNM/Grade stage. **(C)** The mRNA expression level of TAZ/WNT10B was upregulated in ccRCC tissues. ccRCC, clear cell renal cell carcinoma. ***P < 0.001; **P < 0.01; *P < 0.05.

such as tumor-associated macrophages (TAMs) (36) and regulatory T cells (Tregs) (37). In addition, TAZ promotes immune evasion of tumor cells by regulating the expression of immune checkpoints. Feng et al. indicated that tumor cell-derived lactate activated the TAZ/PD-L1 axis to enhance tumor evasion from the immune response (38). Similarly, a recent study also reported that the TAZ/YAP/TEAD signaling pathway increased PD-L1 promoter activity and induced immune evasion of tumors (39). In our study, we found that the expression of TAZ was highly positively associated with PD-1, which suggested that TAZ was a potential therapeutic target of immunotherapy in ccRCC.

To study the specific molecular mechanisms of TAZ, WGCNA and GSEA were performed and indicated that WNT10B is a potential downstream target of TAZ. WNT10B (Wnt Family Member 10B) is a regulator encoding secreted proteins and activating the Wnt signaling cascade (40). It has been reported that the Wnt signaling pathway is closely involved in regulating immune checkpoints. Notably, the expression of PD-L1 has been proven to be regulated by MYC, which is a well-documented target of the Wnt signaling pathway (41). Moreover, inhibiting the Wnt/β-catenin axis can promote antitumor immunity by suppressing PD-L1 expression (42). In this study, we also found that TAZ was significantly positively correlated with WNT10B and that high WNT10B predicted poor OS/DFS in ccRCC. These findings suggested that the TAZ/WNT10B axis might regulate tumor immunity by activating the WNT signaling pathway.

In conclusion, the TAZ/WNT10B axis (ferroptosis-related pathway) is regarded as a tumor immune-related regulatory pathway *via* integrated bioinformatics analysis. Further analysis revealed that immune checkpoints are potential targets of the TAZ/WNT10B pathway. Therefore, the TAZ/WNT10B axis is expected

to be a novel therapeutic target of immunotherapy in ccRCC. However, the specific mechanisms still require further research.

DATA AVAILABILITY STATEMENT

Publicly available datasets were analyzed in this study. This data can be found here: TCGA-KIRC, https://www.cancer.gov/tcga and ICGC-RECA-EU, https://dcc.icgc.org https://science.sciencemag.org/content/suppl/2018/01/03/science.aan5951.DC1.

ETHICS STATEMENT

The studies involving human participants were reviewed and approved by Human Research Ethics Committee of Huazhong University of Science and Technology (HUST). The patients/participants provided their written informed consent to participate in this study. Written informed consent was obtained from the individual(s) for the publication of any potentially identifiable images or data included in this article.

AUTHOR CONTRIBUTIONS

XZ designed this study. TX and SG performed data collection and analysis. TX, SG, HR, and JL performed the majority of the experiments. TX and SG wrote the manuscript and contributed to preparing and making figures and tables. YL, DL, and JT collected the clinical samples and managed the clinical data. JT and JS reviewed the relevant literature. HY and XZ provided conceptual advice and critically reviewed the manuscript. All authors contributed to the article and approved the submitted version.

FUNDING

This study was supported by the Key Research and Development Plan in China (grant no. 2017YFB1303100), the National Natural Science Foundation of China (grant nos. 81672524, 81672528, and 81874090), the Hubei Provincial Natural Science Foundation of China (grant no. 2018CFA038), the Independent Innovation Foundation of Huazhong University of Science and Technology (grant no. 118530309), and the Clinical Research Physician Program of Tongji Medical College, Huazhong University of Science and Technology (grant no. 5001530015).

ACKNOWLEDGMENTS

We would like to express our gratitude to all the members who participated in the discussion and assisted in this study.

REFERENCES

1. Moch H, Cubilla AL, Humphrey PA, Reuter VE, Ulbright TM. The 2016 WHO Classification of Tumours of the Urinary System and Male Genital Organs-Part A: Renal, Penile, and Testicular Tumours. *Eur Urol* (2016) 70:93–105. doi: 10.1016/j.eururo.2016.02.029
2. Siegel RL, Miller KD, Jemal A. Cancer Statistics, 2020. *CA Cancer J Clin* (2020) 70:7–30. doi: 10.3322/caac.21590
3. Campbell S, Uzzo RG, Allaf ME, Bass EB, Cadeddu JA, Chang A, et al. Renal Mass and Localized Renal Cancer: AUA Guideline. *J Urol* (2017) 198:520–9. doi: 10.1016/j.juro.2017.04.100
4. Ljungberg B, Bensalah K, Canfield S, Dabestani S, Hofmann F, Hora M, et al. EAU Guidelines on Renal Cell Carcinoma: 2014 Update. *Eur Urol* (2015) 67:913–24. doi: 10.1016/j.eururo.2015.01.005
5. Deleuze A, Saout J, Dugay F, Peyronnet B, Mathieu R, Verhoest G, et al. Immunotherapy in Renal Cell Carcinoma: The Future Is Now. *Int J Mol Sci* (2020) 21:2532. doi: 10.3390/ijms21072532
6. Carosella ED, Ploussard G, LeMaoult J, Desgrandchamps F. A Systematic Review of Immunotherapy in Urologic Cancer: Evolving Roles for Targeting of CTLA-4, PD-1/PD-L1, and HLA-G. *Eur Urol* (2015) 68:267–79. doi: 10.1016/j.eururo.2015.02.032
7. Rotte A. Combination of CTLA-4 and PD-1 Blockers for Treatment of Cancer. *J Exp Clin Cancer Res* (2019) 38:255. doi: 10.1186/s13046-019-1259-z
8. Fares CM, Van Allen EM, Drake CG, Allison JP, Hu-Lieskovan S. Mechanisms of Resistance to Immune Checkpoint Blockade: Why Does Checkpoint Inhibitor Immunotherapy Not Work for All Patients? *Am Soc Clin Oncol Educ Book* (2019) 39:147–64. doi: 10.1200/edbk_240837
9. Dixon SJ, Lemberg KM, Lamprecht MR, Skouta R, Zaitsev EM, Gleason CE, et al. Ferroptosis: An Iron-Dependent Form of Nonapoptotic Cell Death. *Cell* (2012) 149:1060–72. doi: 10.1016/j.cell.2012.03.042
10. Stockwell BR, Friedmann Angeli JP, Bayir H, Bush AI, Conrad M, Dixon SJ, et al. Ferroptosis: A Regulated Cell Death Nexus Linking Metabolism, Redox Biology, and Disease. *Cell* (2017) 171:273–85. doi: 10.1016/j.cell.2017.09.021
11. Yan N, Zhang J. Iron Metabolism, Ferroptosis, and the Links With Alzheimer's Disease. *Front Neurosci* (2019) 13:1443. doi: 10.3389/fnins.2019.01443
12. Guiney SJ, Adlard PA, Bush AI, Finkelstein DI, Ayton S. Ferroptosis and Cell Death Mechanisms in Parkinson's Disease. *Neurochem Int* (2017) 104:34–48. doi: 10.1016/j.neuint.2017.01.004
13. Li Y, Feng D, Wang Z, Zhao Y, Sun R, Tian D, et al. Ischemia-Induced ACSL4 Activation Contributes to Ferroptosis-Mediated Tissue Injury in Intestinal Ischemia/Reperfusion. *Cell Death Differ* (2019) 26:2284–99. doi: 10.1038/s41418-019-0299-4
14. Hassannia B, Vandenabeele P, Vanden Berghe T. Targeting Ferroptosis to Iron Out Cancer. *Cancer Cell* (2019) 35:830–49. doi: 10.1016/j.ccell.2019.04.002
15. Zhang Y, Shi J, Liu X, Feng L, Gong Z, Koppula P, et al. BAP1 Links Metabolic Regulation of Ferroptosis to Tumour Suppression. *Nat Cell Biol* (2018) 20:1181–92. doi: 10.1038/s41556-018-0178-0
16. Wang W, Green M, Choi JE, Gijón M, Kennedy PD, Johnson JK, et al. CD8(+) T Cells Regulate Tumour Ferroptosis During Cancer Immunotherapy. *Nature* (2019) 569:270–4. doi: 10.1038/s41586-019-1170-y
17. Lang X, Green MD, Wang W, Yu J, Choi JE, Jiang L, et al. Radiotherapy and Immunotherapy Promote Tumoral Lipid Oxidation and Ferroptosis via Synergistic Repression of SLC7A11. *Cancer Discov* (2019) 9:1673–85. doi: 10.1158/2159-8290.cd-19-0338
18. Miao D, Margolis CA, Gao W, Voss MH, Li W, Martini DJ, et al. Genomic Correlates of Response to Immune Checkpoint Therapies in Clear Cell Renal Cell Carcinoma. *Science* (2018) 359:801–6. doi: 10.1126/science.aan5951
19. Love MI, Huber W, Anders S. Moderated Estimation of Fold Change and Dispersion for RNA-Seq Data With Deseq2. *Genome Biol* (2014) 15:550. doi: 10.1186/s13059-014-0550-8

20. Robinson MD, McCarthy DJ, Smyth GK. Edger: A Bioconductor Package for Differential Expression Analysis of Digital Gene Expression Data. *Bioinformatics* (2009) 26:139–40. doi: 10.1093/bioinformatics/btp616
21. Shannon P, Markiel A, Ozier O, Baliga NS, Wang JT, Ramage D, et al. Cytoscape: A Software Environment for Integrated Models of Biomolecular Interaction Networks. *Genome Res* (2003) 13:2498–504. doi: 10.1101/gr.1239303
22. Friedman J, Hastie T, Tibshirani R. Regularization Paths for Generalized Linear Models *via* Coordinate Descent. *J Stat Softw* (2010) 33:1–22. doi: 10.18637/jss.v033.i01
23. Ritchie ME, Phipson B, Wu D, Hu Y, Law CW, Shi W, et al. Limma Powers Differential Expression Analyses for RNA-Sequencing and Microarray Studies. *Nucleic Acids Res* (2015) 43:e47. doi: 10.1093/nar/gkv007
24. Subramanian A, Tamayo P, Mootha VK, Mukherjee S, Ebert BL, Gillette MA, et al. Gene Set Enrichment Analysis: A Knowledge-Based Approach for Interpreting Genome-Wide Expression Profiles. *Proc Natl Acad Sci USA* (2005) 102:15545–50. doi: 10.1073/pnas.0506580102
25. Hänzelmann S, Castelo R, Guinney J. GSVA: Gene Set Variation Analysis for Microarray and RNA-Seq Data. *BMC Bioinf* (2013) 14:7. doi: 10.1186/1471-2105-14-7
26. Yu G, Wang LG, Han Y, He QY. Clusterprofiler: An R Package for Comparing Biological Themes Among Gene Clusters. *Omics* (2012) 16:284–7. doi: 10.1089/omi.2011.0118
27. Langfelder P, Horvath S. WGCNA: An R Package for Weighted Correlation Network Analysis. *BMC Bioinf* (2008) 9:559. doi: 10.1186/1471-2105-9-559
28. Inthagard J, Edwards J, Roseweir AK. Immunotherapy: Enhancing the Efficacy of This Promising Therapeutic in Multiple Cancers. *Clin Sci* (2019) 133:181–93. doi: 10.1042/cs20181003
29. Parikh M, Bajwa P. Immune Checkpoint Inhibitors in the Treatment of Renal Cell Carcinoma. *Semin Nephrol* (2020) 40:76–85. doi: 10.1016/j.semnephrol.2019.12.009
30. Postow MA, Sidlow R, Hellmann MD. Immune-Related Adverse Events Associated With Immune Checkpoint Blockade. *N Engl J Med* (2018) 378:158–68. doi: 10.1056/NEJMra1703481
31. Zanconato F, Cordenonsi M, Piccolo S. YAP/TAZ at the Roots of Cancer. *Cancer Cell* (2016) 29:783–803. doi: 10.1016/j.ccell.2016.05.005
32. Jang W, Kim T, Koo JS, Kim SK, Lim DS. Mechanical Cue-Induced YAP Instructs Skp2-Dependent Cell Cycle Exit and Oncogenic Signaling. *EMBO J* (2017) 36:2510–28. doi: 10.15252/embj.201696089
33. Mason DE, Collins JM, Dawahare JH, Nguyen TD, Lin Y, Voytik-Harbin SL, et al. YAP and TAZ Limit Cytoskeletal and Focal Adhesion Maturation to Enable Persistent Cell Motility. *J Cell Biol* (2019) 218:1369–89. doi: 10.1083/jcb.201806065
34. Yang WH, Huang Z, Wu J, Ding CC, Murphy SK, Chi JT. A TAZ-ANGPTL4-NOX2 Axis Regulates Ferroptotic Cell Death and Chemoresistance in Epithelial Ovarian Cancer. *Mol Cancer Res* (2020) 18:79–90. doi: 10.1158/1541-7786.Mcr-19-0691
35. Yang WH, Ding CC, Sun T, Rupprecht G, Lin CC, Hsu D, et al. The Hippo Pathway Effector TAZ Regulates Ferroptosis in Renal Cell Carcinoma. *Cell Rep* (2019) 28:2501–8.e4. doi: 10.1016/j.celrep.2019.07.107
36. Zhao X, Wang X, You Y, Wen D, Feng Z, Zhou Y, et al. Nogo-B Fosters HCC Progression by Enhancing Yap/Taz-Mediated Tumor-Associated Macrophages M2 Polarization. *Exp Cell Res* (2020) 391:111979. doi: 10.1016/j.yexcr.2020.111979
37. Geng J, Yu S, Zhao H, Sun X, Li X, Wang P, et al. The Transcriptional Coactivator TAZ Regulates Reciprocal Differentiation of T(H)17 Cells and T (reg) Cells. *Nat Immunol* (2017) 18:800–12. doi: 10.1038/ni.3748
38. Feng J, Yang H, Zhang Y, Wei H, Zhu Z, Zhu B, et al. Tumor Cell-Derived Lactate Induces TAZ-Dependent Upregulation of PD-L1 Through GPR81 in Human Lung Cancer Cells. *Oncogene* (2017) 36:5829–39. doi: 10.1038/onc.2017.188
39. Janse van Rensburg HJ, Azad T, Ling M, Hao Y, Snetsinger B, Khanal P, et al. The Hippo Pathway Component TAZ Promotes Immune Evasion in Human Cancer Through PD-L1. *Cancer Res* (2018) 78:1457–70. doi: 10.1158/0008-5472.Can-17-3139
40. Wend P, Wend K, Krum SA, Miranda-Carboni GA. The Role of WNT10B in Physiology and Disease. *Acta Physiol (Oxf)* (2012) 204:34–51. doi: 10.1111/j.1748-1716.2011.02296.x
41. Casey SC, Tong L, Li Y, Do R, Walz S, Fitzgerald KN, et al. MYC Regulates the Antitumor Immune Response Through CD47 and PD-L1. *Science* (2016) 352:227–31. doi: 10.1126/science.aac9935
42. Wong C, Chen C, Wu Q, Liu Y, Zheng P. A Critical Role for the Regulated wnt-myc Pathway in Naive T Cell Survival. *J Immunol* (2015) 194:158–67. doi: 10.4049/jimmunol.1401238

Conflict of Interest: The authors declare that the research was conducted in the absence of any commercial or financial relationships that could be construed as a potential conflict of interest.

frontiers in Oncology

CASE REPORT
published: 15 October 2021
doi: 10.3389/fonc.2021.735077

Complete Response of Hereditary Leiomyomatosis and Renal Cell Cancer (HLRCC)-Associated Renal Cell Carcinoma to Pembrolizumab Immunotherapy: A Case Report

Tao Wang[1,2†], *Yan Huang*[1†], *Xing Huang*[1,2], *Zheng Lv*[1,2], *Shuo Tian*[1,2], *Xin Ma*[1*] *and Xu Zhang*[1*]

[1] Department of Urology, The Third Medical Centre, Chinese People's Liberation Army (PLA) General Hospital, Beijing, China, [2] Medical School of Chinese People's Liberation Army (PLA), Beijing, China

OPEN ACCESS

Edited by:
Walter J. Storkus, University of Pittsburgh, United States

Reviewed by:
Rafael Jimenez, Mayo Clinic, United States
Leonard Joseph Appleman, University of Pittsburgh, United States

***Correspondence:**
Xin Ma
urologist@foxmail.com
Xu Zhang
xzhang301@163.com

[†]*These authors have contributed equally to this work*

Specialty section:
This article was submitted to Genitourinary Oncology, a section of the journal Frontiers in Oncology

Received: *02 July 2021*
Accepted: *28 September 2021*
Published: *15 October 2021*

Citation:
Wang T, Huang Y, Huang X, Lv Z, Tian S, Ma X and Zhang X (2021) Complete Response of Hereditary Leiomyomatosis and Renal Cell Cancer (HLRCC)-Associated Renal Cell Carcinoma to Pembrolizumab Immunotherapy: A Case Report. Front. Oncol. 11:735077. doi: 10.3389/fonc.2021.735077

Hereditary leiomyomatosis and renal cell cancer (HLRCC) is a rare autosomal dominant disorder that results from a germline mutation in the fumarate hydratase (*FH*) gene; it manifests as cutaneous leiomyomas, uterine fibroids, and renal cell cancer (RCC). Patients with HLRCC-associated RCC (HLRCC-RCC) have aggressive clinical courses, but there is no standardized therapy for advanced HLRCC-RCC. Here, we describe aggressive HLRCC in a 26-year-old man who presented with RCC that exhibited a novel heterozygous germline insertion mutation in exon 2 of the *FH* gene (c.191dupA: p.N64fs). Systemic lymph node metastasis had already occurred. The patient underwent robot-assisted laparoscopic resection of the right kidney, but new metastases appeared within 5 months postoperatively. Histological staining of the resected tumor showed high expression levels of programmed cell death-ligand 1 (PD-L1) and programmed cell death-1 (PD-1). The patient was treated with anti-PD-1 antibody as first-line therapy. After 2 years of immune checkpoint inhibitor (ICI) treatment, all lesions had disappeared; this response was maintained at 51 months. To our knowledge, this is the first successful treatment of HLRCC-RCC with single-agent immunotherapy. Our approach might be effective for patients with advanced HLRCC-RCC.

Keywords: hereditary leiomyomatosis and renal cell cancer (HLRCC), mutation, immunotherapy, follow-up, complete response (CR)

INTRODUCTION

Hereditary leiomyomatosis and renal cell cancer (HLRCC) is an autosomal dominant disorder that results from a germline mutation of the fumarate hydratase (*FH*) gene on chromosome 1q42.1 (1, 2). Individuals with *FH* germline mutations are at risk of developing multiple cutaneous and uterine leiomyomas, as well as renal cell carcinoma (RCC) (3). HLRCC-associated RCC (HLRCC-RCC) was defined as a distinct entity in the 2016 World Health Organization classification (4). Importantly, patients with HLRCC-RCC usually have poor clinical courses.

FH acts as a tumor suppressor gene that encodes an enzyme in the tricarboxylic acid cycle; this enzyme catalyzes the conversion of fumarate to malate. Intracellular fumarate accumulation leads to the overexpression of hypoxia-inducible factor-1α with resulting pseudohypoxia, which induces angiogenesis and appears to cause tumorigenesis (5).

There are no standard therapies or consensus for advanced HLRCC-RCC. Novel methods (e.g., targeted therapy and immunotherapy) might improve the prognosis of advanced RCC, which would also provide new insights regarding HLRCC. Here, we describe an aggressive HLRCC in a 26-year-old man who exhibited a novel heterozygous germline insertion mutation in exon 2 of the *FH* gene (c.191dupA:p.N64fs). He achieved complete response (CR) to pembrolizumab immunotherapy, an anti-programmed cell death-1 (PD-1) antibody. To our knowledge, this is the first report of pembrolizumab monotherapy producing CR in advanced HLRCC-RCC. The successful outcome in this case may provide new insights for the management of HLRCC.

CASE PRESENTATION

The patient was a 26-year-old man with an unremarkable medical history. A painless left supraclavicular lymph node was found incidentally in early 2017; it was considered malignant. Ultrasound-guided biopsy of this left lymph node indicated metastasis of renal adenocarcinoma. Positron emission tomography (PET)-computed tomography (CT) showed that the right kidney volume was increased, the lower part of the right kidney contained an irregular cystic mass, and the internal glucose metabolism was uneven (**Figure 1A** and **Supplementary Figure 2A**). There were multiple enlarged lymph nodes in the neck (zones III–V), bilateral clavicle areas, posterior mediastinum, and posterior phrenic angle space, as well as adjacent to the abdominal aorta and iliac vessels; all of these enlarged lymph nodes were considered malignant (**Figure 3C**).

Because the patient's father and grandfather both died of kidney cancer (**Figure 1B**), HLRCC was suspected. Whole-exome sequencing of genomic DNA from blood and cancerous tissues was performed after the patient had provided informed consent. The sequencing results revealed a previously unidentified germline insertion mutation in exon 2 of the *FH* gene (c.191dupA:p.N64fs); the mutation rate was strongly enhanced in the tumor tissue. Sanger sequencing confirmed these findings (**Figures 1C, D**) and supported a diagnosis of HLRCC-RCC.

The patient underwent robot-assisted laparoscopic resection of the right kidney and retroperitoneal lymphadenectomy (**Supplementary Figure 2B**). Postoperative pathology revealed RCC with papillary and tubular structures, accompanied by metastasis of the inferior vena cava lymph nodes and invasion of the renal sinus and perinephric fat. The tumor measured 8.5 cm × 6.5 cm × 6 cm and was World Health Organization/International Society of Urologic Pathologists grade III. The microstructure was characterized by thick papillae lined with large tumor cells containing abundant, granular, and eosinophilic cytoplasm; large nuclei were present with prominent eosinophilic nucleoli surrounded by clear halos (**Figure 2A** and **Supplementary Figure 1A**). Immunohistochemistry indicated high expression levels of programmed cell death-ligand 1 (PD-L1) (tumor

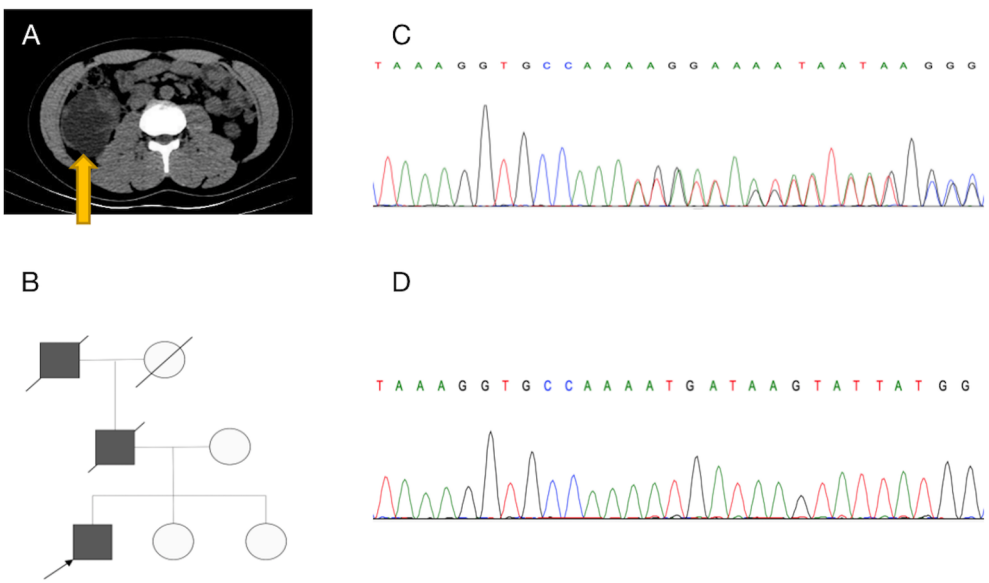

FIGURE 1 | Diagnosis of hereditary leiomyomatosis and renal cell cancer-associated renal cell carcinoma (HLRCC-RCC). **(A)** Transverse CT revealed a large mass in the lower middle part of the right kidney. **(B)** Pedigree of the family with three patients. The black symbols represent the affected members with renal carcinoma, and the arrow indicates the proband. **(C, D)** Genetic testing identified a novel fumarate hydratase (FH) germline mutation (c.191dupA:p.N64fs), which confirmed the diagnosis of HLRCC-RCC. **(C)** A heterozygous mutation was identified in blood, and **(D)** a homozygous mutation was identified in tumor tissue.

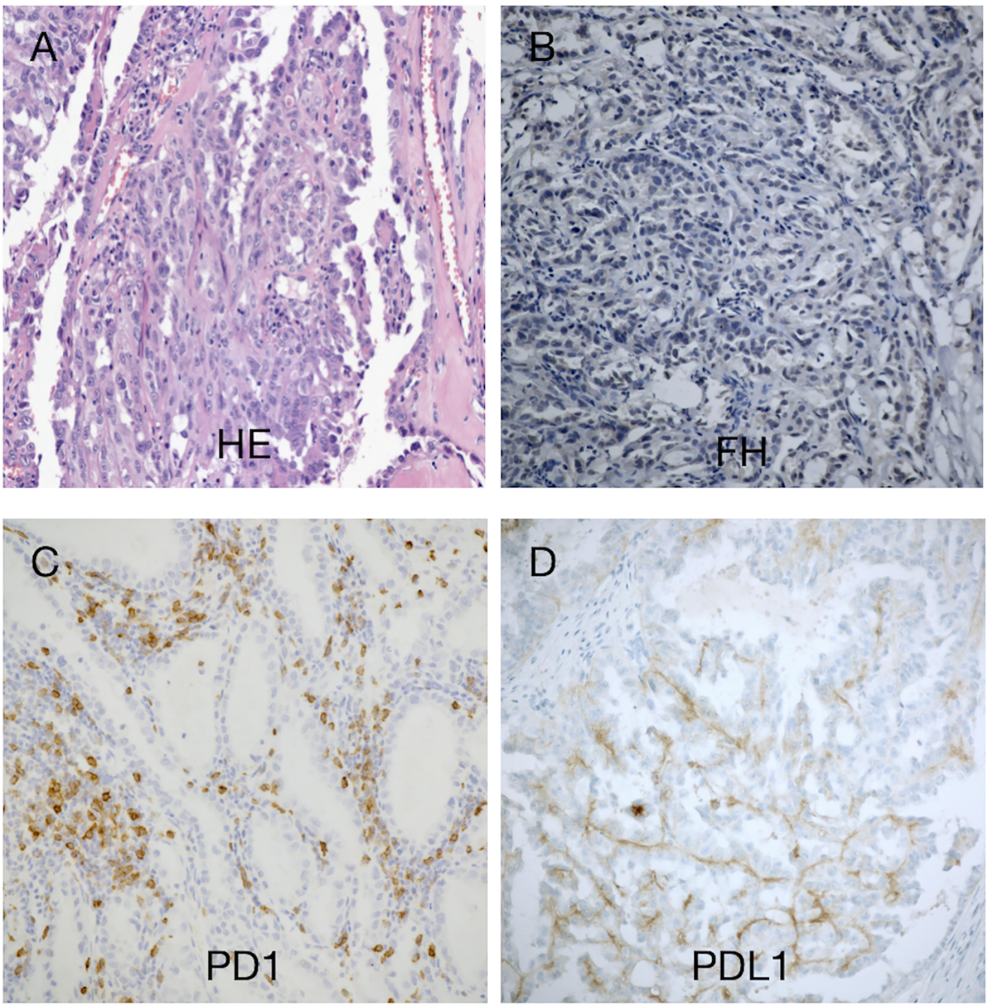

FIGURE 2 | Histomorphological findings in our patient with hereditary leiomyomatosis and renal cell cancer syndrome. **(A)** Hematoxylin–eosin staining showed a renal cell carcinoma with papillary and tubular structures. **(B)** Immunohistochemistry revealed absence of fumarate hydratase (FH) expression in tumor cells, supporting the diagnosis of FH-deficient RCC. **(C, D)** There were few tumor-infiltrating lymphocytes (TILs). Approximately 30% of the tumor cells exhibited programmed cell death-ligand 1 (PD-L1) expression. TILs exhibited programmed cell death-1 (PD-1) expression (35%). Magnification, ×100.

cells +30%) and PD-1 (lymphocytes +35%) (**Figures 2C, D**). FH staining of the tumor tissue revealed the loss of FH expression (**Figure 2B** and **Supplementary Figure 1B**).

At 4 months postoperatively, CT revealed multiple nodules on the retroperitoneal lymph nodes, peritoneum, and right pleural nodules, suggestive of metastasis (**Figure 3A**). The patient was immediately treated with pembrolizumab using the standard triweekly regimen (100 mg per treatment). The main side effect during treatment was immune enteritis. After 8 months of pembrolizumab treatment, the patient's abovementioned metastatic lesions were significantly reduced or even disappeared (**Figure 3B**). After 24 months of treatment, PET-CT showed that the fluorodeoxyglucose (FDG) metabolism of the lesions had normalized, indicative of CR (**Figure 3D**). A third PET-CT in April 2021 still showed no disease progression (**Figure 3E**). The timeline is shown in **Figure 4**.

DISCUSSION

HLRCC is a rare autosomal dominant disorder caused by heterozygous germline mutations in the *FH* gene (1q42.3-43). Approximately 15% of patients with HLRCC develop RCC. Most patients with HLRCC develop aggressive RCC that demonstrates papillary morphology and early metastasis (3). Here, we described a patient with HLRCC-RCC who exhibited a novel heterozygous germline FH mutation and was cured with pembrolizumab. While receiving immune checkpoint inhibitor (ICI) treatment, the patient's only complaint was mild enteritis. The patient achieved CR after 2 years of pembrolizumab treatment, with improved symptoms and controlled metastasis. To our knowledge, this is the first case of successful single-agent immunotherapy for HLRCC-RCC, providing new insights for the management of HLRCC.

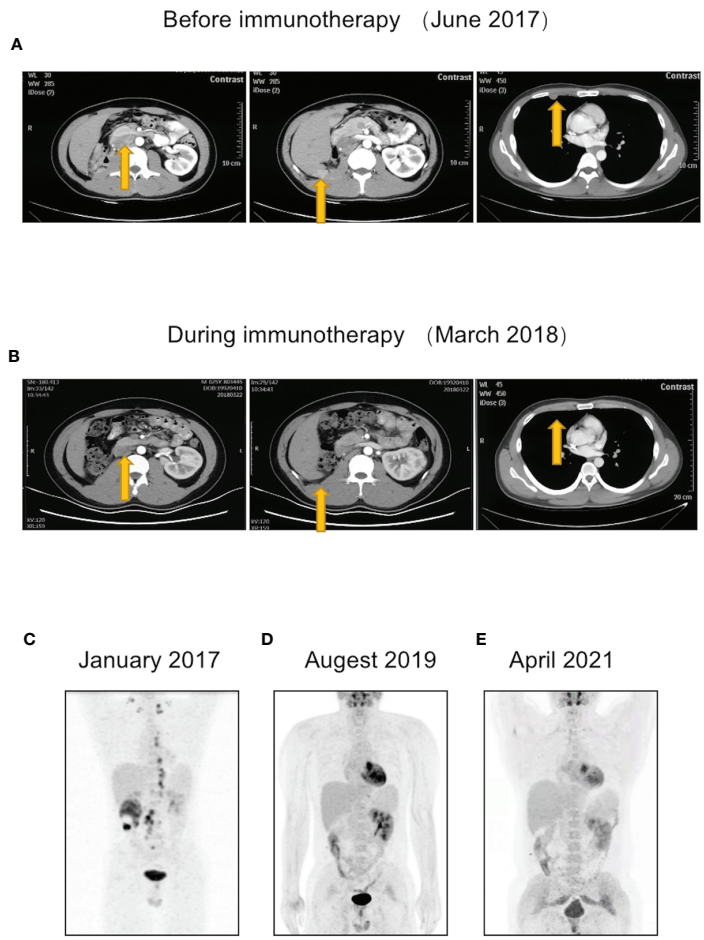

FIGURE 3 | The patient had new metastatic lesions postoperatively but showed a response during immunotherapy and eventually achieved complete response (CR). **(A)** At 4 months postoperatively, CT revealed metastatic lesions on retroperitoneal lymph nodes, peritoneum, and right pleural nodules. **(B)** After 8 months of pembrolizumab treatment, the patient's abovementioned metastatic lesions were significantly reduced or even disappeared. **(C–E)** Changes in patient's PET-CT. **(C)** Preoperative PET-CT showed multiple systemic lymph node metastases. **(D)** After 2 years of immunotherapy, PET-CT showed that the metastases had disappeared. **(E)** A third PET-CT in April 2021 confirmed the patient's CR maintenance status.

Prompt excision of HLRCC-associated kidney tumors is critical for preventing metastasis (3). However, no standard therapies or consensus management approaches have been established for advanced HLRCC-RCC. The PD-1/PD-L1 axis is currently a therapeutic target for various treatment-resistant neoplasms. Checkpoint inhibitors may also be effective in patients with HLRCC-RCC. There have been several reports of HLRCC-RCC treatment with ICIs, which have attracted attention as a new therapeutic option. Antitumor efficacy has been achieved by targeted therapy and ICI combinations in patients with variant histology RCC (6, 7). A recent study reported the achievement of CR in a patient with HLRCC-RCC after 31 weeks of ICI combination treatment (nivolumab plus ipilimumab) (8). Another study showed that ICI treatment led to improved progression-free survival compared with antiangiogenic monotherapy (9). Several cases of papillary RCC were treated effectively with nivolumab (10–12). A single-arm phase II study of pembrolizumab demonstrated an overall response rate of 25.4% in papillary RCC (13). The Society for Immunotherapy of Cancer also recommended single-agent anti-PD-1 as the first-line treatment for papillary RCC (14).

PD-1/PD-L1 has been shown to improve the prognosis of patients with HLRCC (15). A multicenter phase II study of atezolizumab and bevacizumab for patients with metastatic RCC involving variant histology revealed an overall response rate in PD-L1-positive patients of 60% (n = 9) vs. 19% (n = 4) in PD-L1-negative patients (16). In the report of CR after combined ICI treatment, approximately half of the tumor cells exhibited PD-L1 expression (8). The immunohistochemical staining in our patient showed strong PD-1/PD-L1 expression. Thus, PD-1 and PD-L1 may be useful as predictors or biomarkers of treatment effects in future studies.

The establishment of systemic therapy for HLRCC-RCC is an unmet need. The findings in our case suggest that ICI treatment

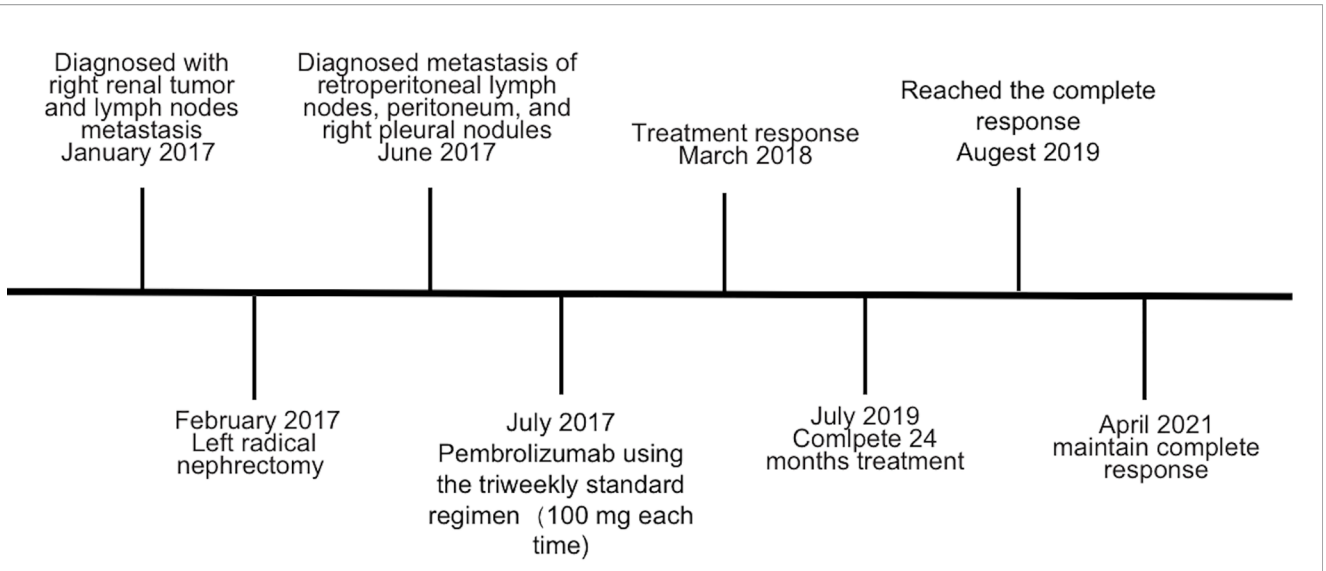

FIGURE 4 | Timeline of the case.

is an effective therapeutic option, although long-term survival results are not available. Additional cases of immunotherapy in patients with HLRCC should be collected to determine the role of its treatment in HLRCC.

CONCLUSIONS

A novel *FH* gene mutation was found in a patient with HLRCC-RCC. He achieved CR after pembrolizumab monotherapy; this response was maintained at 51 months. Immunotherapy for HLRCC merits further studies in additional patients.

DATA AVAILABILITY STATEMENT

The datasets presented in this study can be found in online repositories. The names of the repository/repositories and accession number(s) can be found in the article/**Supplementary Material**.

ETHICS STATEMENT

The studies involving human participants were reviewed and approved by Ethical Committee of PLA General Hospital. The patients/participants provided their written informed consent to participate in this study.

AUTHOR CONTRIBUTIONS

TW and YH: performed the research and wrote the article. XH and ZL: performed the experiments and collected patient data. ST: assisted with laboratory experiments and produced radiology images. XM and XZ: contributed to patient samples and treated patients. All authors contributed to the article and approved the submitted version.

FUNDING

The study was supported by the National Natural Science Foundation of China (Grand Nos. 81770790 and 81970665).

ACKNOWLEDGMENTS

We would like to thank the patient who agreed to participate in this study.

SUPPLEMENTARY MATERIAL

The Supplementary Material for this article can be found online at: https://www.frontiersin.org/articles/10.3389/fonc.2021.735077/full#supplementary-material

Supplementary Figure 1 | Magnifying Hematoxylin–eosin image and the internal control of FH. **(A)** Hematoxylin–eosin staining showed the prominent nucleoli and perinucleolar halo, which is so characteristic of this entity.Magnification 400× **(B)** *FH* staining showed positive in the tissues of FH wild-type patients, proving the effectiveness of our immunohistochemistry process.Magnification 100×.

Supplementary Figure 2 | Additional computed tomography information. **(A)** Axial images at different levels before operation. **(B)** Images at post-operative baseline.

REFERENCES

1. Alam NA, Bevan S, Churchman M, Barclay E, Barker K, Jaeger EE, et al. Localization of a Gene (MCUL1) for Multiple Cutaneous Leiomyomata and Uterine Fibroids to Chromosome 1q42.3-Q43. *Am J Hum Genet* (2001) 68 (5):1264–9. doi: 10.1086/320124
2. Sanz-Ortega J, Vocke C, Stratton P, Linehan WM, Merino MJ. Morphologic and Molecular Characteristics of Uterine Leiomyomas in Hereditary Leiomyomatosis and Renal Cancer (HLRCC) Syndrome. *Am J Surg Pathol* (2013) 37(1):74–80. doi: 10.1097/PAS.0b013e31825ec16f
3. Menko FH, Maher ER, Schmidt LS, Middelton LA, Aittomaki K, Tomlinson I, et al. Hereditary Leiomyomatosis and Renal Cell Cancer (HLRCC): Renal Cancer Risk, Surveillance and Treatment. *Fam Cancer* (2014) 13(4):637–44. doi: 10.1007/s10689-014-9735-2
4. Moch H, Cubilla AL, Humphrey PA, Reuter VE, Ulbright TM. The 2016 WHO Classification of Tumours of the Urinary System and Male Genital Organs-Part A: Renal, Penile, and Testicular Tumours. *Eur Urol* (2016) 70 (1):93–105. doi: 10.1016/j.eururo.2016.02.029
5. Koivunen P, Hirsila M, Remes AM, Hassinen IE, Kivirikko KI, Myllyharju J. Inhibition of Hypoxia-Inducible Factor (HIF) Hydroxylases by Citric Acid Cycle Intermediates: Possible Links Between Cell Metabolism and Stabilization of HIF. *J Biol Chem* (2007) 282(7):4524–32. doi: 10.1074/jbc.M610415200
6. Rini BI, Plimack ER, Stus V, Gafanov R, Hawkins R, Nosov D, et al. Pembrolizumab Plus Axitinib *Versus* Sunitinib for Advanced Renal-Cell Carcinoma. *N Engl J Med* (2019) 380(12):1116–27. doi: 10.1056/NEJMoa1816714
7. Motzer RJ, Penkov K, Haanen J, Rini B, Albiges L, Campbell MT, et al. Avelumab Plus Axitinib Versus Sunitinib for Advanced Renal-Cell Carcinoma. *N Engl J Med* (2019) 380(12):1103–15. doi: 10.1056/NEJMoa1816047
8. Iribe Y, Furuya M, Shibata Y, Yasui M, Funahashi M, Ota J, et al. Complete Response of Hereditary Leiomyomatosis and Renal Cell Cancer (HLRCC)-Associated Renal Cell Carcinoma to Nivolumab and Ipilimumab Combination Immunotherapy by: A Case Report. *Fam Cancer* (2021) 20 (1):75–80. doi: 10.1007/s10689-020-00195-0
9. Sun G, Zhang X, Liang J, Pan X, Zhu S, Liu Z, et al. Integrated Molecular Characterization of Fumarate Hydratase-Deficient Renal Cell Carcinoma. *Clin Cancer Res* (2021) 27(6):1734–43. doi: 10.1158/1078-0432.CCR-20-3788
10. Geynisman DM. Anti-Programmed Cell Death Protein 1 (PD-1) Antibody Nivolumab Leads to a Dramatic and Rapid Response in Papillary Renal Cell Carcinoma With Sarcomatoid and Rhabdoid Features. *Eur Urol* (2015) 68 (5):912–4. doi: 10.1016/j.eururo.2015.07.008
11. Ruiz-Banobre J, Anido U, Abdulkader I, Antunez-Lopez J, Lopez-Lopez R, Garcia-Gonzalez J. Long-Term Response to Nivolumab and Acute Renal Failure in a Patient With Metastatic Papillary Renal Cell Carcinoma and a PD-L1 Tumor Expression Increased With Sunitinib Therapy: A Case Report. *Front Oncol* (2016) 6:250. doi: 10.3389/fonc.2016.00250
12. Adrianzen Herrera DA, Fleisig SB, Gartrell BA. Impressive and Durable Response to Nivolumab in a Patient With Metastatic Type 2 Papillary Renal Cell Carcinoma: On-Label But Without Evidence. *Invest New Drugs* (2017) 35 (5):665–8. doi: 10.1007/s10637-017-0469-5
13. McDermott DF, Lee JL, Ziobro M, Suarez C, Langiewicz P, Matveev VB, et al. Open-Label, Single-Arm, Phase II Study of Pembrolizumab Monotherapy as First-Line Therapy in Patients With Advanced Non-Clear Cell Renal Cell Carcinoma. *J Clin Oncol* (2021) 39(9):1029–39. doi: 10.1200/JCO.20.02365
14. Rini BI, Battle D, Figlin RA, George DJ, Hammers H, Hutson T, et al. The Society for Immunotherapy of Cancer Consensus Statement on Immunotherapy for the Treatment of Advanced Renal Cell Carcinoma (RCC). *J Immunother Cancer* (2019) 7(1):354. doi: 10.1186/s40425-019-0813-8
15. Llamas-Velasco M, Requena L, Kutzner H, Scharer L, Rutten A, Hantschke M, et al. Fumarate Hydratase Immunohistochemical Staining may Help to Identify Patients With Multiple Cutaneous and Uterine Leiomyomatosis (MCUL) and Hereditary Leiomyomatosis and Renal Cell Cancer (HLRCC) Syndrome. *J Cutan Pathol* (2014) 41(11):859–65. doi: 10.1111/cup.12396
16. McGregor BA, McKay RR, Braun DA, Werner L, Gray K, Flaifel A, et al. Results of a Multicenter Phase II Study of Atezolizumab and Bevacizumab for Patients With Metastatic Renal Cell Carcinoma With Variant Histology and/or Sarcomatoid Features. *J Clin Oncol* (2020) 38(1):63–70. doi: 10.1200/JCO.19.01882

Conflict of Interest: The authors declare that the research was conducted in the absence of any commercial or financial relationships that could be construed as a potential conflict of interest.

frontiers in Oncology

CASE REPORT
published: 08 November 2021
doi: 10.3389/fonc.2021.764352

Persistent Response to a Combination Treatment Featuring a Targeted Agent and an Immune Checkpoint Inhibitor in a Patient With Collecting Duct Renal Carcinoma: A Case Report and Literature Review

Weimin Zhou[1], *Ji Huang*[1], *Qiuming He*[1], *Qingfeng Luo*[2], *Xiaofang Zhang*[2], *Xuewei Tao*[3], *Hanzhi Dong*[4] *and Xinhua Tu*[1*]

[1] Department of Urology, Jiangxi Cancer Hospital of Nanchang University, Jiangxi Cancer Center, Nanchang, China, [2] Department of Pathology, Jiangxi Cancer Hospital of Nanchang University, Jiangxi Cancer Center, Nanchang, China, [3] Department of Radiology, Jiangxi Cancer Hospital of Nanchang University, Jiangxi Cancer Center, Nanchang, China, [4] Department of Internal Medical Oncology, Jiangxi Cancer Hospital of Nanchang University, Jiangxi Cancer Center, Nanchang, China

OPEN ACCESS

Edited by:
Walter J. Storkus, University of Pittsburgh, United States

Reviewed by:
Elena Verzoni, Istituto Nazionale dei Tumori (IRCCS), Italy
Leonard Joseph Appleman, University of Pittsburgh, United States

***Correspondence:**
Xinhua Tu
Tuxinhua2020@163.com

Specialty section:
This article was submitted to Genitourinary Oncology, a section of the journal Frontiers in Oncology

Received: *25 August 2021*
Accepted: *25 October 2021*
Published: *08 November 2021*

Citation:
Zhou W, Huang J, He Q, Luo Q, Zhang X, Tao X, Dong H and Tu X (2021) Persistent Response to a Combination Treatment Featuring a Targeted Agent and an Immune Checkpoint Inhibitor in a Patient With Collecting Duct Renal Carcinoma: A Case Report and Literature Review. Front. Oncol. 11:764352. doi: 10.3389/fonc.2021.764352

Collecting duct carcinoma (CDC) is a rare and highly aggressive subtype of kidney cancer that is associated with a poor prognosis. At present, there is no effective treatment for CDC. Herein, we report a case of metastatic CDC treated with a combination of a tyrosine kinase inhibitor and an immune checkpoint inhibitor. A 67-year-old male was diagnosed with CDC with lung and bone metastasis. Pazopanib and camrelizumab were administered after cytoreductive nephrectomy. The patient achieved a partial response after one cycle of treatment; however, he then experienced serious drug-induced hepatic injury. Therefore, we discontinued camrelizumab and administered monotherapy with pazopanib. Three months later, the cancer had progressed and axitinib and sintilimab were administered. The patient achieved a partial response, accompanied by the complete disappearance of the metastatic lesion in the lung. The patient had an excellent physical status after 11 months. This is the first reported case of metastatic CDC successfully treated with a combination of a tyrosine kinase inhibitor and an immune checkpoint inhibitor. This form of combination treatment may be an effective option for treating metastatic CDC.

Keywords: collecting duct carcinoma, kidney cancer, immunotherapy, targeted therapy, immune checkpoint inhibitor

INTRODUCTION

Renal collecting duct carcinoma (CDC), also referred to as Bellini duct carcinoma, is a subtype of renal cell carcinoma (RCC) with unique clinical and pathological characteristics. This is a rare condition and accounts for only 0.4–2.0% of RCC cases (1–3). CDC originates from distal convoluted tubules of the kidney (3) and is characterized by high rates of invasiveness and early

metastasis, as well as a poor prognosis. According to a previous study, >70% of patients with CDC had distant metastasis at their initial diagnosis; their median overall survival (OS) was approximately 13 months (4). The biological characteristics of CDC are similar to those of urothelial carcinoma (5).

Thus far, there is a lack of effective treatment options for metastatic CDC (mCDC) (6). The combination of gemcitabine with platinum salt chemotherapy showed efficacy in a previous study involving 23 cases of mCDC (7). In this previous cohort, one complete and five partial responses (objective response rate: 26%) were observed; however, the median progression-free survival (PFS) and OS were only 7.1 and 10.5 months, respectively (7). Nevertheless, platinum-based chemotherapy is considered a standard therapeutic regimen for mCDC. Targeted agents (e.g., sorafenib, temsirolimus, sunitinib, and cabozantinib) have shown activity in certain mCDC cases (8, 9). Although immune checkpoint inhibitors (ICIs) may be effective against some mCDCs, the benefit of monotherapy with these agents is limited (10). In earlier studies, three cases of mCDC receiving a combination immunotherapy of nivolumab, a programmed cell death 1 (PD-1) antibody, and ipilimumab, a cytotoxic T-lymphocyte associated protein 4 (CTLA4) antibody, the first-line therapy for clear cell RCC (ccRCC), all achieved excellent disease control (11, 12).

The combination of immunotherapy and targeted therapy plays a joint role in the treatment of advanced ccRCC and is recommended as a first-line therapy. However, the efficacy of combination immunotherapy and targeted therapy against CDC remains unclear. Herein, we report a case that demonstrated the efficacy of the combination of targeted therapy and PD-1 antibody against mCDC.

CASE PRESENTATION

In October 2019, a 67-year-old man was admitted to our hospital due to left flank pain. He was initially diagnosed with a left renal tumor based on ultrasound examination. The patient had a history of controlled hypertension for approximately 10 years, but no personal or family history of other systemic disorders. Contrast-enhanced computed tomography (CT) revealed the presence of a malignant mass (5.2 cm × 4.3 cm) (**Figures 1A, B**). Chest CT revealed multiple nodules in the right lower lung, indicating metastasis (**Figure 1C**). Whole-body bone scanning by emission CT suggested vertebral (T12) metastasis (**Figure 1D**). The Eastern Cooperative Oncology Group score of the patient was 1. Routine blood and blood biochemistry tests did not yield abnormal findings. Based on these findings, the patient was diagnosed with advanced left renal carcinoma graded cT2N×M1.

According to the criteria established by the International Metastatic Renal Cell Carcinoma Database Consortium (IMDC), the prognostic risk associated with one risk factor was intermediate. Thus, cytoreductive nephrectomy was recommended, and pathological examination confirmed CDC (**Figure 2A**). Immunohistochemistry was used to examine the presence of several key markers: paired box 8-negative (PAX8;

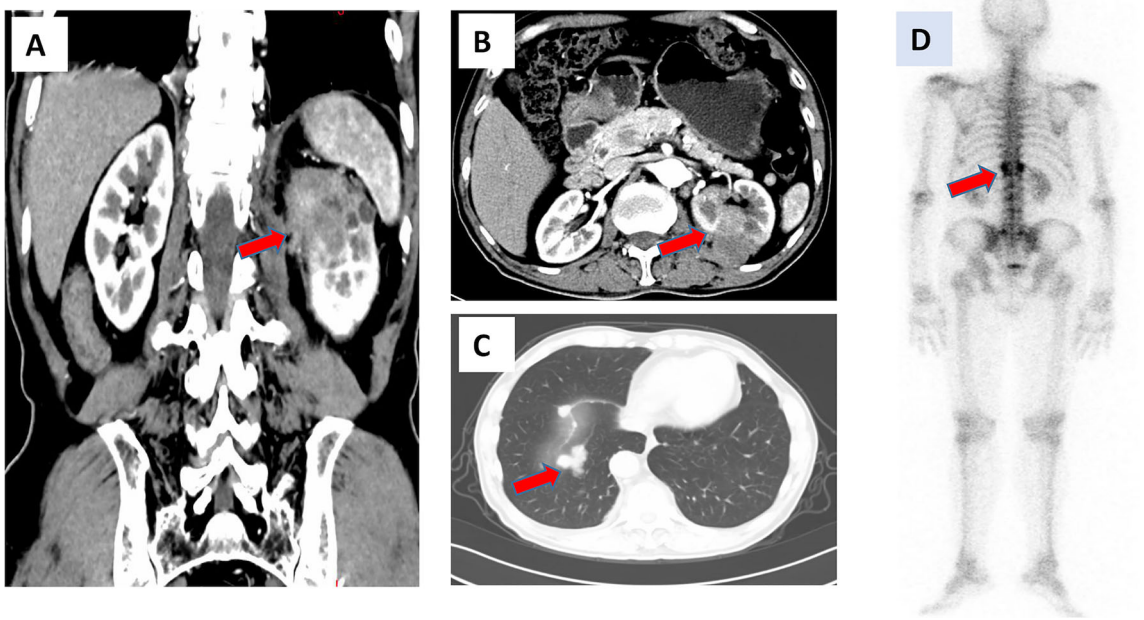

FIGURE 1 | Radiological examination at initial visit. **(A, B)** Contrast-enhanced CT scan of the abdomen showing a malignant mass in the left kidney. **(C)** Chest CT scan showing metastatic nodules in the right lower lung. **(D)** Whole body bone scan showing abnormal T12 vertebration. CT, computed tomography.

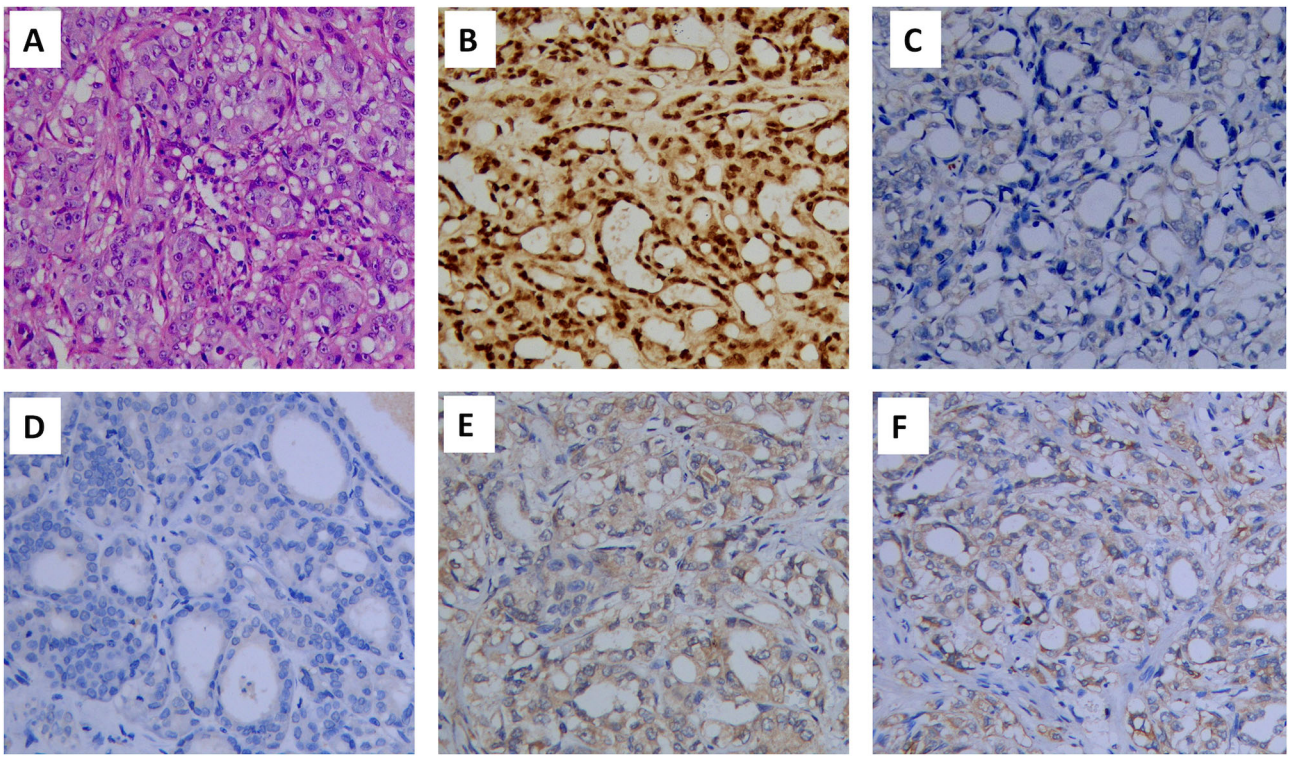

FIGURE 2 | Hematoxylin and eosin (HE) staining and immunohistochemical staining of the renal tumor (×200): **(A)** HE staining, **(B)** PAX8 (positive), **(C)** p63 (negative), **(D)** CD10(negative), **(E)** vinculin (positive) and **(F)** PD-L1(positive). PAX8, paired box 8; PD-L1, programmed cell death 1 ligand 1.

positive), p63 (negative), CD10 (negative), and vinculin (positive) (**Figures 2B–E**). Immunohistochemistry was positive for programmed cell death 1 ligand 1 (PD-L1) (**Figure 2F**). Next, we performed genetic profiling using a customized panel consisting of 618 genes to investigate potential actionable somatic and pathogenic germline variants (**Supplemental Table 1**). Sequencing analysis did not identify pathogenic or likely pathogenic germline variants in this sample. However, four somatic alterations with uncertain clinical significance were detected: ERBB receptor feedback inhibitor 1 (ERRFI1) S138fs; speckle type BTB/POZ protein (SPOP) S55fs; E1A binding protein p300 (EP300) S457I; and TEK receptor tyrosine kinase (TEK) R673H. However, none of these findings supported the potential response to any of the therapies approved by the Food and Drug Administration. We recommended a treatment strategy involving the combination of a targeted agent and ICI, which has shown excellent therapeutic results in the treatment of ccRCC. The patient was fully informed and aware of the off-label use of the drugs. Pazopanib (400 mg, *per os*, once daily) and the PD-1 monoclonal antibody camrelizumab (200 mg, intravenous gtt, once every 3 weeks) were administered. Following one cycle of therapy, the patient experienced a reduction in appetite and developed severe drug-induced hepatic injury. However, chest CT showed remarkable shrinkage of the metastases, indicating a partial response (**Figures 3A, B**). Subsequently, glucocorticosteroid therapy was administered. Liver function recovered three weeks later. Immunotherapy was discontinued, and monotherapy with pazopanib was initiated.

Five months later, the patient presented with cough, dyspnea, and lumbar pain. Chest CT showed malignant pleural effusion and pleural metastasis (**Figure 3C**); this was confirmed by the cytological examination of pleural effusion. Considering the response of the patient to the previous combination strategy, axitinib (5 mg, *per os*, twice daily) and the PD-1 monoclonal antibody sintilimab (200 mg, intravenous gtt, once every 3 weeks) were duly administered. The symptoms of the patient were gradually alleviated and completely disappeared after five cycles of treatment. Except for hypertension, there was no occurrence of obvious adverse reactions. Chest CT revealed a marked reduction of pleural effusion (**Figure 3D**). In April 2021, after 11 months of treatment, examinations confirmed the complete disappearance of the metastatic lesion in the lung. The last follow-up examination was performed in July 2021. Chest and abdomen CT did not reveal the presence of abnormal lesions (**Figure 3E**) and demonstrated improvement in the osteogenic structure at the site of vertebral metastasis (**Figure 3E**). The patient had an excellent physical status that was similar to that of a healthy person. Thereafter, the patient remained tumor-free for >14 months after receiving the combination therapy (**Figure 4**).

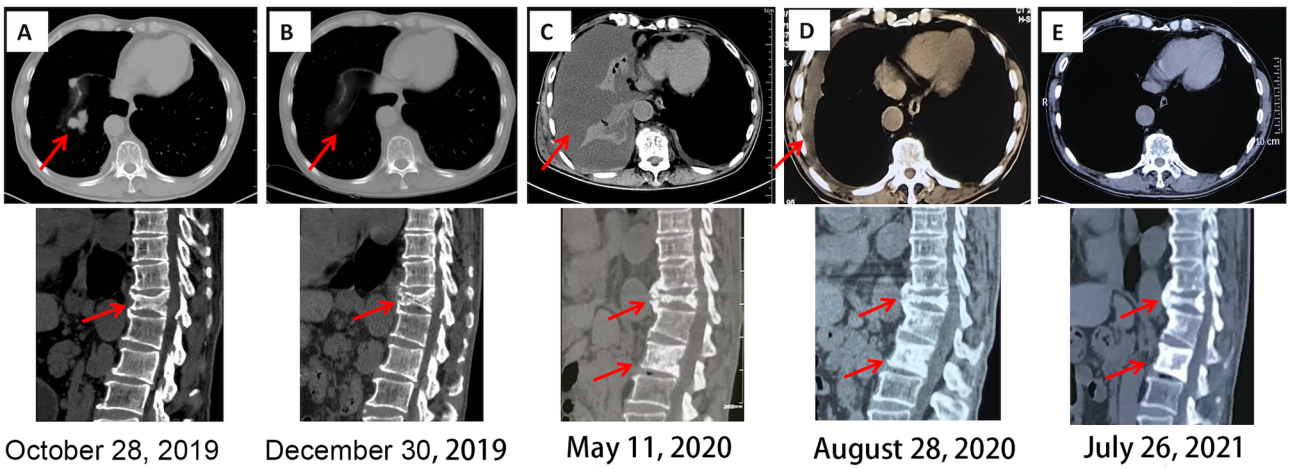

FIGURE 3 | Chest and spinal CT imaging manifestations after treatment. **(A)** First diagnosis. **(B)** After one cycle of pazopanib and camrelizumab. **(C)** Discontinuation of camrelizumab and monotherapy involving pazopanib for 5 months. **(D)** Three months after the combination treatment of axitinib and sintilimab. **(E)** Fourteen months after the combination treatment of axitinib and sintilimab. CT, computed tomography.

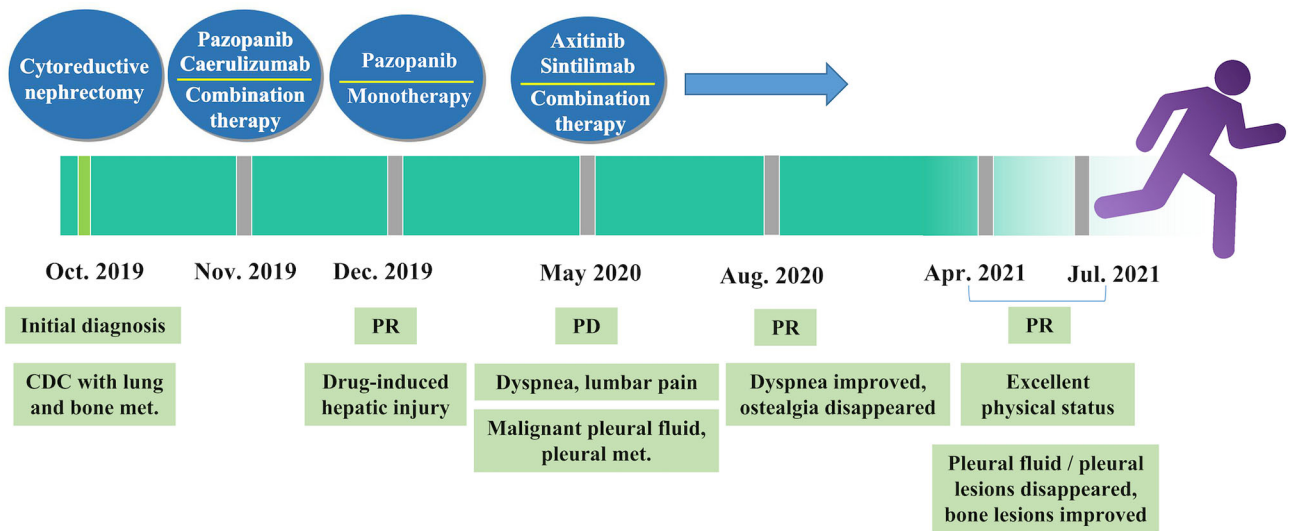

FIGURE 4 | Timeline of treatment. CDC, collecting duct carcinoma; met., metastasis; PD, progressive disease; PR, partial response.

DISCUSSION

Research has shown that 40–70% of patients with CDC have metastatic spread at their initial presentation, and most patients die within 1–3 years from the time of primary diagnosis (13–15). To the best of our knowledge, this is the first reported case of the successful treatment of mCDC through the combination of a targeted agent and immunotherapy.

Cytotoxic chemotherapy plays an important role in the management of non-ccRCC, such as sarcomatoid RCC, renal medullary carcinoma, and CDC. In a previous multicenter prospective study, 23 patients with mCDC were treated with a combination of gemcitabine and either cisplatin or carboplatin as first-line therapy; these agents are often used as standard chemotherapy for urothelial carcinoma (7). Analysis revealed a response rate of 26% and an OS of 10.5 months, indicating that chemotherapy is an option for the treatment of CDC. Thus, the National Comprehensive Cancer Network Kidney Cancer Panel made an appropriate recommendation (16). Another study reported that the triple combination of bevacizumab, gemcitabine, and platinum salt, prolonged progression-free survival (median: 15.1 months) and OS (median: 27.8 months)

in five cases of mCDC (17). However, in a prospective phase II trial of metastatic renal medullary and mCDC, this triple combination strategy was associated with low response rates and severe toxicity (18).

The role of targeted agents for the treatment of non-ccRCC warrants further investigation. Data suggested that the targeted therapies approved for ccRCC may offer benefits to patients with non-ccRCC. A previous retrospective study analyzed seven patients with mCDC who received treatment with targeted agents (i.e., sorafenib, temsirolimus, or sunitinib) as first-line therapy (8). The results showed long-lasting disease control in two cases (OS: 49 and 19 months, respectively) and early progression of disease with a very short survival period of 4 months in the remaining five patients (8). In another study, cabozantinib was used in four patients with mCDC; two patients achieved a partial response with relief times of 10 and 11 months, respectively (19). Overall, the response rates to monotherapy with a targeted agent are significantly lower for CDC when compared to ccRCC.

Currently, ICIs are an important treatment option for metastatic ccRCC. Checkpoint antibodies alter the interaction between immune cells and antigen-presenting cells, including tumor cells. These agents can augment the anti-tumor immune response and have shown promise in numerous indications. In metastatic ccRCC, monotherapy with ICI has shown limited benefit, whereas the combination of ICIs or targeted agent/ICIs has displayed encouraging efficacy (20, 21). However, there is a lack of evidence regarding the effects of combination therapy for CDC. CDC is found an immunogenic disease with a high level of immune lymphocyte infiltration, particularly in metastatic cases, suggesting that immunotherapy may be feasible for mCDC (3). In a previous study, Danno et al. (12) reported two cases of mCDC treated with combination immunotherapy consisting of nivolumab and ipilimumab. One patient achieved stable disease for 23 months, while the other achieved a partial response after four cycles of treatment. Similarly, another CDC case with multiple lymph node metastases achieved a complete response after therapy with nivolumab and ipilimumab (11).

Sintilimab and camrelizumab are both immunoglobulin G4 (IgG4) monoclonal PD-1 antibodies that are derived from humans. These antibodies block the binding of PD-1 to PD-L1 or PD-L2 (22, 23). These two drugs have been developed independently in China and have shown excellent clinical benefits in the treatment of relapsed or refractory Hodgkin's lymphoma (24), non-small-cell lung cancer (25), and hepatocellular carcinoma (26). Pazopanib and axitinib are multitargeted tyrosine kinase inhibitors (TKIs) and have shown efficacy when combined with ICIs (21, 27). In the present case, the combination of both pazopanib/camrelizumab and axitinib/sintilimab exerted an obvious therapeutic effect. This finding suggested that the strategy of combining targeted agents and ICIs for the treatment of ccRCC may also benefit patients with CDC. However, this combination therapy may increase the incidence of adverse reactions. Although our patient achieved good results following the administration of pazopanib and camrelizumab, he subsequently developed a severe liver function reaction; his symptoms improved after the discontinuation of treatment. It is currently established that combination therapy with standard doses of pazopanib plus PD-1 antibody is associated with a high risk of hepatotoxicity (28, 29). Grade 3 transaminase elevation has been reported in up to 90% of patients (29). However, treatment with low-dose pazopanib (≤400 mg daily) may avoid the hepatoxicity. A retrospective analysis of 13 patients with metastatic RCC who received combination treatment with nivolumab and low dose pazopanib showed no hepatotoxicity, while only one patient on pazopanib starting dose 800 mg developed elevated transaminases (27). Therefore, the success of combination regimens based on ICIs and TKIs may depend on the selection of the antiangiogenic component and dosage (28).

Multidisciplinary treatment is important for advanced CDC. Cytoreductive nephrectomy is typically carried out for both diagnostic and therapeutic purposes (13). It has been shown that patients in the early stages of CDC with no lymph and distant metastasis can benefit from cytoreductive surgery (30). A retrospective analysis of 851 patients with metastatic non-ccRCC from the Surveillance, Epidemiology and End Results (SEER) database (2001–2014) revealed that, among all histological subtypes (including CDC), the cancer-specific mortality was invariably lower in patients who underwent cytoreductive nephrectomy than in those who did not (31). Recently, Sui et al. (4) conducted a retrospective study of 577 patients with CDC. Multivariate analysis revealed a survival benefit of multidisciplinary therapy with surgery plus chemotherapy and/or radiotherapy over single-mode therapy. Watanabe et al. (11) reported a case of mCDC treated with the combination of nivolumab and ipilimumab following cytoreductive nephrectomy, achieving a complete response. However, the mechanism underlying the benefits offered by cytoreductive nephrectomy in patients with mCDC has yet to be elucidated.

To our knowledge, this is the first reported patient with mCDC who was treated with a combination of a TKI and an ICI. The patient achieved a sustained response after the combination of axitinib and sintilimab following cytoreductive nephrectomy. Accumulation of additional cases and prospective studies targeting CDCs through the combination of a TKI and an ICI are warranted to improve the outcomes of this rare disease with few evidence-based treatment options. Furthermore, the use of cytoreductive nephrectomy in mCDC is worthy of reconsideration.

DATA AVAILABILITY STATEMENT

The original contributions presented in the study are included in the article/**Supplementary Material**. Further inquiries can be directed to the corresponding author.

ETHICS STATEMENT

The studies involving human participants were reviewed and approved by Ethics Committee of Jiangxi Cancer Hospital of Nanchang University. The patients/participants provided their written informed consent to participate in this study. Written

informed consent was obtained from the individual(s) for the publication of any potentially identifiable images or data included in this article.

AUTHOR CONTRIBUTIONS

XHT performed the surgery and participated in treatment planning. WZ collected the data and wrote the original draft of the manuscript. JH and QH prepared the draft of the manuscript. QL and XZ analyzed the pathology data. XWT analyzed the imaging data. All authors contributed to the article and approved the submitted version.

ACKNOWLDGMENTS

We are grateful to the patient and his family for their contributions to the study.

SUPPLEMENTARY MATERIAL

The Supplementary Material for this article can be found online at: https://www.frontiersin.org/articles/10.3389/fonc.2021.764352/full#supplementary-material

Supplementary Table 1 | Genetic analysis of 618 genes related to the potential actionable somatic and pathogenic germline variants.

REFERENCES

1. May M, Ficarra V, Shariat SF, Zigeuner R, Chromecki T, Cindolo L, et al. Impact of Clinical and Histopathological Parameters on Disease Specific Survival in Patients With Collecting Duct Renal Cell Carcinoma: Development of a Disease Specific Risk Model. *J Urol* (2013) 190(2):458–63. doi: 10.1016/j.juro.2013.02.035
2. Gupta R, Billis A, Shah RB, Moch H, Osunkoya AO, Jochum W, et al. Carcinoma of the Collecting Ducts of Bellini and Renal Medullary Carcinoma: Clinicopathologic Analysis of 52 Cases of Rare Aggressive Subtypes of Renal Cell Carcinoma With a Focus on Their Interrelationship. *Am J Surg Pathol* (2012) 36:1265–78. doi: 10.1097/PAS.0b013e3182635954
3. Malouf GG, Comperat E, Yao H, Mouawad R, Lindner V, Rioux-Leclercq N, et al. Unique Transcriptomic Profile of Collecting Duct Carcinomas Relative to Upper Tract Urothelial Carcinomas and Other Kidney Carcinomas. *Sci Rep* (2016) 6:30988. doi: 10.1038/srep30988
4. Sui W, Matulay JT, Robins DJ, James MB, Onyeji IC, RoyChoudhury A, et al. Collecting Duct Carcinoma of the Kidney: Disease Characteristics and Treatment Outcomes From the National Cancer Database. *Urol Oncol* (2017) 35(9):540 e13–8. doi: 10.1016/j.urolonc.2017.04.010
5. Kafe H, Verbavatz JM, Cochand-Priollet B, Castagnet P, Vieillefond A. Collecting Duct Carcinoma: An Entity to be Redefined? *Virchows Arch* (2004) 445(6):637–40. doi: 10.1007/s00428-004-1124-z
6. Pagani F, Colecchia M, Sepe P, Apollonio G, Claps M, Verzoni E, et al. Collecting Ducts Carcinoma: An Orphan Disease. Literature Overview and Future Perspectives. *Cancer Treat Rev* (2019) 79:101891. doi: 10.1016/j.ctrv.2019.101891
7. Oudard S, Banu E, Vieillefond A, Fournier L, Priou F, Medioni J, et al. Prospective Multicenter Phase II Study of Gemcitabine Plus Platinum Salt for Metastatic Collecting Duct Carcinoma: Results of a GETUG (Groupe d'Etudes Des Tumeurs Uro-Genitales) Study. *J Urol* (2007) 177(5):1698–702. doi: 10.1016/j.juro.2007.01.063
8. Procopio G, Verzoni E, Iacovelli R, Colecchia M, Torelli T, Mariani L. Is There a Role for Targeted Therapies in the Collecting Ducts of Bellini Carcinoma? Efficacy Data From a Retrospective Analysis of 7 Cases. *Clin Exp Nephrol* (2012) 16(3):464–7. doi: 10.1007/s10157-012-0589-3
9. Mego M, Sycova-Mila Z, Rejlekova K, Rychly B, Obertova J, Rajec J, et al. Sunitinib in the Treatment of Tubulocystic Carcinoma of the Kidney. A Case Report. *Ann Oncol* (2008) 19(9):1655–6. doi: 10.1093/annonc/mdn408
10. Koshkin VS, Barata PC, Zhang T, George DJ, Atkins MB, Kelly WJ, et al. Clinical Activity of Nivolumab in Patients With Non-Clear Cell Renal Cell Carcinoma. *J Immunother Cancer* (2018) 6(1):9. doi: 10.1186/s40425-018-0319-9
11. Watanabe K, Sugiyama T, Otsuka A, Miyake H. Complete Response to Combination Therapy With Nivolumab and Ipilimumab for Metastatic Collecting Duct Carcinoma of the Kidney. *Int Cancer Conf J* (2020) 9 (1):32–5. doi: 10.1007/s13691-019-00389-z
12. Danno T, Iwata S, Niimi F, Honda S, Okada H, Azuma T. Nivolumab and Ipilimumab Combination Immunotherapy for Patients With Metastatic Collecting Duct Carcinoma. *Case Rep Urol* (2021) 2021:9936330. doi: 10.1155/2021/9936330
13. Tokuda N, Naito S, Matsuzaki O, Nagashima Y, Ozono S, Igarashi T, et al. Collecting Duct (Bellini Duct) Renal Cell Carcinoma: A Nationwide Survey in Japan. *J Urol* (2006) 176(1):40–3; discussion 3. doi: 10.1016/S0022-5347(06)00502-7
14. Srigley JR, Delahunt B. Uncommon and Recently Described Renal Carcinomas. *Mod Pathol* (2009) 22(Suppl 2):S2–23. doi: 10.1038/modpathol.2009.70
15. Karakiewicz PI, Trinh QD, Rioux-Leclercq N, de la Taille A, Novara G, Tostain J, et al. Collecting Duct Renal Cell Carcinoma: A Matched Analysis of 41 Cases. *Eur Urol* (2007) 52(4):1140–5. doi: 10.1016/j.eururo.2007.01.070
16. Motzer RJ, Jonasch E, Boyle S, Carlo MI, Manley B, Agarwal N, et al. NCCN Guidelines Insights: Kidney Cancer, Version 1.2021. *J Natl Compr Canc Netw* (2020) 18(9):1160–70. doi: 10.6004/jnccn.2020.0043
17. Pecuchet N, Bigot F, Gachet J, Massard C, Albiges L, Teghom C, et al. Triple Combination of Bevacizumab, Gemcitabine and Platinum Salt in Metastatic Collecting Duct Carcinoma. *Ann Oncol* (2013) 24(12):2963–7. doi: 10.1093/annonc/mdt423
18. Thibault C, Elaidi RT, Fléchon A, Albiges L, Joly C, Barthélémy P, et al. 724p A Prospective Phase II Study of Gemcitabine Plus Platinum in Combination With Bevacizumab for Metastatic Renal Medullary and Collecting Duct Carcinoma (GETUG-AFU 24, BEVABEL Trial) - ScienceDirect. *Ann Oncol* (2020) 31(4):S568. doi: 10.1016/j.annonc.2020.08.796
19. Martinez Chanza N, Xie W, Asim Bilen M, Dzimitrowicz H, Burkart J, Geynisman DM, et al. Cabozantinib in Advanced Non-Clear-Cell Renal Cell Carcinoma: A Multicentre, Retrospective, Cohort Study. *Lancet Oncol* (2019) 20(4):581–90. doi: 10.1016/S1470-2045(18)30907-0
20. Motzer RJ, Penkov K, Haanen J, Rini B, Albiges L, Campbell MT, et al. Avelumab Plus Axitinib Versus Sunitinib for Advanced Renal-Cell Carcinoma. *N Engl J Med* (2019) 380(12):1103–15. doi: 10.1056/NEJMoa1816047
21. Rini BI, Plimack ER, Stus V, Gafanov R, Hawkins R, Nosov D, et al. Pembrolizumab Plus Axitinib Versus Sunitinib for Advanced Renal-Cell Carcinoma. *N Engl J Med* (2019) 380(12):1116–27. doi: 10.1056/NEJMoa1816714
22. Xu J, Zhang Y, Jia R, Yue C, Chang L, Liu R, et al. Anti-PD-1 Antibody SHR-1210 Combined With Apatinib for Advanced Hepatocellular Carcinoma, Gastric, or Esophagogastric Junction Cancer: An Open-Label, Dose Escalation and Expansion Study. *Clin Cancer Res* (2019) 25(2):515–23. doi: 10.1158/1078-0432.CCR-18-2484
23. Shi Y, Su H, Song Y, Jiang W, Sun X, Qian W, et al. Safety and Activity of Sintilimab in Patients With Relapsed or Refractory Classical Hodgkin Lymphoma (ORIENT-1): A Multicentre, Single-Arm, Phase 2 Trial. *Lancet Haematol* (2019) 6(1):e12–9. doi: 10.1016/S2352-3026(18)30192-3
24. Song Y, Wu J, Chen X, Lin T, Cao J, Liu Y, et al. A Single-Arm, Multicenter, Phase II Study of Camrelizumab in Relapsed or Refractory Classical Hodgkin Lymphoma. *Clin Cancer Res* (2019) 25(24):7363–9. doi: 10.1158/1078-0432.CCR-19-1680

25. Yang Y, Wang Z, Fang J, Yu Q, Han B, Cang S, et al. Efficacy and Safety of Sintilimab Plus Pemetrexed and Platinum as First-Line Treatment for Locally Advanced or Metastatic Nonsquamous NSCLC: A Randomized, Double-Blind, Phase 3 Study (Oncology Program by InnovENT Anti-PD-1-11). *J Thorac Oncol* (2020) 15(10):1636–46. doi: 10.1016/j.jtho.2020.07.014
26. Qin S, Ren Z, Meng Z, Chen Z, Chai X, Xiong J, et al. Camrelizumab in Patients With Previously Treated Advanced Hepatocellular Carcinoma: A Multicentre, Open-Label, Parallel-Group, Randomised, Phase 2 Trial. *Lancet Oncol* (2020) 21(4):571–80. doi: 10.1016/S1470-2045(20)30011-5
27. Laccetti AL, Garmezy B, Xiao L, Economides M, Venkatesan A, Gao J, et al. Combination Antiangiogenic Tyrosine Kinase Inhibition and Anti-PD1 Immunotherapy in Metastatic Renal Cell Carcinoma: A Retrospective Analysis of Safety, Tolerance, and Clinical Outcomes. *Cancer Med* (2021) 10(7):2341–9. doi: 10.1002/cam4.3812
28. Amin A, Plimack ER, Ernstoff MS, Lewis LD, Bauer TM, McDermott DF, et al. Safety and Efficacy of Nivolumab in Combination With Sunitinib or Pazopanib in Advanced or Metastatic Renal Cell Carcinoma: The CheckMate 016 Study. *J Immunother Cancer* (2018) 6(1):109. doi: 10.1186/s40425-018-0420-0
29. Chowdhury S, McDermott DF, Voss MH, Hawkins RE, Aimone P, Voi M, et al. A phase I/II Study to Assess the Safety and Efficacy of Pazopanib (PAZ) and Pembrolizumab (PEM) in Patients (pts) with Advanced Renal Cell Carcinoma (aRCC). *J Clin Oncol* (2017) 35:4506. doi: 10.1200/JCO.2017.35.15_suppl.4506
30. Mejean A, Roupret M, Larousserie F, Hopirtean V, Thiounn N, Dufour B. Is There a Place for Radical Nephrectomy in the Presence of Metastatic Collecting Duct (Bellini) Carcinoma? *J Urol* (2003) 169(4):1287–90. doi: 10.1097/01.ju.0000050221.51509.f5
31. Marchioni M, Bandini M, Preisser F, Tian Z, Kapoor A, Cindolo L, et al. Survival After Cytoreductive Nephrectomy in Metastatic Non-Clear Cell Renal Cell Carcinoma Patients: A Population-Based Study. *Eur Urol Focus* (2019) 5(3):488–96. doi: 10.1016/j.euf.2017.11.012

Conflict of Interest: The authors declare that the research was conducted in the absence of any commercial or financial relationships that could be construed as a potential conflict of interest.

Publisher's Note: All claims expressed in this article are solely those of the authors and do not necessarily represent those of their affiliated organizations, or those of the publisher, the editors and the reviewers. Any product that may be evaluated in this article, or claim that may be made by its manufacturer, is not guaranteed or endorsed by the publisher.

frontiers in Oncology

SYSTEMATIC REVIEW
published: 07 December 2021
doi: 10.3389/fonc.2021.735803

Prognostic and Clinicopathological Significance of the Systemic Immune-Inflammation Index in Patients With Renal Cell Carcinoma: A Meta-Analysis

Mingyu Jin[1]*, *Shaoying Yuan*[1], *Yiming Yuan*[2] and *Luqi Yi*[3]

[1] Department of Andrology, Guangdong Hospital of Traditional Chinese Medicine, Zhuhai, China, [2] Andrology Center, Peking University First Hospital, Beijing, China, [3] Department of Urology, Guangdong Hospital of Traditional Chinese Medicine, Zhuhai, China

OPEN ACCESS

Edited by:
Walter J. Storkus,
University of Pittsburgh, United States

Reviewed by:
Ronald James Fecek,
Lake Erie College of Osteopathic Medicine, United States
Antonella Argentiero,
Istituto Nazionale dei Tumori (IRCCS), Italy

***Correspondence:**
Mingyu Jin
15919152830@163.com

Specialty section:
This article was submitted to Genitourinary Oncology, a section of the journal Frontiers in Oncology

Received: 03 July 2021
Accepted: 17 November 2021
Published: 07 December 2021

Citation:
Jin M, Yuan S, Yuan Y and Yi L (2021) Prognostic and Clinicopathological Significance of the Systemic Immune-Inflammation Index in Patients With Renal Cell Carcinoma: A Meta-Analysis. Front. Oncol. 11:735803. doi: 10.3389/fonc.2021.735803

Background: The systemic immune-inflammation index (SII) is a hematological parameter based on neutrophil, platelet, and lymphocyte counts. Studies that have investigated the prognostic value of SII in patients with renal cell carcinoma (RCC) have reported controversial results. In this study, we systematically investigated the prognostic value of SII in patients with RCC.

Methods: We systematically searched English articles in the PubMed, Embase, Web of Science, and Cochrane Library databases up to October 2021. Hazard ratios (HRs) and odds ratios (ORs) with 95% confidence intervals (CIs) were used to obtain pooled results.

Results: The meta-analysis included 10 studies that enrolled 3,180 patients. A high SII was associated with poor overall survival (HR 1.75, 95% CI 1.33–2.30, p<0.001) in patients with RCC. However, a high SII was not shown to be a significant prognostic factor for progression-free survival/disease-free survival (HR 1.22, 95% CI 0.84–1.76, p=0.293) or poor cancer-specific survival (HR 1.46, 95% CI 0.68–3.12, p=0.332) in patients with RCC. A high SII was correlated with male sex (OR 1.51, 95% CI 1.11–2.04, p=0.008), Fuhrman grade G3–G4 (OR 1.80, 95% CI 1.08–3.00, p=0.024), and poor risk based on the International Metastatic Renal Cell Carcinoma Database Consortium criteria (OR 19.12, 95% CI 9.13–40.06, p<0.001).

Conclusion: A high SII was independently associated with poor survival outcomes in patients with RCC. Additionally, an elevated SII indicated more aggressive disease. The SII may serve as a useful cost-effective prognostic indicator in patients with RCC.

Keywords: systemic immune-inflammation index, prognosis, meta-analysis, renal cell carcinoma, survival

INTRODUCTION

Renal cell carcinoma (RCC) is the third most common cancer of the urinary system and accounts for 2.2% of all human malignancies (1). Approximately 25%–30% of patients with RCC present with metastases at the time of diagnosis (2). Among patients diagnosed with early-stage and localized disease, 25% develop recurrence or metastasis after radical surgical resection (3). Immune checkpoint inhibitors are widely accepted as an essential component of RCC treatment following rapid advances in immunotherapy for the management of RCC (4, 5). The prognosis of patients with RCC remains poor; the 5-year survival rate is only 12% for stage IV metastatic disease (6). Prognostic markers are clinically useful for improved management of patients with RCC. Therefore, identification of novel and reliable prognostic indicators is urgently required to improve survival of patients with RCC (7).

The role of the immune system in various stages of cancer progression has been extensively investigated over the last few years (8). Inflammation-based prognostic scores such as platelet-to-lymphocyte ratio (9), lymphocyte to monocyte ratio (10), and prognostic nutritional index (11) are cost-effective and reliable prognostic tools that are widely used in patients with cancer (10, 12). Many studies have shown that the systemic immune-inflammation index (SII) is a useful prognostic marker for several malignant tumors, including pancreatic (13), gallbladder (14), non-small-cell lung (15), and laryngeal cancer (16), as well as for cholangiocarcinoma (17). Studies have investigated the prognostic value of SII in patients with RCC; however, the results are inconsistent (18–25). Therefore, in this meta-analysis, we investigated the role of SII as a prognostic indicator of RCC and also the correlation between SII and clinicopathological features of RCC.

MATERIALS AND METHODS

Study Guideline and Ethics Statement

This meta-analysis was performed in accordance with the Preferred Reporting Items for Systematic Reviews and Meta-Analyses guidelines (26). All data used in this meta-analysis were based on previous studies; therefore, ethical approval and patient consent were not required for this study.

Search Strategy

The English databases of PubMed, Embase, Web of Science, and Cochrane Library were systematically searched up to October 2021. We used the following search terms: systemic immune-inflammation index OR SII AND renal cell carcinoma OR kidney cancer AND prognosis OR survival OR outcomes OR prognostic. The citation lists of the relevant studies were also manually checked for additional eligible articles. We selected only English publications.

Inclusion and Exclusion Criteria

The inclusion criteria were as follows: (1) studies that investigated the association between the SII and prognosis in patients diagnosed with RCC, (2) availability of hazard ratios (HRs) and 95% confidence intervals (CIs) for survival outcomes or data required to calculate these values, (3) an appropriately defined SII based on the following formula: platelet count × neutrophil count/lymphocyte count, (4) availability of a cutoff value to divide the SII into high or low SII groups and, (5) articles published in English. The exclusion criteria were as follows: (1) case reports, reviews, meeting abstracts, letters, and comments, (2) duplicate articles with patient overlap, (3) insufficient data for detailed analysis and, (4) animal studies. The survival endpoints included overall survival (OS), progression-free survival (PFS), disease-free survival (DFS), and cancer-specific survival (CSS).

Data Extraction and Quality Assessment

Two investigators (M.J. and S.Y.) independently extracted information from all studies included in this meta-analysis, and any disagreements were resolved by discussion with a third investigator (Y.Y.). The following data were extracted: first author, publication year, country, sample size, sex, age, study period, survival outcomes, follow-up, cancer type, treatment methods used, cut-off value of the SII, number of patients with high and low SII scores, and HRs and 95% CIs for OS, PFS, DFS, and CSS. The Newcastle–Ottawa quality assessment scale (NOS) (27) was used to assess the quality of the included studies. The NOS assesses the quality of studies with regard to the following aspects: subject selection, comparability of the subject, and clinical outcomes. The NOS score ranged from 0 to 9, and studies with NOS scores ≥6 were considered high-quality studies.

Statistical Analysis

Pooled HRs and 95% CIs were calculated to determine the role of the SII as a prognostic marker in patients with RCC. Pooled HR >1 (without 95% CI overlapping 1) indicated that a high SII correlated with poor prognosis. Heterogeneity among studies was assessed using the χ2-based Q test and I^2 statistics. The I^2>50% and Ph<0.10 indicated significant heterogeneity, and a random-effects model was used for analysis; a fixed-effects model was used in other cases. Subgroup analyses were performed to confirm the source of heterogeneity. The pooled odds ratios (ORs) and 95% CIs were used to determine the association between SII and clinicopathological factors. Pooled OR>1 (without 95% CI overlapping 1) suggested that a high SII was associated with poor clinicopathological outcomes. Potential publication bias was evaluated using the Begg's test (28). All data analyses were performed using the Stata 12.0 software (Stata Corp LP, College Station, TX, USA). A P value <0.05 (two-tailed) was considered statistically significant.

RESULTS

Study Selection

Figure 1 shows a detailed flow diagram of the study selection process. The initial literature search yielded 138 studies, of which 46 were included in the analysis after exclusion of duplicates. After

screening of titles and abstracts, 32 studies were discarded and the full text was reviewed in 14. Four studies with insufficient survival data were eliminated. Finally, data of 10 studies that included 3,180 patients (18–25, 29, 30) were analyzed in this meta-analysis.

Characteristics of Included Studies

Table 1 summarizes the main characteristics of all studies included in our research. The total sample size was 3,180 and ranged from 31 to 646. Three studies were performed in Turkey (19, 24, 30), two in Italy (21, 23), and one each in India (18), China (22), Japan (25), Austria (29), and Poland (20), respectively. The included studies were published between 2016 and 2021 and all were English publications. All 10 studies investigated the association between SII and OS (18–25, 29, 30), three investigated the association between SII and PFS (18, 23, 30), one between SII and DFS (24), and two between SII and CSS (22, 29). Eight studies recruited patients with metastatic RCC (18–21, 23, 25, 29, 30), and two studies enrolled patients with localized disease (22, 24). The cut-off values of SII ranged from 529 to 1,375 (median 730). All included studies were shown to be high-quality studies (NOS scores ≥6).

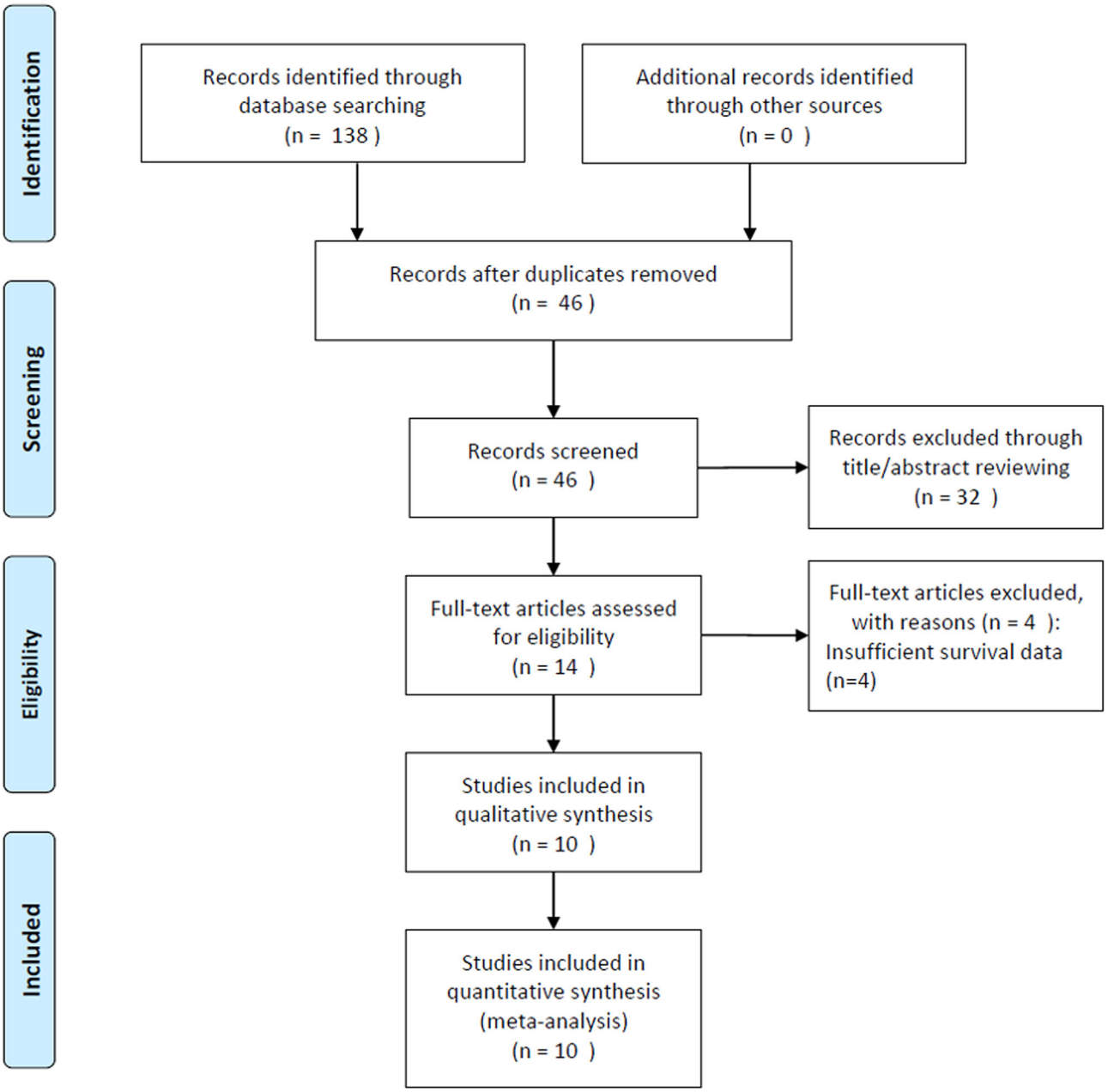

FIGURE 1 | Flow diagram of included studies for this meta-analysis.

TABLE 1 | Main characteristics of all included studies.

Author	Year	Country	Sample size	Sex (M/F)	Age (year) Median(range)	Study period	Survival outcome	Follow-up (month)	Cancer type	Treatment methods	Cut-off value	No. of patients with high/low SII	NOS score
Barua	2019	India	31	21/10	Mean: 55	2012-2017	OS, PFS	16.5	mRCC	Surgery	883	17/14	7
Bugdayci	2021	Turkey	187	149/38	61 (34-86)	2012-2019	OS	15	mRCC	Surgery+ TKIs	730	94/93	7
Chrom	2019	Poland	502	339/163	62 (22-88)	2008-2016	OS	52.5	mRCC	TKIs	730	208/294	8
De Giorgi	2019	Italy	313	235/78	65 (40-84)	2015-2016	OS	24	mRCC	ICIs	1375	96/217	7
Hu	2020	China	646	394/252	Mean: 54.77	2010-2013	OS, CSS	84	Localized RCC	Surgery	529	163/483	7
Lolli	2016	Italy	335	238/97	63 (27-88)	2006-2014	OS, PFS	49	mRCC	TKIs	730	126/209	9
Ozbek	2020	Turkey	176	111/65	Mean: 65.32	NR	OS, DFS	NR	Localized RCC	Surgery	830	52/124	6
Teishima	2020	Japan	179	145/34	65.5 (40-85)	2008-2018	OS	24	mRCC	TKIs	730	73/106	8
Laukhtina	2021	Austria	613	NR	65	NR	OS, CSS	31	mRCC	Surgery	710	298/315	7
Yilmaz	2021	Turkey	198	135/63	63 (29–87)	2012-2019	OS, PFS	24(1-70)	mRCC	TKIs	1291	91/107	8

RCC, renal cell carcinoma; mRCC, metastatic renal cell carcinoma; TKIs, tyrosine kinase inhibitors; OS, overall survival; PFS, progression-free survival; DFS, disease-free survival; CSS, cancer-specific survival; ICIs, immune checkpoint inhibitors; NR, not reported; NOS, Newcastle-Ottawa Scale.

Association Between the Systemic Immune-Inflammation Index and Survival Outcomes in Patients With Renal Cell Carcinoma

The prognostic value of SII for OS was determined based on data from 10 studies that included 3,180 patients (18–25, 29, 30). The pooled HR and 95% CI are as follows: HR 1.75, 95% CI 1.33–2.30, p<0.001 (**Table 2** and **Figure 2**). A random-effects model was used owing to significant heterogeneity (I^2 = 92.4%, Ph<0.001). Studies were stratified based on region, cancer type, cut-off value, treatment methods, and sample size for subgroup analyses. A high SII was associated with poor OS, regardless of geographical region, cancer type, and treatment methods (**Table 2**). A high SII was significantly correlated with poor OS at cut-off values ≤730 (HR 1.81, 95% CI 1.41–2.30, p<0.001) (**Table 2**). Four studies that included 740 patients (18, 23, 24, 30) reported an association between SII and PFS/DFS in patients with RCC. Results of pooled data were as follows: HR 1.22, 95% CI 0.84–1.76, p=0.293, which indicate that SII was not a significant prognostic factor for PFS/DFS in patients with RCC (**Table 2** and **Figure 3**). Additionally, subgroup analysis indicated that a cut-off level ≤730 was of prognostic value for poor PFS/DFS in patients with RCC (**Table 2**). Data obtained from two studies (22, 29) showed that a high SII was not associated with poor CSS (pooled data HR 1.46, 95% CI 0.68–3.12, p=0.332) (**Table 2** and **Figure 4**). Subgroup analysis of CSS was not performed because of the limited sample size.

Correlation Between the Systemic Immune-Inflammation Index and Clinicopathological Factors in Patients With Renal Cell Carcinoma

Five studies (19, 21, 22, 24, 25) reported an association between SII and clinicopathological characteristics in RCC; sex (male vs. female), histopathological type (clear cell [ccRCC] vs. non-ccRCC), Fuhrman grade (G3–G4 vs. G1–G2), T stage (T3–T4 vs. T1–T2), sarcomatoid differentiation (present vs. absent), and the International Metastatic Renal Cell Carcinoma Database Consortium (IMDC) risk score (poor vs. favorable/intermediate) were associated with SII. The results showed that a high SII was correlated with male sex (OR 1.51, 95% CI 1.11–2.04, p=0.008), Fuhrman grade G3–G4 (OR 1.80, 95% CI 1.08–3.00, p=0.024), and poor risk based on IMDC criteria (OR 19.12, 95% CI 9.13–40.06, p<0.001) (**Figure 5** and **Table 3**). However, we observed no significant association between the SII and histopathological cancer type (OR 1.04, 95% CI 0.72–1.51, p=0.840), T stage (OR 1.76, 95% CI 0.62–5.01, p=0.292), or sarcomatoid differentiation (OR 1.74, 95% CI 0.50–6.06, p=0.382) (**Figure 5** and **Table 3**).

Publication Bias

As shown in **Figure 6**, we observed no significant publication bias in our meta-analysis based on funnel plots and Begg's test (p=0.592 for OS, p=0.734 for PFS/DFS, and p=1 for CSS).

DISCUSSION

The SII has been reported as a useful prognostic indicator in many solid tumors, including gallbladder (31), pancreatic (13), and colorectal cancer (32), as well as in intrahepatic cholangiocarcinoma (33). Studies have investigated the association between SII and survival outcomes in patients with RCC (18–25, 29, 30); however, the results remain controversial. In the current meta-analysis, we analyzed data of 10 studies that included 3,180 patients and quantitatively investigated the role of SII as a prognostic indicator in RCC. Pooled data showed that a

TABLE 2 | Subgroup analyses of SII for prognosis in patients with RCC.

Subgroups	No. of studies	No. of patients	Effects model	HR (95%CI)	p	Heterogeneity I^2(%)	Ph
OS							
Total	10	3,180	Random	1.75 (1.33-2.30)	<0.001	92.4	<0.001
Region							
Asia	6	1,417	Random	1.62 (1.12-2.34)	0.010	85.4	<0.001
Non-Asia	4	1,763	Random	1.92 (1.33-2.78)	0.001	88	<0.001
Cancer type							
Localized RCC	2	822	Fixed	1.96 (1.41-2.71)	<0.001	0	0.363
mRCC	8	2,358	Random	1.70 (1.26-2.30)	0.001	93.2	<0.001
Cut-off value							
≤730	6	2,462	Random	1.81 (1.41-2.30)	<0.001	72.5	0.003
>730	4	718	Random	1.64 (0.92-2.93)	0.096	92.2	<0.001
Treatments							
Surgery	4	1,466	Random	1.37 (1.03-1.81)	0.029	85.5	<0.001
TKIs	4	1,214	Fixed	1.87 (1.58-2.20)	<0.001	27.8	0.245
Surgery + TKIs	1	187	–	2.08 (1.40-3.09)	<0.001	–	–
ICIs	1	313	–	2.99 (2.07-4.31)	<0.001	–	–
Sample size							
≤200	5	771	Random	1.51 (1.04-2.18)	0.029	82.2	<0.001
>200	5	2,409	Random	1.97 (1.42-2.73)	<0.001	85.0	<0.001
PFS/DFS							
Total	4	740	Random	1.22 (0.84-1.76)	0.293	85.9	<0.001
Region							
Asia	3	405	Fixed	1.02 (1.00-1.04)	0.048	0	0.943
Non-Asia	1	335	–	1.84 (1.43-2.36)	<0.001	–	–
Cancer type							
Localized RCC	1	176	–	1.14 (0.53-2.43)	0.738	–	–
mRCC	3	564	Random	1.23 (0.81-1.88)	0.330	90.6	<0.001
Cut-off value							
≤730	1	335	–	1.84 (1.43-2.36)	<0.001	–	–
>730	3	405	Fixed	1.02 (1.00-1.04)	0.048	0	0.943
Treatments							
Surgery	2	207	Fixed	1.02 (1.00-1.04)	0.047	0	0.777
TKIs	2	533	Random	1.38 (0.74-2.55)	0.311	83.6	0.014
Sample size							
≤200	3	405	Fixed	1.02 (1.00-1.04)	0.048	0	0.943
>200	1	335	-0	1.84 (1.43-2.36)	<0.001	–	–
CSS							
Total	2	1,259	Random	1.46 (0.68-3.12)	0.332	81.5	0.020

RCC, renal cell carcinoma; mRCC, metastatic renal cell carcinoma; TKIs, tyrosine kinase inhibitors; OS, overall survival; PFS, progression-free survival; DFS, disease-free survival; CSS, cancer-specific survival; ICIs, immune checkpoint inhibitors.

high SII was associated with poor OS but not with PFS/DFS or CSS in patients with RCC. Furthermore, a high SII was also correlated with a high Fuhrman grade and poor IMDC risk scores. In this meta-analysis, we observed that a high SII indicated poor survival outcomes and aggressive histopathological features in patients with RCC. To our knowledge, this is the first meta-analysis that investigated the prognostic value of the SII in patients with RCC. The immune system plays a critical role in tumor development *via* various mechanisms including tumor initiation, angiogenesis, and metastasis (34). The tumor microenvironment (TME) can trigger immune inflammatory responses and facilitate tumor progression (35). For example, natural killer and CD8+ T cells in the TME can recognize and eliminate more immunogenic cancer cells during the early stages of tumor development (36). Moreover, M2-type tumor-associated macrophages are protumorigenic and promote angiogenesis, lymphangiogenesis, and cancer cell proliferation and metastasis in the TME (37).

The SII, calculated using blood test parameters, is a useful prognostic indicator based on the following underlying mechanisms: (a) neutrophils participate in different stages of tumor progression *via* production of a variety of cytokines (38). Neutrophils in the TME release various cytokines and chemokines such as reactive oxygen species and transforming growth factor (TGF)-β to educate themselves and other cell types to differentiate into a pro-cancer phenotype (39, 40). (b) Platelets stimulate thrombopoiesis and tumor angiogenesis *via* production of TGF-β, promotion of adhesion, and prevention of cell death (41). (c) Cytotoxic lymphocytes play an important role in the cell-mediated immunological destruction of tumor cells (42). Lymphocytosis represents activation of the immune response and is associated with prolonged survival in patients with cancer (43). Therefore, a high SII, which could be secondary to elevated neutrophil or platelet counts, and/or low lymphocyte counts, is correlated with poor survival outcomes in patients with RCC. Notably, our results also indicate that a high SII was

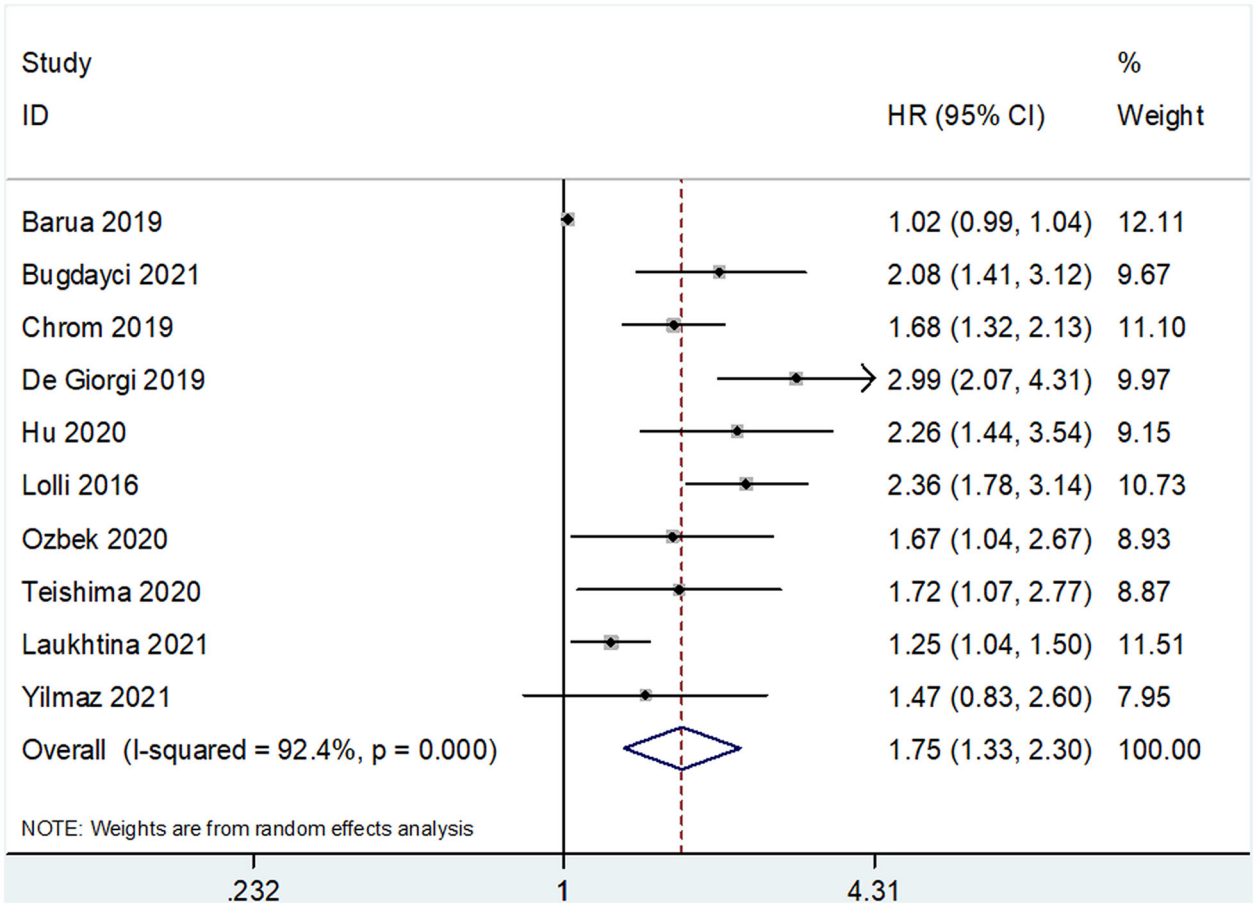

FIGURE 2 | Forest plots showing the association between SII and overall survival (OS) in renal cell carcinoma (RCC).

associated with a high Fuhrman grade and poor IMDC risk scores. The Fuhrman grade and IMDC risk scores reflect aggressiveness of the cancer; therefore, patients with a high SII tend to show tumor progression or recurrence after initial treatment.

Recent meta-analyses have investigated the prognostic role of SII in many cancer types, including hepatocellular (44), gastric (45), breast (46), and colorectal cancer (47). A meta-analysis that included 2,796 patients reported that a high SII was associated with poor prognosis in patients with hepatocellular carcinoma (44). Fu et al. observed that a high SII was significantly associated with poor OS and DFS in patients with gastric cancer (45). Huang et al. also reported that a high SII was associated with poor OS, PFS, and CSS in patients with urologic cancers (48). A recent meta-analysis observed that a high SII predicts poor survival outcomes in patients with gynecological cancers (49). The results of the aforementioned meta-analyses are consistent with our findings. Moreover, we observed an association between the SII and Fuhrman grade and IMDC risk scores in patients with RCC, which highlights the clinical usefulness of the SII to identify patients at high risk of tumor progression.

In a recent study, the authors performed transcriptome profiling of all three subgroups of RCC using machine learning and bioinformatics analysis (50); transcriptomic data of 891 patients were extracted from The Cancer Genome Atlas (TCGA) database; ccRCC samples obtained from mixed subgroups showed an inverse correlation between mitochondrial and angiogenesis-related genes in the TCGA database and external validation cohorts (50). Moreover, affiliation to the mixed subgroup was associated with a significantly shorter OS in patients with ccRCC and longer OS in patients with chromophobe RCC (50). These findings reported by Marquardt et al. (50) indicate heterogeneity among various histopathological subtypes of RCC, which can be attributed to the different gene clusters in each subgroup. These findings highlight the heterogeneity among recruited patients because the histopathological types were not the same.

Following are the limitations of this meta-analysis: (i) The relatively small sample size is a drawback of this research; this meta-analysis included only 10 studies that investigated 3,180 patients. Large-scale studies are warranted in future to provide deeper insight into this subject. (ii) The cut-off values of SII

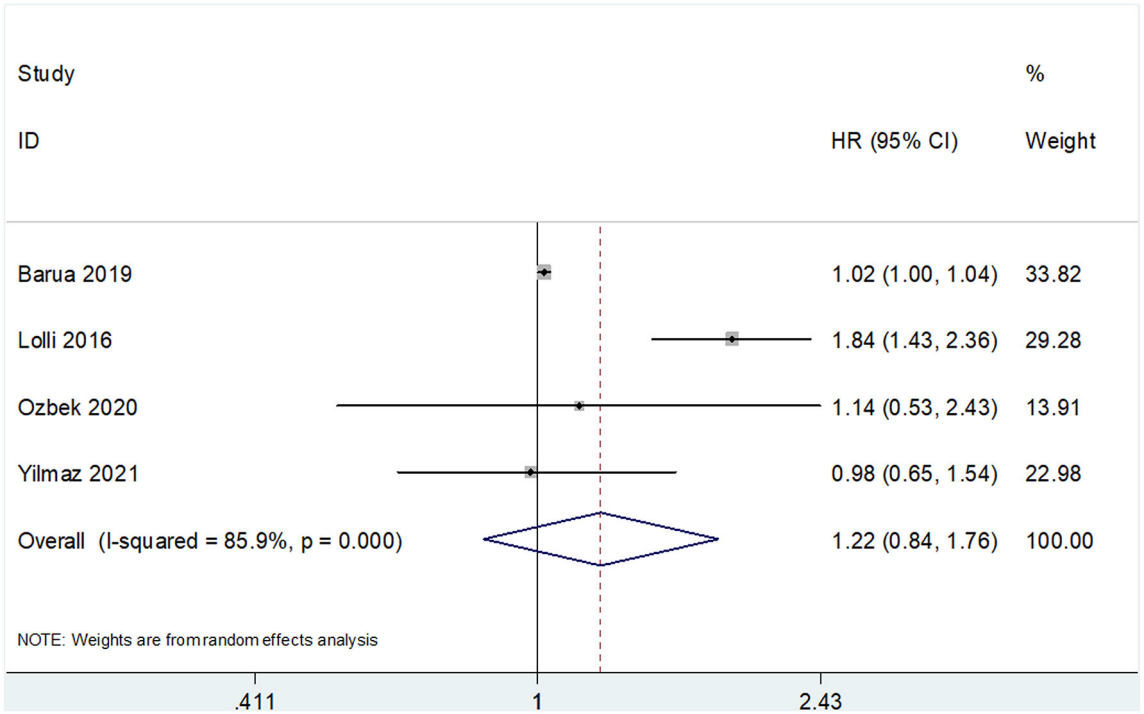

FIGURE 3 | Forest plots showing the association between SII and progression-free survival (PFS)/disease-free survival (DFS) in RCC.

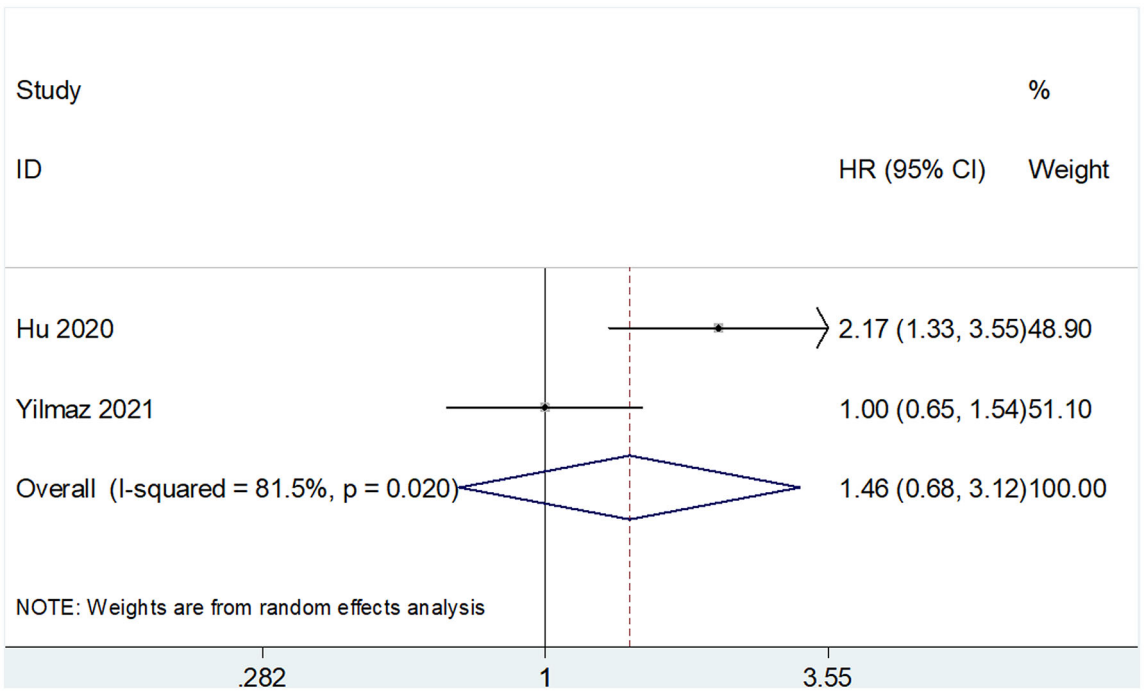

FIGURE 4 | Forest plots showing the association between SII and cancer-specific survival (CSS) in RCC.

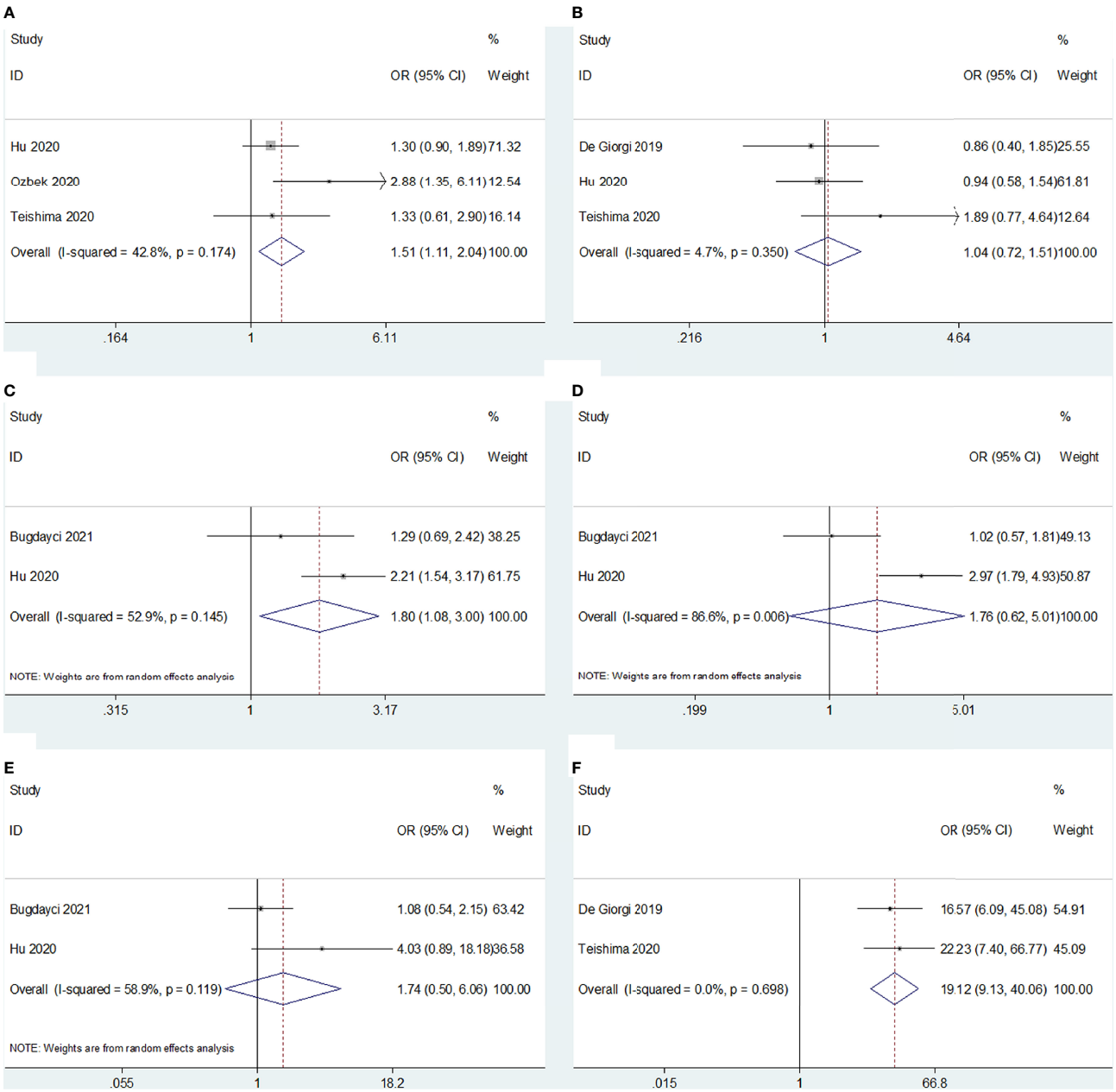

FIGURE 5 | Forest plots of the association between SII and clinicopathological features of RCC. **(A)** Sex; **(B)** Histological type; **(C)** Fuhrman grade; **(D)** T stage; **(E)** Sarcomatoid differentiation, and **(F)** IMDC risk.

TABLE 3 | The meta-analysis of association between SII and clinicopathological factors in patients with RCC.

Variables	No. of studies	No. of patients	Effects model	OR (95%CI)	p	Heterogeneity I^2(%)	Ph
Sex (male vs female)	3	1,001	Fixed	1.51(1.11-2.04)	0.008	42.8	0.174
Histological type (non-clear cell vs clear cell)	3	1,138	Fixed	1.04(0.72-1.51)	0.840	4.7	0.350
Fuhrman grade (G3-G4 vs G1-G2)	2	833	Random	1.80(1.08-3.00)	0.024	52.9	0.145
T stage (T3-T4 vs T1-T2)	2	833	Random	1.76(0.62-5.01)	0.292	86.6	0.006
Sarcomatoid differentiation (present vs absent)	2	833	Random	1.74(0.50-6.06)	0.382	58.9	0.119
IMDC risk (poor vs favorable/intermediate)	2	492	Fixed	19.12(9.13-40.06)	<0.001	0	0.698

IMDC, International Metastatic Renal Cell Carcinoma Database Consortium.

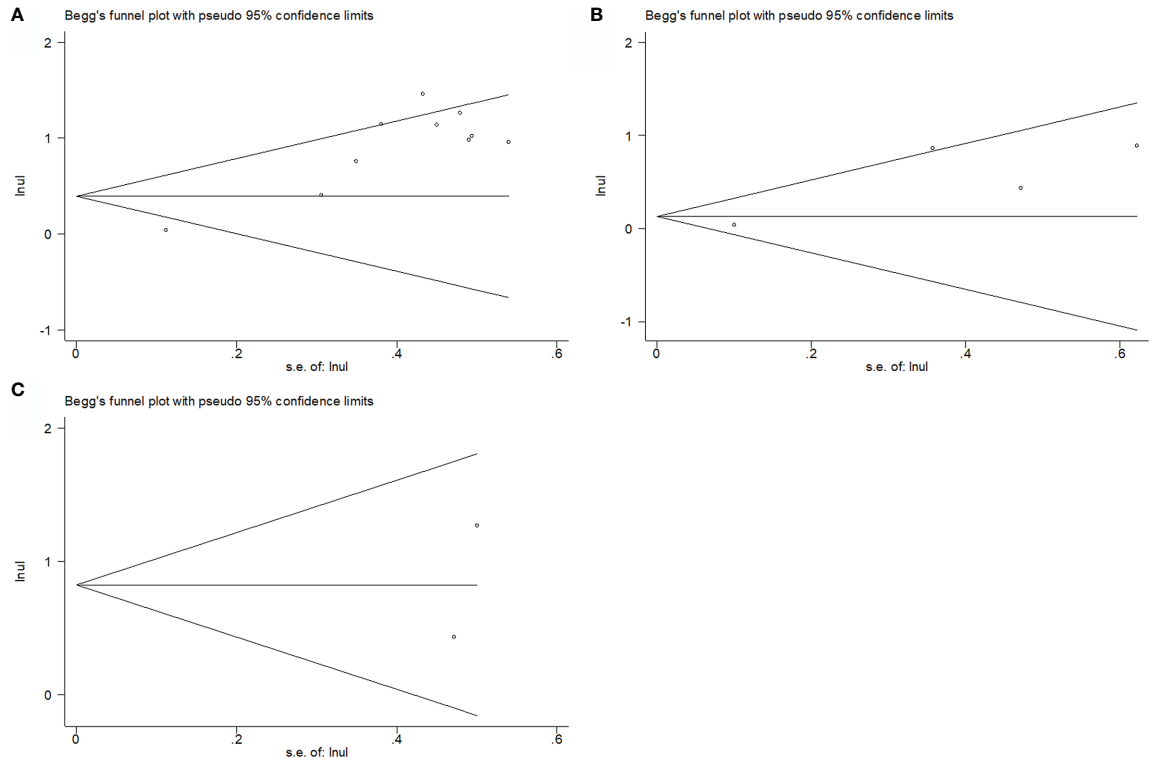

FIGURE 6 | Publication bias assessment using Begg funnel plot. **(A)** Begg's test for OS; **(B)** Begg's test for PFS/DFS; **(C)** Begg's test for CSS.

varied across the included studies, which may have contributed to a selection bias. (iii) Most studies were retrospectively designed; therefore, the inherent flaws associated with retrospective studies may have introduced heterogeneity in the meta-analysis, although we did not detect publication bias.

CONCLUSIONS

This meta-analysis highlights that a high SII was independently associated with poor survival outcomes in patients with RCC. Additionally, a high SII indicates greater aggressiveness of the malignancy. The SII may serve as a useful cost-effective prognostic indicator in patients with RCC.

DATA AVAILABILITY STATEMENT

The original contributions presented in the study are included in the article/supplementary material. Further inquiries can be directed to the corresponding author.

AUTHOR CONTRIBUTIONS

MJ and SY provided the study conception and design. YY and LY contributed to the drafting of the article and final approval of the submitted version. All authors provided the analyses and interpretation of the data and completion of figures and tables. All authors contributed to the article and approved the submitted version.

REFERENCES

1. Bray F, Ferlay J, Soerjomataram I, Siegel RL, Torre LA, Jemal A. Global Cancer Statistics 2018: GLOBOCAN Estimates of Incidence and Mortality Worldwide for 36 Cancers in 185 Countries. *CA: Cancer J Clin* (2018) 68 (6):394–424. doi: 10.3322/caac.21492
2. Hammers HJ, Plimack ER, Infante JR, Rini BI, McDermott DF, Lewis LD, et al. Safety and Efficacy of Nivolumab in Combination With Ipilimumab in Metastatic Renal Cell Carcinoma: The CheckMate 016 Study. *J Clin Oncol Off J Am Soc Clin Oncol* (2017) 35(34):3851–8. doi: 10.1200/jco.2016.72.1985
3. MacLennan S, Imamura M, Lapitan MC, Omar MI, Lam TB, Hilvano-Cabungcal AM, et al. Systematic Review of Oncological Outcomes Following Surgical Management of Localised Renal Cancer. *Eur Urol* (2012) 61(5):972–93. doi: 10.1016/j.eururo.2012.02.039
4. Xu WX, Atkins MB, McDermott DF. Checkpoint Inhibitor Immunotherapy in Kidney Cancer. *Nat Rev Urol* (2020) 17(3):137–50. doi: 10.1038/s41585-020-0282-3
5. Deleuze A, Saout J, Dugay F, Peyronnet B, Mathieu R, Verhoest G, et al. Immunotherapy in Renal Cell Carcinoma: The Future Is Now. *Int J Mol Sci* (2020) 21(7):2532. doi: 10.3390/ijms21072532

6. Padala SA, Barsouk A, Thandra KC, Saginala K, Mohammed A, Vakiti A, et al. Epidemiology of Renal Cell Carcinoma. *World J Oncol* (2020) 11(3):79–87. doi: 10.14740/wjon1279
7. Scholtes MP, Alberts AR, Ifle IG, Verhagen P, van der Veldt AAM, Zuiverloon TCM. Biomarker-Oriented Therapy in Bladder and Renal Cancer. *Int J Mol Sci* (2021) 22(6):2832. doi: 10.3390/ijms22062832
8. Diaz-Montero CM, Rini BI, Finke JH. The Immunology of Renal Cell Carcinoma. *Nat Rev Nephrol* (2020) 16(12):721–35. doi: 10.1038/s41581-020-0316-3
9. Wang Z, Peng S, Wang A, Xie H, Guo L, Jiang N, et al. Platelet-Lymphocyte Ratio Acts as an Independent Predictor of Prognosis in Patients With Renal Cell Carcinoma. *Clinica chimica acta; Int J Clin Chem* (2018) 480:166–72. doi: 10.1016/j.cca.2018.02.014
10. Li M, Deng Q, Zhang L, He S, Rong J, Zheng F. The Pretreatment Lymphocyte to Monocyte Ratio Predicts Clinical Outcome for Patients With Urological Cancers: A Meta-Analysis. *Pathology Res Pract* (2019) 215(1):5–11. doi: 10.1016/j.prp.2018.10.026
11. Yasar HA, Bir Yucel K, Arslan C, Ucar G, Karakaya S, Bilgin B, et al. The Relationship Between Prognostic Nutritional Index and Treatment Response in Patients With Metastatic Renal Cell Cancer. *J Oncol Pharm Pract Off Publ Int Soc Oncol Pharm Practitioners* (2020) 26(5):1110–6. doi: 10.1177/1078155219883004
12. Hu X, Wang Y, Yang WX, Dou WC, Shao YX, Li X. Modified Glasgow Prognostic Score as a Prognostic Factor for Renal Cell Carcinomas: A Systematic Review and Meta-Analysis. *Cancer Manage Res* (2019) 11:6163–73. doi: 10.2147/cmar.S208839
13. Bittoni A, Pecci F, Mentrasti G, Crocetti S, Lupi A, Lanese A, et al. Systemic Immune-Inflammation Index: A Prognostic Tiebreaker Among All in Advanced Pancreatic Cancer. *Ann Trans Med* (2021) 9(3):251. doi: 10.21037/atm-20-3499
14. Sun LJ, Jin YK, Hu WM, Zhang MY, Jin B, Xu HF, et al. The Impacts of Systemic Immune-Inflammation Index on Clinical Outcomes in Gallbladder Carcinoma. *Front Oncol* (2020) 10:554521. doi: 10.3389/fonc.2020.554521
15. Huang TS, Zhang HQ, Zhao YZ, Li YP, Wang GF, Zhang YB, et al. Systemic Immune-Inflammation Index Changes Predict Outcome in Stage III Non-Small-Cell Lung Cancer Patients Treated With Concurrent Chemoradiotherapy. *Future Oncol* (2021) 17(17):2141–9. doi: 10.2217/fon-2020-1272
16. Akkas EA, Yucel B. Prognostic Value of Systemic Immune Inflammation Index in Patients With Laryngeal Cancer. *Eur Arch Oto-Rhino-Laryngology* (2021) 278(6):1945–55. doi: 10.1007/s00405-021-06798-2
17. Tsilimigras DI, Moris D, Mehta R, Paredes AZ, Sahara K, Guglielmi A, et al. The Systemic Immune-Inflammation Index Predicts Prognosis in Intrahepatic Cholangiocarcinoma: An International Multi-Institutional Analysis. *Hpb* (2020) 22(12):1667–74. doi: 10.1016/j.hpb.2020.03.011
18. Barua SK, Singh Y, Baruah SJ, PR T, Bagchi PK, Sarma D, et al. Predictors of Progression-Free Survival and Overall Survival in Metastatic Non-Clear Cell Renal Cell Carcinoma: A Single-Center Experience. *World J Oncol* (2019) 10 (2):101–11. doi: 10.14740/wjon1188
19. Bugdayci Basal F, Karacin C, Bilgetekin I, Oksuzoglu OB. Can Systemic Immune-Inflammation Index Create a New Perspective for the IMDC Scoring System in Patients With Metastatic Renal Cell Carcinoma? *Urol Int* (2021) 105 (7-8):666–73. doi: 10.1159/000513456
20. Chrom P, Zolnierek J, Bodnar L, Stec R, Szczylik C. External Validation of the Systemic Immune-Inflammation Index as a Prognostic Factor in Metastatic Renal Cell Carcinoma and Its Implementation Within the International Metastatic Renal Cell Carcinoma Database Consortium Model. *Int J Clin Oncol* (2019) 24(5):526–32. doi: 10.1007/s10147-018-01390-x
21. De Giorgi U, Procopio G, Giannarelli D, Sabbatini R, Bearz A, Buti S, et al. Association of Systemic Inflammation Index and Body Mass Index With Survival in Patients With Renal Cell Cancer Treated With Nivolumab. *Clin Cancer Res an Off J Am Assoc Cancer Res* (2019) 25(13):3839–46. doi: 10.1158/1078-0432.Ccr-18-3661
22. Hu X, Shao YX, Yang ZQ, Dou WC, Xiong SC, Li X. Preoperative Systemic Immune-Inflammation Index Predicts Prognosis of Patients With Non-Metastatic Renal Cell Carcinoma: A Propensity Score-Matched Analysis. *Cancer Cell Int* (2020) 20:222. doi: 10.1186/s12935-020-01320-w
23. Lolli C, Basso U, Derosa L, Scarpi E, Sava T, Santoni M, et al. Systemic Immune-Inflammation Index Predicts the Clinical Outcome in Patients With Metastatic Renal Cell Cancer Treated With Sunitinib. *Oncotarget* (2016) 7 (34):54564–71. doi: 10.18632/oncotarget.10515
24. Ozbek E, Besiroglu H, Ozer K, Horsanali MO, Gorgel SN. Systemic Immune Inflammation Index Is a Promising Non-Invasive Marker for the Prognosis of the Patients With Localized Renal Cell Carcinoma. *Int Urol Nephrol* (2020) 52 (8):1455–63. doi: 10.1007/s11255-020-02440-y
25. Teishima J, Inoue S, Hayashi T, Mita K, Hasegawa Y, Kato M, et al. Impact of the Systemic Immune-Inflammation Index for the Prediction of Prognosis and Modification of the Risk Model in Patients With Metastatic Renal Cell Carcinoma Treated With First-Line Tyrosine Kinase Inhibitors. *Can Urological Assoc J = J l'Association Des urologues du Canada* (2020) 14(11): E582–e7. doi: 10.5489/cuaj.6413
26. Moher D, Liberati A, Tetzlaff J, Altman DG, Grp P. Preferred Reporting Items for Systematic Reviews and Meta-Analyses: The PRISMA Statement. *Ann Internal Med* (2009) 151(4):264–W64. doi: 10.7326/0003-4819-151-4-200908180-00135
27. Stang A. Critical Evaluation of the Newcastle-Ottawa Scale for the Assessment of the Quality of Nonrandomized Studies in Meta-Analyses. *Eur J Epidemiol* (2010) 25(9):603–5. doi: 10.1007/s10654-010-9491-z
28. Begg CB, Mazumdar M. Operating Characteristics of a Rank Correlation Test for Publication Bias. *Biometrics* (1994) 50(4):1088–101. doi: 10.2307/2533446
29. Laukhtina E, Pradere B, D'Andrea D, Rosiello G, Luzzago S, Pecoraro A, et al. Prognostic Effect of Preoperative Systemic Immune-Inflammation Index in Patients Treated With Cytoreductive Nephrectomy for Metastatic Renal Cell Carcinoma. *Minerva Urol Nephrol* (2021). doi: 10.23736/s2724-6051.21.04023-6
30. Yılmaz H, Yılmaz A, Demirağ G. Prognostic Significance of Hemoglobin-to-Red Cell Distribution Width Ratio in Patients With Metastatic Renal Cancer. *Future Oncol (London England)* (2021) 17(29):3853–64. doi: 10.2217/fon-2021-0040
31. Chen H, Huang ZW, Sun B, Wang AK, Wang YR, Shi H, et al. The Predictive Value of Systemic Immune Inflammation Index for Postoperative Survival of Gallbladder Carcinoma Patients. *J Surg Oncol* (2021) 124(1):59–66. doi: 10.1002/jso.26470
32. Li J, Shao JJ, Zhang XL, Chen X, Zhao WJ, Qian HY, et al. Prognostic Value of the Pretreatment Systemic Immune-Inflammation Index in Patients With Colorectal Cancer. *Gastroenterol Res Pract* (2020) 2020:8781674. doi: 10.1155/2020/8781674
33. Ren A, Li ZQ, Cheng PR, Zhang XZ, Deng RH, Ma Y. Systemic Immune-Inflammation Index Is a Prognostic Predictor in Patients With Intrahepatic Cholangiocarcinoma Undergoing Liver Transplantation. *Mediators Inflamm* (2021) 2021:6656996. doi: 10.1155/2021/6656996
34. Singh R, Mishra MK, Aggarwal H. Inflammation, Immunity, and Cancer. *Mediators Inflamm* (2017) 2017:6027305. doi: 10.1155/2017/6027305
35. Gonzalez H, Hagerling C, Werb Z. Roles of the Immune System in Cancer: From Tumor Initiation to Metastatic Progression. *Genes Dev* (2018) 32(19-20):1267–84. doi: 10.1101/gad.314617.118
36. Teng MW, Galon J, Fridman WH, Smyth MJ. From Mice to Humans: Developments in Cancer Immunoediting. *J Clin Invest* (2015) 125(9):3338–46. doi: 10.1172/jci80004
37. Mantovani A, Marchesi F, Malesci A, Laghi L, Allavena P. Tumour-Associated Macrophages as Treatment Targets in Oncology. *Nat Rev Clin Oncol* (2017) 14(7):399–416. doi: 10.1038/nrclinonc.2016.217
38. Tecchio C, Scapini P, Pizzolo G, Cassatella MA. On the Cytokines Produced by Human Neutrophils in Tumors. *Semin Cancer Biol* (2013) 23(3):159–70. doi: 10.1016/j.semcancer.2013.02.004
39. Wu LY, Saxena S, Awaji M, Singh RK. Tumor-Associated Neutrophils in Cancer: Going Pro. *Cancers* (2019) 11(4):564. doi: 10.3390/cancers11040564
40. Shaul ME, Fridlender ZG. Neutrophils as Active Regulators of the Immune System in the Tumor Microenvironment. *J Leukoc Biol* (2017) 102(2):343–9. doi: 10.1189/jlb.5MR1216-508R
41. Labelle M, Begum S, Hynes RO. Direct Signaling Between Platelets and Cancer Cells Induces an Epithelial-Mesenchymal-Like Transition and Promotes Metastasis. *Cancer Cell* (2011) 20(5):576–90. doi: 10.1016/j.ccr.2011.09.009

42. Ferrone C, Dranoff G. Dual Roles for Immunity in Gastrointestinal Cancers. *J Clin Oncol Off J Am Soc Clin Oncol* (2010) 28(26):4045–51. doi: 10.1200/jco.2010.27.9992
43. Gooden MJ, de Bock GH, Leffers N, Daemen T, Nijman HW. The Prognostic Influence of Tumour-Infiltrating Lymphocytes in Cancer: A Systematic Review With Meta-Analysis. *Br J Cancer* (2011) 105(1):93–103. doi: 10.1038/bjc.2011.189
44. Wang B, Huang Y, Lin T. Prognostic Impact of Elevated Pre-Treatment Systemic Immune-Inflammation Index (SII) in Hepatocellular Carcinoma: A Meta-Analysis. *Med (Baltimore)* (2020) 99(1):e18571. doi: 10.1097/md.0000000000018571
45. Fu S, Yan J, Tan Y, Liu D. Prognostic Value of Systemic Immune-Inflammatory Index in Survival Outcome in Gastric Cancer: A Meta-Analysis. *J Gastrointest Oncol* (2021) 12(2):344–54. doi: 10.21037/jgo-20-252
46. Wang Y, Cong ZJ, Li ZG, Huang GL. Clinicopathological and Prognostic Importance of Systemic Immune Inflammation Index (SII) in Breast Cancer Patients: A Meta-Analysis. *Int J Clin Exp Med* (2020) 13(8):5527–49.
47. Dong M, Shi Y, Yang J, Zhou Q, Lian Y, Wang D, et al. Prognostic and Clinicopathological Significance of Systemic Immune-Inflammation Index in Colorectal Cancer: A Meta-Analysis. *Ther Adv Med Oncol* (2020) 12:1758835920937425. doi: 10.1177/1758835920937425
48. Huang Y, Gao Y, Wu Y, Lin H. Prognostic Value of Systemic Immune-Inflammation Index in Patients With Urologic Cancers: A Meta-Analysis. *Cancer Cell Int* (2020) 20:499. doi: 10.1186/s12935-020-01590-4
49. Ji Y, Wang H. Prognostic Prediction of Systemic Immune-Inflammation Index for Patients With Gynecological and Breast Cancers: A Meta-Analysis. *World J Surg Oncol* (2020) 18(1):197. doi: 10.1186/s12957-020-01974-w
50. Marquardt A, Solimando AG, Kerscher A, Bittrich M, Kalogirou C, Kübler H, et al. Subgroup-Independent Mapping of Renal Cell Carcinoma-Machine Learning Reveals Prognostic Mitochondrial Gene Signature Beyond Histopathologic Boundaries. *Front Oncol* (2021) 11:621278. doi: 10.3389/fonc.2021.621278

Conflict of Interest: The authors declare that the research was conducted in the absence of any commercial or financial relationships that could be construed as a potential conflict of interest.

frontiers in Oncology

ORIGINAL RESEARCH
published: 17 March 2022
doi: 10.3389/fonc.2022.755936

Systematic Analysis of the Expression and Prognosis of Fcγ Receptors in Clear Cell Renal Cell Carcinoma

*Wenyuan Nie, Yong Yao, Benjun Luo, Jiyin Zhu, Shaocheng Li, Xiaoteng Yang, Tao Luo, Wei Liu and Shibing Yan**

Department of Urology, Medical Center Hospital of Qionglai City, Chengdu, China

OPEN ACCESS

Edited by:
Viktor Grünwald, Universitätsklinikum Essen, Germany

Reviewed by:
Antonella Argentiero, National Cancer Institute Foundation (IRCCS), Italy
Dan Bai, Northwestern Polytechnical University, China

***Correspondence:**
Shibing Yan
ysburomas2003@126.com

Specialty section:
This article was submitted to Genitourinary Oncology, a section of the journal Frontiers in Oncology

Received: *09 August 2021*
Accepted: *17 February 2022*
Published: *17 March 2022*

Citation:
Nie W, Yao Y, Luo B, Zhu J, Li S, Yang X, Luo T, Liu W and Yan S (2022) Systematic Analysis of the Expression and Prognosis of Fcγ Receptors in Clear Cell Renal Cell Carcinoma. Front. Oncol. 12:755936. doi: 10.3389/fonc.2022.755936

Background: Clear cell renal cell carcinoma (ccRCC) remains a common malignancy in the urinary system. Although dramatic progress was made in multimodal therapies, the improvement of its prognosis continues to be unsatisfactory. The antibody-binding crystallizable fragment (Fc) γ receptors (FcγRs) are expressed on the surface of leukocytes, to mediate antibody-induced cell-mediated anti-tumor responses when tumor-reactive antibodies are present. FcγRs have been studied extensively in immune cells, but rarely in cancer cells.

Methods: ONCOMINE, UALCAN, GEPIA, TIMER, TISIDB, Kaplan–Meier Plotter, SurvivalMeth, and STRING databases were utilized in this study.

Results: Transcriptional levels of FcγRs were upregulated in patients with ccRCC. There was a noticeable correlation between the over expressions of FCGR1A/B/C, FCGR2A, and clinical cancer stages/tumor grade in ccRCC patients. Besides, higher transcription levels of FcγRs were found to be associated with poor overall survival (OS) in ccRCC patients. Further, high DNA methylation levels of FcγRs were also observed in ccRCC patients, and higher DNA methylation levels of FcγRs were associated with shorter OS. Moreover, we also found that the expression of FcγRs was significantly correlated with immune infiltrates, namely, immune cells (NK, macrophages, Treg, cells) and immunoinhibitor (IL-10, TGFB1, and CTLA-4).

Conclusions: Our study demonstrated that high DNA methylation levels of FcγRs lead to their low mRNA, protein levels, and poor prognosis in ccRCC patients, which may provide new insights into the choice of immunotherapy targets and prognostic biomarkers.

Keywords: clear cell renal cell carcinoma, Fcγ receptor, prognostic value, bioinformatics analysis, tumor microenvironment

INTRODUCTION

Renal cell carcinoma (RCC) is one of the most common malignancies of the urinary system, which accounts for 3–5% of all new cases of cancer worldwide (1). Clear cell RCC (ccRCC) is the main type of RCC that accounts for 75–82% of the incidence (2). Although immunotherapy strategies of metastatic RCC have been partially improved in recent decades, namely, cytokines, monoclonal antibodies, immuno checkpoint inhibitors(ICI), and chimeric antigen receptor (CAR) modified immune cells therapy, the improvement in the clinical results of the patient still remained unsatisfactory duo to the multiple immune escape mechanisms of kidney cancer (3).

The family of Fc receptors for IgG (FcγRs) are membrane-bound glycoproteins, expressed by several types of circulating and tissue-resident leukocytes (4, 5), which act as a bridge between specific antibodies and effector cell functions to make innate immunity and adaptive immunity closely related (6). To date, three different classes of FcγRs, known as FcγRI, FcγRII, and FcγRIII, have fully recognized in humans (7). FcγRI, which exists on the membrane surface of monocytes and macrophages, has a high affinity with IgG (8). Three genes encoding FcγRI have been identified, which are *FCGR1A*, *FCGR1B*, and *FCGR1C*, whereas only *FCGR1A* expresses the functional FcγRI, *FCGR1B/C* are duplicated pseudogenes of *FCGR1A* (9, 10). Contrary to FcγRI, FcγRII, and FcγRIII exhibit low affinity for monomeric IgG, but they are capable of binding IgG–antigen complexes through high avidity, multimeric interactions (11). Three different FcγRII have been identified, FcγRIIa, FcγRIIb, and FcγRIIc are encoded by *FCGR2A*, *FCGR2B*, and *FCGR2C* respectively and mainly expressing on B lymphocytes, granulocytes, monocytes, macrophages, and dendritic cells (12, 13). FcγRIIb is the sole inhibitory FcγR which can counterbalance the signaling activity of the activating FcγRs. Two classes of FcγRIII (FcγRIIIa and FcγRIIIb) are encoded by the *FCGR3A* and *FCGR3B* genes. FcγRIIIa is widely expressed by macrophages, NK cells, and monocyte subsets, while FcγRIIIb expression is restricted to neutrophils (14, 15).

FcγRs are involved in anti-tumor immunity in the following ways. 1. FcγRs expressed by natural killer (NK) cells and macrophages engage with antibody (IgG), triggering antibody-dependent cellular cytotoxicity (ADCC) of tumor cells (16, 17); 2. Anti-tumor antibodies bind to phagocytic surface FcγRs to enhance the phagocytic function of phagocytosis (18). 3. Anti-tumor antibodies can bind to the corresponding tumor antigen to form an immune complex, where the IgG FC segment can bind to the FcγRs on the APC surface, thus enriching the antigen, facilitating the APC presentation of tumor antigens to T cells (19).

In the past few years, polymorphisms in some members of the FcγRs have been reported in studies which lead to a different response to monoclonal antibodies in cancer (20), whereas abnormal expression of FcγRs in cancer has not been reported yet. In this present study, bioinformatics was performed initially to address this problem by analyzing the expression, DNA methylation, and prognosis of FcγRs and their relations with individual cancer stages and tumor grade in ccRCC patients. Furthermore, we also analyzed the predicted functions and pathways of FcγRs and their 88 co-expression genes.

Abbreviations: ccRCC, clear cell renal cell carcinoma; FcγRs, antibody-binding crystallizable fragment γ receptors; TCGA, The Cancer Genome Atlas; GO, Gene Ontology; KEGG, Kyoto Encyclopedia of Genes and Genomes; BP, biological processes; CC, cellular components; MF, molecular functions; OS, over survival; DFS, disease free survival.

MATERIALS AND METHODS

Ethics Statement

The study has been admitted by the Institutional Review Board of the Medical Central Hospital of Qionglai. All written informed consent had already been obtained since all the data were retrieved from the online databases.

ONCOMINE Database

ONCOMINE is a publicly accessible online genome-wide expression analysis platform, covering 715 datasets and 86,733 samples of cancer (21). ONCOMINE was utilized to analyze expression differences of the FcγRs gene family in multiple tumor tissues and the corresponding adjacent normal tissues. The threshold was determined according to the following values: p-value of 0.001, fold change of 1.5, and gene ranking the top 10%. In this study, the cell color is determined by the best gene rank percentile for the analysis within the cell, and the Student's t-test was applied to generate a p-value.

UALCAN

UALCAN is a comprehensive and interactive web resource for analyzing cancer OMICS data (TCGA, MET500, and CPTAC) (22). In our study, UALCAN was used to illustrate the distinct expression levels of tumor and normal tissues of ccRCC. Student's t-test was used to generate a p-value and the p-value cutoff was 0.05.

GEPIA

Gene Expression Profiling Interactive Analysis (GEPIA) is a newly developed interactive platform for elaborating the RNA sequencing expression data of 9,736 tumors and 8,587 normal samples from the TCGA and the Genotype-tissue Expression dataset, utilizing a standard processing pipeline (23). In this study, GEPIA was used to compare the association with cancer type staging of eight FcγRs members. The Student's t-test was used to generate a p-value and the p-value cutoff was 0.05.

TIMER2.0

TIMER is a comprehensive resource for systematical analysis of immune infiltrates across diverse cancer types. The 2.0 version of the webserver provides abundances of immune infiltrates estimated by multiple immune deconvolution methods, and allows users to generate high-quality figures dynamically to explore tumor immunological, clinical, and genomic features comprehensively (TIMER2.0 for analysis of tumor-infiltrating

immune cells). In this study, we used TIMER2.0 to assess the correlation between FcγRs expression levels and immune cell infiltration and to assess the correlation between clinical outcomes and immune cell infiltration and FcγRs expression.

TISIDB

TISIDB is a web portal for tumor and immune system interaction, and a valuable resource for cancer immunology research and therapy, which integrates multiple heterogeneous data types (TISIDB: an integrated repository portal for tumor-immune system interactions). In this study, we used TISIDB to assess the correlation between FcγRs mRNA expression levels and immunoinhibitors expression levels or cancer grade of ccRCC.

Kaplan–Meier Plotter

The Kaplan–Meier plotter is an online database to assess the effect of gene expression on survival in 21 cancer types (24). We used this online tool to evaluate the prognostic value of FcγRs mRNA levels in ccRCC patients. The overall survival (OS) and recurrence-free survival (RFS) of patients were analyzed with a 50% (Median) cutoff for both low and high expression groups. The statically significant difference was considered when a p-value is <0.05. Information on the number of patients, median values of mRNA expression, 95% confidence interval (CI), hazard ratio (HR), and P-value can be found on the Kaplan–Meier plotter web page.

Multivariate Regression Analysis of ccRCC Data in The Cancer Genome Atlas (TCGA) Database

We have downloaded RNA-sequencing, clinical, pathological, and follow-up data of 603 ccRCC patients from the TCGA-KIRC dataset. A total of 484 cases with complete data were screened out for multivariate regression analysis.

SurvivalMeth

SurvivalMeth is a web server to investigate the effect of DNA methylation-related functional elements on prognosis, and multiple kinds of commonly used functional elements associated with DNA methylation are considered (25). The frequently used data from the TCGA, the CCLE, and the GEO were prestored into SurvivalMeth, namely, 81 DNA methylation profiles in 13,371 samples across 36 cancers, covering more than 480,000 DNA methylation sites locating in 19,000 coding genes, 1,689,653 super enhancers, 1,304,902 CTCF binding regions, 77,634 repeat elements and multiple functional elements such as CpG island, shore, shelf, promoter, gene body, exon, etc.

STRING

STRING is a database of known and predicted protein–protein direct (physical) and indirect (functional) interactions (26). The protein–protein interactions (PPI) network of FcγRs co-expressed genes was visualized using the online tool of STRING with the species setting to *Homo sapiens* and a combined score of >0.7 was considered statistically significant. The nodes meant proteins; the edges meant the interaction of proteins and we hide disconnected nodes in the network.

DAVID

Functions of FcγRs and 88 co-expression genes significantly were analyzed by the Gene Ontology (GO) and the Kyoto Encyclopedia of Genes and Genomes (KEGG) in the Database for Annotation, Visualization, and Integrated Discovery (DAVID) (24). Gene ontology analyses focus on three domains: biological processes (BP), cellular components (CC), and molecular functions (MF), and such analyses are commonly used to predict the functional roles of FcγRs mutations and 80 genes significantly associated with FcγRs mutations, while the KEGG analysis can define the pathways related to the FcγRs mutations and 80 co-expressed genes associated with FcγRs mutations. Only terms with p-value of <0.05 were considered as significant.

RESULTS

Aberrant Expression of FcγRs in Patients With ccRCC

Differential mRNA expression levels of FcγRs were profiled in tumor and adjacent normal tissues of multiple cancer types using Oncomine platform. mRNA levels of FcγR family were remarkably upregulated in four cancer types, namely, brain and CNS, breast, head and neck colorectal and kidney, while mRNA levels of FcγRs were downregulated in leukemia and lung cancer (**Figure 1A**). **Table 1** shows that mRNA expression levels of *FCGR1A/B*, *FCGR2A/B/C*, and *FCGR3B* were remarkably upregulated in ccRCC in multiple datasets. As shown in **Figure 1B**, eight FcγRs are expressed abnormally in different tumor tissues. mRNA expression levels of *FCGR1A/B/C*, *FCGR2A/B/C*, and *FCGR3A* were remarkably upregulated in ccRCC tissues compared with normal tissues. The protein expression levels of FcγRs were analyzed using the CPTAC online tool of UALCAN platform. It was observed that only *FCGR1A* expresses the functional FcγRI, whereas *FCGR1B/C* represents duplicated pseudogenes of *FCGR1A* (6). **Figure 1C** showed that the protein expression levels of *FCGR1A*, *FCGR2A/B*, and *FCGR3A* were downregulated in ccRCC tissues compared with normal tissues.

Correlation Between Transcriptional Levels of FcγRs and Tumor Stages and Cancer Grade of ccRCC Patients

We used the GEPIA dataset to analyze the relationship between transcriptional levels of different FcγRs members with tumor stages of ccRCC patients. The results showed that the mRNA levels of *FCGR1A/B/C* and *FCGR3A* were correlated with the tumor stages of ccRCC patients, whereas the mRNA levels of *FCGR2A/B/C* and *FCGR3B* did not markedly differ among tumor stages (**Figure 2A**). The reason why the mRNA expression of FCGR2A/B/C and FCGR3B in ccRCC did not appear to be significantly different among tumor stages may be their unique roles in anti-tumor immunity. Likewise, cancer grades analysis by TISIDB indicated that mRNA expressions of *FCGR1A/B*,

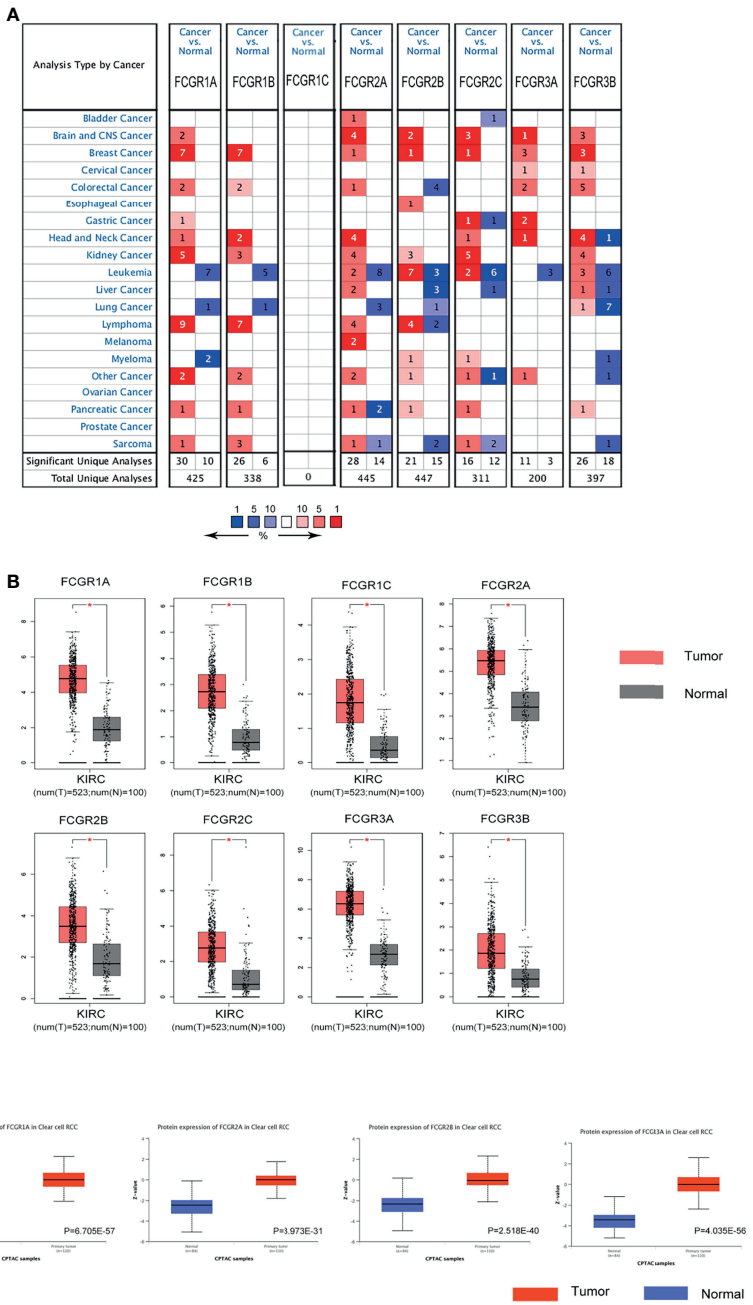

FIGURE 1 | The expression of FCγRs in ccRCC. **(A)** The figure shows the numbers of datasets with statistically significant mRNA upregulation (red) or downregulated expression (blue) of FCγRs. Student's t-test was used to compare the different mRNA levels. Cutoff of p-value and fold change were as following: p-value: 0.01, fold change: 2, gene rank: 10%, data type: mRNA. **(B)** The mRNA expression of different FCγRs in ccRCC tissues and adjacent normal tissues (GEPIA). All the FCγRs mRNA expressions were found to be upregulated in ccRCC compared to normal samples. *p <0.01. **(C)** The protein levels of *FCGR1A*, *FCGR2A/B*, and *FCGR3A* were found to be upregulated in ccRCC tissues compared to normal tissues (UALCAN).

FCGR2A/B/C, and *FCGR3A* correlated with cancer grade of ccRCC (**Figure 2B**). In short, the results above suggested that mRNA expressions of FcγRs (except for *FCGR3B*) were positively correlated with individual tumor stages or cancer grades of patients.

The Prognostic Value of FcγRs in Patients With ccRCC

To evaluate the prognostic value of the FCGR gene family in ccRCC progression, we analyze the correlation between FcγRs transcription levels and clinical outcomes including overall

TABLE 1 | Remarkable changes of FcγRs mRNA expression level between ccRCC and normal tissues (ONCOMINE).

	Types of PAAD vs. normal	Fold Change	t-test	P-value	
FCGR1A	ccRCC vs. Normal	3.623	9.036	4.57E–08	Gumz (27)
	ccRCC vs. Normal	2.856	6.211	0.0000179	Lenburg (28)
	Non-Hereditary ccRCC vs. Normal	7.552	8.972	5.46E–10	Beroukhim (29)
	Hereditary ccRCC vs. Normal	7.431	10.208	1.21E–09	Beroukhim (29)
	ccRCC vs. Normal	11.288	10.468	0.00000119	Yusenko (30)
FCGR1B	ccRCC vs. Normal	2.14	6.5	0.0000219	Lenburg (28)
	Non-Hereditary ccRCC vs. Normal	5.369	7.956	2.8E–09	Beroukhim (29)
	Hereditary ccRCC vs. Normal	5.47	9.463	1.35E–09	Beroukhim (29)
FCGR2A	ccRCC vs. Normal	2.829	8.636	4.35E–08	Gumz (27)
	ccRCC vs. Normal	2.261	4.97	0.0000706	Lenburg (28)
	Non-Hereditary ccRCC vs. Normal	4.659	8.597	0.000000215	Beroukhim (29)
	Hereditary ccRCC vs. Normal	6.143	10.413	4.63E–08	Beroukhim (29)
FCGR2B	ccRCC vs. Normal	5.212	4.849	0.0000777	Gumz (27)
	Hereditary ccRCC vs. Normal	3.466	6.29	0.00000059	Beroukhim (29)
	Non-Hereditary ccRCC vs. Normal	2.844	5.369	0.00000786	Beroukhim (29)
FCGR2C	Papillary Renal Cell Carcinoma vs. Normal	4.799	7.231	0.00000082	Yusenko (30)
	ccRCC vs. Normal	6.779	11.343	0.00000085	Yusenko (30)
	ccRCC vs. Normal	2.805	7.224	0.000000812	Gumz (27)
	Non-Hereditary ccRCC vs. Normal	3.15	7.08	0.000000799	Beroukhim (29)
	Hereditary ccRCC vs. Normal	4.139	9.021	0.00000006	Beroukhim (29)
FCGR3B	Non-Hereditary ccRCC vs. Normal	9.706	7.8	6.54E–09	Beroukhim (29)
	Hereditary ccRCC vs. Normal	15.915	11.751	8.03E–10	Beroukhim (29)
	ccRCC vs. Normal	9.204	4.699	0.0000895	Gumz (27)
	ccRCC vs. Normal	2.814	8.701	3.2E–09	Jones (31)

survival (OS) and disease-free survival (DFS) using the Kaplan–Meier Plotter database. ccRCC patients were divided into low and high-risk groups based on cutoff value. As shown in **Figure 3A**, high transcription levels of FcγRs were correlated with shorter OS in ccRCC. Nevertheless, high transcription levels of *FCGR2B/C* were correlated with longer DFS in ccRCC, and no significant correlation was observed between DFS and other FcγRs (**Figure 3B**). We downloaded and screened the gene expression and clinical data of 485 ccRCC patients from the TCGA database (**Supplementary Table 1**) for multivariate Cox regression survival analysis. The results showed that the effects of *FCGR1A*, *FCGR1B*, and *FCGR1C* on prognosis were still significant after correcting for conventional prognostic factors (**Table 2**; **Supplementary Table 2**).

Correlation Between FcγRs DNA Methylation Levels and Clinical Outcomes in Patients With ccRCC

Genome-wide DNA methylation array and clinical outcome profiles of renal tissues were explored on the SurvivalMeth platform to investigate the DNA methylation levels of FcγRs and their relationships with clinical outcomes of ccRCC patients. Methylation levels of ccRCC were tested in Illumina Infnium HumanMethylation 450 array and Illumina Infnium HumanMethylation27 array in 535 tumors versus 357 normal renal tissues (318 tumors vs. 160 normal with HumanMethylation450 array; 217 tumors vs. 197 normal with HumanMethylation27 array). Lower DNA methylation levels of *FCGR1A/B/C*, *FCGR2A*, and *FCGR3A/B* were detected in ccRCC tissues, comparing with normal tissues (**Figure 4A**), whereas, the DNA methylation levels of *FCGR2A/B* did not differ significantly between tumors and normal tissues. Moreover, lower *FCGR1A/B/C* and *FCGR3A* DNA methylation levels were associated with shorter OS, while lower *FCGR2A* DNA methylation level was associated with longer OS (**Figure 4B**; **Table 3**).

PPI and Functional Enrichment Analysis of FcγRs and Their 88 Co-Expression Genes in ccRCC Patients

We then analyzed significant coexpression genes with FcγRs using the co-expression analysis module in the UAICAN database and listed in **Supplementary Table 3**. A total of 88 upregulated genes were significantly associated with FcγRs expression. Subsequently, the 88 genes were analyzed using GO and KEGG tools in DAVID, and constructed a PPI network by STRING. **Figure 5A** exposed that the activation of immune response-related genes, namely, C1QA, C1QB and, C1QC and adaptive immune response participant genes, such as LAIR1, LILRB4, CD4, and CD86 were closely connected with FcγRs alterations. The first 21 Kyoto Encyclopedia of Genes and Genomes (KEGG) pathways of FcγRs and their 88 Co-expression genes are illustrated in **Figure 5B**. Among them, Phagosom, FcγR-mediated phagocytosis, Cytokine–cytokine receptor interaction, Toll-like receptor signaling pathway and Natural killer cell mediated cytotoxicity are significantly associated with anti-tumor immunity of ccRCC. In addition, GO (Gene Ontology) analysis including molecular functions (MF), cellular components (CC), and biological processes (BP) are shown in **Figures 5C–E**. Most results of GO analysis were associated with immune responses.

Correlation of FcγRs Expression Levels With Immune Infiltration in ccRCC

TIMER and TISIDB online analysis tools were used to evaluate the relationship between the expression levels of FcγRs and the

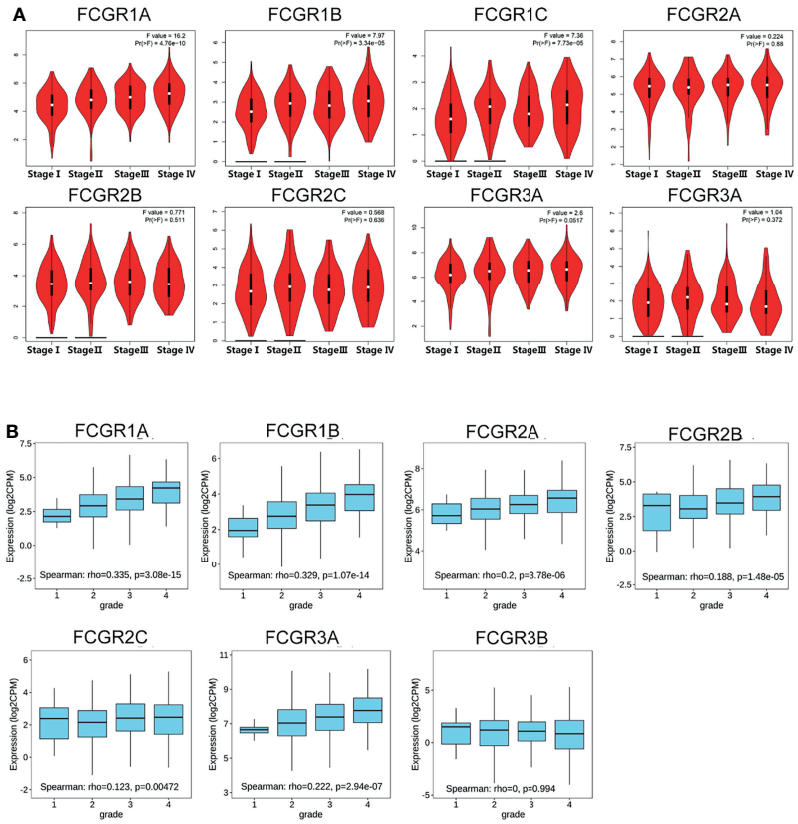

FIGURE 2 | Correlation between FCgRs family expression and tumor stage/cancer grade in ccRCC patients. **(A)** mRNA expressions of FCGR1A/B/C and FCGR3A were significantly related to individual tumor stage (GEPIA) of patients, **(B)** mRNA levels of FCgRs except FCGR3B were associated with the individual cancer grade (TISIDB) of patients.

level of immune infiltration in ccRCC. It was found that FcγRs are involved in immunosuppression regulation and immune cell infiltration, which might affect the clinical outcome of ccRCC patients. The analysis results showed that $CD4^+$ T and NK were negatively correlated with FcγRs expression levels, whereas Treg and M2 macrophage cells were positively correlated with FcγRs expression levels (**Figure 6**). The result of the TISIDB online analysis shows that immunoinhibitors, namely, IL-10 and CTLA-4 were positively correlated with all the FcγRs expression levels. TGFB1 was positively correlated with *FCGR1A/B/C*, *FCGR2A/B*, and *FCGR3A* (**Figure 7**).

DISCUSSION

In the past few decades, monoclonal antibodies (mAbs) that directly target tumor cells have become powerful tools in the fight against cancer, by triggering elimination of cancer cells through FcγRs-mediated antibody-dependent cellular cytotoxicity (ADCC) or, phagocytosis (ADCP) and activating FcγRs on antigen-presenting cells (APC) to promote APC maturation (26). FcγRs were reported to be essential in anti-tumor immunity. FcγRI was demonstrated to play a central role in antibody therapy of experimental melanoma (32). DeLillo and Ravetch showed that the initial ADCC-mediated elimination of tumor cells is dependent on activating human FcgRIIIa using a murine model of EL4 lymphoma (33). The authors also demonstrated that the immune complex binding to FCγRIIa is an essential step in the activation of the T cell-dependent vaccinal effect. Indeed, patients carrying the allelic variants of *FCGR2A*, *FCGR2C*, and *FCGR3A* which exhibit increased affinity for human IgG demonstrated better responsiveness to anti-tumor antibody therapy in cases of B cell lymphomas, colorectal, renal, and breast cancers (20, 34–37).

Abnormal FcγRs expression was rarely reported in tumors. Only *FCGR2B* has been identified to be selectively expressed by metastasis melanoma that impairs the tumor susceptibility to FcγR-dependent innate effector responses, which might explain in part the low response of melanoma patients treated with anti-idiotype (38). In the present study, we found that all FcγRs members have remarkably high expression in ccRCC, and patients with higher FcγRs expression levels exhibit a worse prognosis. Among them, *FCGR1A/B/C* and *FCGR3A* more highly express in ccRCC. Then we analyzed the DNA methylation levels of the FcγRs and found that almost all FCGR genes have high methylation levels in

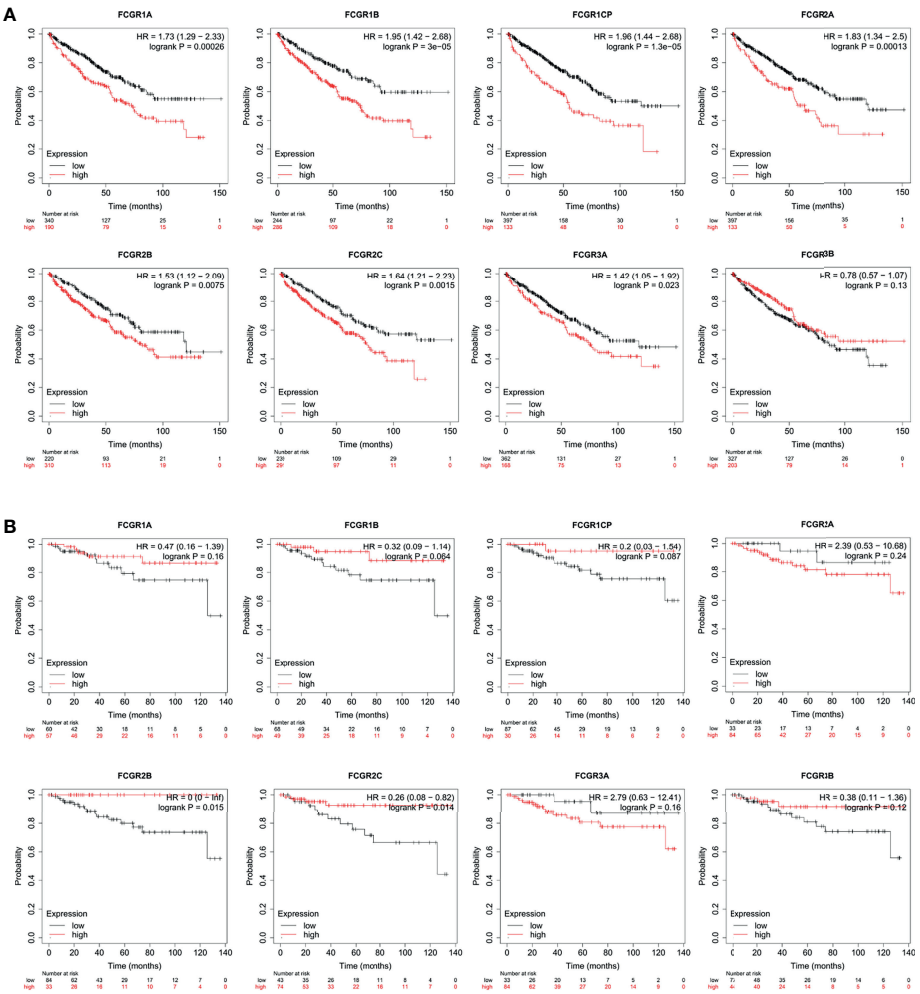

FIGURE 3 | Prognostic feature of mRNA expression of distinct FCgRs in ccRCC patients (Kaplan–Meier plotter). The OS **(A)** and FPS **(B)** survival curves comparing patients with high (red) and low (black) FCgRs expression in ccRCC were plotted using the Kaplan–Meier plotter database at the threshold of p-value of <0.05.

ccRCC, and patients with higher methylation levels have a worse prognosis. The above results indicate that the low DNA methylation levels of the FcγRs in ccRCC were likely to decrease their transcription levels, which in turn affects the prognosis of the patient.

RCC is an extremely heterogeneous cancer, in which a complex immune microenvironment provides favorable conditions for tumor immune escape (39). RCC consists of three major histopathologic groups—ccRCC), papillary (pRCC), and chromophobe RCC (chRCC). Pan-RCC clustering according to

TABLE 2 | The Summary Results of Cox Regression Survival Analysis.

	Coefficient	Z_value	HR	Lower (95%)	Upper (95%)	P-value
FCGR1A	0.4544	2.7858	1.5753	1.1442	2.1687	0.0053
FCGR1B	0.5154	3.1135	1.6743	1.2104	2.316	0.0018
FCGR1C	0.7155	4.2799	2.0452	1.4738	2.8382	<0.0001
FCGR2A	0.2864	1.8138	1.3316	0.9772	1.8145	0.0697
FCGR2B	0.2243	1.4302	1.2514	0.9203	1.7017	0.1527
FCGR2C	0.2624	1.6728	1.3001	0.956	1.7681	0.0944
FCGR3A	0.1823	1.1595	1.2	0.8817	1.6331	0.2463
FCGR3B	-0.0413	-0.2594	0.9596	0.7025	1.3107	0.7954

TABLE 3 | The Summary Results of Kaplan–Meier Plots.

	Concordance (CI)	Rsquare	HR	Lower (95%)	Upper (95%)	P-value
FCGR1A	0.551273	0.005437	1.660288	1.115112	2.471999	0.01388
FCGR1B	0.6050909	0.0510752	2.373975	1.5645872	3.6020732	0.0006167
FCGR1C	0.57315	0.01565	1.68973	1.06181	2.68898	0.01221
FCGR2A	0.58606	0.02623	0.54579	0.26666	1.11711	0.03313
FCGR3A	0.548061	0.017906	2.549054	1.60572	4.04658	0.002245
FCGR3B	0.612	0.04607	1.35641	0.8914	2.06402	0.13678

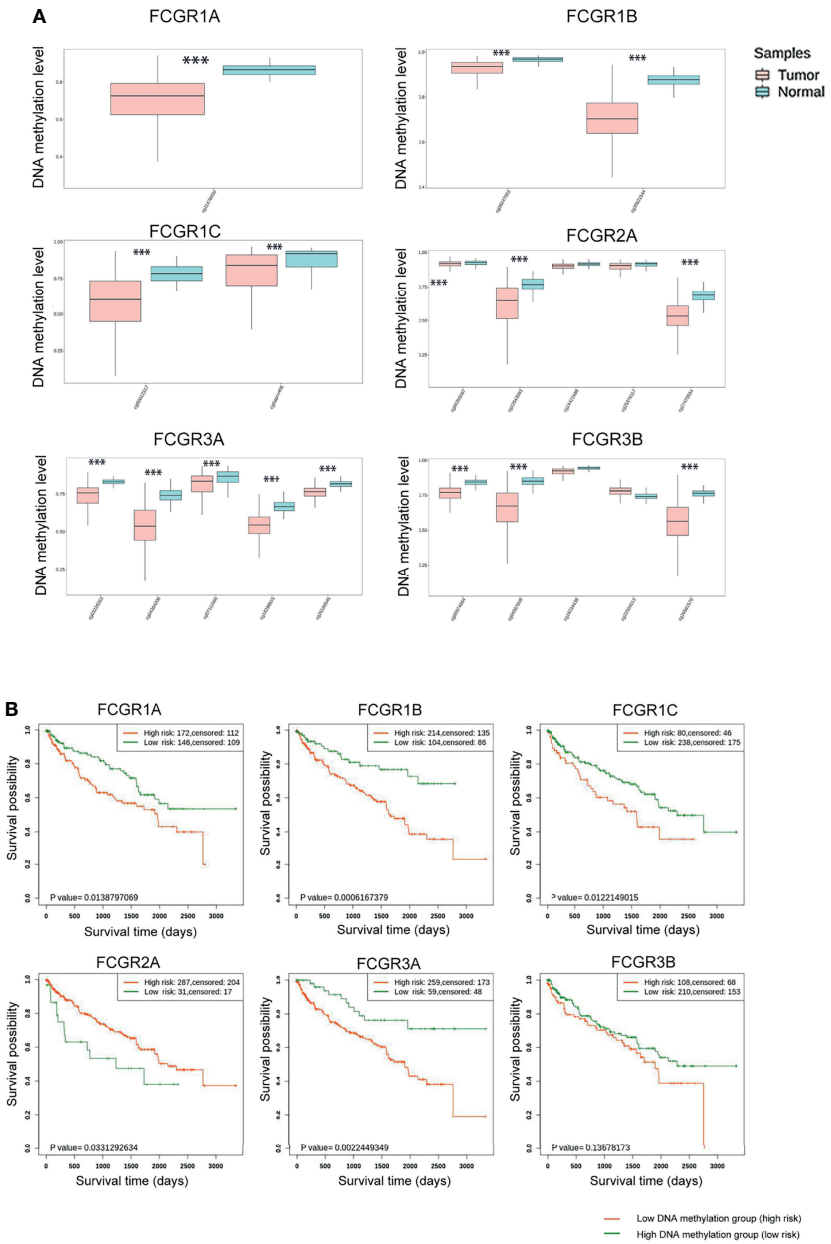

FIGURE 4 | SurvivalMeth analysis of FCγRs. **(A)** FCγRs DNA methylation were enhanced in ccRCC tissues compared with normal renal tissues (***p <0.001). **(B)** The prognostic value of different FCγRs DNA methylation levels in ccRCC patients in the OS curve.

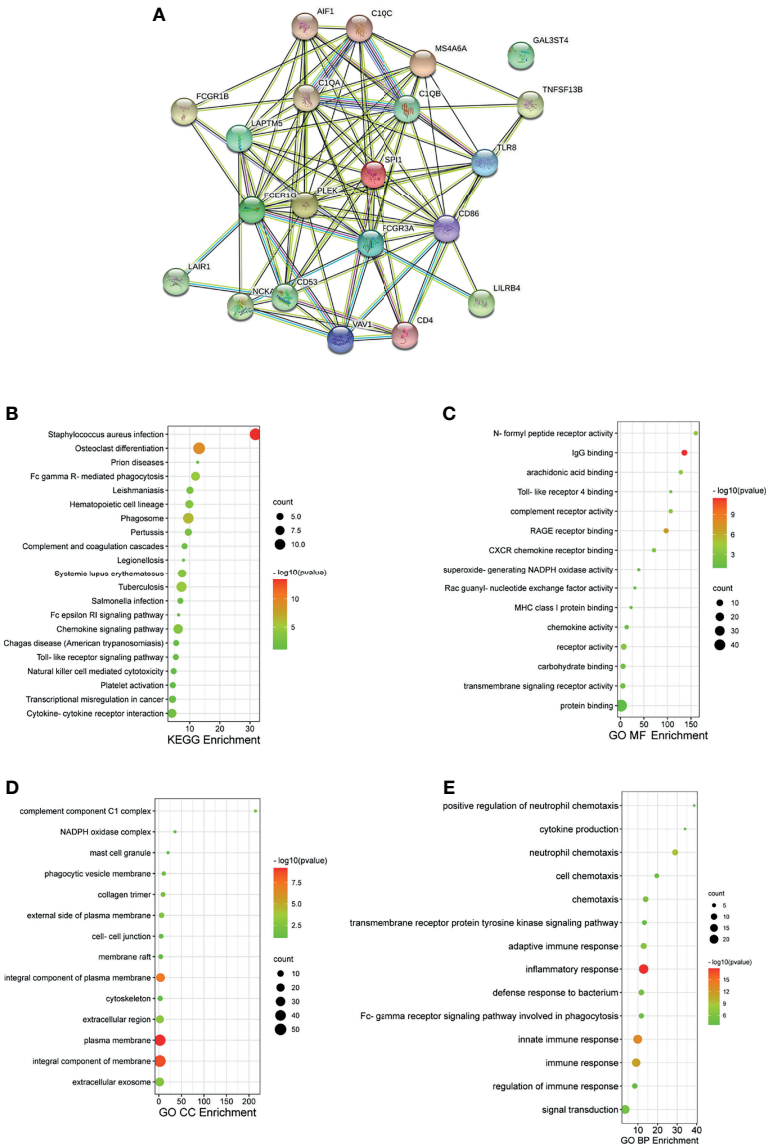

FIGURE 5 | PPI and functional enrichment analysis of FCγRs and their 88 co-expression genes in ccRCC patients (STRING and DAVID). **(A)** PPI network. The nodes meant proteins; the edges meant the interaction of proteins **(B)** KEGG enriched terms. **(C)** GO MF enriched terms. **(D)** GO CC enriched terms. **(E)** GO BP enriched terms.

RNA-sequencing data revealed a distinct histology-independent RCC subgroup characterized by strengthened mitochondrial and weakened angiogenesis-related gene signatures (40). RCC cells may induce cytokine expression, such as IL-10 and TGF-β, in the tumor microenvironment (TME), leading to an immunosuppressive tumor state and promoting immune escape (41–43). Tumor-related immunosuppressive cells, namely, regulatory T cells and tumor-associated macrophages, also play an "accomplice" role in the immunosuppressive tumor state (42). In the present study immune infiltration analysis showed that the expression of FcγRs was negatively correlated with infiltration levels of NK and macrophage M2 cells which were the major immune cells that eliminate tumor cells through ADCC or ADCP. Whereas the infiltration level of macrophage M1 and Treg cells was positively correlated with the expression of FcγRs which would contribute to the immunosuppressive state in ccRCC. The infiltration level of $CD4^+$ T cells is negatively correlated with the expression levels of *FCGR1A/B/C* and *FCGR3A* and positively correlated with the expression of *FCGR2C*. NK cells and macrophages M1 are the primary cells that exert anti-tumor immunity through ADCC. High expression of FcγRs in tumor cells may competitively bind to anti-tumor monoclonal antibodies, thereby inhibiting the activation of ADCC, resulting in low infiltrate levels of NK cells in tumor tissues. Macrophages M2 and Treg cells play an immunosuppressive role in most tumor microenvironments, and the increased level of infiltration of both in ccRCC may lead to

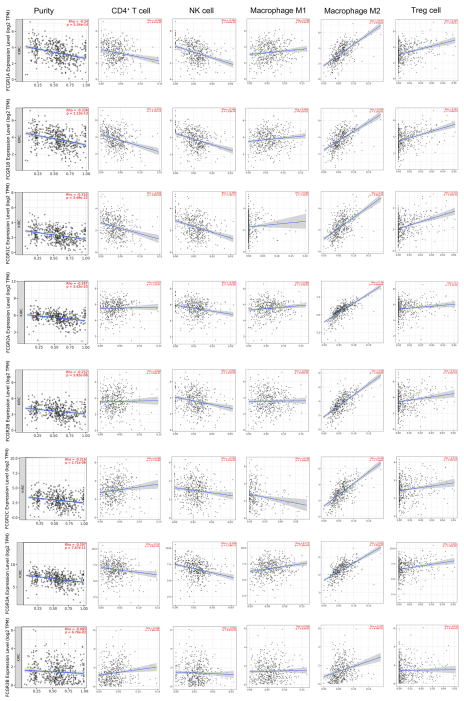

FIGURE 6 | The relationship between FCγRs Expression Levels and Immune Infiltration Levels in ccRCC (TIMER). The correlation between the abundance of immune cell and the expression of FCγRs in ccRCC.

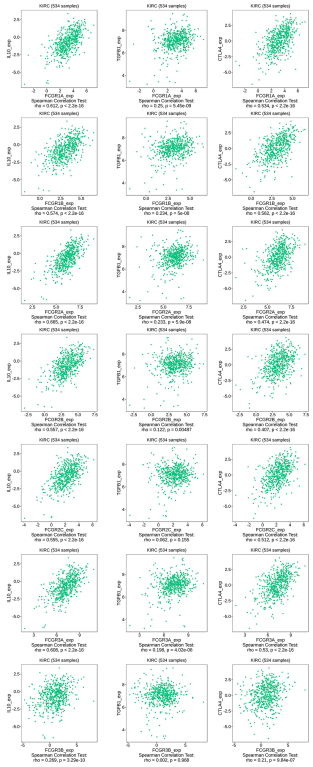

FIGURE 7 | The relationship between FCγRs Expression Levels and Immunoinhibitor in ccRCC (TISIDB).

suppression of anti-tumor immunity, leading to a poor prognosis for patients. Further infiltration analysis of immune-related factors in the TISIDB online tool shows that immunosuppressive factors like IL-10, TGFB1, and CTLA-4 are positively related to FcγRs gene expression in ccRCC. In short, the increase of FcγRs expression level in ccRCC is likely to inhibit anti-tumor immune response by inhibiting the effect of ADCC and promoting the infiltration of immunosuppressive cells and immunosuppressive factors.

Emerging evidence indicates that angiogenesis and immunosuppression frequently occur simultaneously in tumor (44). Sasha et al. demonstrated that humanized or human IgG1 antibodies inhibited angiogenesis by binding to FcγRI of macrophages, resulting in reduced infiltration of macrophages in the tumor microenvironment (45). High expression of FCGR1 in ccRCC may compete with macrophages for binding to human IgG1 antibodies, thus inhibiting their antiangiogenic effects. The expression of FCγRs in ccRCC may simultaneously promote angiogenesis and immunosuppression.

To conclude, our research indicates that DNA methylation levels of FcγRs in ccRCC decreased and mRNA levels increased in ccRCC, which were both associated with poor clinical outcomes. FcγRs can be used as potential survival prognostic biomarkers and therapeutic target for ccRCC. The correlation between the expression of FcγRs and immune infiltration suggests that FcγRs may be involved in anti-tumor immunity in ccRCC. Our results indicated that FcγRs not only can be used as a risk factor for survival of patients with ccRCC but also reflect their immune status. Targeting the FcγRs might go a long way to find more appropriate prognostic factors for ccRCC as well as facilitate the development of novel immunotherapies.

DATA AVAILABILITY STATEMENT

The original contributions presented in the study are included in the article/**Supplementary Material**. Further inquiries can be directed to the corresponding author.

AUTHOR CONTRIBUTIONS

WN conceived the project and wrote the manuscript. SL, BL, JZ, and WL participated in data analysis. YY and TL participated in discussion and language editing. SY reviewed the manuscript. All authors listed have made a substantial, direct, and intellectual contribution to the work and approved it for publication.

SUPPLEMENTARY MATERIAL

The Supplementary Material for this article can be found online at: https://www.frontiersin.org/articles/10.3389/fonc.2022.755936/full#supplementary-material

REFERENCES

1. Siegel RL, Miller KD, Fuchs HE, Jemal A. Cancer Statistics, 2021. *CA Cancer J Clin* (2021) 71:7–33. doi: 10.3322/caac.21654
2. Casuscelli J, Vano YA, Fridman WH, Hsieh JJ. Molecular Classification of Renal Cell Carcinoma and Its Implication in Future Clinical Practice. *Kidney Cancer* (2017) 1:3–13. doi: 10.3233/KCA-170008
3. Ljungberg B, Albiges L, Abu-Ghanem Y, Bensalah K, Dabestani S, Fernández-Pello S, et al. European Association of Urology Guidelines on Renal Cell Carcinoma: The 2019 Update. *Eur Urol* (2019) 75:799–810. doi: 10.1016/j.eururo.2019.02.011
4. Nimmerjahn F, Ravetch JV. Fcgamma Receptors as Regulators of Immune Responses. *Nat Rev Immunol* (2008) 8:34–47. doi: 10.1038/nri2206
5. Bournazos S, Woof JM, Hart SP, Dransfield I. Functional and Clinical Consequences of Fc Receptor Polymorphic and Copy Number Variants. *Clin Exp Immunol* (2009) 157:244–54. doi: 10.1111/j.1365-2249.2009.03980.x
6. Bournazos S, Ravetch JV. Fcγ Receptor Pathways During Active and Passive Immunization. *Immunol Rev* (2015) 268:88–103. doi: 10.1111/imr.12343
7. Ahmed AA, Giddens J, Pincetic A, Lomino JV, Ravetch JV, Wang LX, et al. Structural Characterization of Anti-Inflammatory Immunoglobulin G Fc Proteins. *J Mol Biol* (2014) 426:3166–79. doi: 10.1016/j.jmb.2014.07.006
8. Wang X, Mathieu M, Brezski RJ. IgG Fc Engineering to Modulate Antibody Effector Functions. *Protein Cell* (2018) 9:63–73. doi: 10.1007/s13238-017-0473-8
9. Ernst LK, Duchemin AM, Miller KL, Anderson CL. Molecular Characterization of Six Variant Fcgamma Receptor Class I (CD64) Transcripts. *Mol Immunol* (1998) 35:943–54. doi: 10.1016/S0161-5890(98)00079-0
10. Ernst LK, van de Winkel JG, Chiu IM, Anderson CL. Three Genes for the Human High Affinity Fc Receptor for IgG (Fc Gamma RI) Encode Four Distinct Transcription Products. *J Biol Chem* (1992) 267:15692–700. doi: 10.1016/S0021-9258(19)49591-4
11. Sondermann P, Kaiser J, Jacob U. Molecular Basis for Immune Complex Recognition: A Comparison of Fc-Receptor Structures. *J Mol Biol* (2001) 309:737–49. doi: 10.1006/jmbi.2001.4670
12. Anania JC, Chenoweth AM, Wines BD, Hogarth PM. The Human Fcγrii (CD32) Family of Leukocyte FcR in Health and Disease. *Front Immunol* (2019) 10:464. doi: 10.3389/fimmu.2019.00464
13. Jessup CF, Ridings J, Ho A, Nobbs S, Roberton DM, Macardle P, et al. The Fc Receptor for IgG (Fc Gamma RII; CD32) on Human Neonatal B Lymphocytes. *Hum Immunol* (2001) 62:679–85. doi: 10.1016/S0198-8859(01)00257-9
14. Bandukwala HS, Clay BS, Tong J, Mody PD, Cannon JL, Shilling RA, et al. Signaling Through Fc Gamma RIII is Required for Optimal T Helper Type (Th)2 Responses and Th2-Mediated Airway Inflammation. *J Exp Med* (2007) 204:1875–89. doi: 10.1084/jem.20061134
15. Barb AW. Fc γ Receptor Compositional Heterogeneity: Considerations for Immunotherapy Development. *J Biol Chem* (2021) 296:100057. doi: 10.1074/jbc.REV120.013168
16. Seidel UJ, Schlegel P, Lang P. Natural Killer Cell Mediated Antibody-Dependent Cellular Cytotoxicity in Tumor Immunotherapy With Therapeutic Antibodies. *Front Immunol* (2013) 4:76. doi: 10.3389/fimmu.2013.00076
17. Vivier E, Tomasello E, Baratin M, Walzer T, Ugolini S. Functions of Natural Killer Cells. *Nat Immunol* (2008) 9:503–10. doi: 10.1038/ni1582
18. Vidarsson G, Dekkers G, Rispens T. IgG Subclasses and Allotypes: From Structure to Effector Functions. *Front Immunol* (2014) 5:520. doi: 10.3389/fimmu.2014.00520
19. de Jong JM, Schuurhuis DH, Ioan-Facsinay A, Welling MM, Camps MG, van der Voort EI, et al. Dendritic Cells, But Not Macrophages or B Cells, Activate Major Histocompatibility Complex Class II-Restricted CD4+ T Cells Upon Immune-Complex Uptake In Vivo. *Immunology* (2006) 119:499–506. doi: 10.1111/j.1365-2567.2006.02464.x
20. Mellor JD, Brown MP, Irving HR, Zalcberg JR, Dobrovic A. A Critical Review of the Role of Fc Gamma Receptor Polymorphisms in the Response to Monoclonal Antibodies in Cancer. *J Hematol Oncol* (2013) 6:1. doi: 10.1186/1756-8722-6-1
21. Rhodes DR, Yu J, Shanker K, Deshpande N, Varambally R, Ghosh D, et al. ONCOMINE: A Cancer Microarray Database and Integrated Data-Mining Platform. *Neoplasia* (2004) 6:1–6. doi: 10.1016/S1476-5586(04)80047-2
22. Nagy Á, Lánczky A, Menyhárt O, Győrffy B. Validation of miRNA Prognostic Power in Hepatocellular Carcinoma Using Expression Data of Independent Datasets. *Sci Rep* (2018) 8:9227. doi: 10.1038/s41598-018-27521-y
23. Szklarczyk D, Gable AL, Lyon D, Junge A, Wyder S, Huerta-Cepas J, et al. STRING V11: Protein-Protein Association Networks With Increased Coverage, Supporting Functional Discovery in Genome-Wide Experimental Datasets. *Nucleic Acids Res* (2019) 47:D607–d613. doi: 10.1093/nar/gky1131
24. Huang da W, Sherman BT, Lempicki RA. Bioinformatics Enrichment Tools: Paths Toward the Comprehensive Functional Analysis of Large Gene Lists. *Nucleic Acids Res* (2009) 37:1–13. doi: 10.1093/nar/gkn923
25. Zhang C, Zhao N, Zhang X, Xiao J, Li J, Lv D, et al. SurvivalMeth: A Web Server to Investigate the Effect of DNA Methylation-Related Functional Elements on Prognosis. *Brief Bioinform* (2021) 22:3. doi: 10.1093/bib/bbaa162
26. Scott AM, Wolchok JD, Old LJ. Antibody Therapy of Cancer. *Nat Rev Cancer* (2012) 12:278–87. doi: 10.1038/nrc3236
27. Gumz ML, Zou H, Kreinest PA, Childs AC, Belmonte LS, LeGrand SN, et al. Secreted Frizzled-Related Protein 1 Loss Contributes to Tumor Phenotype of Clear Cell Renal Cell Carcinoma. *Clin Cancer Res* (2007) 13:4740–9. doi: 10.1158/1078-0432.CCR-07-0143
28. Lenburg ME, Liou LS, Gerry NP, Frampton GM, Cohen HT, Christman MF. Previously Unidentified Changes in Renal Cell Carcinoma Gene Expression Identified by Parametric Analysis of Microarray Data. *BMC Cancer* (2003) 3:31. doi: 10.1186/1471-2407-3-31
29. Beroukhim R, Brunet JP, Di Napoli A, Mertz KD, Seeley A, Pires MM, et al. Patterns of Gene Expression and Copy-Number Alterations in Von-Hippel Lindau Disease-Associated and Sporadic Clear Cell Carcinoma of the Kidney. *Cancer Res* (2009) 69:4674–81. doi: 10.1158/0008-5472.CAN-09-0146
30. Yusenko MV, Kuiper RP, Boethe T, Ljungberg B, van Kessel AG, Kovacs G. High-Resolution DNA Copy Number and Gene Expression Analyses Distinguish Chromophobe Renal Cell Carcinomas and Renal Oncocytomas. *BMC Cancer* (2009) 9:152. doi: 10.1186/1471-2407-9-152
31. Jones J, Otu H, Spentzos D, Kolia S, Inan M, Beecken WD, et al. Gene Signatures of Progression and Metastasis in Renal Cell Cancer. *Clin Cancer Res* (2005) 11:5730–9. doi: 10.1158/1078-0432.CCR-04-2225
32. Bevaart L, Jansen MJ, van Vugt MJ, Verbeek JS, van de Winkel JG, Leusen JH. The High-Affinity IgG Receptor, FcgammaRI, Plays a Central Role in Antibody Therapy of Experimental Melanoma. *Cancer Res* (2006) 66:1261–4. doi: 10.1158/0008-5472.CAN-05-2856
33. Smith P, DiLillo DJ, Bournazos S, Li F, Ravetch JV. Mouse Model Recapitulating Human Fcγ Receptor Structural and Functional Diversity. *Proc Natl Acad Sci USA* (2012) 109:6181–6. doi: 10.1073/pnas.1203954109
34. Weng WK, Levy R. Two Immunoglobulin G Fragment C Receptor Polymorphisms Independently Predict Response to Rituximab in Patients With Follicular Lymphoma. *J Clin Oncol* (2003) 21:3940–7. doi: 10.1200/JCO.2003.05.013
35. Cartron G, Dacheux L, Salles G, Solal-Celigny P, Bardos P, Colombat P, et al. Therapeutic Activity of Humanized Anti-CD20 Monoclonal Antibody and Polymorphism in IgG Fc Receptor FcgammaRIIIa Gene. *Blood* (2002) 99:754–8. doi: 10.1182/blood.V99.3.754
36. Bibeau F, Lopez-Crapez E, Di Fiore F, Thezenas S, Ychou M, Blanchard F, et al. Impact of Fc{gamma}RIIa-Fc{gamma}RIIIa Polymorphisms and KRAS Mutations on the Clinical Outcome of Patients With Metastatic Colorectal Cancer Treated With Cetuximab Plus Irinotecan. *J Clin Oncol* (2009) 27:1122–9. doi: 10.1200/JCO.2008.18.0463
37. Erbe AK, Wang W, Goldberg J, Gallenberger M, Kim K, Carmichael L, et al. FCGR Polymorphisms Influence Response to IL2 in Metastatic Renal Cell Carcinoma. *Clin Cancer Res* (2017) 23:2159–68. doi: 10.1158/1078-0432.CCR-16-1874
38. Cassard L, Cohen-Solal JF, Fournier EM, Camilleri-Broët S, Spatz A, Chouaïb S, et al. Selective Expression of Inhibitory Fcgamma Receptor by Metastatic Melanoma Impairs Tumor Susceptibility to IgG-Dependent Cellular Response. *Int J Cancer* (2008) 123:2832–9. doi: 10.1002/ijc.23870
39. Hsieh JJ, Purdue MP, Signoretti S, Swanton C, Albiges L, Schmidinger M, et al. Renal Cell Carcinoma. *Nat Rev Dis Primers* (2017) 3:17009. doi: 10.1038/nrdp.2017.9
40. Marquardt A, Solimando AG, Kerscher A, Bittrich M, Kalogirou C, Kübler H, et al. Subgroup-Independent Mapping of Renal Cell Carcinoma-Machine Learning Reveals Prognostic Mitochondrial Gene Signature Beyond

Histopathologic Boundaries. *Front Oncol* (2021) 11:621278. doi: 10.3389/fonc.2021.621278
41. Gooden MJ, de Bock GH, Leffers N, Daemen T, Nijman HW. The Prognostic Influence of Tumour-Infiltrating Lymphocytes in Cancer: A Systematic Review With Meta-Analysis. *Br J Cancer* (2011) 105:93–103. doi: 10.1038/bjc.2011.189
42. Jian Y, Yang K, Sun X, Zhao J, Huang K, Aldanakh A, et al. Current Advance of Immune Evasion Mechanisms and Emerging Immunotherapies in Renal Cell Carcinoma. *Front Immunol* (2021) 12:639636. doi: 10.3389/fimmu.2021.639636
43. Busse A, Asemissen A, Nonnenmacher A, Ochsenreither S, Fusi A, Braun F, et al. Systemic Immune Tuning in Renal Cell Carcinoma: Favorable Prognostic Impact of TGF-β1 mRNA Expression in Peripheral Blood Mononuclear Cells. *J Immunother* (2011) 34:113–9. doi: 10.1097/CJI.0b013e3181fb6580
44. Liu Y, Cao X. Characteristics and Significance of the Pre-Metastatic Niche. *Cancer Cell* (2016) 30:668–81. doi: 10.1016/j.ccell.2016.09.011
45. Bogdanovich S, Kim Y, Mizutani T, Yasuma R, Tudisco L, Cicatiello V, et al. Human IgG1 Antibodies Suppress Angiogenesis in a Target-Independent Manner. *Signal Transduct Target Ther* (2016) 1:15001. doi: 10.1038/sigtrans.2015.1

Conflict of Interest: The authors declare that the research was conducted in the absence of any commercial or financial relationships that could be construed as a potential conflict of interest.

Advantages of publishing in Frontiers

OPEN ACCESS
Articles are free to read for greatest visibility and readership

FAST PUBLICATION
Around 90 days from submission to decision

HIGH QUALITY PEER-REVIEW
Rigorous, collaborative, and constructive peer-review

TRANSPARENT PEER-REVIEW
Editors and reviewers acknowledged by name on published articles

Frontiers
Avenue du Tribunal-Fédéral 34
1005 Lausanne | Switzerland

Visit us: www.frontiersin.org
Contact us: frontiersin.org/about/contact

REPRODUCIBILITY OF RESEARCH
Support open data and methods to enhance research reproducibility

DIGITAL PUBLISHING
Articles designed for optimal readership across devices

FOLLOW US
@frontiersin

IMPACT METRICS
Advanced article metrics track visibility across digital media

EXTENSIVE PROMOTION
Marketing and promotion of impactful research

LOOP RESEARCH NETWORK
Our network increases your article's readership